

Maritime Tsunami Hazard Assessment for the City of Bainbridge Island's Eagle Harbor, Washington

Technical Report

November 2024

Alex Dolcimascolo  
Washington Geological Survey  
Washington State Department of Natural Resources

Submitted to the  
Washington State Emergency Management Division and  
Washington Geological Survey  
for  
Tsunami Maritime Response and Mitigation Strategy

## Contents

|  |    |
|--|----|
| 1. Introduction .....  | 4  |
| 2. Earthquake sources.....   | 5  |
| 2.1 Cascadia subduction zone earthquake (Cascadia Extended L1) ..... | 5  |
| 2.2 Seattle fault (SF-L) .....                                       | 8  |
| 3. Topography and bathymetry .....                                   | 11 |
| 3.1 Study DEMs.....  | 11 |
| 4. Study area.....   | 13 |
| 4.1 Fgmax selection improvements and limitations .....               | 15 |
| 4.2 Dry land below Mean High Water .....                             | 15 |
| 5. Model uncertainties and limitations .....                         | 15 |
| 5.1 Tide stage and sea level rise .....                              | 15 |
| 5.2 The built environment .....                                      | 16 |
| 5.3 Bottom friction .....  | 16 |
| 5.4 Tsunami modification of bathymetry and topography .....          | 16 |
| 6. Fgmax results.....  | 17 |
| 6.1 Maximum onshore flow depths.....                                 | 19 |
| 6.2 Maximum speeds.....  | 21 |
| 6.3 Minimum water depths.....  | 23 |
| 7. Gauge output results .....  | 25 |
| 7.1 Synthetic tide gauge locations.....                              | 25 |
| 7.2 Synthetic gauge plots.....                                       | 28 |
| Acknowledgments .....  | 29 |
| Data availability.....   | 29 |
| References .....   | 30 |
| Appendix A. GeoClaw output and version information.....              | 35 |
| A.1 GeoClaw Version 5.9.0 .....                                      | 36 |
| Appendix B. Gauge report summaries.....                              | 37 |
| Appendix C. All study gauge plots.....                               | 42 |

## 1. Introduction

This Tsunami Hazard Assessment (THA) tests tsunamis from two earthquake sources, the Cascadia subduction zone (CSZ) and the Seattle fault (SF), at two sea-level tide stages (mean high water [MHW] and mean low water [MLW]) for the City of Bainbridge Island's Eagle Harbor, Washington. The modeled tsunami results from this study are useful for estimating potential current speeds, inundation depths, minimum water depths, and wave arrival times. The data from this modeling study is used in the Tsunami Maritime Response and Mitigation Strategy for Eagle Harbor, prepared by Washington's Emergency Management Division, to aid in planning and preparing the maritime community for a tsunami. This maritime guidance document is a collaboration between Washington Emergency Management Division, the Washington State Department of Natural Resources' Washington Geological Survey, and the City of Bainbridge Island.

An fgmax region is a fixed grid (fg) that saves the maximum (max) values of model variables attained over the duration of the simulation. These variables include water depth (h), and water speed (s) derived from the velocity components ( $s = \sqrt{u^2 + v^2}$ ), as well as other quantities of interest derived from the depth (h) and horizontal momenta (hu and hv; the quantities modeled in the shallow water equations). The tsunami modeling for this project consists of one distinct fgmax region covering all of Eagle Harbor, Bainbridge Island at 1/9<sup>th</sup> arc-second resolution (Figure 1). This large fgmax region records and saves each model variable in a single job run. However, each tsunami source and assigned tidal stage require a separate job run; model results from each job run are stored in individual multivariable netCDF files. Thus, two earthquake sources (CSZ and SF), two sea level scenarios (MHW and MLW), and one model resolution (1/9<sup>th</sup> arc-second) need a total of four job runs, yielding four unique netCDF files. See Appendix A for further discussion of the data format. All digital elevation models (DEMs) and project data utilize World Geodetic System 1984 (WGS84, EPSG:4326) as the standard coordinate system for this study.

The tsunami modeling for this study was done using GeoClaw, version 5.10.0 (Clawpack Development Team, 2024). GeoClaw open-source software is available at <http://www.clawpack.org/geoclaw>. The exact version of the code used in the simulations reported here is also available by request from the Washington Geological Survey (WGS) at the Washington State Department of Natural Resources (WADNR). GeoClaw simulates tsunami generation, propagation, and inundation. This model, which solves the nonlinear shallow water equations and uses Adaptive Mesh Refinement (AMR) to focus fine computational grids around the defined fgmax regions, has undergone extensive verification and validation (Berger and others, 2011; LeVeque and others, 2011). GeoClaw has been accepted as a validated model by the U.S. National Tsunami Hazard Mitigation Program (NTHMP) after conducting multiple benchmark tests as part of an NTHMP benchmarking workshop (González and others, 2011). The following THA generally follows the format of previous reports developed by the University of Washington Tsunami Modeling Group (UWTMG; <http://depts.washington.edu/ptha/projects/index.html>) and the WGS. Some of the text in this report describes modeling methods developed by the UWTMG and WGS and is also used in those earlier reports.





Figure 1. Outline of the 1/9<sup>th</sup> arc-second resolution fgmax region covering the study domain for the Eagle Harbor maritime strategy.

## 2. Earthquake sources

This study tests two earthquake sources: 1) a local Cascadia subduction zone (CSZ) megathrust event with moment magnitude  $M_w$  9.0 (denoted Cascadia Extended L1), and 2) a very local Seattle fault (SF) scenario analogous to the prehistorical event from 923 C.E. (Black and others, 2023; denoted SF-L developed by the NOAA Center for Tsunami Research (NTRC) at Pacific Marine Environmental Laboratory [PMEL] in Seattle, Washington).

### 2.1 Cascadia subduction zone earthquake (Cascadia Extended L1)

This study assesses a hypothetical tsunami generated by a megathrust event of the Cascadia subduction zone (CSZ). The CSZ spans from Northern California to British Columbia and has been seismically quiet since the year 1700 (Jacoby and others, 1997; Satake and others, 2003; Yamaguchi and others, 1997; Atwater and others, 2005). However, geologic evidence of submerged coastal areas and tsunami deposits (Atwater and Hemphill-Haley, 1997; Atwater and others, 2004), in addition to offshore sedimentary evidence (Goldfinger and others, 2012; Goldfinger and others, 2017), reveals that Cascadia has had at least 23 approximate magnitude 9 earthquakes in the last 10,000 years. In addition, global

positioning data show that Cascadia is currently building seismic stress, portending a future great earthquake (Burgette and others, 2009; Yousefi and others, 2020). The USGS estimates that there is a 10-14% chance of a magnitude 9 earthquake, and a 30% chance of a magnitude 8 on the CSZ within the next 50 years (Petersen and others, 2002).

The CSZ fault model used for this study is a derivative of the L1 scenario (Witter and others, 2011; 2013, coined the CSZ Extended L1 scenario. It's predecessor, the  $M_w$ 9.0 L1 scenario, is one of 15 scenarios based on an analysis of offshore data spanning 10,000 years for a THA of Bandon, Oregon (Witter and others, 2011). The L1 scenario's earthquake rupture terminates at around 48°N along the northern edge of the Juan de Fuca Plate (southern end of Vancouver Island, British Columbia). Due to Bandon's proximity to the southern part of the CSZ, a full-margin earthquake rupture propagating into the more northern Explorer Plate, which could be significant to Washington's Salish Sea (Dolcimascolo and others, 2021), was not considered. The  $M_w$ 9.0 Extended L1 scenario, developed by NTCR at PMEL, solves this problem by extending the earthquake rupture up to the northern end of Vancouver Island, accommodating the Explorer Plate possibility (Gica and Arcas, 2015). The rupture geometry of this fault model still includes a surface-rupturing splay fault structure that amplifies tsunami waves, like the L1 scenario. The tsunami generated from this scenario consists of very large waves along the Pacific coast that enter the Strait of Juan de Fuca and into Puget Sound to reach Eagle Harbor. Figure 2 displays the crustal and seafloor deformation produced by the Extended L1 model; modeled coseismic subsidence is negligible within this project's study area. Washington State has adopted the Extended L1 scenario (and the original L1) as the "maximum considered" CSZ tsunami scenario. The L-category source models have an estimated mean recurrence interval of ~3,333 years (Witter and others, 2013). This is a close and conservative approximation to design requirements for critical facilities in the international building code for seismic hazards that build to the engineering standard of a 2,500-year event (International Code Council, 2015).

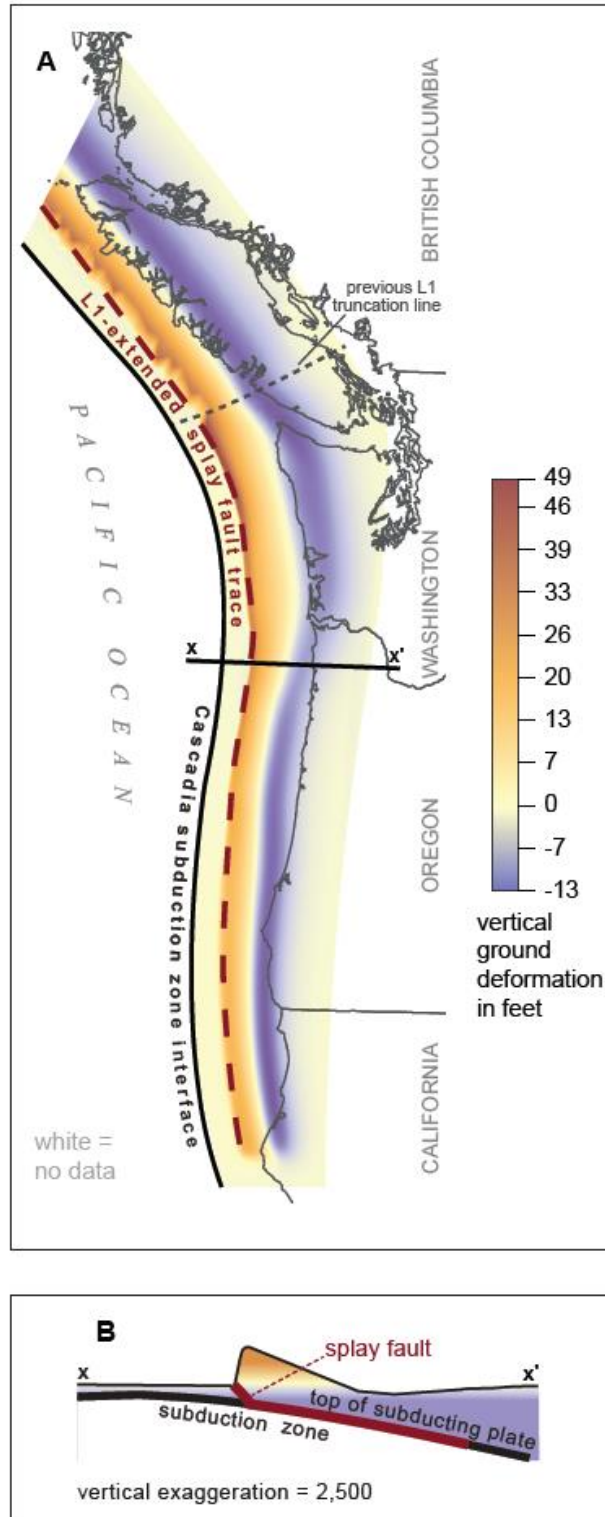


**Figure 2.** Vertical ground deformation for the Extended L1 scenario modified by NTCR at PMEL (Gica and Arcas, 2015). This earthquake scenario has a maximum uplift of 15.08 meters (~49 feet) offshore and a maximum subsidence of -3.98 meters (~-13 feet) near the shore/onshore. B. Splay fault model diagram corresponding to the X-X' line in subfigure A.

## 2.2 Seattle fault (SF-L)

The Seattle fault extends from the Cascade Range foothills to Hood Canal, cutting across Seattle, Puget Sound, and Bainbridge Island. Large earthquake events on this fault can generate tsunami waves that immediately impact Bainbridge Island and the Eagle Harbor study area, with just minutes of warning due to its proximity to the fault.

The Seattle fault model used for this study is the same source used in recent tsunami modeling assessments completed by the UWTMG, the NCTR at PMEL, and the WGS (Table 1; LeVeque and others, 2018; Titov and others, 2018; Adams and others, 2019; LeVeque and others, 2019; Dolcimascolo and others, 2022). Figure 3 displays the crustal and seafloor deformation produced by this scenario; modeled coseismic subsidence is ~5-6 feet within Eagle Harbor.

Previous tsunami hazard assessments have disagreed on the magnitude of this source model. For example, different groups have referred to the magnitude of this earthquake as either Mw 7.3 (Titov and others, 2003) or Mw 7.54 (LeVeque and others, 2019). However, this scenario is a geomorphic model and slip values are only constrained by documented land level changes within the Puget Sound (listed in Table 2) from the 923 C.E. event (Black and others, 2023; Titov and others, 2003). Therefore, this Seattle fault model should not be associated with an official magnitude (T. Walsh, Pers. Comm., 2020).

Table 1: The six sub-fault segments of the Seattle fault scenario used in this study with the updated down-dip width values (Venturato and others, 2007) that produced the deformation in Figure 3. I numbered the segments from west to east. Although I list point coordinates for the top center of each segment, Titov and others (2003) did not specify latitude and longitude. Discussions and examinations between the UWTMG and NCTR at PMEL determined these coordinate locations.

| Segment | Longitude<br>(°W) | Latitude<br>(°N) | Depth<br>(mi) | Approximate<br>length (mi) | Approximate<br>width (mi) | Strike<br>(°) | Dip<br>(°) | Approximate<br>slip (ft) |
|---------|-------------------|------------------|---------------|----------------------------|---------------------------|---------------|------------|--------------------------|
| 1       | -122.7599344      | 47.6115777       | 0.3 (0.5 km)  | 9.44 (15.2 km)             | 22 (35 km)                | 87.9          | 60         | 3 (1 m)                  |
| 2       | -122.6165584      | 47.6157655       | 0.3 (0.5 km)  | 3.9 (6.3 km)               | 22 (35 km)                | 86.6          | 60         | 3 (1 m)                  |
| 3       | -122.5154909      | 47.6132604       | 0.3 (0.5 km)  | 5.5 (8.9 km)               | 22 (35 km)                | 96.0          | 60         | 49 (12 m)                |
| 4       | -122.4397627      | 47.6000508       | 0.3 (0.5 km)  | 2.0 (3.2 km)               | 22 (35 km)                | 128.8         | 60         | 26 (11 m)                |
| 5       | -122.3474066      | 47.5826645       | 0.3 (0.5 km)  | 7.15 (11.5 km)             | 22 (35 km)                | 99.3          | 60         | 13 (4 m)                 |
| 6       | -122.1735094      | 47.5847905       | 0.3 (0.5 km)  | 9.26 (14.9 km)             | 22 (35 km)                | 81.0          | 60         | 3 (1 m)                  |

Due to uncertainty about the proper magnitude for this earthquake source model, the tsunami modeling groups in Washington have collectively adopted the SF-L notation for this larger Seattle fault scenario (LeVeque and others, 2018), which is being used for this assessment. Since the original specification of the SF-L model, many additional land-level change observations have been made (e.g. ten Brink and others, 2006; Martin, 2011; Table 2) and improved models for the subfault geometry have also been produced (Kelsey and others, 2008; Nelson and others, 2014; Pratt and others, 2015). Once a new source model for the Seattle fault zone is developed and peer-reviewed, a new tsunami hazard assessment will be necessary to update these results.

Table 2: Observed land-level changes from the last Seattle Fault earthquake in 923 CE (Black and others, 2023). Other sites at Lynch Cove, Burley, and Oakland Bay (not included in this table) also show at least 7 ft (2 m) of uplift, but they are relatively far from the Seattle Fault (22 to 37 miles [35 to 60 km]) and so their relationship to the Seattle Fault is not clear (Bucknam and others, 1992; Sherrod, 2001; Fig. 3). The land-level changes at these sites could be a result of a series of earthquakes occurring in a short time interval (several hundred years apart) on additional faults within the Puget Lowland and are unlikely to be from a single earthquake (Buckham and others, 1992).

| Site location                 | Approximate land-level change (ft) | Incorporated into the modeled earthquake scenario, SF-L? | Reference  |
|-------------------------------|------------------------------------|--|--|
| Restoration Point             | +23 (+7 m)                         | Yes  | Bucknam and others (1992); Sherrod and others (2000)   |
| Alki Point                    | +13 (+4 m)                         | Yes  | Bucknam and others (1992)                              |
| Gorst                         | +10 (+3 m)                         | No   | Martin (2011)  |
| Eagle Harbor (southern shore) | +10 (+3 m)                         | No   | Bucknam and others, 1992); ten Brink and others (2006) |
| West Point                    | <-3 (<-1 m)                        | Yes  | Atwater and Moore (1992)                               |
| Winslow                       | <-3 (<-1 m)                        | No   | Bucknam and others (1992)                              |
| Indianola                     | 0 (0 m)                            | No   | ten Brink and others (2006)                            |

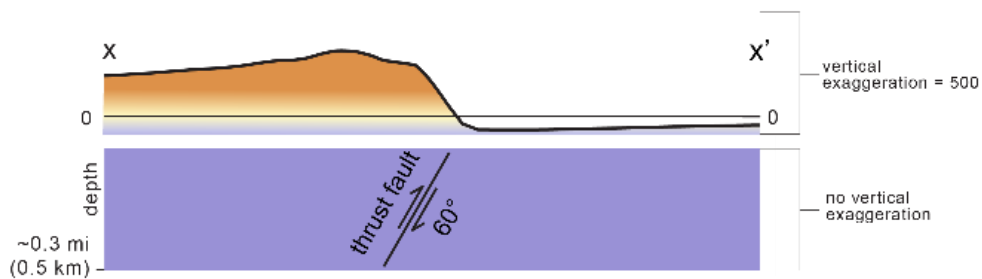
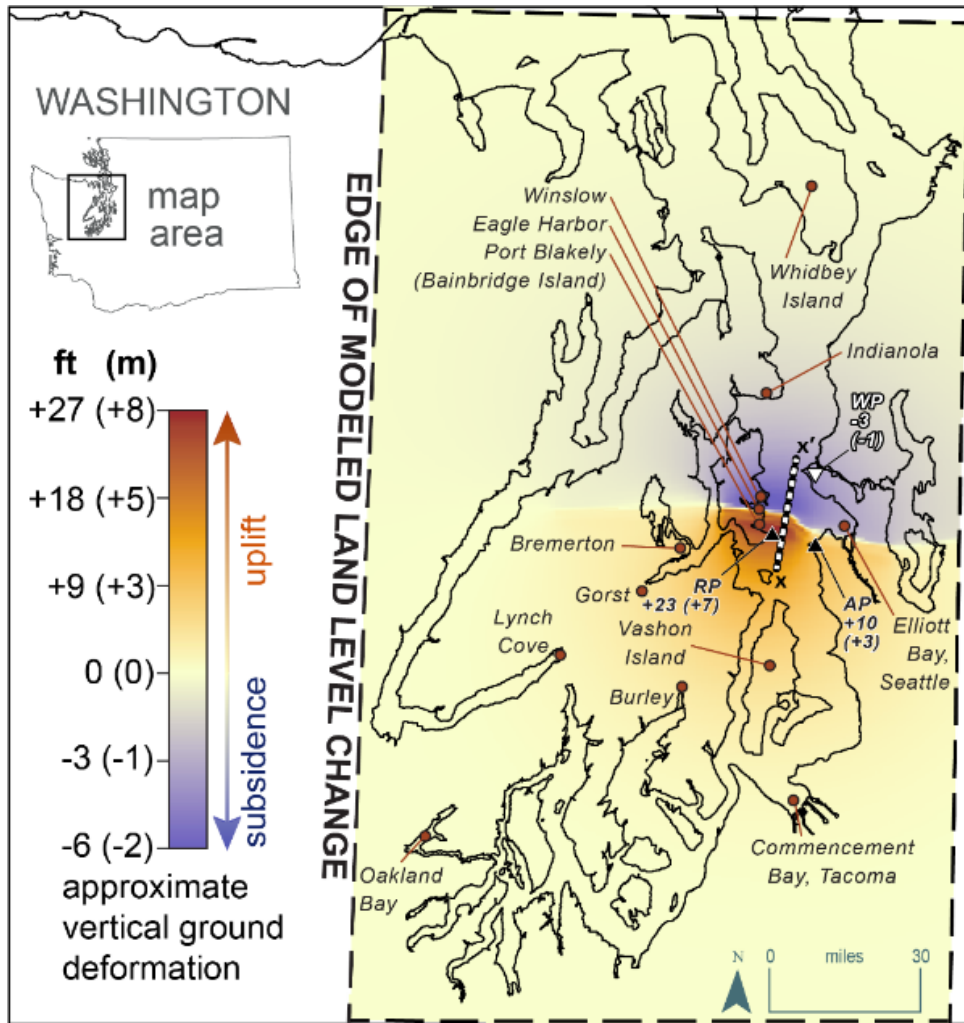


Figure 3: (A) Map of assigned surface deformation from the Seattle Fault scenario developed by Titov and others (2003). The dashed black line outlines the edge of modeled land-level change within the study area. The X—X' line denotes the area of a cross section, represented in subfigure B. This Seattle fault scenario reproduces the observed land level change at Alki Point (AP; Bucknam and others, 1992), Restoration Point (RP; Bucknam and others, 1992), and West Point (WP; Atwater and Moore, 1992) from the last SFZ earthquake that ruptured in 923 C.E. (shown in black [uplift] and white [subsidence] triangles). (B) Thrust fault model diagram corresponding to the X—X' line in subfigure A.



### 3. Topography and bathymetry

Digital Elevation Models (DEMs) are needed by the GeoClaw modeling software to effectively track the movement of tsunami waves from the source to the study area. The footprints of the DEMs used in this study were developed/hosted by the NOAA National Centers for Environmental Information (NCEI) and are listed in Table 2. All DEMs used in this study are vertically referenced to mean high water (MHW), so that the “0” elevation reference point for model outputs is MHW. For the mean low water (MLW) simulations, the MHW DEM was also used, but sea level was set to -2.334 m (-7.657 ft) below zero, agreeing with the tides and currents data from the nearest NOAA tide station in Elliot Bay, Seattle, Washington (#9447130; NOAA, 2024). All DEMs used in this study are projected in the World Geodetic System 1984 (WGS84, EPSG:4326) coordinate system. Note that published DEMs may have errors, or the landscape may have changed since the DEM was initially developed.

Table 2. DEMs used in this tsunami modeling study.

| Name   | Resolution  | Source          |
|--|---|-----------------|
| ETOPO 2022<br>Global Relief Model  | 30 arc-second   | NOAA NCEI, 2022 |
| Strait of Juan de Fuca (Sjdf)  | 2 arc-second  | NOAA NGDC, 2015 |
| Port Townsend (PT)   | 2 arc-second  | NOAA NGDC, 2011 |
| Puget Sound (PS)   | 2 arc-second  | NOAA NGDC, 2014 |
| CUEM merged<br>(ncei19_n47x50_w122x25_mhw.nc,<br>ncei19_n47x50_w122x50_mhw.nc,<br>ncei19_n47x50_w122x75_mhw.nc,<br>ncei19_n47x50_w123x00_mhw.nc,<br>ncei19_n47x50_w123x25_mhw.nc,<br>ncei19_n47x75_w122x25_mhw.nc,<br>ncei19_n47x75_w122x50_mhw.nc,<br>ncei19_n47x75_w122x75_mhw.nc,<br>ncei19_n47x75_w123x00_mhw.nc,<br>ncei19_n47x75_w123x25_mhw.nc,<br>ncei19_n48x00_w122x25_mhw.nc,<br>ncei19_n48x00_w122x50_mhw.nc,<br>ncei19_n48x00_w122x75_mhw.nc,<br>ncei19_n48x00_w123x00_mhw.nc) | 1/9 arc-second for the study<br>area (specified extent:<br>-122.60°W, -122.31°E, 47.48°N,<br>47.75°N) | CIRES, 2020     |

#### 3.1 Study DEMs

The highest resolution model outputs for this study were run on a DEM covering all of Eagle Harbor, Bainbridge Island with 1/9 arc-second grid points (1/9 arc-second both in longitude and latitude; CIRES,

2020; referred to as EH for this project). I also used three additional DEMs covering the Strait of Juan de Fuca (NOAA NGDC, 2015; referred to as SJDf), the greater Port Townsend region (NOAA NDGC, 2011; referred to as PT), and the broader Puget Sound (NOAA NGDC, 2014; referred to as PS). These three DEMs were all coarsened to 2 arc-second using a pre-processing script that subsampled every sixth point in each direction. These coarsened DEM supplies topography and bathymetry coverage leading up to Eagle Harbor and its adjacent areas to capture the nearfield tsunami domain. Lastly, the simulations also use the ETOPO 2022 30 arc-second ice surface Global Relief Model (NCEI, 2022) to cover the entire modeling domain (including offshore areas in the Pacific Ocean), which is necessary for the CSZ runs due to this tsunami source initiating ~70 miles offshore in the Pacific Ocean. Figure 4 displays the extents of all DEMs used in this assessment, apart from the ETOPO 2022 Global Relief Model used in the Pacific. Only the 2 arc-second PS DEM was used for the Seattle fault runs, in addition to the 1/9 arc-second EH DEM, since Eagle Harbor and the Seattle fault scenario deformation are contained entirely within this DEM extent.

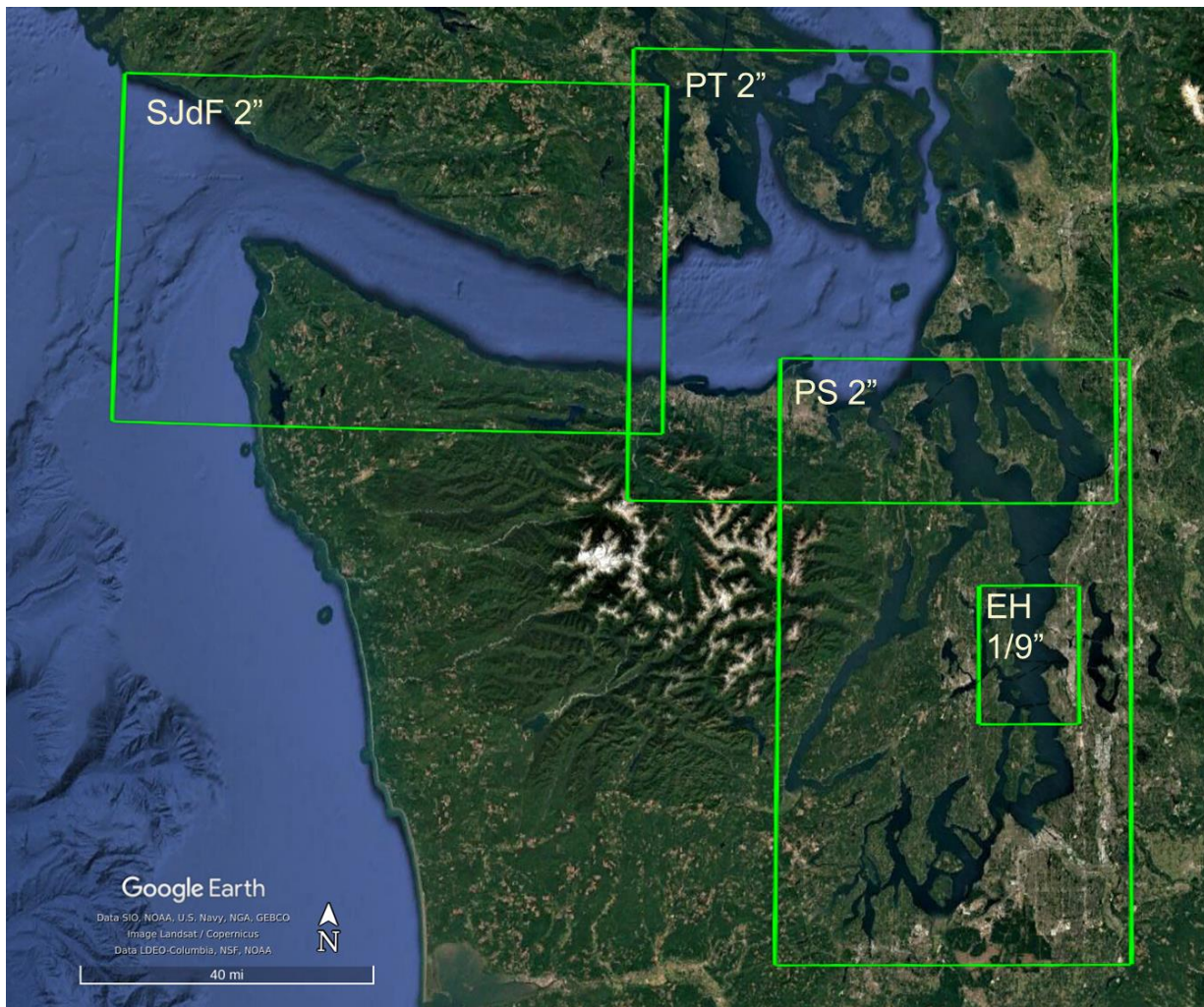


Figure 4. DEMs used in this study. The sources of the different resolution DEMs are listed in Table 2. All DEMs shown are used for the CSZ simulations, and only the PS and EH DEMs are used in the SF simulations. All simulations (CSZ and SF) used the ETOPO 2022 30 arc-second Global Relief Model (not shown; NCEI, 2022).



## 4. Study area

This study defines one 1/9<sup>th</sup> arc-second (Eagle Harbor) fgmax region (refer to Figure 1). This fgmax region uses a fixed set of points (independent of adaptive mesh refinement [AMR]) on which the maximum of each quantity of interest is monitored over the course of the simulation. The quantities monitored are the flow depth, flow speed, and momentum flux. These fgmax points also monitor the time of the maximum values and the first wave arrival at each grid point. Furthermore, all fgmax points lie on a grid with spacing based on their respective resolution and align with the DEM grids. Table 3 gives an overview of the number of points included in the Eagle Harbor fgmax region and Figure 5 provides visuals of this fgmax region.

Table 3: The total number of fgmax points in the Eagle Harbor fgmax region that is used in this tsunami hazard assessment. This fgmax region only contains grid points for which the topography elevation is less than 15 m above MHW in the specified region boundaries. The column labeled “extent” defines the boundary GPS coordinates (west, east, south, north) of the fgmax region derived from the CUDEM merged tiles listed in Table 2. A pre-processing script was used to select a “ruled rectangle” polygon of fgmax points using a “marching front” algorithm (refer to Section 4.1; [https://www.clawpack.org/ruled\\_rectangles.html](https://www.clawpack.org/ruled_rectangles.html); Clawpack Development Team, 2024). The column labeled “Count” gives the number of fgmax points in the region. See Section 6 for sample results of the maximum values monitored in each job run.

| <b>Fgmax region</b> | <b>Extent</b>                         | <b>Count</b> | <b>Resolution</b> |
|---------------------|---------------------------------------|--------------|-------------------|
| Eagle Harbor        | -122.550, -122.480,<br>47.605, 47.640 | 1,040,374    | 1/9”              |

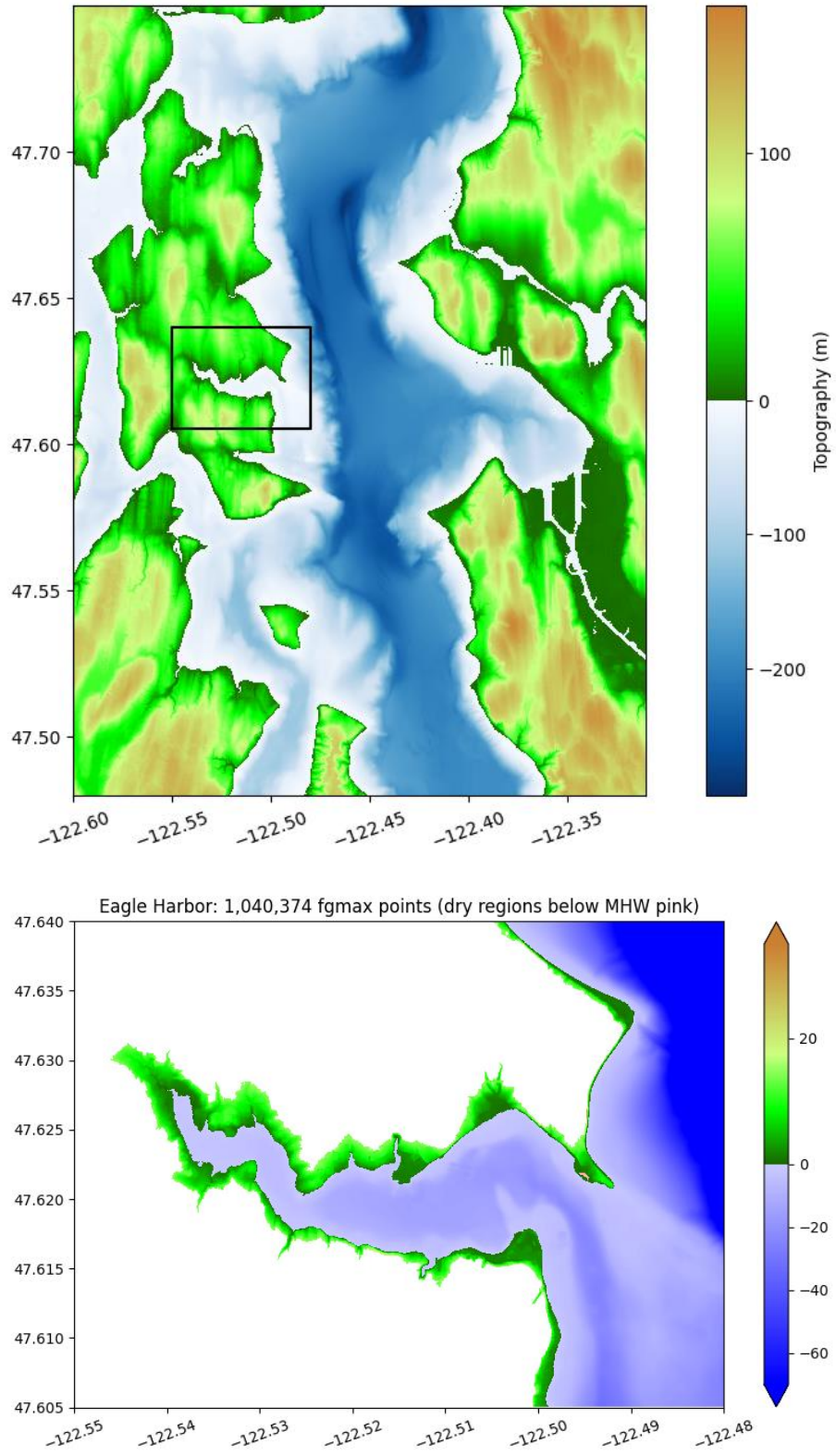


Figure 5: Specified extent used to select fgmax points for the Eagle Harbor fgmax region (top). 1,040,374 points selected in the ruled rectangle fgmax region (bottom; [https://www.clawpack.org/ruled\\_rectangles.html](https://www.clawpack.org/ruled_rectangles.html)).

## 4.1 Fgmax selection improvements and limitations

The fgmax region selected for this project was specified in a pre-processing script that only selects grid points that return topography elevations below a specified limit,  $Z_{max}$ . For the current project,  $Z_{max}$  is set to 15 meters. This pre-processing script is available upon request by the WGS. Additionally, if only onshore inundation and nearshore currents need to be modeled, there is also the capability to set a maximum depth threshold (e.g. -60 or -40 meters). This would then only select fgmax points within the polygon or rectangle boundary where the bathymetry elevation is both above the specified value and less than  $Z_{max}$ . Note that this project includes all water points in each fgmax polygon to model currents farther from shore and did not include a maximum depth threshold. To run the code with many fgmax points efficiently, the UWTMG also improved the way the GeoClaw code internally handled the fgmax points. This resulted in a substantial computational speedup, while still monitoring values in the same manner as in previous versions of GeoClaw. Refer to LeVeque and others (2019) for a more complete summary of all improvements developed when selecting fgmax points and increasing computation efficiency.

## 4.2 Dry land below Mean High Water

Few locations in the fgmax region represent dry land with elevations below MHW, though protected from inundation under normal conditions. The standard GeoClaw software would initialize these points with water up to the level of MHW at the start of the simulation. Inadvertently, GeoClaw would flood these locations even if no tsunami arrived, which can be a misleading result. Moreover, for locations where the tsunami does reach land below MHW, there would be very different wave dynamics if the tsunami moved over an initially flooded artificial lake rather than moving over dry land. In these scenarios, the maximum depths recorded would be very different, with the former being incorrect. For example, water entering an artificial lake will spread out rapidly and eventually raise the level everywhere by a small amount. On the other hand, the same quantity of water overtopping a dike or levee and moving across dry land will quickly decelerate due to high bottom friction, giving higher maximum depth near the dike and little or no flooding farther inland. To deal with this problem, the UWTMG first developed a capability used in their project that modeled Whatcom County (Adams and others, 2019) and then improved upon it in the Island and Skagit County project (LeVeque and others, 2019) that forces these areas dry prior to tsunami wave arrival. Documentation of this “force dry” capability has been built into the GeoClaw code since v5.7.0 and is used in this current project. The locations that were subject to this problem were effectively forced dry and were saved as a variable in the input netCDF file needed to run the tsunami simulation (Appendix B). This file is available upon request from the WGS.

## 5. Model uncertainties and limitations

The inputs to the GeoClaw model include the earthquake sources, the DEMs used, and the fgmax areas (discussed in sections 2-4). In addition, other geophysical parameters are designated. Some physical processes are not included in these simulations, which use the two-dimensional shallow water equations. See below for the discussion of these parameters and their potential effect on the modeling results.

### 5.1 Tide stage and sea level rise

The simulations for this study were run at both mean high water (MHW) and mean low water (MLW)

tidal datums. The MHW datum is conservative for tsunami inundation depths as the deeper tidal stage amplifies flooding over land. The MLW datum is often conservative for tsunami currents, in that current speeds tend to increase at lower water levels in shallow areas. The MLW datum is also conservative for minimum water depths to infer maximum drawdown values. Running simulations at both MHW and MLW tidal stages capture the range of variability of expected conditions within Eagle Harbor, Bainbridge Island during a tsunami event. The DEMs used near the study location are referenced to the MHW datum (= 0), except for the Strait of Juan de Fuca and ETOPO1 DEMs which are referenced to NAVD88. This is not a concern because those datasets cover parts of the model at coarse resolution. The simulations at MLW used the same DEMs (referenced to MHW), but sea level was set in GeoClaw at -2.334 m (7.657 feet) to approximate MLW. The MLW level was obtained from data collected by the NOAA tide gauge #9447130 located in Seattle, WA (NOAA, 2011). While consideration of future sea level rise is important for planning, this study does not account for potential sea level rise projections.

## 5.2 The built environment

The topographic DEMs used in this study are “bare earth” and are created by stripping the land surface of built structures, buildings, and vegetation. The presence of structures and vegetation can alter tsunami flow patterns and generally impede inland flow. To some extent, the lack of structures in the model makes the model results more conservative because structures can reduce inland penetration of the tsunami wave. Actual tsunami flows are likely to interact with structures that may impede flow and cause water to pile up in some areas. Additionally, bare earth DEMs may lead to simulations with higher flow velocities because there is nothing to slow the flows. Actual tsunami flows may also be slowed by structures, or conversely may speed up in areas where the flow is channelized, such as between buildings. Structures also contribute to debris that interacts with tsunami flows. In some cases, structures may be necessary to best model an area.

## 5.3 Bottom friction

Each simulation uses the value 0.025 for Manning’s Roughness Coefficient. This is a standard value used in tsunami modeling and corresponds to a gravelly earth surface material. Using 0.025 is conservative in some sense, because the presence of trees, structures, and vegetation would justify the use of a larger value, which might tend to reduce the inland flow. On the other hand, larger friction values can lead to deeper flow in some areas, since the water may pile up more as it advances more slowly across the topography.

## 5.4 Tsunami modification of bathymetry and topography

Scour, erosion, and deposition all happen in a tsunami. These topographic and bathymetric changes will inherently alter flow patterns of the tsunami wave. The erosion of natural berms or ridges along the coastline (or manufactured levies, dikes, or breakwaters) by the tsunami could increase more extensive flooding. On the other hand, the movement of material in a tsunami also requires an expenditure of tsunami energy, which could reduce the inland extent of inundation. These complex changes to the land are largely uncertain in a tsunami, and GeoClaw does not account for erosional or bathymetric/topographic change during simulations. Because there is no active modification to the topography and bathymetry in these results, the modeling dynamics of flow presented here may not entirely predict future tsunami behavior in the study area.

## 6. Fgmax results

This section contains figures of modeling results from each job run. The WGS at the Washington State Department of Natural Resources developed these model results into high-quality graphics for the final maritime guidance publication and products. The fgmax plots that follow show simplistic visual representations of the maximum onshore flow depths, maximum speeds, and minimum water depths recorded over the full simulation time for each source (12 hours for the CSZ scenario and 3 hours for the SF scenario) at mean high water (MHW) and mean low water (MLW) tidal stages. To query the specific values of each grid cell within the simulated fgmax region, the data files (in netCDF format) are available from the WGS upon request (refer to Appendix A).

The deepest onshore inundation depths (flooding over dry land) in the fgmax area are generated from the SF-L scenario event at MHW. At this tide stage, average flow depths range from 5-6 meters (16-20) feet near the Bainbridge Island City Dock, and ~4 meters (~13 feet) at the ferry terminal maintenance yard. Additionally, inundation depths from the SF-L scenario simulated at MLW is also significant along all shorelines of Eagle Harbor. Figure 7 shows onshore flow depths for the SF-L scenario at both MHW and MLW tidal stages. On the contrary, the CSZ scenario produces minimal inundation depths within the Eagle Harbor study area, with few exceptions in locations nearest the shoreline, and the low-lying areas adjacent to Hawley Cove Park, the west side of Wing Point, and the Head of the Bay. Inundation becomes negligible from the CSZ simulation run using the MLW tidal stage (Figure 8).

Maximum speeds are shown in meters/second for the SF scenario in Figure 9, and for the CSZ scenario in Figure 10 at MHW and MLW tidal stages. Modeled results suggest that the maximum current speeds for a given location can form at either MHW or MLW tidal stages. When combining the results from both tide stages, the SF scenario generates currents that exceed 4.5 meters/second (9+ knots) in many areas throughout the study area, including the mouth and offshore of Eagle Harbor, the nearshore region just south of the ferry maintenance yard, and much of Eagle Harbor west of ~-122.518°W (where the width of the harbor decreases towards the head of the bay. Many offshore gyres also form in the SF tsunami scenarios throughout the study area—one of note forming south of the Williamson Landing Marina, which moves in the northeast direction towards the City Dock between 19 and 28 minutes of the simulations (following the main inundating wave peak). To generalize the overall current velocities from the SF scenario, speeds are greatest west of the City Dock and at the entrance to Eagle Harbor offshore Wing Point and Pritchard Park. The tsunami modeling also suggests that speeds are fastest near shorelines and slowest in the center of the harbor, such as between Eagle Harbor Marina and the ferry terminal maintenance yard) where modeled maximum speeds yield between ~2-3 m/s (~4-6 knots).

In the CSZ scenarios, modeled current speeds are comparatively less with much of the region between the ferry terminal maintenance yard and Eagle Harbor Marina yielding values less than 1.5 m/s (3 knots). Additionally, the tsunami modeling shows that the inlet immediately west of the ferry terminal maintenance yard (~-122.516°W, 47.622°N) is fairly protected from increased current speeds, suggesting a potential last-resort offshore staging area for ships in the event of a CSZ-induced tsunami. Furthermore, the CSZ tsunami modeling captured speeds of 2-3 m/s (4-6 knots) at both the head and mouth of Eagle Harbor, and just offshore in central Puget Sound. Only the area south of Williamson Landing Marina (where the harbor decreases in width towards the head of the bay; ~-122.525°W, 47.619°N) shows modeled speeds greater than 4.5 m/s (9 knots) from these CSZ scenarios, posing significant risk to the local marinas west of the City Dock.

Minimum water depth values are important for understanding the potential drawdown of water

preceding or between tsunami wave crests. In marinas, this can result in vessels becoming stranded and possibly tipped prior to (or following) the next wave crest arrival. The low tide simulations resulted in greater drawdowns for both the SF (Figure 11) and CSZ (Figure 12) scenarios. When comparing the two tsunami sources, the modeled CSZ scenario produced slightly greater reaches of 3-feet or less water depths from shore than the SF scenario throughout the study area. Areas of greatest differences include within the head of the bay and at the mouth of the bay offshore Wing Point and Pritchard Park. These differences are likely results of 1) the CSZ earthquake source generating a longer tsunami wavelength than the SF earthquake source, and 2) the local subsidence that impacts the study area from the SF source. This subsidence seems to slightly diminishes the overall impact of the trough-phase of the modeled tsunami as local sea-level recovers and flows back into the subsided areas during the onset of the first inundating waves within less than 10 minutes of earthquake. The “change in water height” tide gauge plots for the SF scenarios (Appendix C) capture the impact that subsidence has on overall offshore wave heights relative to the post-earthquake conditions.

## 6.1 Maximum onshore flow depths

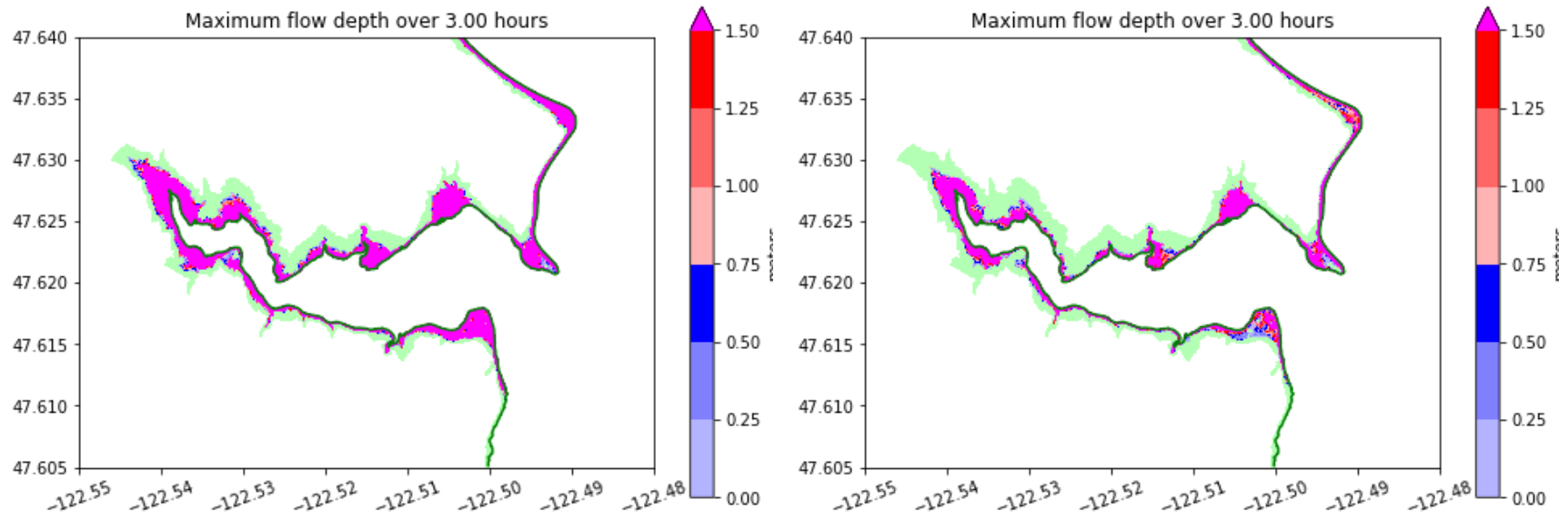


Figure 7: Seattle fault (large) scenario, maximum onshore depths attained over 3 hours for MHW simulation (left), and MLW simulation (right). Green coloring represents non-inundated dry land within the selected fgmax region. Model resolution: 1/9<sup>th</sup> arc-second.

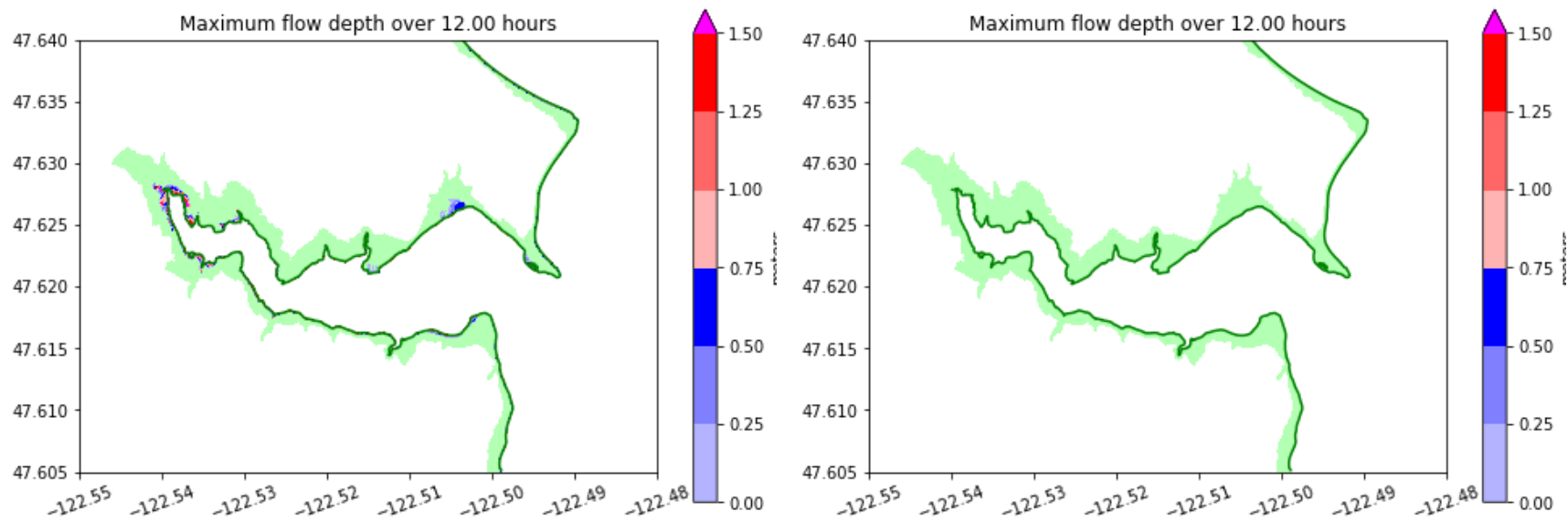


Figure 8: Cascadia subduction zone scenario, maximum onshore depths attained over 12 hours for MHW simulation (left), and MLW simulation (right). Green coloring represents non-inundated dry land within the selected fgmax region. Model resolution: 1/9<sup>th</sup> arc-second.



## 6.2 Maximum speeds

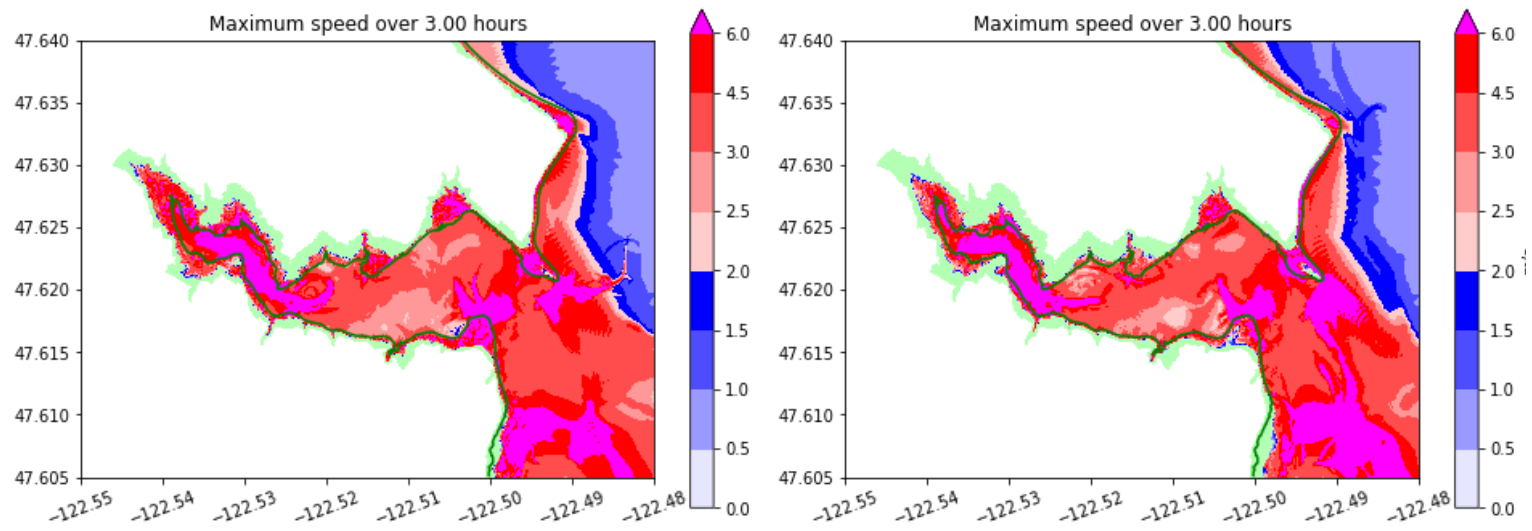


Figure 9: Seattle fault (large), maximum speeds attained over 3 hours for MHW simulation (left), and MLW simulation (right). Green coloring represents non-inundated dry land within the selected fgmax region. Model resolution: 1/9<sup>th</sup> arc-second.

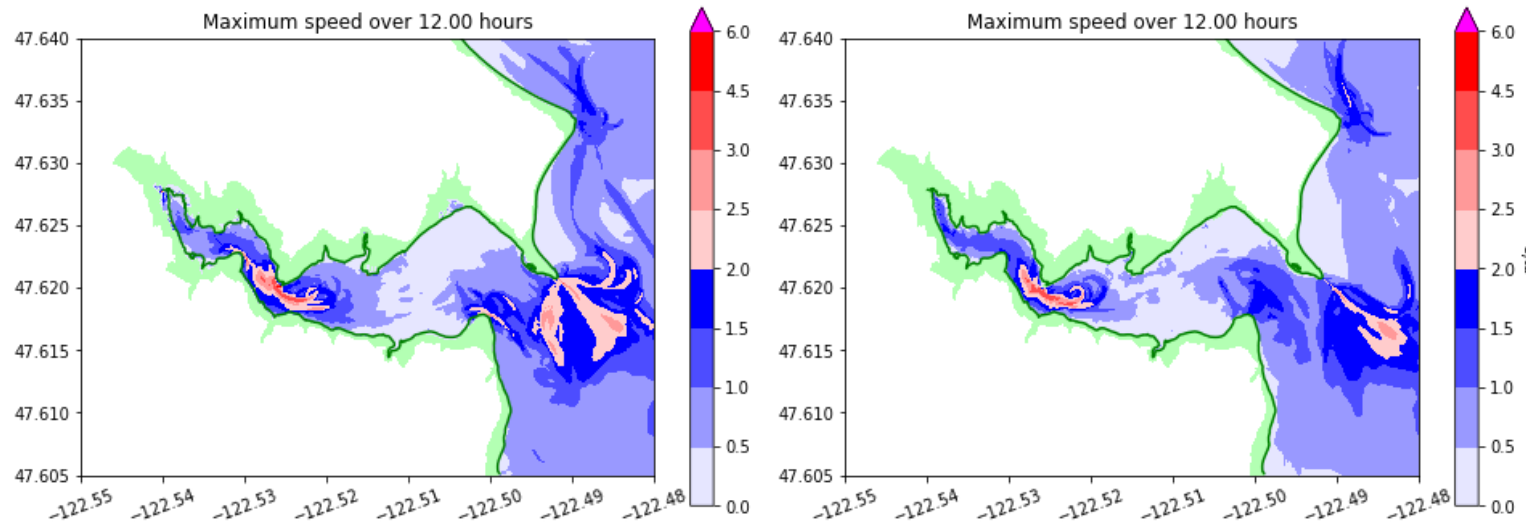


Figure 10: Cascadia subduction zone scenario, maximum speeds attained over 12 hours for MHW simulation (left), and MLW simulation (right). Green coloring represents non-inundated dry land within the selected fgmax region. Model resolution: 1/9<sup>th</sup> arc-second.

### 6.3 Minimum water depths

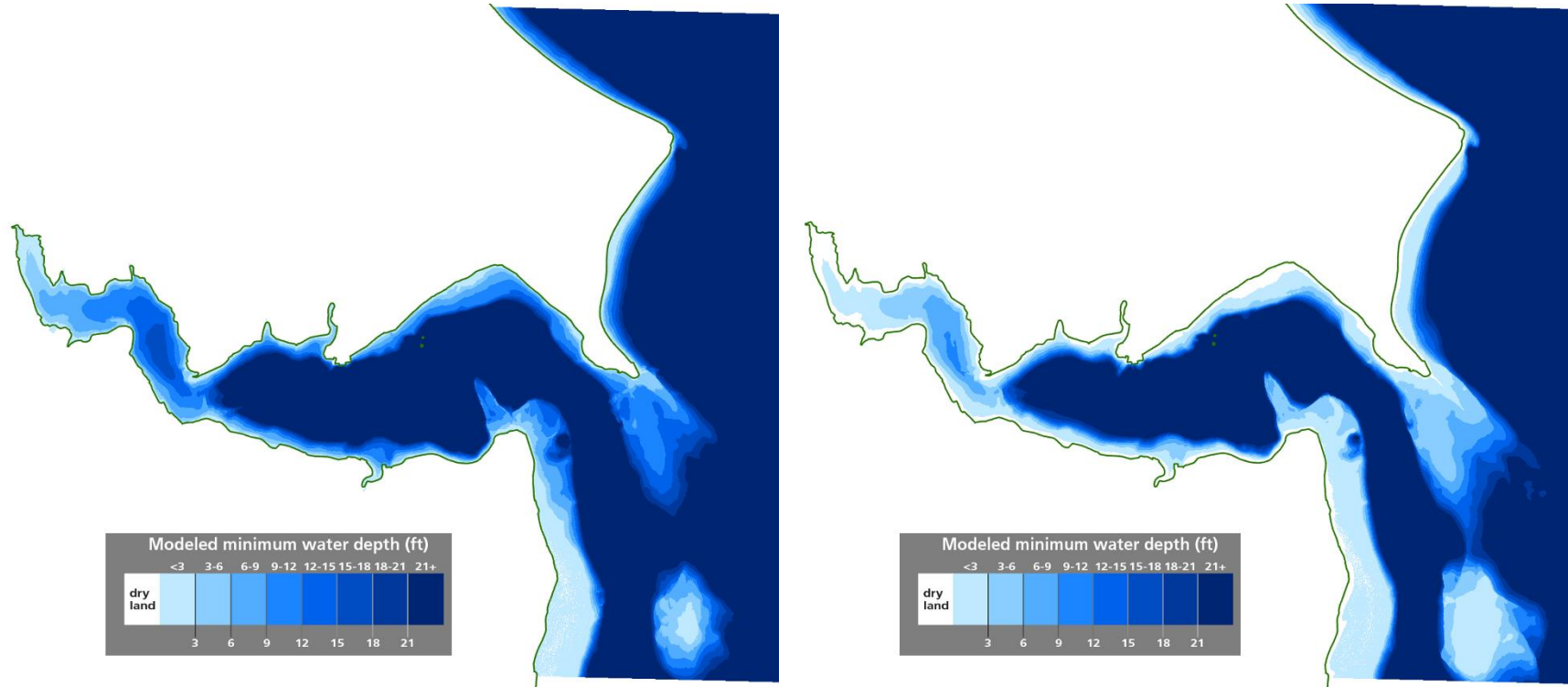


Figure 11: Seattle fault (large) scenario, minimum water depths attained over 3 hours for MHW simulation (left), and MLW simulation (right). Lightest blue represents water depths of three feet or less. Darkest blue represents water depths greater than 21 feet. Model resolution: 1/9<sup>th</sup> arc-second.

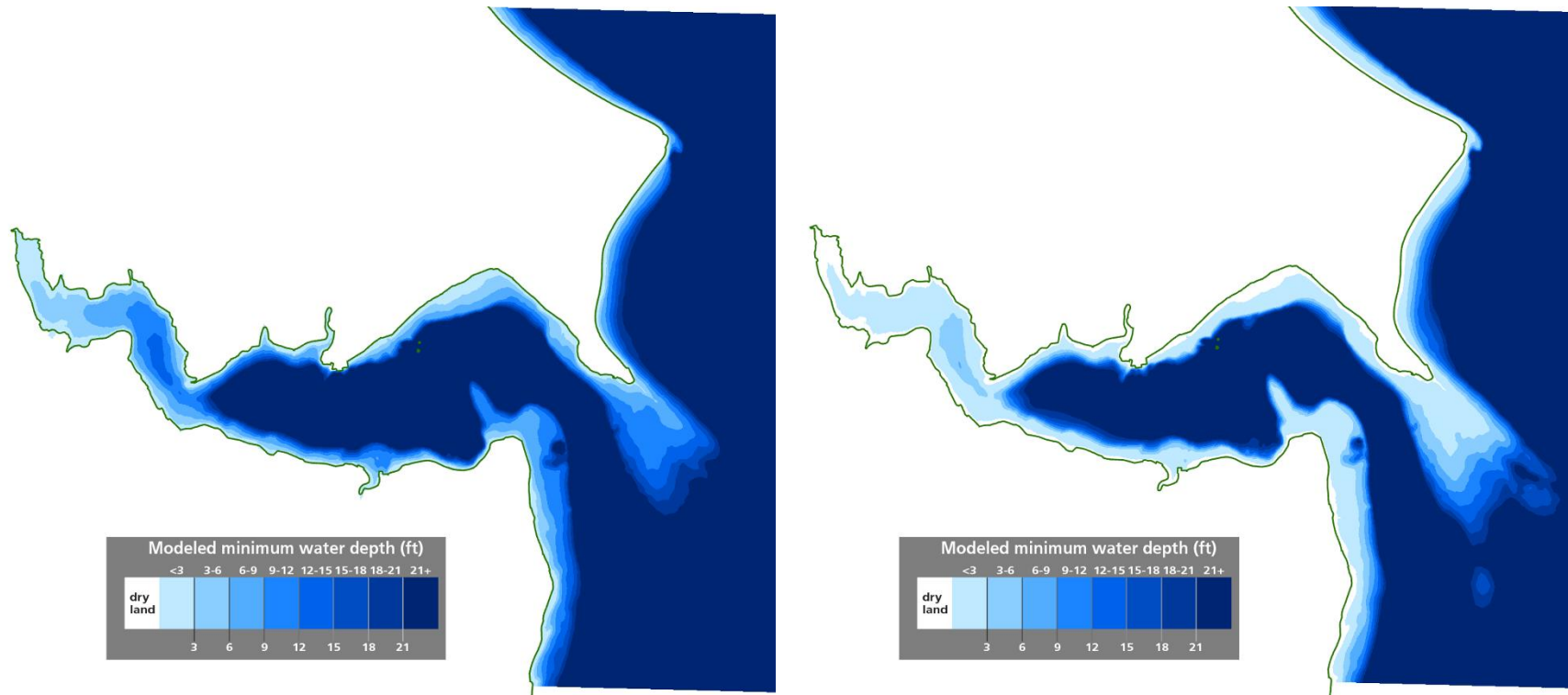


Figure 12: Cascadia subduction zone scenario, minimum water depths attained over 12 hours for MHW simulation (left), and MLW simulation (right). Lightest blue represents water depths of three feet or less. Darkest blue represents water depths greater than 21 feet. Model resolution: 1/9<sup>th</sup> arc-second.

## 7. Gauge output results

### 7.1 Synthetic tide gauge locations

Figure 13 shows the locations of the 35 simulated synthetic tide gauges used to capture time series of the flow depth/surface elevation, and current velocity at specified locations for each simulation. All 35 gauges are used in both the CSZ and SF scenario job runs and modeled at the highest resolution (1/9 arc-second). Figure 14 captures a zoomed view of the gauges in the center of Eagle Harbor near the Ferry Terminal, Bainbridge Island City Dock (and marinas west), and Eagle Harbor Marina on the southern shoreline. All gauges are located offshore, being placed in water. Table 4 summarizes the geographic location for each gauge.

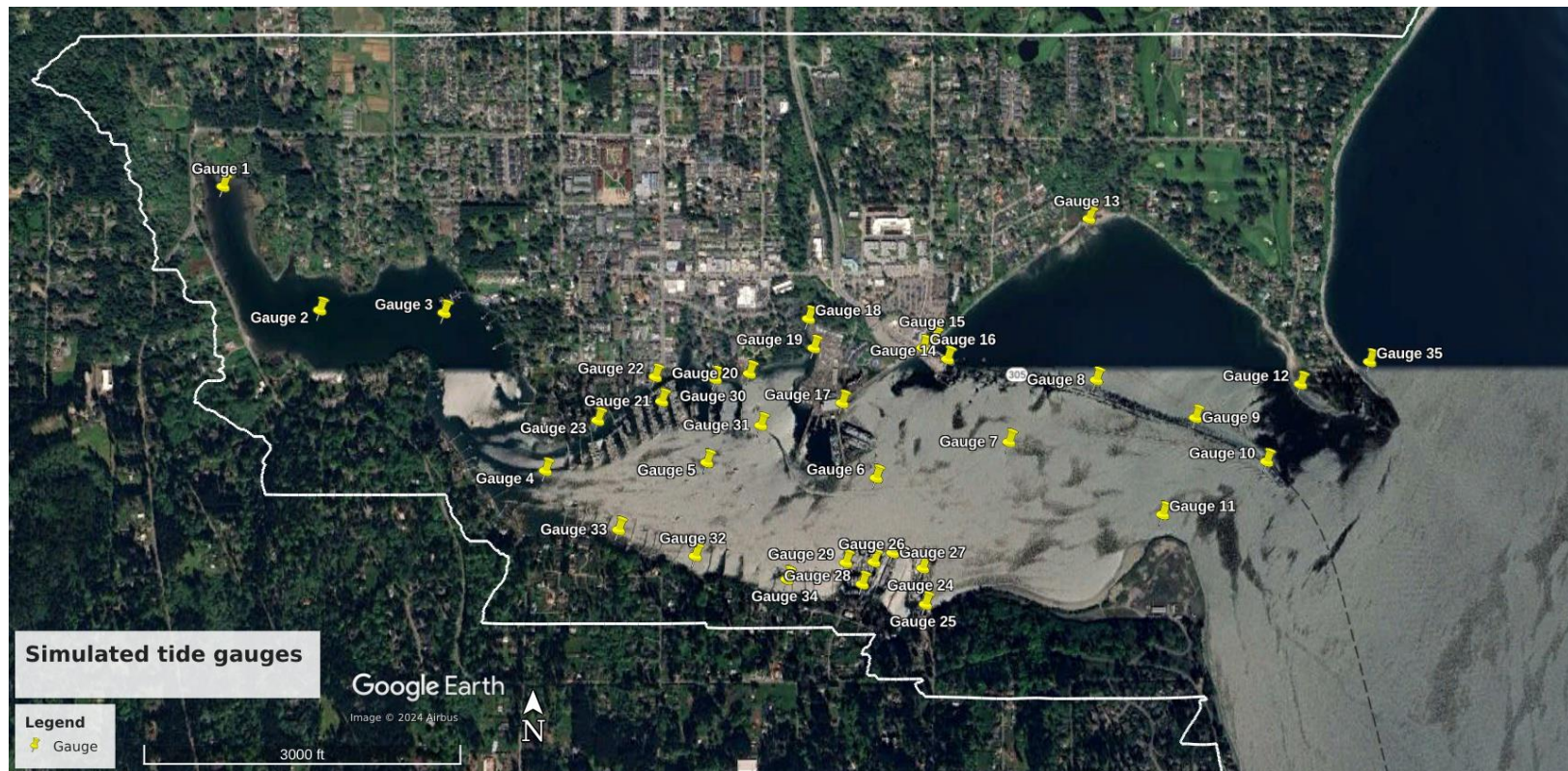


Figure 13. All 35 synthetic tide gauge locations in this study.



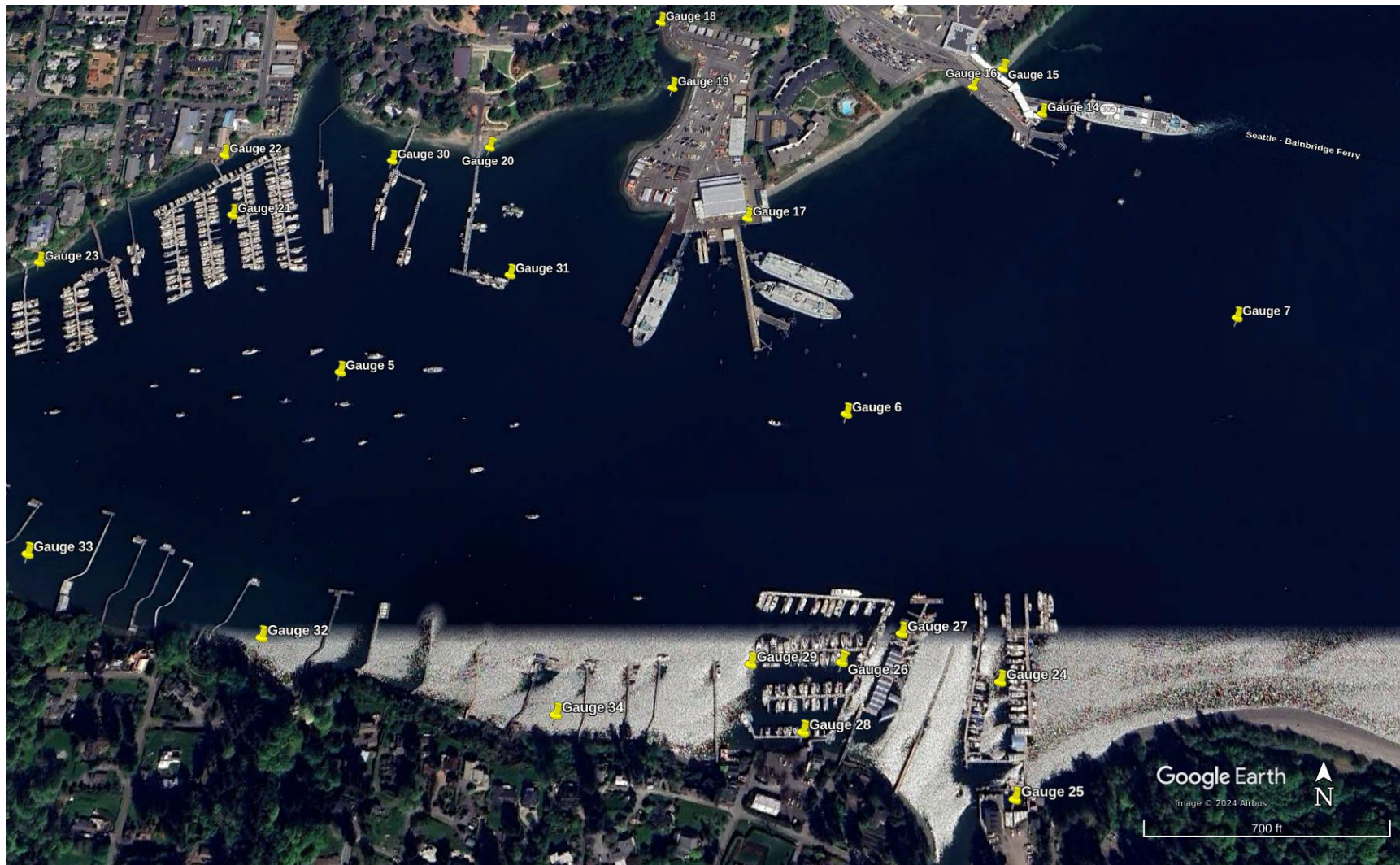


Figure 14. Zoomed view of the tide gauges placed in Eagle Harbor.

Table 4. Locations of all modeled synthetic tide gauges in this study. These gauges are also shown in map view in Figures 13 and 14. Each gauge records the results for both the Cascadia subduction zone and Seattle fault scenarios at either mean high water (MHW) or mean low water (MLW).

| Number | Latitude   | Longitude    | Description                          |
|--------|------------|--------------|--------------------------------------|
| 1      | 47.6269394 | -122.5386636 | Northeast Eagle Harbor               |
| 2      | 47.6236179 | -122.5347751 | center channel 1                     |
| 3      | 47.6235448 | -122.5298304 | center channel 2                     |
| 4      | 47.6193188 | -122.5257788 | center channel 3                     |
| 5      | 47.6195408 | -122.5193796 | center channel 4                     |
| 6      | 47.6191303 | -122.5126762 | center channel 5                     |
| 7      | 47.6200883 | -122.5074046 | center channel 6                     |
| 8      | 47.6217451 | -122.5039281 | center channel 7                     |
| 9      | 47.6207328 | -122.500005  | center channel 8 (DEM tile boundary) |
| 10     | 47.6195639 | -122.4971937 | channel entrance                     |
| 11     | 47.6181532 | -122.5013354 | offshore Pritchard Park              |
| 12     | 47.6216316 | -122.4958303 | West of Wing Point Rd NE             |
| 13     | 47.6260679 | -122.5041835 | South of Hawley Cove Park            |
| 14     | 47.6223055 | -122.5098302 | Bainbridge Island Ferry Terminal 1   |
| 15     | 47.6228278 | -122.5103546 | Bainbridge Island Ferry Terminal 2   |
| 16     | 47.6226046 | -122.5108047 | Bainbridge Island Ferry Terminal 3   |
| 17     | 47.6211288 | -122.5140212 | Offshore WSF Maintenance Facility    |
| 18     | 47.6233859 | -122.5153542 | Offshore Waterfront Trail bridge     |
| 19     | 47.6226021 | -122.5151386 | West of WSF parking lot              |
| 20     | 47.6219176 | -122.5176936 | Exotic Aquatic Kayaks Dock           |
| 21     | 47.6211716 | -122.5211719 | Winslow Wharf Marina center          |
| 22     | 47.62183   | -122.5214312 | Winslow Wharf Marina nearshore       |
| 23     | 47.6206623 | -122.5237021 | Offshore Williamson Landing Marina   |
| 24     | 47.6167265 | -122.5108386 | Bainbridge Island Marina center      |
| 25     | 47.6157705 | -122.5107418 | Bainbridge Island Marina nearshore   |
| 26     | 47.6168901 | -122.5127642 | Eagle Harbor Marina center           |
| 27     | 47.6171336 | -122.5120236 | North of eagle harbor houseboats     |
| 28     | 47.6163068 | -122.5132347 | Eagle Harbor Marina nearshore        |
| 29     | 47.6168746 | -122.5138773 | West of Eagle Harbor                 |
| 30     | 47.6217714 | -122.5190526 | Police boat location                 |
| 31     | 47.6205316 | -122.5172453 | Bainbridge Island City Dock          |
| 32     | 47.6170583 | -122.5198249 | private dock center                  |
| 33     | 47.61776   | -122.5228421 | private dock west                    |
| 34     | 47.6164393 | -122.516201  | private dock east                    |
| 35     | 47.6222302 | -122.4930758 | East of Wing Point                   |

## 7.2 Synthetic gauge plots

The individual gauge plots show time series outputs of the flow depth ( $h$ ), fluctuations in the water heights ( $\Delta h$ ; incorporating local subsidence impacts), surface elevation ( $\eta$ ; the variation in the waveform amplitude relative to the pre-earthquake water surface elevation [0; regional MHW]), and speed for both the CSZ and SF scenarios at MHW and MLW from each individual simulated tide gauge (Appendix B [summary tables]; Appendix C). All gauges were simulated at the highest level of refinement (or resolution; 1/9 arc-second; level 8 for CSZ runs; level 7 for SF runs). The “TopoBathy” subplots beneath the surface elevation plots indicate the elevation of each tide gauge relative to the modeled tidal datum (including any coseismic land level changes). Negative “TopoBathy” numbers record the offshore water depth at the location of which the simulated tide gauge is placed. The speed is shown as a time series of speed vs time ( $\sqrt{u^2 + v^2}$ ), in addition to the individual E—W ( $u$ ) and N—S ( $v$ ) velocity components. The  $u$ — $v$  plane located in the lower right plot for each event also allows one to see how the E—W component,  $u$ , of the speed compares to the N—S component,  $v$ , which can help discern the dominant direction of the tsunami current if one exists. On the other hand, the speed vs time plots simply show one-dimensional current speeds over the course of the simulation. Note that the vertical and horizontal axes on the gauge plots vary by location, parameter, and duration. The vertical scale is set by the maximum values in each plot to better show each individual result.



## Acknowledgments

I thank the City of Bainbridge Island and Bainbridge Island Police Department for their local expertise in identifying areas for synthetic tide gauge locations and advising the modeling scope of this study. I acknowledge the work of NOAA's National Centers of Environmental Information for providing all 1/9 arc-second DEM tiles covering central Puget Sound necessary to complete the high-resolution modeling for this maritime-specific project. I also acknowledge the NOAA Center for Tsunami Research (NCTR) at the Pacific Marine Environmental Laboratory in Seattle for providing the earthquake deformation files for the Cascadia subduction zone Extended L1 and Seattle fault large (SF-L) earthquake fault models. This work is supported by the Washington Geological Survey. The Tsunami Maritime Response and Mitigation Strategy study is funded by NOAA Award #NA23NWS4670022. This does not constitute an endorsement by NOAA.

## Data availability

The computer code and input data used in this study has been archived and is available on request from the Washington Geological Survey. The DEMs used in this study are available from the National Centers for Environmental Information (NCEI) at [www.ncei.noaa.gov](http://www.ncei.noaa.gov). NCEI provides these referenced to the MHW and NAVD88 vertical datums. NAVD88 can be converted to MHW with NOAA's VDatum tool: <https://vdatum.noaa.gov/vdatumweb/>.

## References

- Adams, L.M.; González, F. I.; LeVeque, R.J., 2019, Tsunami Hazard Assessment of Whatcom County, Washington Project Report – Version 2, [webpage]: University of Washington. [accessed Jan. 22, 2024, at [http://depts.washington.edu/ptha/WA\\_EMD\\_Whatcom/](http://depts.washington.edu/ptha/WA_EMD_Whatcom/)]
- Atwater, B. F.; Hemphill-Haley, Eileen, 1997, Recurrence intervals for great earthquakes of the past 3,500 years at northeastern Willapa Bay, Washington: U.S. Geological Survey Professional Paper 1576, 108 p. [<https://doi.org/10.3133/pp1576>]
- Atwater, B. F.; Satoko, Musumi-Rokkaku; Kenji, Satake; Yoshinobu, Tsuji; Kazue, Ueda; Yamaguchi, D. K., 2005, The orphan tsunami of 1700—Japanese clues to a parent earthquake in North America: U.S. Geological Survey in association with University of Washington Press, U.S. Geological Survey Professional Paper 1707, 135 p. [<https://doi.org/10.3133/pp1707>]
- Atwater, B. F.; Tuttle, M. P.; Schweig, E. S.; Rubin, C. M.; Yamaguchi, D. K.; Hemphill-Haley, Eileen, 2004, Earthquake recurrence inferred from paleoseismology. IN Gillespie, A. R.; Porter, S. C.; Atwater, B. F., editors, The Quaternary period in the United States: Developments in Quaternary Science, v. 1, p. 331-350.
- Atwater, B. F.; Moore, A. L., 1992, A tsunami about 1000 years ago in Puget Sound, Washington: Science, v. 258, no. 5088, p. 1614–1617. [<https://doi.org/10.1126/science.258.5088.1614>]
- Black, B. A.; Pearl, J. K.; Pearson, C. L.; Pringle, P. T.; Frank, D. C.; Page, M. T.; Buckley, B.M.,; Cook, E.R.; Harley, G.L.; King, K.J., Hughes, J.F.; Reynolds, D.J.; Sherrod, B. L., 2023, A multifault earthquake threat for the Seattle metropolitan region revealed by mass tree mortality: Science advances, v. 9 no. 39, p. eadh4973.
- Berger, M. J.; George, D. L.; LeVeque, R. J.; Mandli, K. T., 2011, The GeoClaw software for depth-averaged flows with adaptive refinement: Advances in Water Resources, v. 34, no. 9, p. 1195–1206. [<https://doi.org/10.1016/j.advwatres.2011.02.016>]
- Bucknam, R. C.; Hemphill-Haley, Eileen; Leopold, E. B., 1992, Abrupt uplift within the past 1700 years at southern Puget Sound, Washington: Science, v. 258, no. 5088, p. 1611–1614. [<https://doi.org/10.1126/science.258.5088.1611>]
- Burgette, R. J.; Weldon, R. J.; Schmidt, D. A., 2009, Interseismic uplift rates for western Oregon and along-strike variation in locking on the Cascadia subduction zone: Journal of Geophysical Research Solid Earth, v. 114, no. B1, 24 p. [<https://doi.org/10.1029/2008JB005679>]
- Cooperative Institute for Research in Environmental Sciences (CIRES) at the University of Colorado, Boulder, 2020, Continuously Updated Digital Elevation Model (CUDEM)—1/9 Arc-second resolution bathymetric-topographic tiles for central Puget Sound (ncei19\_n47x50\_w122x25\_mhw.nc, ncei19\_n47x50\_w122x50\_mhw.nc, ncei19\_n47x50\_w122x75\_mhw.nc, ncei19\_n47x50\_w123x00\_mhw.nc, ncei19\_n47x50\_w123x25\_mhw.nc, ncei19\_n47x75\_w122x25\_mhw.nc, ncei19\_n47x75\_w122x50\_mhw.nc, ncei19\_n47x75\_w122x75\_mhw.nc, ncei19\_n47x75\_w123x00\_mhw.nc, ncei19\_n47x75\_w123x25\_mhw.nc,

ncei19\_n48x00\_w122x25\_mhw.nc, ncei19\_n48x00\_w122x50\_mhw.nc, ncei19\_n48x00\_w122x75\_mhw.nc, ncei19\_n48x00\_w123x00\_mhw.nc), Washington: NOAA National Centers for Environmental Information. [<https://doi.org/10.25921/ds9v-ky35>]

Clawpack Development Team, Clawpack software, 2024, Version 5.10.0, <http://www.clawpack.org>, DOI 10.17605/osf.io/kmw6h

Dolcimascolo, Alexander; Eungard, D. W.; Allen, Corina; LeVeque, R. J.; Adams, L. M.; Arcas, Diego; Titov, V. V.; González, F. I.; Moore, Christopher, 2022, Tsunami inundation, current speeds, and arrival times simulated from a large Seattle Fault earthquake scenario for Puget Sound and other parts of the Salish Sea: Washington Geological Survey Map Series 2022-03, 16 sheets, scale 1:48,000, 51 p. text. [[https://fortress.wa.gov/dnr/geologydata/tsunami\\_hazard\\_maps/ger\\_ms2022-03\\_tsunami\\_hazard\\_seattle\\_fault.zip](https://fortress.wa.gov/dnr/geologydata/tsunami_hazard_maps/ger_ms2022-03_tsunami_hazard_seattle_fault.zip)]

Dolcimascolo, Alexander; Eungard, D. W.; Allen, Corina; LeVeque, R. J.; Adams, L. M.; Arcas, Diego; Titov, V. V.; González, F. I.; Moore, Christopher; Garrison-Laney, C. E.; Walsh, T. J., 2021, Tsunami hazard maps of the Puget Sound and adjacent waters—Model results from an extended L1 Mw 9.0 Cascadia subduction zone megathrust earthquake scenario: Washington Geological Survey Map Series 2021-01, 16 sheets, scale 1:48,000, 49 p. text. [[https://fortress.wa.gov/dnr/geologydata/tsunami\\_hazard\\_maps/ger\\_ms2021-01\\_tsunami\\_hazard\\_puget\\_sound.zip](https://fortress.wa.gov/dnr/geologydata/tsunami_hazard_maps/ger_ms2021-01_tsunami_hazard_puget_sound.zip)]

Gica, Edison; Arcas, Diego, 2015, Tsunami inundation modeling of Seattle and Tacoma due to a Cascadia subduction zone earthquake: National Oceanic and Atmospheric Administration Center for Tsunami Research unpublished report, 44 p.

Goldfinger, Chris; Galer, Steve; Beeson, Jeffrey; Hamilton, Tark; Black, Bran; Romsos, Chris; Patton, Jason; Nelson, C. H.; Hausmann, Rachel; Morey, Ann, 2017, The importance of site selection, sediment supply, and hydrodynamics: A case study of submarine paleoseismology on the northern Cascadia margin, Washington, USA: *Marine Geology*, v. 384, no. 17, p. 25–46. [<https://doi.org/10.1016/j.margeo.2016.06.008>]

Goldfinger, Chris; Nelson, C. H.; Morey, A. E.; Johnson, J. E.; Patton, J. R.; Karabanov, E. B.; Gutierrez-Pastor, Julia; Eriksson, A. T.; Gracia, Eulalia; Dunhill, Gita; Enkin, R. J.; Dallimore, Audrey; Vallier, Tracy, 2012, Turbidite event history—Methods and implications for Holocene paleoseismicity of the Cascadia Subduction Zone: U.S. Geological Survey Professional Paper 1661-F, 170 p. [<https://doi.org/10.3133/pp1661F>]

González, F. I.; LeVeque, R. J.; Chamberlain, Paul; Hirai, Bryant; Varkovitsky, Jonathan; George, D. L., 2011, Validation of the GeoClaw model—NTHMP MMS tsunami inundation model validation workshop: University of Washington, 84 p. [<https://depts.washington.edu/clawpack/links/nthmp-benchmarks/geoclaw-results.pdf>] NTHMP Model Benchmarking Workshop, <http://depts.washington.edu/clawpack/links/nthmp-benchmarks/geoclaw-results.pdf>.

International Code Council, 2015, 2015 International Building Code, 690 p. [<https://codes.iccsafe.org/content/IBC2015>]

- Jacoby, G. C.; Bunker, D. E.; Benson, B. E., 1997, Tree-ring evidence for an A.D. 1700 Cascadia earthquake in Washington and northern Oregon: *Geology*, v. 25, no. 11, p. 999–1002. [[https://doi.org/10.1130/0091-7613\(1997\)025<0999:TREFAA>2.3.CO;2](https://doi.org/10.1130/0091-7613(1997)025<0999:TREFAA>2.3.CO;2)]
- Kelsey and others, 2008
- LeVeque, R. J.; Adams, L. M.; González, F. I., 2019, Tsunami Hazard Assessment of Portions of Island and Skagit Counties, Washington [webpage]: University of Washington. [accessed Jan. 22, 2024, at [http://depts.washington.edu/ptha/IslandSkagitTHA\\_2019/](http://depts.washington.edu/ptha/IslandSkagitTHA_2019/)]
- LeVeque, R., González, F., and Adams, L., 2018, Tsunami Hazard Assessment of Snohomish County, Washington, Project Report – Version 2, [http://faculty.washington.edu/rjl/pubs/THA\\_Snohomish/index.html](http://faculty.washington.edu/rjl/pubs/THA_Snohomish/index.html).
- LeVeque, R. J.; George, D. L.; Berger, M. J., 2011, Tsunami modelling with adaptively refined finite volume methods: *Acta Numerica*, v. 20, p. 211–289. [<https://doi.org/10.1017/S0962492911000043>]
- Martin, M. E., 2011, Coastal marsh stratigraphy as an indicator of past earthquakes, Puget Lowland, Washington State: University of Washington Doctor of Philosophy thesis, 186 p.
- (NOAA) National Centers for Environmental Information. 2022, ETOPO 2022 15 Arc-Second Global Relief Model: NOAA National Centers for Environmental Information. <https://doi.org/10.25921/fd45-gt74> . Accessed [May 28, 2024 at [https://www.ngdc.noaa.gov/thredds/catalog/global/ETOPO2022/30s/30s\\_surface\\_elev\\_netcdf/catalog.html?dataset=globalDatasetScan/ETOPO2022/30s/30s\\_surface\\_elev\\_netcdf/ETOPO\\_2022\\_v1\\_30s\\_N90W180\\_surface.nc](https://www.ngdc.noaa.gov/thredds/catalog/global/ETOPO2022/30s/30s_surface_elev_netcdf/catalog.html?dataset=globalDatasetScan/ETOPO2022/30s/30s_surface_elev_netcdf/ETOPO_2022_v1_30s_N90W180_surface.nc)].
- (NOAA) National Geophysical Data Center (NGDC), 2015, Strait of Juan de Fuca, Washington 1/3 Arc-second NAVD88 Coastal Digital Elevation Model: NOAA National Centers for Environmental Information. [accessed May 28, 2024 at <https://www.ncei.noaa.gov/metadata/geoportal/rest/metadata/item/gov.noaa.ngdc.mgg.dem:11514/html>].
- NOAA National Geophysical Data Center, 2014, Puget Sound, Washington 1/3 Arc-second MHW Coastal Digital Elevation Model: NOAA National Centers for Environmental Information. [accessed May 28, 2024 at <https://www.ncei.noaa.gov/metadata/geoportal/rest/metadata/item/gov.noaa.ngdc.mgg.dem:5165/html>].
- NOAA National Geophysical Data Center, 2011, Port Townsend, Washington 1/3 Arc-second MHW Coastal Digital Elevation Model: NOAA National Centers for Environmental Information. [accessed May 28, 2024 at <https://www.ncei.noaa.gov/metadata/geoportal/rest/metadata/item/gov.noaa.ngdc.mgg.dem:1786/html>]
- National Oceanic and Atmospheric Administration, 2011, Datums for 9447130, Seattle, WA [webpage]: National Oceanic and Atmospheric Administration. [accessed Jun. 11, 2024, at <https://tidesandcurrents.noaa.gov/datums.html?id=9447130>]

- Nelson, A. R.; Personius, S. F.; Sherrod, B. L.; Kelsey, H. M.; Johnson, S. Y.; Bradley, L. A.; Wells, R. E., 2014, Diverse rupture modes for surface-deforming upper plate earthquakes in the southern Puget Lowland of Washington State: *Geosphere*, v. 10, no. 4, p. 769–796. [https://doi.org/10.1130/GES00967.1]
- Petersen, M. D.; Cramer, C. H.; Frankel, A. D., 2002, Simulations of seismic hazard for the Pacific Northwest of the United States from earthquakes associated with the Cascadia subduction zone: *Pure and Applied Geophysics*, v. 159, no. 9, p. 2147–2168.
- Pratt, T. L.; Troost, K. G.; Odum, J. K.; Stephenson, W. J., 2015, Kinematics of shallow backthrusts in the Seattle Fault zone, Washington State: *Geosphere*, v. 11, no. 6, p. 1948–1974. [https://doi.org/10.1130/GES01179.1]
- Satake, Kenji; Wang, Kelin; Atwater, B. F., 2003, Fault slip and seismic moment of the 1700 Cascadia earthquake inferred from Japanese tsunami descriptions: *Journal of Geophysical Research*, v. 108, no. B11, 17 p. [https://doi.org/10.1029/2003JB002521]
- Sherrod, B. L., 2001, Evidence for earthquake-induced subsidence about 1100 yr ago in coastal marshes of southern Puget Sound, Washington: *GSA Bulletin*, v. 113, no. 10, p. 1299–1311. [https://doi.org/10.1130/0016-7606(2001)113<1299:EFEISA>2.0.CO;2]
- ten Brink, U. S.; Song, J.; Bucknam, R. C., 2006, Rupture models for the AD 900–930 Seattle Fault earthquake from uplifted shorelines: *Geology*, v. 34, no. 7, p. 585–588. [https://doi.org/10.1130/G22173.1]
- Titov, V. V.; Arcas, Diego; Moore, C. W.; LeVeque, R. J.; Adams, L. M.; González, F. I., 2018, Tsunami hazard assessment of Bainbridge Island, Washington—Project Report: Washington State Emergency Management Division, 43 p. [http://depts.washington.edu/ptha/WA\_EMD\_Bainbridge/BainbridgeIslandTHA.pdf].
- Titov, V. V.; González, F. I.; Mofjeld, H. O.; Venturato, A. J., 2003, NOAA TIME Seattle tsunami mapping project: Procedures, data sources, and products: NOAA Technical Memorandum OAR PMEL-124. [https://www.pmel.noaa.gov/pubs/PDF/tito2572/tito2572.pdf]
- Venturato, A. J.; Arcas, Diego; Titov, V. V.; Mofjeld, H. O.; Chamberlin, C. C.; González, F. I., 2007, Tacoma, Washington, tsunami hazard mapping project: Modeling tsunami inundation from Tacoma and Seattle fault earthquakes: NOAA Technical Memorandum OAR PMEL-132, 23 p. [https://repository.library.noaa.gov/view/noaa/11070]
- Witter, R. C.; Zhang, Y. J.; Wang, Kelin; Priest, G. R.; Goldfinger, Chris; Stimely, L. L.; English, J. T.; Ferro, P. A., 2011, Simulating tsunami inundation at Bandon, Coos County, Oregon, using hypothetical Cascadia and Alaska earthquake scenarios: Oregon Department of Geology and Mineral Industries Special Paper 43, 57 p. [http://www.oregongeology.org/pubs/sp/p-SP-43.htm]
- Witter, R. C.; Zhang, Y. J.; Wang, Kelin; Priest, G. R.; Goldfinger, Chris; Stimely, Laura; English, J. T.; Ferro, P. A., 2013, Simulated tsunami inundation for a range of Cascadia megathrust earthquake scenarios at Bandon, Oregon, USA: *Geosphere*, v. 9, no. 6, p. 1783–1803. [https://doi.org/10.1130/GES00899.1]

Yamaguchi, D. K.; Atwater, B. F.; Bunker, D. E.; Benson, B. E.; Reid, M. S., 1997, Tree-ring dating the 1700 Cascadia earthquake: *Nature*, v. 389, p. 922–923. [<https://doi.org/10.1038/40048>]

Yousefi, Maryam; Milne, Glenn; Li, Shaoyang; Wang, Kelin; Bartholet, Alan, 2020, Constraining interseismic deformation of the Cascadia subduction zone: new insights from estimates of vertical land motion over different timescales: *Journal of Geophysical Research: Solid Earth*, v. 125, no. 3, article e2019JB018248. [<https://doi.org/10.1029/2019JB018248>]

## Appendix A. GeoClaw output and version information

Output was delivered as netCDF for each source (Cascadia subduction zone and Seattle fault), at high tide (MHW) and low tide (MLW).

The netCDF files contain multiple field variables. A pre-processing script generates a few variables before the initiation of the GeoClaw run based on the fgmax region as part of the input. Following the GeoClaw run, the fgmax output generates other variables. Note that all variables are stored on two-dimensional uniform grids as defined by the lon and lat arrays. Only the points on this grid where fgmax point == 1 are used as fgmax points and only at these points is fgmax output available.

Values created as part of the GeoClaw input:

- lon: longitude, x (degrees),
- lat: latitude, y (degrees),
- Z: topography value Z from the DEM, relative to MHW (m),
- fgmax point: 1 if this point is used as an fgmax point, 0 otherwise,
- force\_dry\_init: 1 if this point is initialized as usual, 0 if this point is forced to be dry, regardless of initial topography value.

Values created based on the GeoClaw output:

- dz: Co-seismic surface deformation interpolated to each point (m),
- B: post-seismic topography value B from GeoClaw at gauge location (m),
- h: maximum depth of water over simulation (m),
- s: maximum speed over simulation (m/s),
- hss: maximum momentum  $hs^2$  over simulation ( $m^3/s^2$ ),
- hmin: minimum depth of water over simulation (m),
- arrival\_time\*: apparent arrival time (rising wave  $> 0.05$  m) of tsunami (s),
- tfirstPOS: time of first positive wave arrival ( $h-h_0 > 0.1016$  m) of tsunami (s)
- tfirstNEG: time of first negative wave arrival ( $h-h_0 < 0.1016$  m) of tsunami (s)
- tfirstAdvis: time of first “advisory-level” wave arrival ( $h-h_0 > 0.3048$  m) of tsunami (s)
- tfirstDRAW: time of first significant falling wave arrival ( $h-h_0 > 0.3048$  m) of tsunami (s)
- tfirstWarn: time of first “warning-level” wave arrival ( $h-h_0 > 0.9144$  m) of tsunami (s)

\* Because the arrival\_time variable is defined by changes in B in the initial modeling code, it is only valid where  $dz = 0$  (CSZ-based runs only) as any local uplift or subsidence would automatically trigger an “arrival time.”

In addition, the netCDF files contain the following metadata values:

- tfinal: final time of GeoClaw simulation (seconds),
- history: record of times data was added to file,
- outdir: location of output directory where data was found,
- run\_finished: date and time run finished,

The fgmax points align exactly with the 1/9" DEM points. The finest level computational finite volume grid also aligns so that cell centers are exactly at the fgmax points, and Z in the netCDF file is the value from the DEM at this point. However, by integrating a piecewise bilinear function that interpolates the 1/9" DEM obtains the topography value B used in a grid cell in GeoClaw, which is not exactly equal to Z initially. Moreover, B is the value after any co-seismic deformation associated with the event.

## A.1 GeoClaw Version 5.10.0

The modeling for this project used GeoClaw Version 5.10.0. GeoClaw is open source, part of the Clawpack software, and available at <http://www.clawpack.org>. Refer to the official [version 5.10.0 release notes](#) to view changes and modifications from previous GeoClaw versions.



## Appendix B. Gauge report summaries

The following subheadings of this appendix include summary tables for all simulated tide gauges from each modeled earthquake source (Cascadia subduction zone and Seattle fault [CSZ and SF, respectively]) and tidal level (Mean High Water [MHW] and Mean Low Water [MLW]). The variables within each table are defined as:

- B0: pre-seismic bathymetry/topography elevation (m)
- B: post-seismic bathymetry/topography elevation (m)
- dzi: co-seismic surface deformation (m)
- max h: maximum depth of water over simulation (m)
- min h: minimum depth of water over simulation (m)
- max zeta: maximum surface elevation (eta) offshore above MHW; or maximum depth (h) onshore (m)
- max  $\Delta h^*$ : maximum change in water depth/height ( $h_0-h$ ; [ $\max \text{zeta}-\text{dzi}$ ]) over simulation (m)
- max eta post-earthquake: post-seismic maximum surface elevation ( $B + h$ ) above MHW (m) over simulation (m)
- max s: maximum speed over simulation (m/s)
- max  $h_s$ : maximum momentum over simulation ( $m^2/s$ )
- max  $h_h$ : maximum momentum flux  $h_s^2$  over simulation ( $m^3/s^2$ )
- tmax: time of maximum zeta over simulation (minutes)
- tmin: time of minimum zeta over simulation (minutes)
- tfirstPOS: time of first rising wave arrival ( $\text{zeta} > 0.1016$  m) over simulation (minutes)
- tfirstNEG: time of first falling wave arrival ( $\text{zeta} < 0.1016$  m) over simulation (minutes)
- tfirstDRAW\*\*: time of first significant fall wave arrival ( $h_0-h > 0.3048$  m) over simulation (minutes)
- tfirstADVIS: time of first “advisory-level” wave arrival ( $h-h_0 > 0.3048$  m) over simulation (minutes). This threshold matches the Advisory Alert-level defined by the National Tsunami Hazard Mitigation Program (NTHMP)
- tfirstWARN: time of first “warning-level” wave arrival ( $h-h_0 > 0.9144$  m) over simulation (minutes). This threshold matches the Warning Alert-level defined by the NTHMP

\* Note: max  $\Delta h$  only varies from max zeta and max eta post-quake for SF runs. This is because of local subsidence impacting this variable, which is negligible for the CSZ scenario in Eagle Harbor. Coseismic subsidence generated by the SF-L scenario causes the land/seafloor and water surface levels to drop simultaneously within this study area. Following this drop, the water surface level would rebound back to the pre-earthquake conditions over the course of the simulated tsunami, but the land/seafloor would not. The rate at which the water surface level recovers is not captured in the tsunami simulation. Thus, determining offshore wave amplitude is challenging where land level changes exist because amplitude refers to the height above water surface level. This becomes a dynamic and uncertain variable where there are coseismic elevation changes. Rather, because flow depth (h) does not change during coseismic impacts, I instead report the change in water depth (max  $\Delta h$ ) over the simulation to capture the maximum impact of the tsunami water height. This value represents both the tsunami wave amplitude and the amount of sea-level recovery following the earthquake in the zone of coseismic impact. This value may not always represent the largest wave amplitude, which is generally the first wave in this study area. When no coseismic impacts occur, max  $\Delta h$  is the same as max zeta and/or max h (if the gauge is onshore).

\*\*Note: tfirstDRAW timings reported as n/a suggest that either 1) the gauge was placed onshore, or 2) the post-earthquake water depth never falls a foot or more ( $-0.3048$  m) below the water depth ( $h_0$ ) at the time of the earthquake. Zero onshore synthetic tide gauges were included within this tsunami hazard assessment (although some gauges initialized as dry when simulated using the MLW datum).

Scenario: Cascadia subduction zone, MHW

| Gauge | B0     | B      | dzi | max h | min h | max zeta | max Δh | max eta post-quake | max s | max hs | max hss | tmax   | tmin   | tfirstPOS | tfirstNEG | tfirstDRAW | tfirstADVIS | tfirstWARN |
|-------|--------|--------|-----|-------|-------|----------|--------|--------------------|-------|--------|---------|--------|--------|-----------|-----------|------------|-------------|------------|
| 1     | -1.81  | -1.81  | 0   | 3.91  | 0.27  | 2.1      | 3.65   | 2.1                | 0.59  | 1.04   | 0.35    | 292.44 | 372.14 | 143.2     | 0.2       | 93.9       | 144.5       | 147.5      |
| 2     | -3.14  | -3.14  | 0   | 5.11  | 1.75  | 1.97     | 3.36   | 1.97               | 0.87  | 3.27   | 2.83    | 293.27 | 369.5  | 143       | 55.9      | 93.7       | 144.5       | 147.6      |
| 3     | -4.52  | -4.52  | 0   | 6.38  | 3.19  | 1.86     | 3.2    | 1.86               | 1.18  | 6.32   | 7.4     | 292.49 | 248.58 | 142.8     | 55.6      | 93.4       | 144.4       | 147.7      |
| 4     | -4.63  | -4.63  | 0   | 6.23  | 3.33  | 1.6      | 2.9    | 1.6                | 2.36  | 11.01  | 25.91   | 292.29 | 241.49 | 142.2     | 54.9      | 93         | 144.1       | 147.8      |
| 5     | -12.13 | -12.13 | 0   | 13.56 | 10.81 | 1.44     | 2.75   | 1.44               | 1.96  | 23.76  | 46.58   | 290.86 | 240.6  | 141.4     | 54.4      | 92.8       | 143.2       | 147.5      |
| 6     | -14.29 | -14.29 | 0   | 15.65 | 13    | 1.35     | 2.65   | 1.35               | 0.44  | 6.61   | 2.88    | 291.33 | 241.34 | 141.2     | 54.2      | 92.7       | 143.2       | 147.6      |
| 7     | -14.82 | -14.82 | 0   | 16.1  | 13.52 | 1.29     | 2.58   | 1.29               | 0.42  | 6.37   | 2.59    | 291.54 | 241.55 | 141.1     | 54        | 92.7       | 143.1       | 147.8      |
| 8     | -17.51 | -17.51 | 0   | 18.75 | 16.22 | 1.24     | 2.53   | 1.24               | 0.47  | 8.7    | 4.13    | 290.2  | 242.69 | 141       | 54        | 92.6       | 143.1       | 148        |
| 9     | -20.63 | -20.63 | 0   | 21.83 | 19.34 | 1.2      | 2.49   | 1.2                | 0.69  | 14.76  | 10.13   | 290.01 | 242.82 | 141       | 53.8      | 92.5       | 143.1       | 148.2      |
| 10    | -21.67 | -21.67 | 0   | 22.8  | 20.39 | 1.14     | 2.42   | 1.14               | 0.97  | 21.71  | 20.96   | 289.73 | 242.78 | 141       | 53.7      | 92.4       | 143.2       | 148.6      |
| 11    | -3.13  | -3.13  | 0   | 4.32  | 1.83  | 1.19     | 2.49   | 1.19               | 1.78  | 7.58   | 13.52   | 292.48 | 242.87 | 142.1     | 53.9      | 92.5       | 144.3       | 148.3      |
| 12    | -1.47  | -1.47  | 0   | 2.64  | 0.19  | 1.17     | 2.46   | 1.17               | 1.14  | 2.82   | 3.22    | 289.89 | 243.08 | 141       | 53.6      | 92.4       | 143.2       | 148.4      |
| 13    | -0.4   | -0.4   | 0   | 1.66  | 0     | 1.26     | 1.66   | 1.26               | 0.22  | 0.26   | 0.05    | 291.17 | 256.73 | 141       | 53.9      | 92.6       | 143         | 147.9      |
| 14    | -6.31  | -6.31  | 0   | 7.6   | 5.01  | 1.29     | 2.59   | 1.29               | 0.41  | 2.91   | 1.18    | 291.17 | 241.73 | 141.1     | 54.1      | 92.7       | 143.1       | 147.8      |
| 15    | -1.61  | -1.61  | 0   | 2.91  | 0.31  | 1.3      | 2.59   | 1.3                | 0.56  | 1.42   | 0.79    | 291.23 | 241.79 | 141.1     | 54.1      | 92.6       | 143.2       | 147.8      |
| 16    | -2.06  | -2.06  | 0   | 3.36  | 0.76  | 1.3      | 2.6    | 1.3                | 0.53  | 1.48   | 0.78    | 291.21 | 241.72 | 141.2     | 54.1      | 92.7       | 143.2       | 147.8      |
| 17    | -1.49  | -1.49  | 0   | 2.86  | 0.4   | 1.36     | 2.46   | 1.36               | 1.08  | 2.82   | 3.04    | 290.7  | 241.29 | 141.3     | 54.2      | 92.7       | 143.3       | 147.7      |
| 18    | -1.33  | -1.33  | 0   | 2.77  | 0.08  | 1.45     | 2.69   | 1.45               | 0.62  | 1.12   | 0.65    | 291.32 | 240.85 | 141.3     | 54.2      | 92.9       | 143.2       | 147.5      |
| 19    | -2.25  | -2.25  | 0   | 3.68  | 0.95  | 1.43     | 2.74   | 1.43               | 0.31  | 0.88   | 0.27    | 290.78 | 240.58 | 141.3     | 54.2      | 92.9       | 143.2       | 147.5      |
| 20    | -1.69  | -1.69  | 0   | 3.12  | 0.39  | 1.43     | 2.73   | 1.43               | 0.55  | 1.43   | 0.79    | 290.96 | 240.29 | 141.3     | 54.3      | 92.8       | 143.2       | 147.5      |
| 21    | -7.36  | -7.36  | 0   | 8.82  | 6.05  | 1.46     | 2.77   | 1.46               | 0.96  | 6.99   | 6.71    | 290.75 | 240.59 | 141.4     | 54.4      | 92.9       | 143.2       | 147.4      |
| 22    | -2.02  | -2.02  | 0   | 3.49  | 0.71  | 1.47     | 2.77   | 1.47               | 0.43  | 1.14   | 0.41    | 290.72 | 240.57 | 141.4     | 54.4      | 92.9       | 143.2       | 147.4      |
| 23    | -1.8   | -1.8   | 0   | 3.28  | 0.49  | 1.48     | 2.79   | 1.48               | 1.06  | 2.57   | 2.74    | 292.32 | 240.55 | 141.5     | 54.5      | 92.9       | 143.4       | 147.5      |
| 24    | -4.52  | -4.52  | 0   | 5.86  | 3.22  | 1.34     | 2.64   | 1.34               | 0.35  | 1.87   | 0.64    | 291.28 | 241.58 | 141.2     | 54.2      | 92.7       | 143.2       | 147.7      |
| 25    | -2.04  | -2.04  | 0   | 3.38  | 0.74  | 1.34     | 2.64   | 1.34               | 0.11  | 0.33   | 0.04    | 291.32 | 241.95 | 141.2     | 54.1      | 92.7       | 143.1       | 147.6      |
| 26    | -6.89  | -6.89  | 0   | 8.25  | 5.59  | 1.36     | 2.66   | 1.36               | 0.41  | 2.73   | 1.12    | 291.16 | 240.94 | 141.2     | 54.2      | 92.8       | 143.2       | 147.6      |
| 27    | -6.39  | -6.39  | 0   | 7.75  | 5.1   | 1.35     | 2.65   | 1.35               | 0.44  | 2.77   | 1.17    | 291.22 | 241.54 | 141.2     | 54.2      | 92.7       | 143.2       | 147.6      |
| 28    | -2.12  | -2.12  | 0   | 3.49  | 0.83  | 1.37     | 2.67   | 1.37               | 0.4   | 1.26   | 0.5     | 291.24 | 240.99 | 141.2     | 54.2      | 92.8       | 143.2       | 147.6      |
| 29    | -5.86  | -5.86  | 0   | 7.24  | 4.57  | 1.37     | 2.67   | 1.37               | 0.52  | 2.98   | 1.54    | 291.07 | 240.68 | 141.2     | 54.2      | 92.8       | 143.2       | 147.6      |
| 30    | -4.93  | -4.93  | 0   | 6.37  | 3.62  | 1.45     | 2.76   | 1.45               | 0.78  | 4.18   | 3.26    | 290.9  | 240.46 | 141.3     | 54.3      | 92.8       | 143.2       | 147.4      |
| 31    | -12.4  | -12.4  | 0   | 13.82 | 11.1  | 1.42     | 2.72   | 1.42               | 0.68  | 8.76   | 5.94    | 290.9  | 240.61 | 141.3     | 54.3      | 92.8       | 143.2       | 147.5      |
| 32    | -2.46  | -2.46  | 0   | 3.9   | 1.16  | 1.45     | 2.74   | 1.45               | 0.81  | 2.8    | 2.27    | 290.89 | 240.17 | 141.3     | 54.4      | 92.8       | 143.2       | 147.5      |
| 33    | -2.36  | -2.36  | 0   | 3.86  | 1.06  | 1.5      | 2.8    | 1.5                | 0.68  | 1.89   | 1.01    | 290.78 | 240.51 | 141.4     | 54.5      | 92.9       | 143.3       | 147.4      |
| 34    | -2.5   | -2.5   | 0   | 3.9   | 1.2   | 1.4      | 2.7    | 1.4                | 0.36  | 1.22   | 0.44    | 291.2  | 240.3  | 141.3     | 54.2      | 92.8       | 143.2       | 147.5      |
| 35    | -1.72  | -1.72  | 0   | 2.74  | 0.47  | 1.03     | 2.27   | 1.03               | 0.35  | 0.86   | 0.28    | 151.2  | 241.83 | 138.2     | 52.2      | 91         | 140.5       | 147.2      |

Scenario: Cascadia subduction zone, MLW

| Gauge | B0     | B      | dzi | max h | min h | max zeta | max Δh | max eta post-quake | max s | max hs | max hss | tmax   | tmin   | tfirstPOS | tfirstNEG | tfirstDRAW | tfirstADVIS | tfirstWARN |
|-------|--------|--------|-----|-------|-------|----------|--------|--------------------|-------|--------|---------|--------|--------|-----------|-----------|------------|-------------|------------|
| 1     | -1.8   | -1.8   | 0   | 1.39  | 0     | -0.43    | 1.39   | -0.42              | 1.39  | 0.64   | 0.81    | 158.91 | 0      | 153.6     | n/a       | n/a        | 154.1       | 155.6      |
| 2     | -3.14  | -3.14  | 0   | 2.54  | 0.04  | -0.61    | 2.5    | -0.61              | 1.07  | 1.79   | 1.82    | 297.31 | 141.14 | 147.6     | 58.4      | 95.2       | 148.9       | 152.1      |
| 3     | -4.52  | -4.52  | 0   | 3.75  | 0.79  | -0.77    | 2.95   | -0.77              | 1.15  | 3.72   | 4.28    | 296.11 | 377.01 | 146.4     | 57.7      | 94.7       | 148.1       | 151.6      |
| 4     | -4.63  | -4.63  | 0   | 3.67  | 0.88  | -0.96    | 2.79   | -0.96              | 2.75  | 8.2    | 22.56   | 295.06 | 371.84 | 144.7     | 56.2      | 93.8       | 146.5       | 150.5      |
| 5     | -12.13 | -12.13 | 0   | 11.15 | 8.25  | -0.97    | 2.9    | -0.97              | 1.12  | 9.63   | 10.84   | 292.61 | 369.76 | 143.1     | 55.6      | 93.7       | 144.8       | 148.6      |
| 6     | -14.29 | -14.29 | 0   | 13.27 | 10.44 | -1.02    | 2.84   | -1.02              | 0.54  | 6.16   | 3.35    | 292.86 | 368.7  | 143       | 55.4      | 93.6       | 144.7       | 148.6      |
| 7     | -14.82 | -14.82 | 0   | 13.75 | 10.97 | -1.06    | 2.79   | -1.06              | 0.48  | 6.44   | 3.12    | 293.09 | 368.38 | 142.9     | 55.3      | 93.5       | 144.7       | 148.7      |
| 8     | -17.51 | -17.51 | 0   | 16.42 | 13.68 | -1.09    | 2.74   | -1.09              | 0.96  | 14.64  | 14.06   | 293.05 | 368.55 | 142.8     | 55.2      | 93.4       | 144.6       | 148.9      |
| 9     | -20.63 | -20.63 | 0   | 19.49 | 16.82 | -1.14    | 2.67   | -1.14              | 1.43  | 25.94  | 37.14   | 292.43 | 368.59 | 142.7     | 55        | 93.3       | 144.7       | 149.4      |
| 10    | -21.67 | -21.67 | 0   | 20.48 | 17.9  | -1.18    | 2.58   | -1.18              | 1.3   | 24.21  | 31.56   | 291.87 | 368.47 | 142.7     | 54.8      | 93.2       | 144.7       | 149.6      |
| 11    | -3.13  | -3.13  | 0   | 2.01  | 0     | -1.12    | 2.01   | -1.12              | 1.09  | 2      | 2.15    | 292.56 | 132.23 | 142.8     | 55.1      | 93.3       | 144.7       | 149.1      |
| 12    | -1.45  | -1.45  | 0   | 0.31  | 0     | -1.16    | 0.31   | -1.14              | 0.3   | 0.08   | 0.02    | 291.55 | 0      | 149.3     | n/a       | n/a        | 291         | n/a        |
| 13    | -0.35  | -0.35  | 0   | 0     | 0     | -0.35    | 0      | -0.35              | 0     | 0      | 0       | 0      | 0      | n/a       | n/a       | n/a        | n/a         | n/a        |
| 14    | -6.31  | -6.31  | 0   | 5.25  | 2.46  | -1.06    | 2.79   | -1.06              | 0.4   | 1.89   | 0.75    | 293.26 | 368.47 | 142.9     | 55.3      | 93.5       | 144.7       | 148.7      |
| 15    | -1.56  | -1.56  | 0   | 0.56  | 0     | -1.05    | 0.56   | -1                 | 0.17  | 0.07   | 0.01    | 293.35 | 0      | 147.9     | n/a       | n/a        | 149.7       | n/a        |
| 16    | -2.1   | -2.1   | 0   | 1.01  | 0     | -1.05    | 1.01   | -1.09              | 0.39  | 0.32   | 0.12    | 293.46 | 0      | 144.5     | n/a       | n/a        | 146.4       | 151.5      |
| 17    | -0.98  | -0.98  | 0   | 0     | 0     | -0.98    | 0      | -0.98              | 0     | 0      | 0       | 0      | 0      | n/a       | n/a       | n/a        | n/a         | n/a        |
| 18    | -1.18  | -1.18  | 0   | 0.36  | 0     | -0.96    | 0.36   | -0.81              | 0.37  | 0.07   | 0.02    | 292.35 | 0      | 150.7     | n/a       | n/a        | 152.4       | n/a        |
| 19    | -2.32  | -2.32  | 0   | 1.28  | 0     | -0.97    | 1.28   | -1.04              | 0.87  | 0.34   | 0.21    | 292.5  | 0      | 145.2     | n/a       | n/a        | 146         | 149.1      |
| 20    | -1.78  | -1.78  | 0   | 0.71  | 0     | -0.98    | 0.71   | -1.08              | 0.15  | 0.07   | 0.01    | 292.45 | 0      | 146.4     | n/a       | n/a        | 148.1       | n/a        |
| 21    | -7.36  | -7.36  | 0   | 6.39  | 3.48  | -0.96    | 2.91   | -0.96              | 0.57  | 2.82   | 1.61    | 292.53 | 369.82 | 143.1     | 55.6      | 93.7       | 144.8       | 148.5      |
| 22    | -2.23  | -2.23  | 0   | 1.06  | 0     | -0.96    | 1.06   | -1.18              | 0.25  | 0.1    | 0.01    | 292.58 | 0      | 143.7     | n/a       | n/a        | 145.4       | 151.3      |
| 23    | -1.88  | -1.88  | 0   | 0.84  | 0     | -0.96    | 0.84   | -1.04              | 0.38  | 0.25   | 0.08    | 292.69 | 0      | 146       | n/a       | n/a        | 148.2       | n/a        |
| 24    | -4.52  | -4.52  | 0   | 3.49  | 0.66  | -1.03    | 2.83   | -1.03              | 0.39  | 0.88   | 0.27    | 292.25 | 368.33 | 143       | 55.4      | 93.6       | 144.7       | 148.6      |
| 25    | -2.04  | -2.04  | 0   | 1.02  | 0     | -1.02    | 1.02   | -1.02              | 0.69  | 0.07   | 0.05    | 292.05 | 0      | 144.8     | n/a       | n/a        | 146.5       | 151.4      |
| 26    | -6.89  | -6.89  | 0   | 5.87  | 3.03  | -1.02    | 2.84   | -1.02              | 0.26  | 1.22   | 0.31    | 292.78 | 368.65 | 143       | 55.4      | 93.6       | 144.7       | 148.6      |
| 27    | -6.39  | -6.39  | 0   | 5.37  | 2.53  | -1.02    | 2.84   | -1.02              | 0.33  | 1.48   | 0.46    | 292.72 | 368.6  | 143       | 55.4      | 93.6       | 144.7       | 148.6      |
| 28    | -2.13  | -2.13  | 0   | 1.11  | 0     | -1.01    | 1.11   | -1.02              | 0.16  | 0.11   | 0.01    | 292.83 | 0      | 144.3     | n/a       | n/a        | 145.9       | 150.4      |
| 29    | -5.86  | -5.86  | 0   | 4.85  | 2     | -1.01    | 2.85   | -1.01              | 0.3   | 1.14   | 0.3     | 292.81 | 368.72 | 143       | 55.5      | 93.6       | 144.7       | 148.6      |
| 30    | -4.93  | -4.93  | 0   | 3.95  | 1.05  | -0.97    | 2.9    | -0.97              | 0.33  | 0.85   | 0.28    | 292.69 | 369.85 | 143.1     | 55.6      | 93.7       | 144.8       | 148.5      |
| 31    | -12.4  | -12.4  | 0   | 11.42 | 8.54  | -0.99    | 2.88   | -0.99              | 0.44  | 4.15   | 1.82    | 292.55 | 369.4  | 143.1     | 55.6      | 93.7       | 144.8       | 148.6      |
| 32    | -2.54  | -2.54  | 0   | 1.48  | 0     | -0.97    | 1.48   | -1.06              | 0.28  | 0.28   | 0.07    | 292.41 | 326.65 | 143.1     | 55.6      | n/a        | 145.3       | 149.2      |
| 33    | -2.27  | -2.27  | 0   | 1.41  | 0     | -0.96    | 1.41   | -0.87              | 0.46  | 0.34   | 0.1     | 292.91 | 0      | 143.6     | n/a       | n/a        | 144.7       | 148.4      |
| 34    | -2.61  | -2.61  | 0   | 1.5   | 0     | -1       | 1.5    | -1.1               | 0.22  | 0.24   | 0.05    | 292.7  | 460.36 | 143.1     | 55.5      | n/a        | 145.4       | 149.4      |
| 35    | -1.55  | -1.55  | 0   | 0.4   | 0     | -1.31    | 0.4    | -1.15              | 0.08  | 0.03   | 0       | 290.6  | 0      | 146.6     | n/a       | n/a        | 148.6       | n/a        |

Scenario: Seattle fault, MHW

| Gauge | B0     | B      | dzi   | max h | min h | max zeta | max Δh | max eta post-quake | max s | max hs | max hss | tmax  | tmin  | tfirst POS | tfirstNEG | tfirstDRAW | tfirstADVIS | tfirstWARN |
|-------|--------|--------|-------|-------|-------|----------|--------|--------------------|-------|--------|---------|-------|-------|------------|-----------|------------|-------------|------------|
| 1     | -1.81  | -3.45  | -1.64 | 8.67  | 0.73  | 5.22     | 7.94   | 5.22               | 4.87  | 28.22  | 131.07  | 16.68 | 67.81 | 4.5        | 0.2       | 65         | 7.6         | 7.7        |
| 2     | -3.14  | -4.8   | -1.66 | 9.34  | 2.69  | 4.54     | 6.66   | 4.54               | 6.33  | 46.36  | 290.34  | 14.37 | 65.4  | 2.4        | 63        | 64.6       | 6.4         | 6.4        |
| 3     | -4.52  | -6.2   | -1.68 | 10.13 | 4.09  | 3.92     | 6.04   | 3.92               | 6.74  | 58.12  | 387.05  | 13.95 | 66.81 | 0.8        | 5.3       | 63.7       | 5.6         | 5.7        |
| 4     | -4.63  | -6.21  | -1.58 | 10.93 | 3.76  | 4.72     | 7.17   | 4.72               | 6.4   | 51.65  | 325.71  | 13.15 | 61.51 | 4.3        | 0.8       | 10.4       | 4.4         | 4.5        |
| 5     | -12.13 | -13.74 | -1.62 | 18.13 | 9.76  | 4.39     | 8.37   | 4.39               | 5.93  | 60.47  | 357.47  | 12.33 | 24.1  | 0.3        | 2         | 23.7       | 3.4         | 3.8        |
| 6     | -14.29 | -15.91 | -1.62 | 19.31 | 13.96 | 3.4      | 5.35   | 3.4                | 3.09  | 54.91  | 169.63  | 12.08 | 63.14 | 0.3        | 1.2       | 63         | 2.7         | 2.8        |
| 7     | -14.82 | -16.49 | -1.67 | 19.23 | 14.58 | 2.74     | 4.65   | 2.74               | 3.09  | 57.21  | 176.56  | 10.89 | 62.81 | 0.4        | 62.1      | n/a        | 2.2         | 2.3        |
| 8     | -17.51 | -19.24 | -1.72 | 22.45 | 17.43 | 3.21     | 5.02   | 3.21               | 3.6   | 75.62  | 271.75  | 10.71 | 62.37 | 1          | 62.2      | n/a        | 1.7         | 1.9        |
| 9     | -20.63 | -22.33 | -1.7  | 25.65 | 20.6  | 3.31     | 5.04   | 3.31               | 4.47  | 105.11 | 458.68  | 10.32 | 62.15 | 0.6        | 62.1      | n/a        | 1.3         | 1.5        |
| 10    | -21.67 | -23.34 | -1.67 | 27.28 | 21.67 | 3.94     | 5.62   | 3.94               | 4.82  | 128.76 | 611.8   | 2.16  | 0.03  | 0.4        | n/a       | n/a        | 0.9         | 1.2        |
| 11    | -3.13  | -4.73  | -1.6  | 8.48  | 1.51  | 3.75     | 6.97   | 3.75               | 9.47  | 48.75  | 407.07  | 10.48 | 3.39  | 1.3        | 0.3       | 2.1        | 1.4         | 1.5        |
| 12    | -1.48  | -3.21  | -1.73 | 7.19  | 0.22  | 3.98     | 6.97   | 3.98               | 8.19  | 44.45  | 288.73  | 8.27  | 5.64  | 0.3        | 5.5       | 5.5        | 1.1         | 1.4        |
| 13    | -0.4   | -2.16  | -1.77 | 6.18  | 0.02  | 4.02     | 6.16   | 4.02               | 6.36  | 26.88  | 118.35  | 3.33  | 63.41 | 0.9        | 5.9       | 63.3       | 1.7         | 2.5        |
| 14    | -6.3   | -8.03  | -1.72 | 11.42 | 6     | 3.39     | 5.42   | 3.39               | 3.22  | 33.96  | 105.32  | 11.18 | 63.08 | 0.4        | 62.5      | 63.1       | 2.4         | 2.5        |
| 15    | -1.61  | -3.35  | -1.73 | 6.88  | 1.2   | 3.54     | 5.68   | 3.54               | 3.96  | 25.65  | 101.27  | 15.56 | 63.2  | 0.4        | 1.8       | 63         | 2.4         | 2.6        |
| 16    | -2.06  | -3.79  | -1.73 | 7.19  | 1.69  | 3.4      | 5.5    | 3.4                | 3.83  | 27.49  | 105.33  | 15.45 | 63.25 | 0.4        | 1.7       | 63.1       | 2.5         | 2.7        |
| 17    | -1.79  | -3.48  | -1.69 | 6.84  | 1.22  | 3.55     | 5.62   | 3.36               | 6.75  | 21.98  | 148.02  | 12.05 | 59.64 | 0.2        | 3.9       | 59.1       | 2.9         | 2.9        |
| 18    | -1.32  | -3.05  | -1.73 | 7.43  | 0.37  | 4.38     | 7.06   | 4.38               | 5.72  | 22.76  | 129.15  | 5.94  | 60.7  | 0.9        | 2.9       | 3.2        | 1.5         | 4.1        |
| 19    | -2.25  | -3.97  | -1.72 | 8.15  | 1.51  | 4.18     | 6.64   | 4.18               | 4.51  | 23.77  | 71.23   | 11.81 | 23.17 | 0.6        | 2.2       | 22.9       | 1.3         | 3.9        |
| 20    | -1.68  | -3.38  | -1.7  | 7.93  | 1.11  | 4.55     | 6.82   | 4.55               | 2.77  | 17.43  | 48.33   | 12.12 | 60    | 0.3        | 59        | 59.5       | 3.5         | 3.5        |
| 21    | -7.36  | -9.03  | -1.67 | 13.7  | 6.58  | 4.67     | 7.12   | 4.67               | 5.11  | 39.94  | 203.99  | 12.65 | 60.78 | 0.3        | 2.6       | 59.5       | 3.7         | 4          |
| 22    | -2.05  | -3.74  | -1.69 | 8.57  | 1.38  | 4.83     | 7.18   | 4.83               | 3.5   | 15.24  | 42.39   | 4.91  | 61.05 | 0.3        | 3.1       | 59.9       | 3.8         | 4          |
| 23    | -1.81  | -3.45  | -1.65 | 8.31  | 0.69  | 4.86     | 7.63   | 4.86               | 3.41  | 26.92  | 88.32   | 4.99  | 61.16 | 0.2        | 2.7       | 22.8       | 4           | 4.1        |
| 24    | -4.52  | -5.95  | -1.43 | 9.29  | 3.96  | 3.34     | 5.33   | 3.34               | 2.93  | 22.54  | 63.57   | 12.36 | 63.41 | 2.7        | 0.3       | 0.9        | 2.7         | 3          |
| 25    | -2.1   | -3.36  | -1.26 | 7.13  | 1.28  | 3.78     | 5.85   | 3.78               | 3.53  | 23.24  | 78.65   | 12.58 | 63.23 | 2.9        | 0.1       | 0.6        | 2.9         | 3          |
| 26    | -6.89  | -8.33  | -1.44 | 12.09 | 6.37  | 3.76     | 5.72   | 3.76               | 2.42  | 27.27  | 66.06   | 11.97 | 62.97 | 2.9        | 0.2       | 59.5       | 2.9         | 3.2        |
| 27    | -6.39  | -7.87  | -1.47 | 11.45 | 5.93  | 3.59     | 5.53   | 3.59               | 2.71  | 27.98  | 75.89   | 12.07 | 62.84 | 2.8        | 0.3       | 59.5       | 2.8         | 3.2        |
| 28    | -2.08  | -3.42  | -1.34 | 7.41  | 1.41  | 3.99     | 6      | 3.99               | 3.08  | 18.31  | 56.37   | 11.93 | 63.06 | 3.1        | 0.1       | 0.7        | 3.1         | 3.1        |
| 29    | -5.86  | -7.29  | -1.43 | 11.41 | 5.28  | 4.12     | 6.13   | 4.12               | 2.83  | 27.92  | 78.9    | 11.84 | 60    | 3          | 0.2       | 59.4       | 3           | 3.3        |
| 30    | -4.93  | -6.62  | -1.69 | 11.02 | 4.45  | 4.4      | 6.57   | 4.4                | 2.8   | 22.68  | 57.39   | 11.99 | 60.79 | 0.3        | 2         | 59.9       | 3.6         | 3.8        |
| 31    | -12.4  | -14.07 | -1.66 | 18.32 | 11.81 | 4.25     | 6.51   | 4.25               | 3.42  | 53     | 173.98  | 12.26 | 29.03 | 0.3        | 2         | 28.8       | 3.2         | 3.6        |
| 32    | -2.45  | -3.85  | -1.4  | 8.57  | 1.53  | 4.72     | 7.03   | 4.72               | 2.96  | 18.91  | 54.35   | 5.75  | 60.75 | 3.7        | 0.2       | 0.7        | 3.7         | 3.8        |
| 33    | -2.36  | -3.83  | -1.47 | 8.53  | 1.17  | 4.7      | 7.36   | 4.7                | 2.71  | 19.27  | 52.08   | 12.24 | 61.07 | 4          | 0.1       | 2.8        | 4           | 4.1        |
| 34    | -2.5   | -3.83  | -1.33 | 8.59  | 1.68  | 4.76     | 6.91   | 4.76               | 2.72  | 18.03  | 49.05   | 11.85 | 59.87 | 3.3        | 0.1       | 0.5        | 3.3         | 3.5        |
| 35    | -1.72  | -3.46  | -1.74 | 9.87  | 0.83  | 6.41     | 9.04   | 6.41               | 5.07  | 48.92  | 247.63  | 2.05  | 4.13  | 1          | 3.7       | 3.9        | 1.2         | 1.7        |

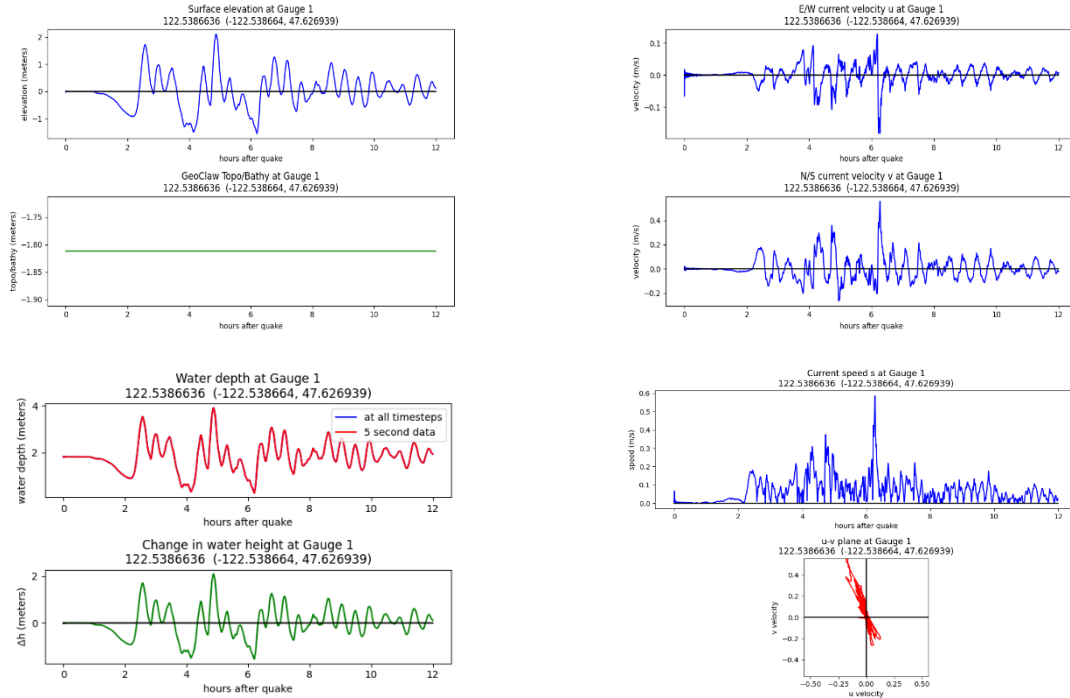
Scenario: Seattle fault, MLW

| Gauge | B0     | B      | dzi   | max h | min h | max zeta | max Δh | max eta post-quake | max s | max hs | max hss | tmax  | tmin  | tfirst POS | tfirstNEG | tfirstDRAW | tfirstADVIS | tfirstWARN |
|-------|--------|--------|-------|-------|-------|----------|--------|--------------------|-------|--------|---------|-------|-------|------------|-----------|------------|-------------|------------|
| 1     | -1.78  | -3.42  | -1.64 | 6     | 0     | 2.55     | 6      | 2.58               | 5.64  | 24.26  | 123.97  | 17.14 | 0     | 8.9        | n/a       | n/a        | 8.9         | 9          |
| 2     | -3.14  | -4.8   | -1.66 | 6.66  | 0.79  | 1.85     | 5.87   | 1.85               | 6.79  | 33.57  | 214.95  | 15.98 | 2.35  | 3.6        | n/a       | n/a        | 7.2         | 7.3        |
| 3     | -4.52  | -6.2   | -1.68 | 8.6   | 2.18  | 2.4      | 6.42   | 2.4                | 6.58  | 34.92  | 215.51  | 14.94 | 6.27  | 1.1        | n/a       | n/a        | 6.3         | 6.3        |
| 4     | -4.63  | -6.21  | -1.58 | 8.31  | 2.07  | 2.1      | 6.24   | 2.1                | 7.02  | 39.92  | 278.46  | 13.46 | 65.24 | 4.7        | 1         | n/a        | 4.8         | 5          |
| 5     | -12.13 | -13.74 | -1.62 | 15.85 | 7.7   | 2.11     | 8.15   | 2.11               | 4.89  | 49.43  | 218.92  | 13.24 | 24.98 | 0.4        | 2.2       | 24.6       | 3.8         | 4.2        |
| 6     | -14.29 | -15.91 | -1.62 | 16.51 | 11.5  | 0.6      | 5.01   | 0.6                | 3.24  | 50.25  | 162.69  | 13.58 | 62.24 | 0.3        | 1.2       | 61.1       | 3           | 3          |
| 7     | -14.82 | -16.49 | -1.67 | 16.82 | 12.25 | 0.33     | 4.57   | 0.33               | 3.83  | 61.57  | 233.32  | 11.41 | 61.25 | 0.4        | 60.2      | n/a        | 2.4         | 2.5        |
| 8     | -17.51 | -19.24 | -1.72 | 20.08 | 15.13 | 0.84     | 4.94   | 0.84               | 4.08  | 75.32  | 307.14  | 11.1  | 60.88 | 1          | 60.8      | n/a        | 1.8         | 2.1        |
| 9     | -20.63 | -22.33 | -1.7  | 23.51 | 18.1  | 1.18     | 5.41   | 1.18               | 5.42  | 109.96 | 596.06  | 10.76 | 6.81  | 0.7        | 6.7       | n/a        | 1.4         | 1.6        |
| 10    | -21.67 | -23.34 | -1.67 | 25.37 | 19.33 | 2.03     | 6.04   | 2.03               | 5.41  | 128.04 | 646.77  | 2.28  | 0.03  | 0.5        | n/a       | n/a        | 1           | 1.2        |
| 11    | -3.13  | -4.73  | -1.6  | 5.7   | 0.44  | 0.97     | 5.26   | 0.97               | 9.6   | 32.78  | 251.5   | 9.53  | 3.87  | 1.6        | 0.4       | 3.8        | 1.7         | 1.7        |
| 12    | -1.59  | -3.32  | -1.73 | 5.48  | 0     | 2.27     | 5.48   | 2.16               | 7.83  | 25.59  | 199.14  | 10.61 | 0     | 1.5        | n/a       | n/a        | 1.5         | 1.6        |
| 13    | -0.38  | -2.15  | -1.77 | 4.28  | 0     | 2.11     | 4.28   | 2.13               | 6.24  | 18.09  | 76.63   | 3.57  | 0     | 2.9        | n/a       | n/a        | 2.9         | 3          |
| 14    | -6.3   | -8.03  | -1.72 | 8.7   | 3.71  | 0.67     | 4.99   | 0.67               | 3.66  | 29.28  | 98.58   | 3.92  | 61.64 | 0.4        | 60.3      | n/a        | 2.6         | 2.7        |
| 15    | -1.73  | -3.46  | -1.73 | 4.1   | 0     | 0.75     | 4.1    | 0.64               | 4.69  | 17.2   | 76.22   | 11.7  | 0     | 2.8        | n/a       | n/a        | 2.8         | 2.9        |
| 16    | -2.05  | -3.78  | -1.73 | 4.37  | 0     | 0.58     | 4.37   | 0.59               | 4.39  | 18.9   | 83      | 11.87 | 0     | 1.3        | n/a       | n/a        | 2.8         | 3          |
| 17    | -1.79  | -3.48  | -1.69 | 4.25  | 0     | 0.95     | 4.25   | 0.77               | 7.31  | 13.68  | 45.43   | 13.68 | 0     | 3.2        | n/a       | n/a        | 3.2         | 3.2        |
| 18    | -1.18  | -2.91  | -1.73 | 5.48  | 0     | 2.43     | 5.48   | 2.57               | 5.67  | 14.08  | 76.65   | 13.98 | 0     | 4.8        | n/a       | n/a        | 4.8         | 4.8        |
| 19    | -2.29  | -4.01  | -1.72 | 6.16  | 0     | 2.19     | 6.16   | 2.14               | 4.72  | 14.47  | 56.75   | 13.68 | 0     | 1.8        | n/a       | n/a        | 4.3         | 4.4        |
| 20    | -1.63  | -3.33  | -1.7  | 5.67  | 0     | 2.29     | 5.67   | 2.33               | 3.37  | 9.83   | 19.9    | 12.52 | 0     | 3.9        | n/a       | n/a        | 3.9         | 3.9        |
| 21    | -7.36  | -9.03  | -1.67 | 11.12 | 4.33  | 2.09     | 6.79   | 2.09               | 3.13  | 25.13  | 78.65   | 12.68 | 63.33 | 0.3        | 3.2       | 61.2       | 4           | 4.4        |
| 22    | -2.1   | -3.79  | -1.69 | 6.16  | 0     | 2.42     | 6.16   | 2.37               | 3.58  | 21.99  | 78.78   | 12.63 | 0     | 4.2        | n/a       | n/a        | 4.2         | 4.3        |
| 23    | -1.79  | -3.44  | -1.65 | 6.51  | 0     | 3.06     | 6.51   | 3.07               | 3.37  | 16.87  | 54.47   | 13.49 | 0     | 4.4        | n/a       | n/a        | 4.4         | 4.7        |
| 24    | -4.52  | -5.95  | -1.43 | 6.79  | 1.48  | 0.84     | 5.31   | 0.84               | 3.6   | 16.73  | 58.67   | 4.7   | 62.06 | 3          | 0.3       | 0.9        | 3           | 3.4        |
| 25    | -2.05  | -3.31  | -1.26 | 4.96  | 0     | 1.6      | 4.96   | 1.65               | 4.37  | 15.47  | 48.3    | 3.96  | 0     | 3.3        | n/a       | n/a        | 3.3         | 3.4        |
| 26    | -6.89  | -8.33  | -1.44 | 9.32  | 3.89  | 0.99     | 5.43   | 0.99               | 2.59  | 20.77  | 53.8    | 13.75 | 61.85 | 3.2        | 0.2       | 60.7       | 3.2         | 3.6        |
| 27    | -6.39  | -7.87  | -1.47 | 8.45  | 3.43  | 0.58     | 5.02   | 0.58               | 2.94  | 22.87  | 67.15   | 13.84 | 61.77 | 3          | 0.2       | 60.6       | 3.1         | 3.5        |
| 28    | -2.19  | -3.53  | -1.34 | 4.99  | 0     | 1.57     | 4.99   | 1.46               | 3.33  | 14.28  | 47.34   | 13.7  | 0     | 3.4        | n/a       | n/a        | 3.4         | 3.5        |
| 29    | -5.86  | -7.29  | -1.43 | 8.7   | 2.85  | 1.41     | 5.85   | 1.41               | 2.99  | 20.23  | 60.55   | 13.62 | 62.63 | 3.3        | 0.2       | 60.7       | 3.3         | 3.6        |
| 30    | -4.93  | -6.62  | -1.69 | 8.82  | 1.99  | 2.2      | 6.83   | 2.2                | 5.36  | 32.15  | 152.06  | 13.35 | 63.37 | 0.3        | 1.9       | 61.4       | 3.9         | 4.2        |
| 31    | -12.4  | -14.07 | -1.66 | 15.78 | 9.47  | 1.71     | 6.31   | 1.71               | 4.17  | 47.2   | 189.02  | 13.38 | 62.42 | 0.3        | 2.3       | 61         | 3.5         | 3.9        |
| 32    | -2.45  | -3.85  | -1.4  | 6.62  | 0     | 2.77     | 6.62   | 2.77               | 4.05  | 13.43  | 50.4    | 12.71 | 25.4  | 4.1        | 0.2       | n/a        | 4.1         | 4.2        |
| 33    | -2.39  | -3.85  | -1.47 | 6.43  | 0     | 2.6      | 6.43   | 2.58               | 3.39  | 15.75  | 51.76   | 13.4  | 10.7  | 4.4        | 0.2       | n/a        | 4.4         | 4.6        |
| 34    | -2.5   | -3.83  | -1.33 | 6.05  | 0     | 2.21     | 6.04   | 2.21               | 3.14  | 12.91  | 38.79   | 13.28 | 65.92 | 3.7        | 0.2       | n/a        | 3.7         | 3.8        |
| 35    | -1.71  | -3.46  | -1.74 | 8.23  | 0     | 4.76     | 8.23   | 4.77               | 7.5   | 45.29  | 258.04  | 2.17  | 0     | 1.3        | n/a       | n/a        | 1.7         | 1.7        |

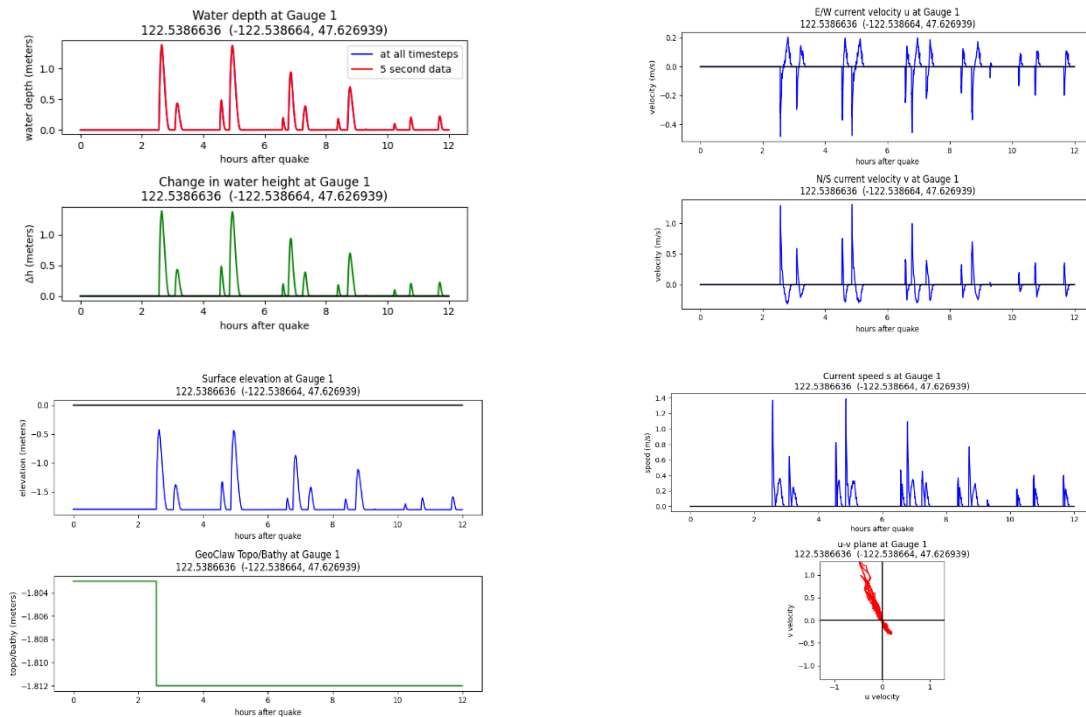
# Appendix C. All study gauge plots

## Gauge 1: Northeast Eagle Harbor

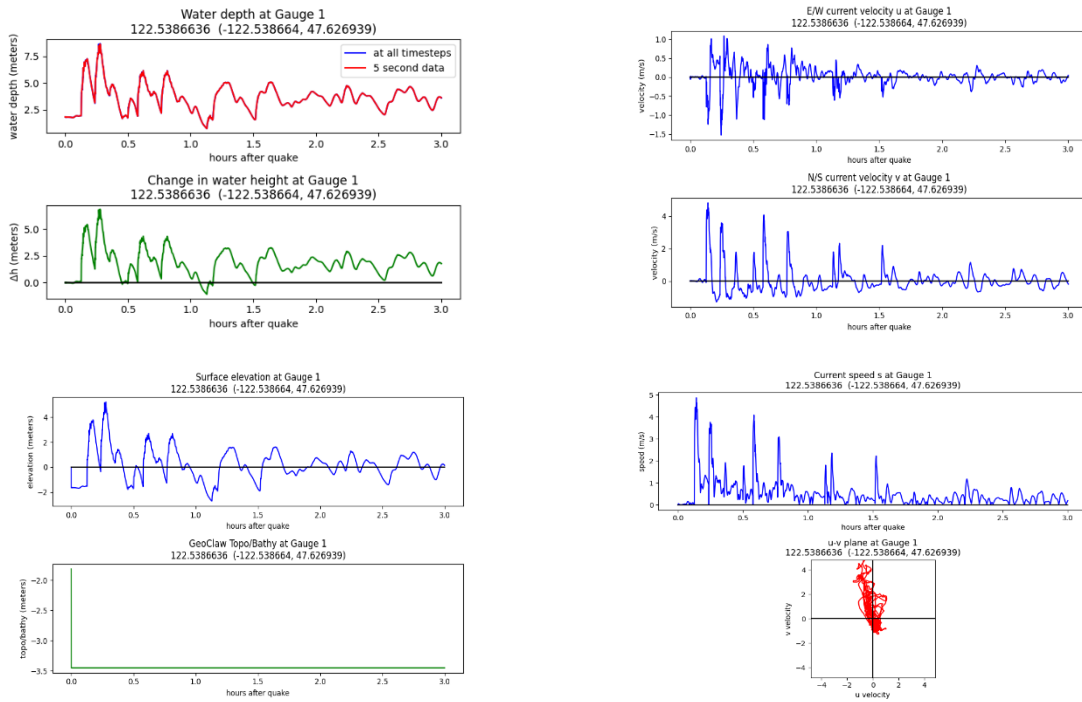
Cascadia subduction zone scenario, MHW:



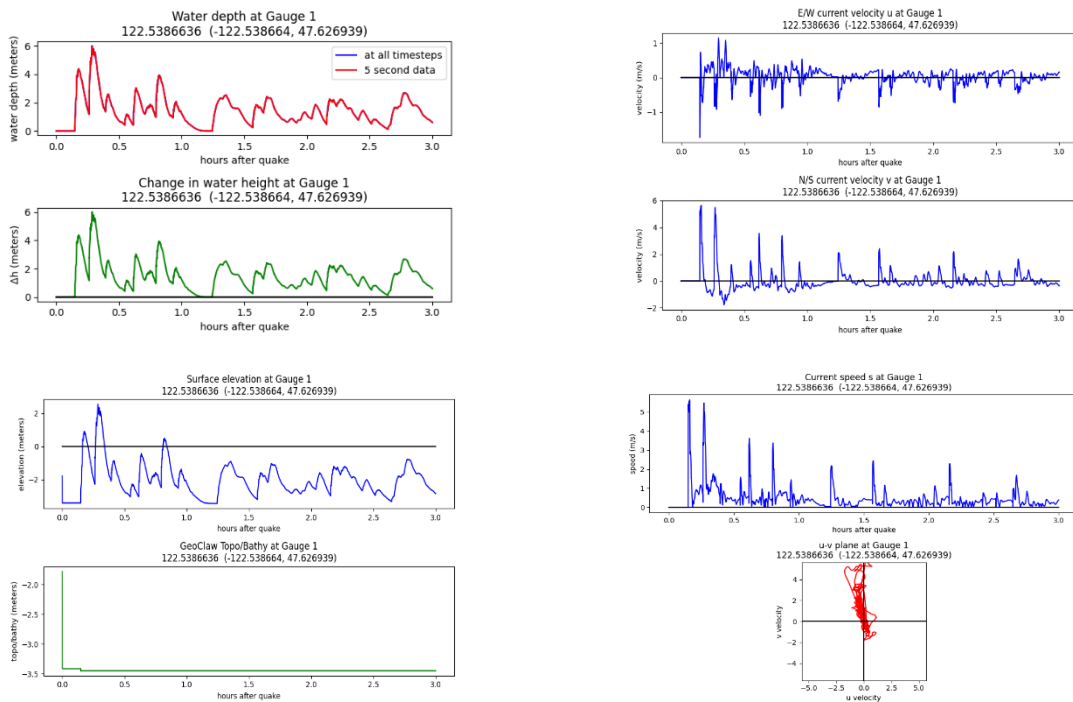
Cascadia subduction zone scenario, MLW:



## Seattle fault scenario, MHW:



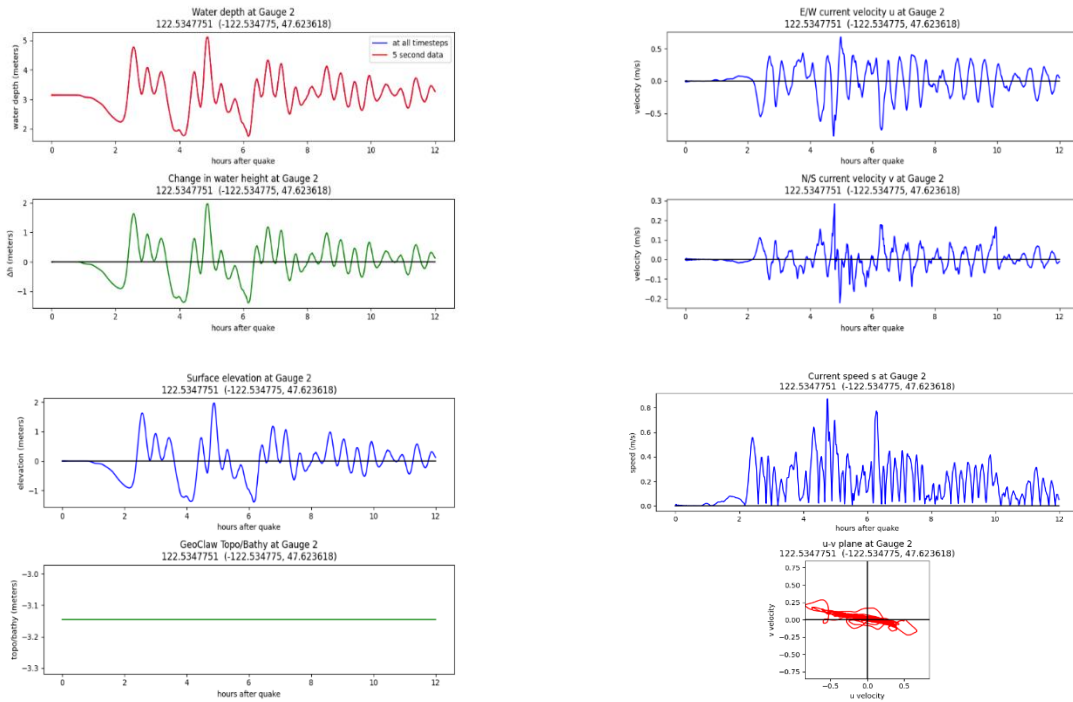
## Seattle fault scenario, MLW:



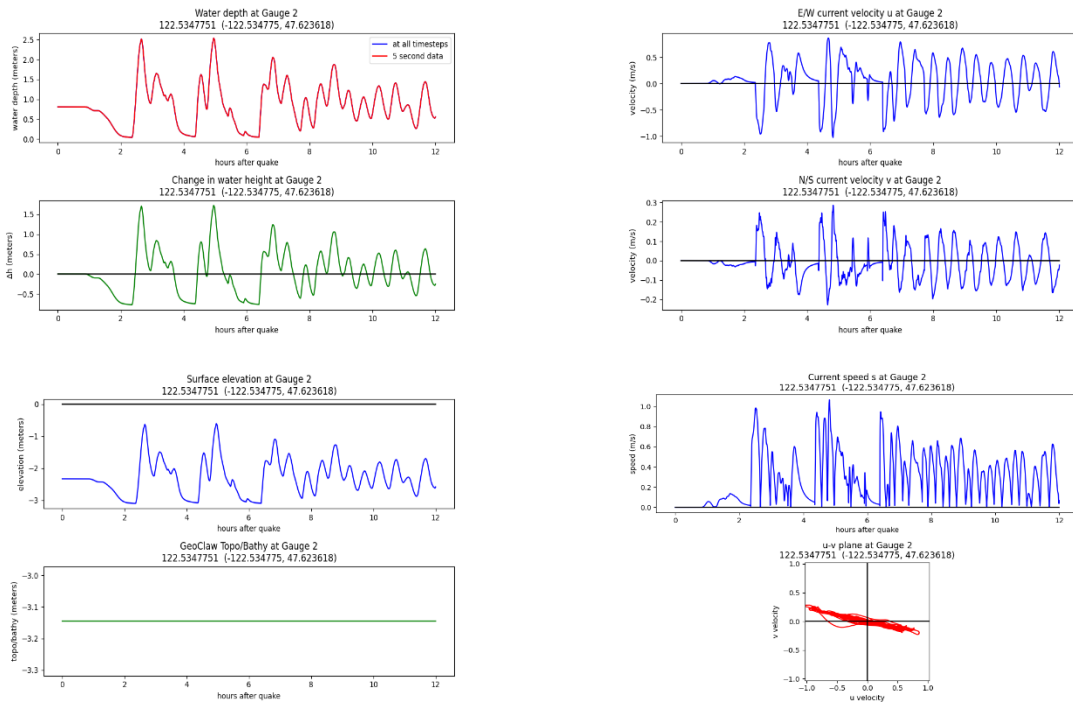


## Gauge 2: Center channel 1

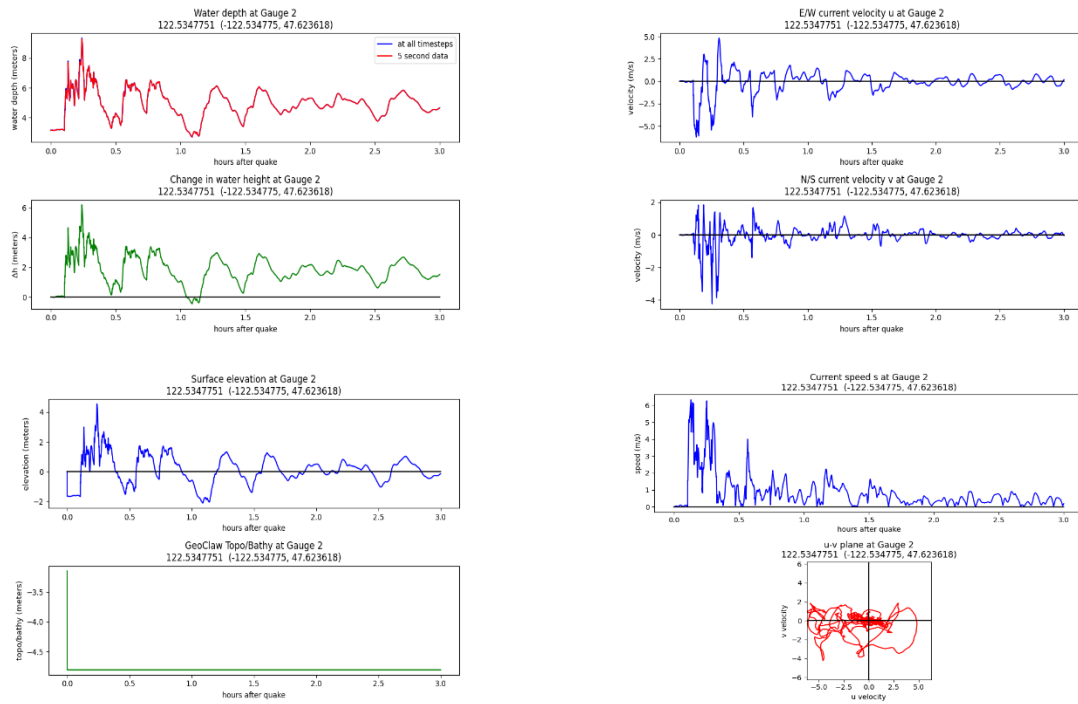
Cascadia subduction zone scenario, MHW:



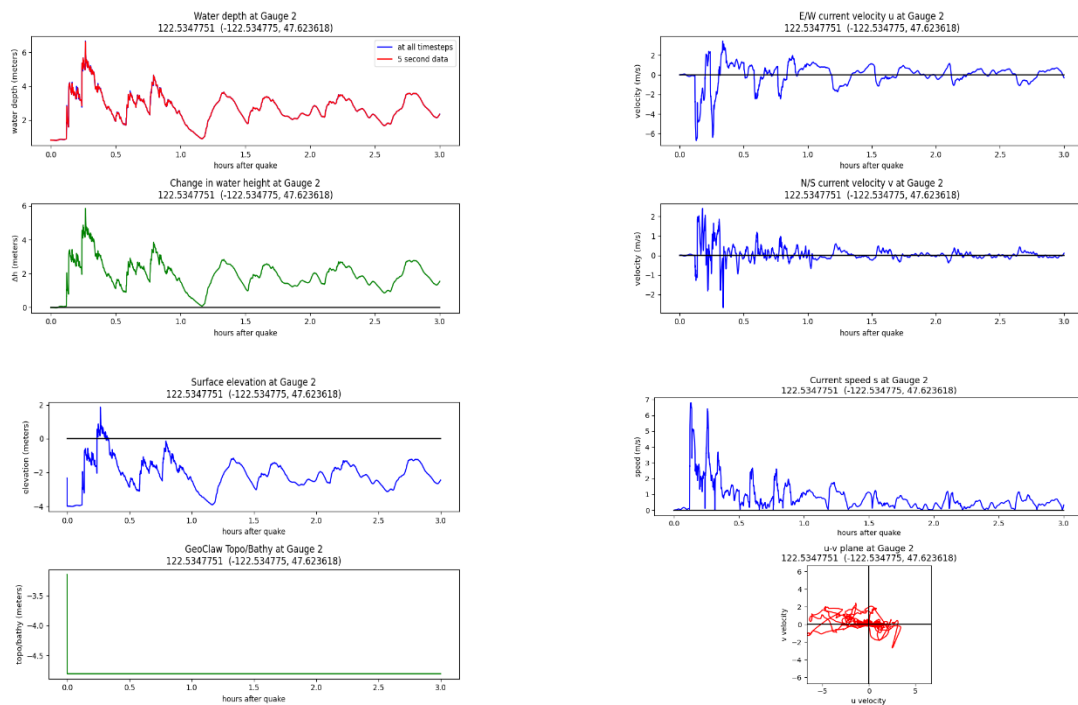
Cascadia subduction zone scenario, MLW:



## Seattle fault scenario, MHW:

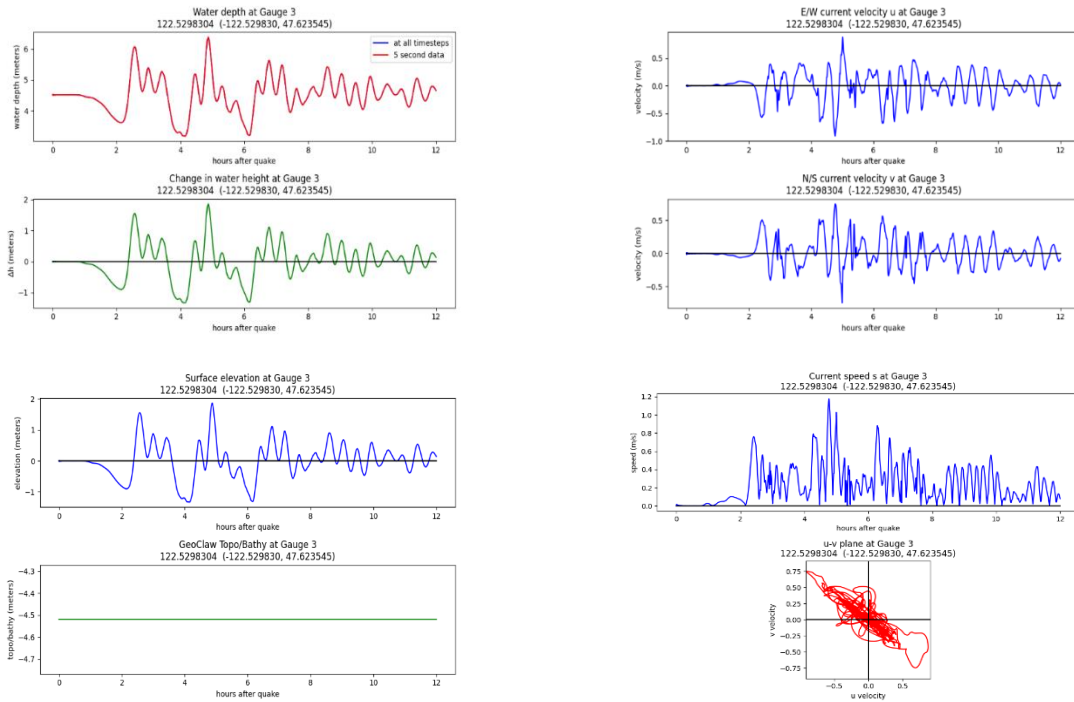


## Seattle fault scenario, MLW:

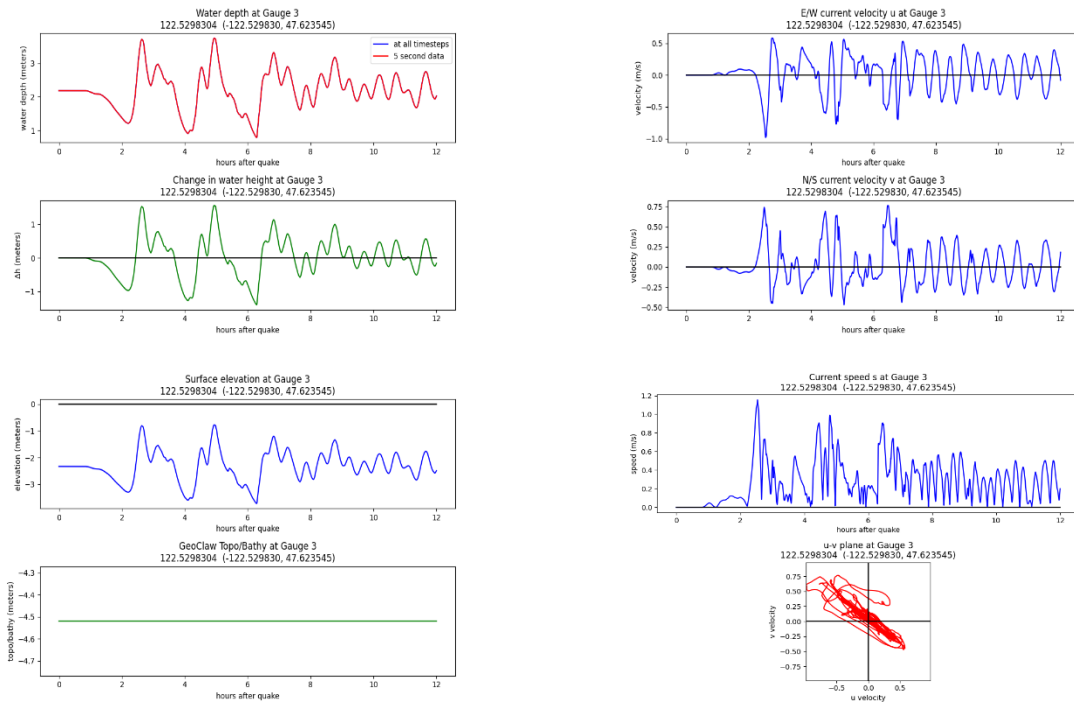


## Gauge 3: Center channel 2

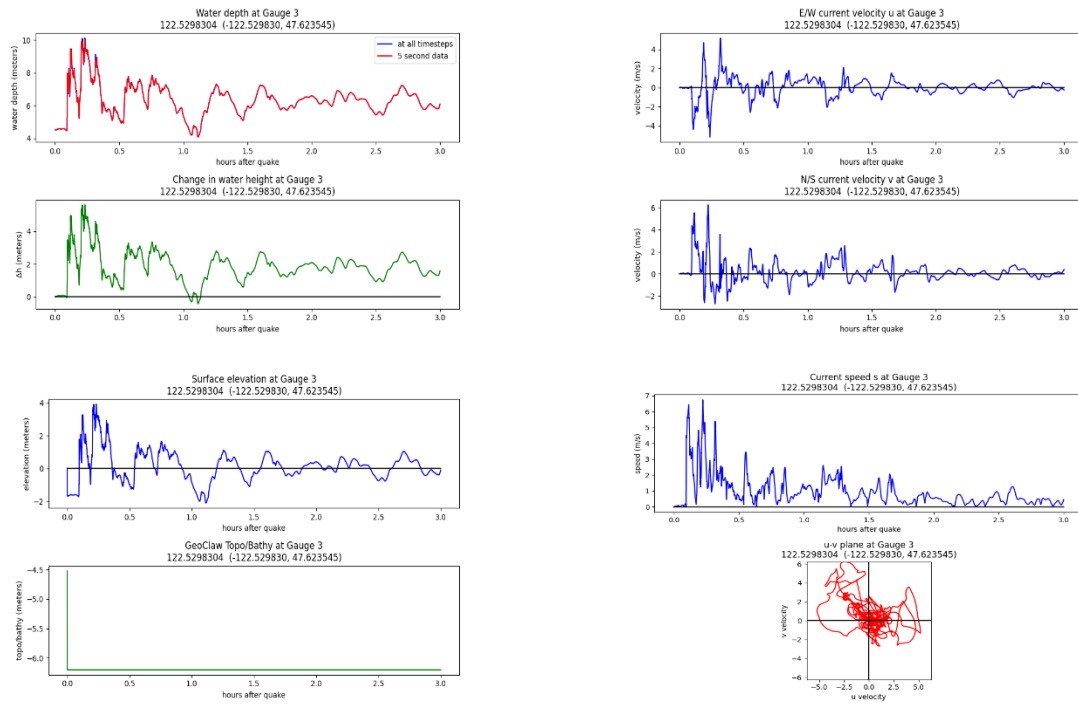
Cascadia subduction zone scenario, MHW:



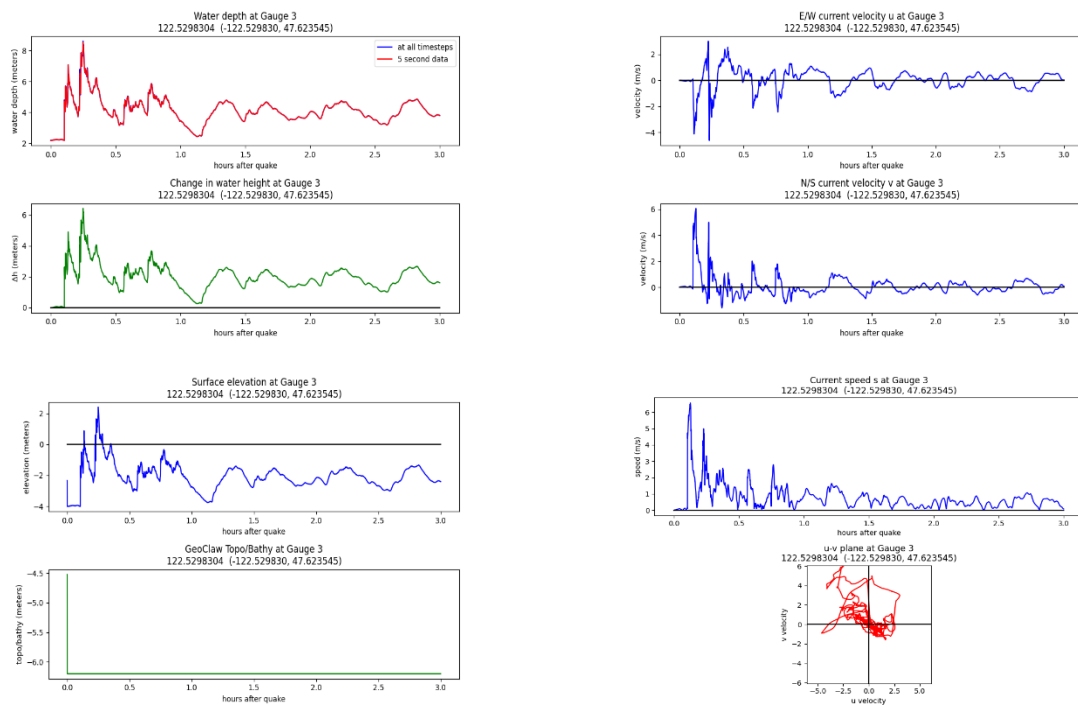
Cascadia subduction zone scenario, MLW:



## Seattle fault scenario, MHW:

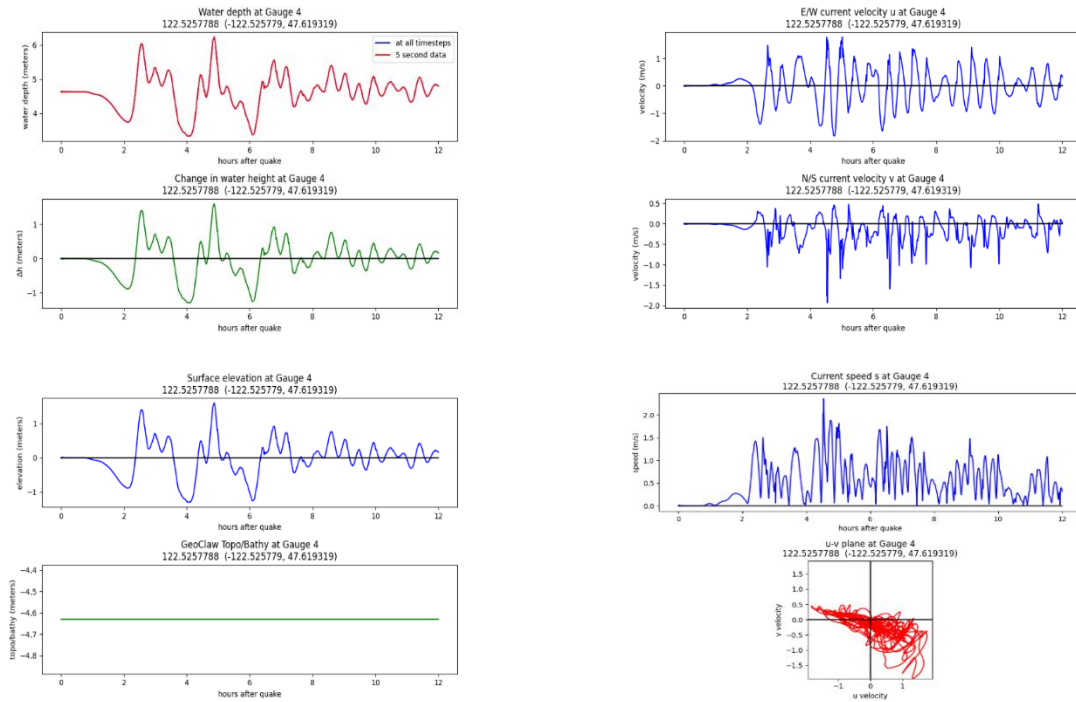


## Seattle fault scenario, MLW:

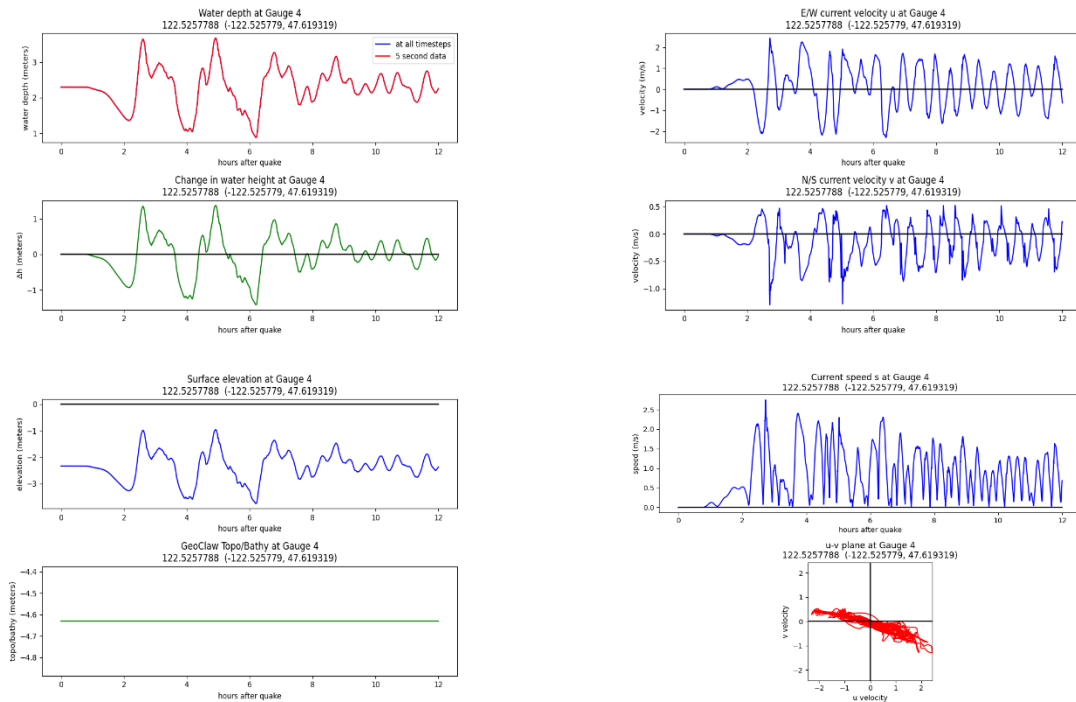


## Gauge 4: Center Channel 3

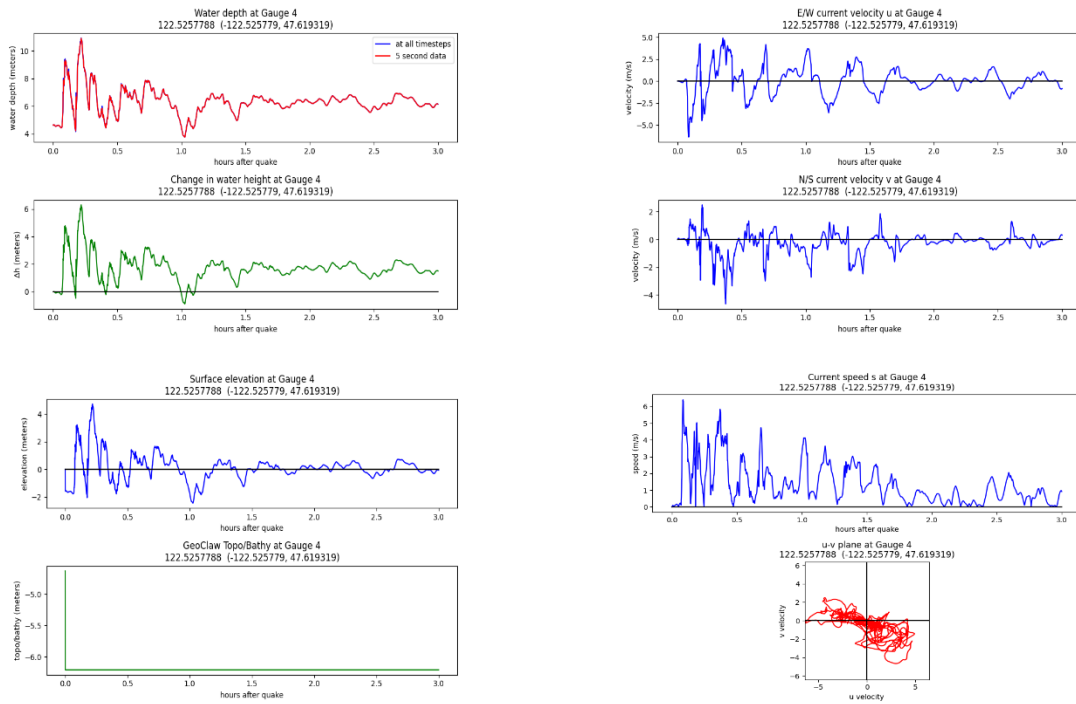
Cascadia subduction zone scenario, MHW:



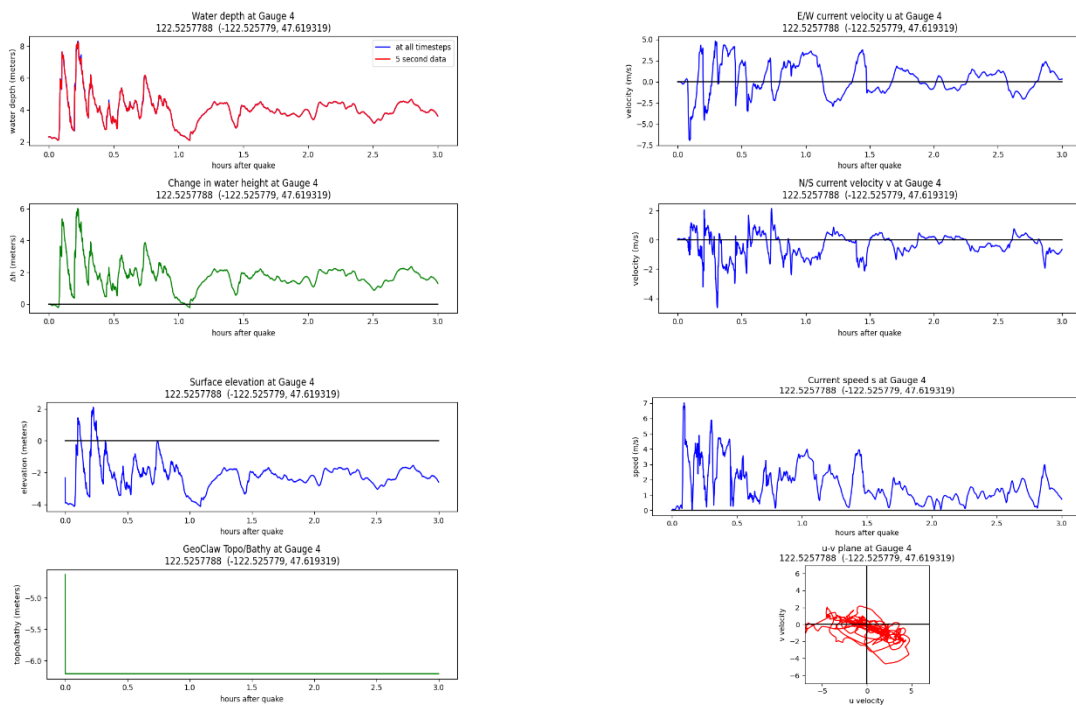
Cascadia subduction zone scenario, MLW:



## Seattle fault scenario, MHW:

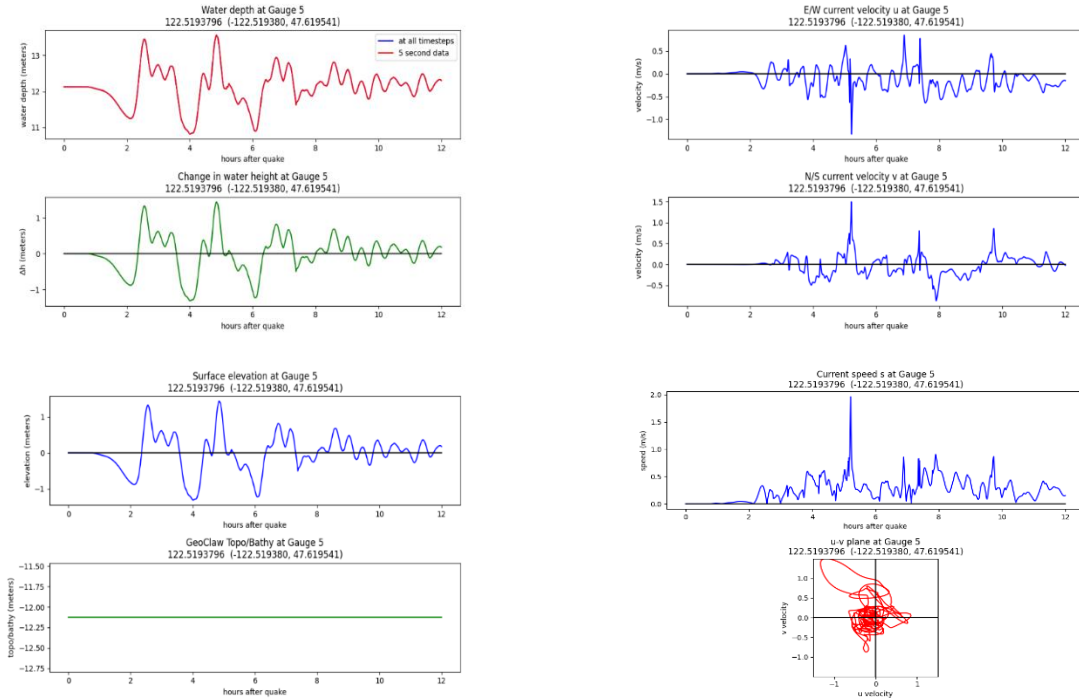


## Seattle fault scenario, MLW:

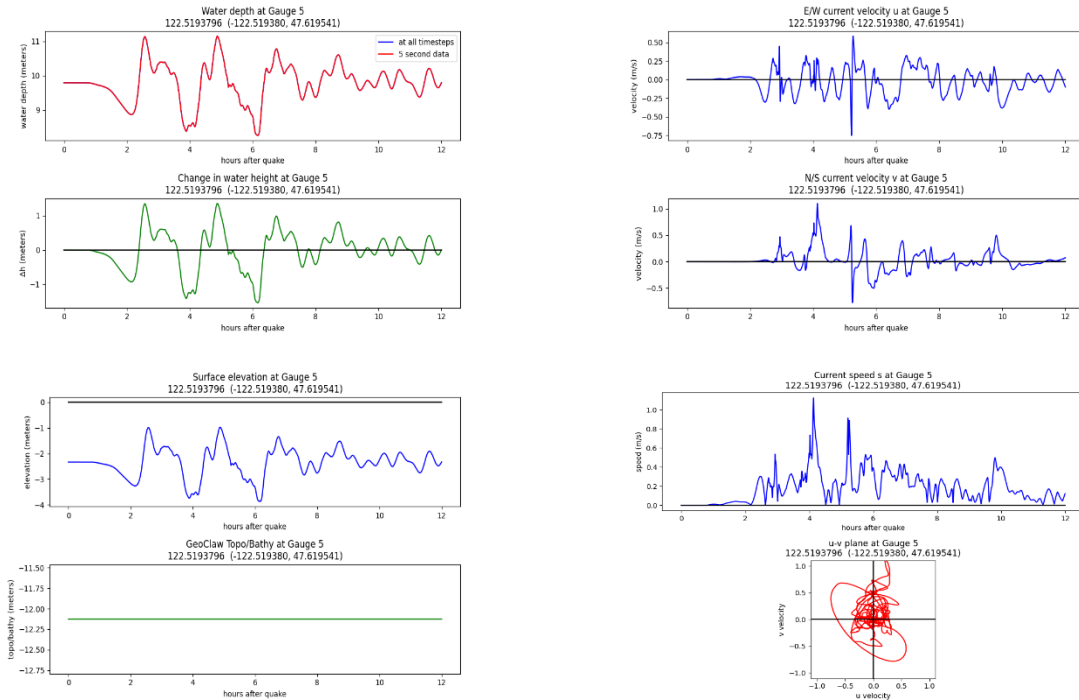


## Gauge 5: Center channel 4

Cascadia subduction zone scenario, MHW:

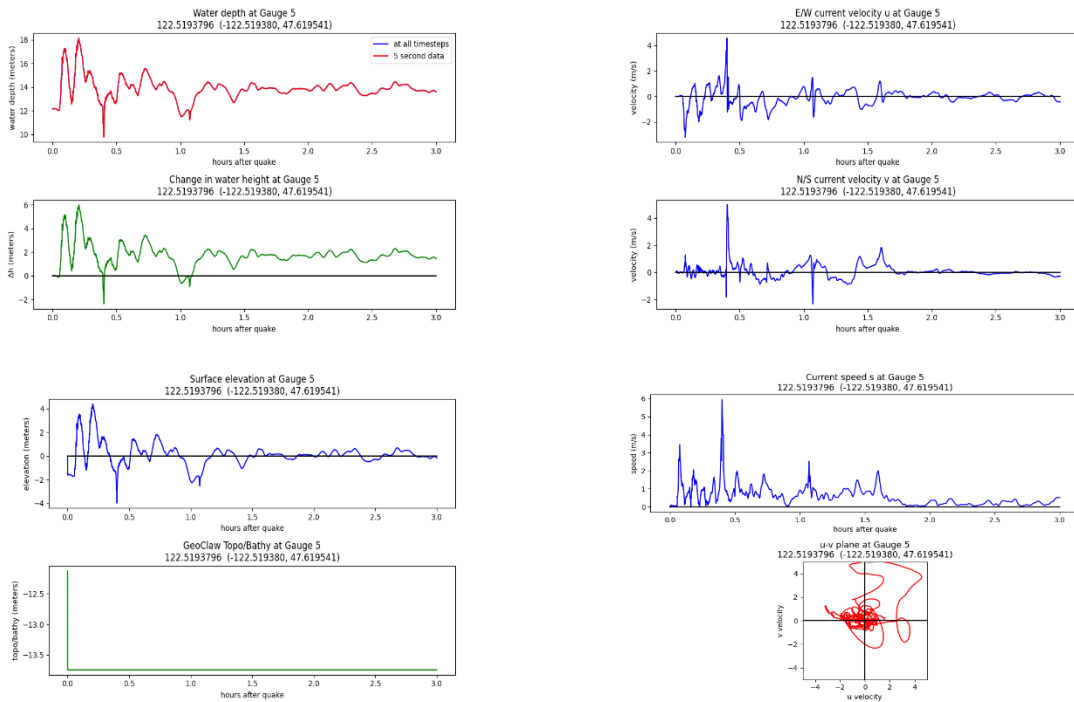


Cascadia subduction zone scenario, MLW:

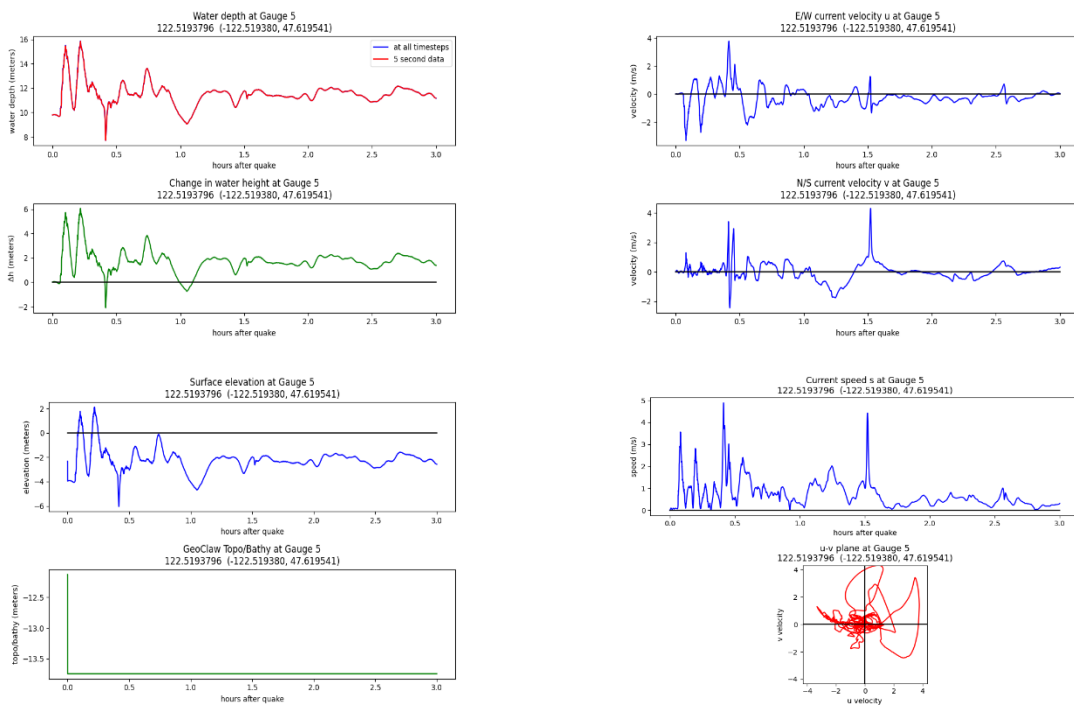




## Seattle fault scenario, MHW:

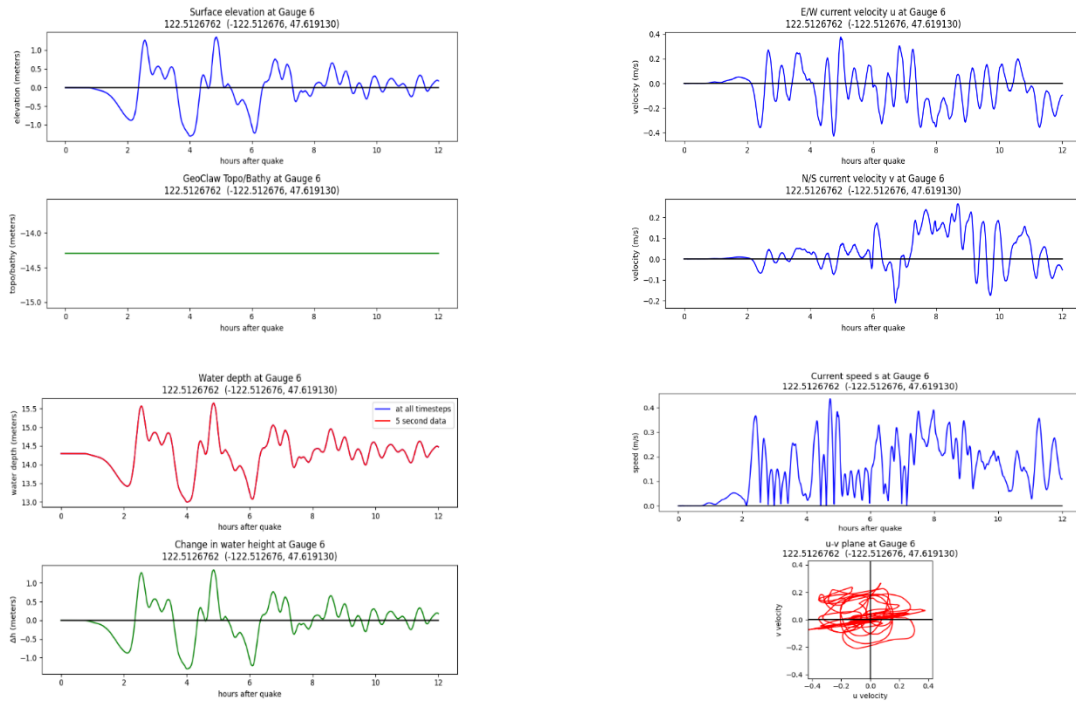


## Seattle fault scenario, MLW:

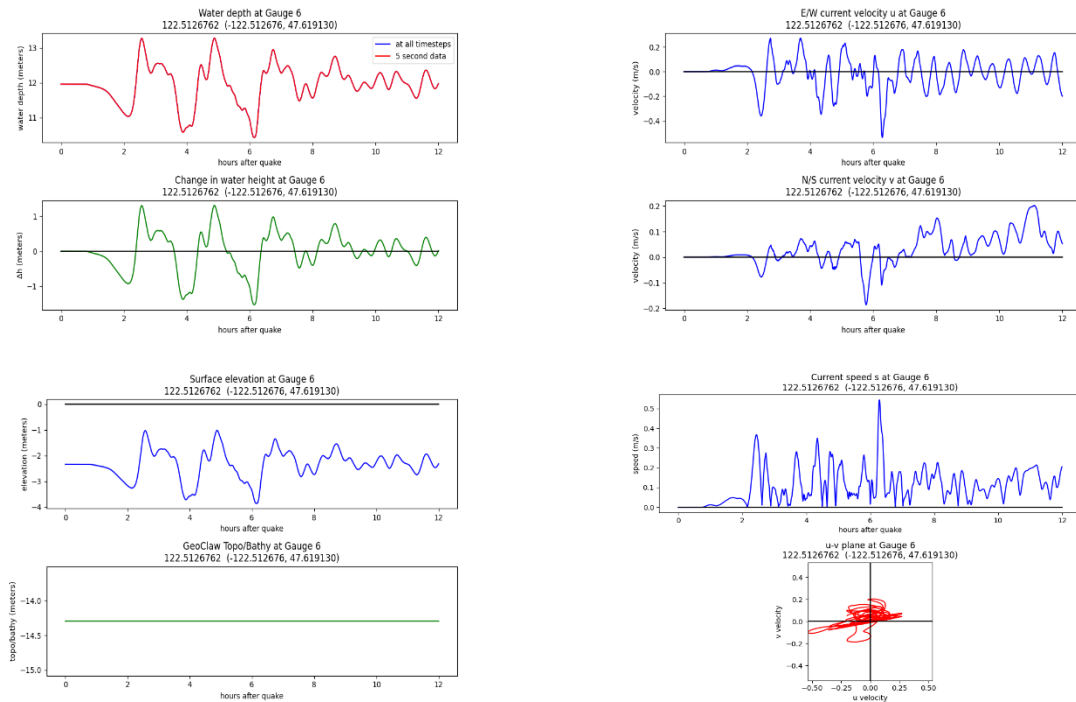


## Gauge 6: Center channel 5

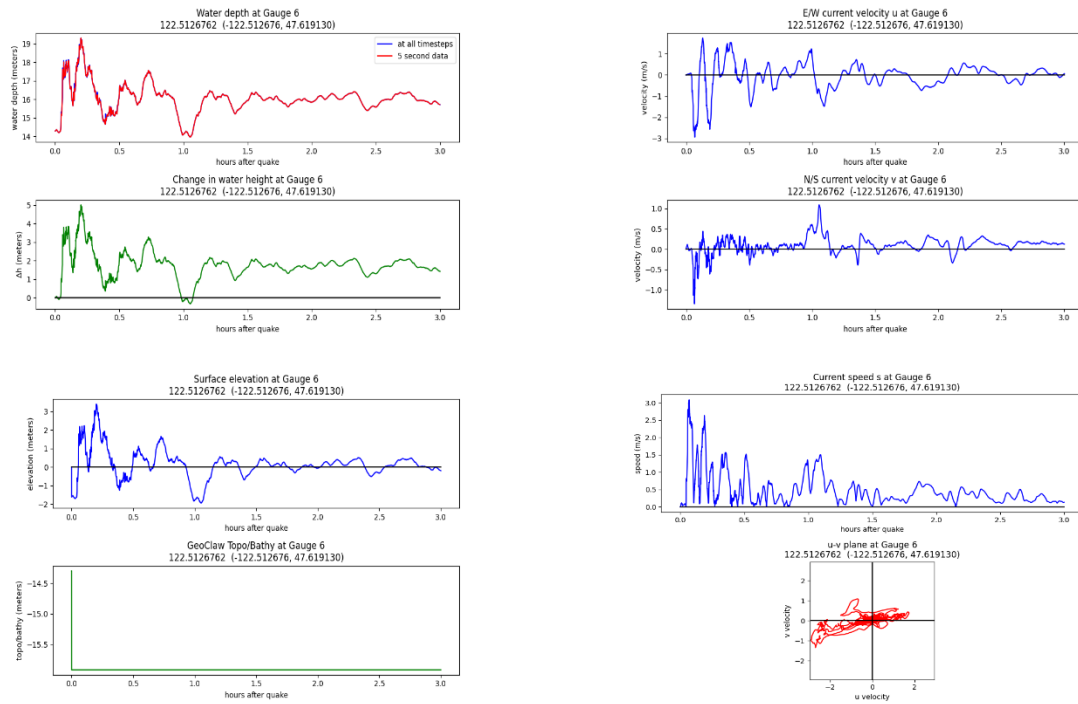
Cascadia subduction zone scenario, MHW:



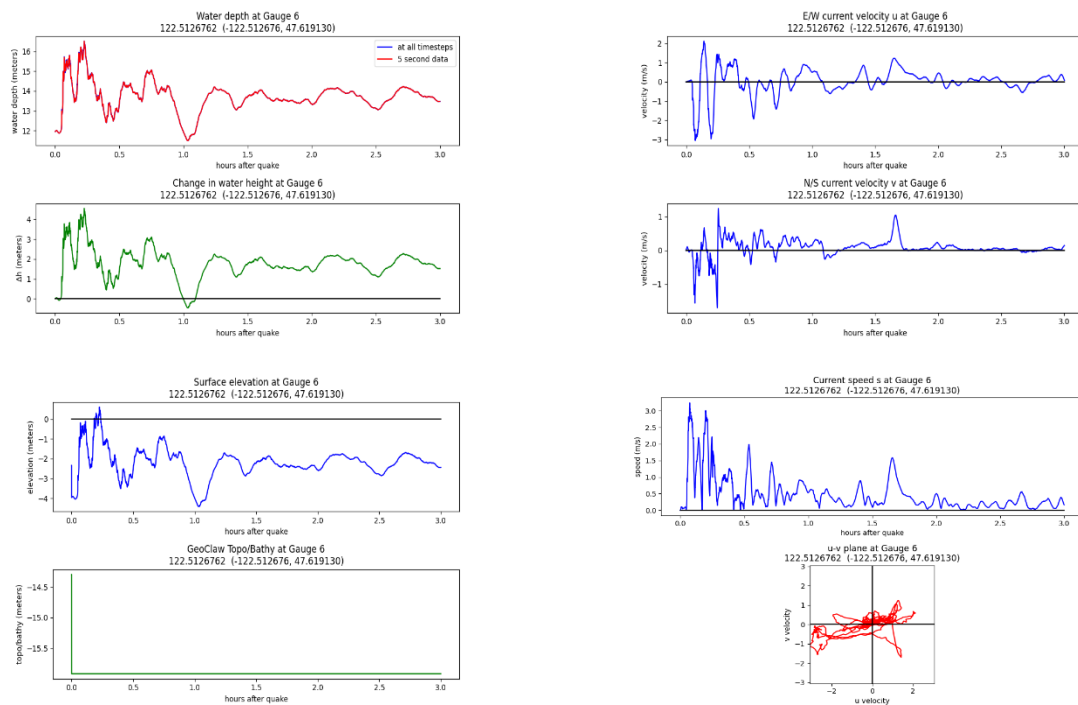
Cascadia subduction zone scenario, MLW:



## Seattle fault scenario, MHW:

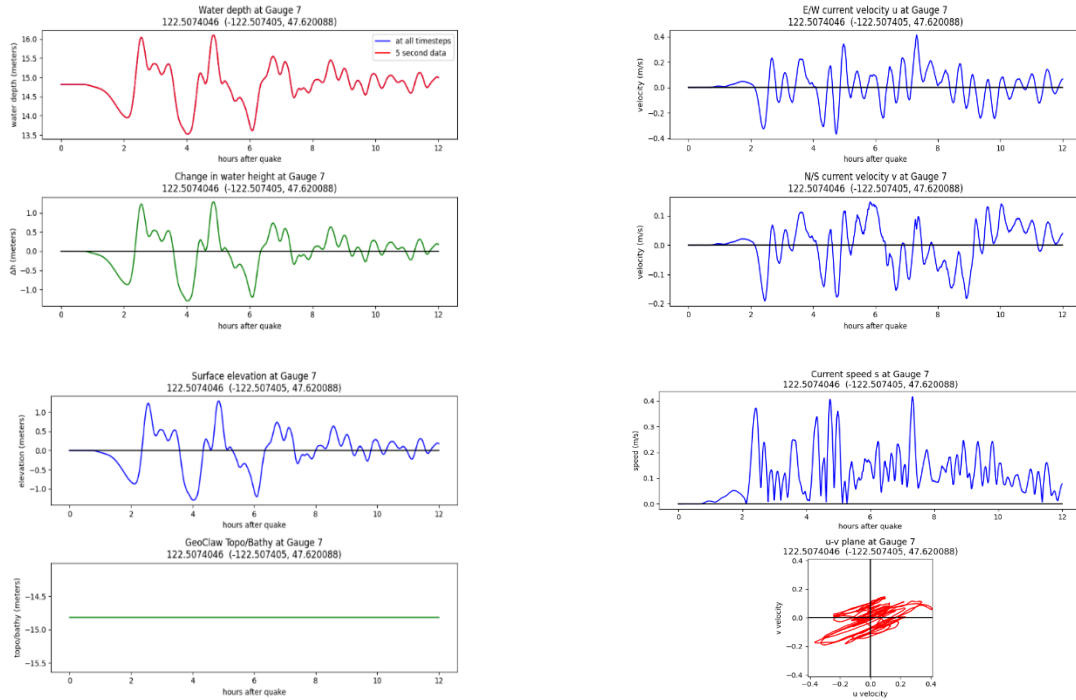


## Seattle fault scenario, MLW:

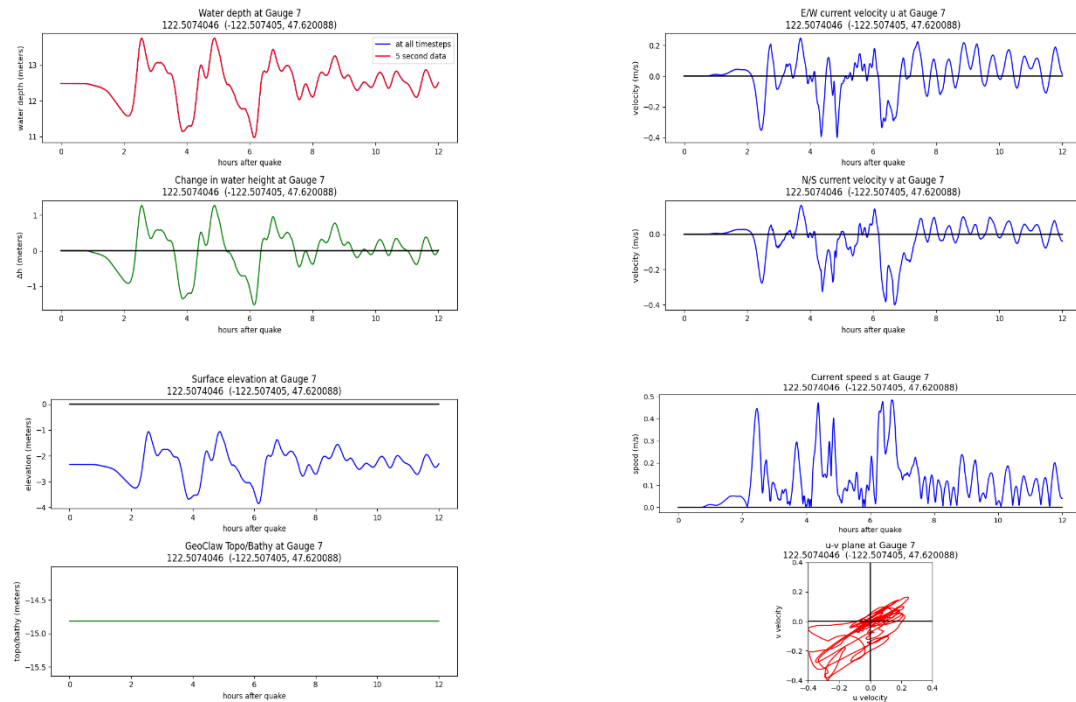


## Gauge 7: Center channel 6

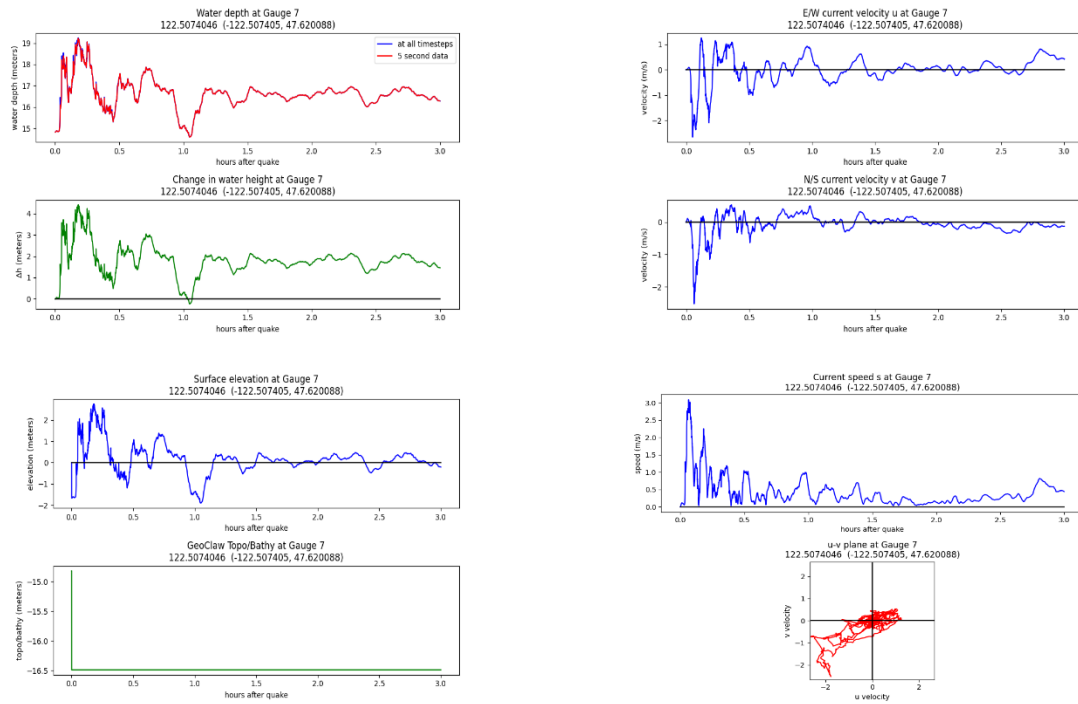
Cascadia subduction zone scenario, MHW:



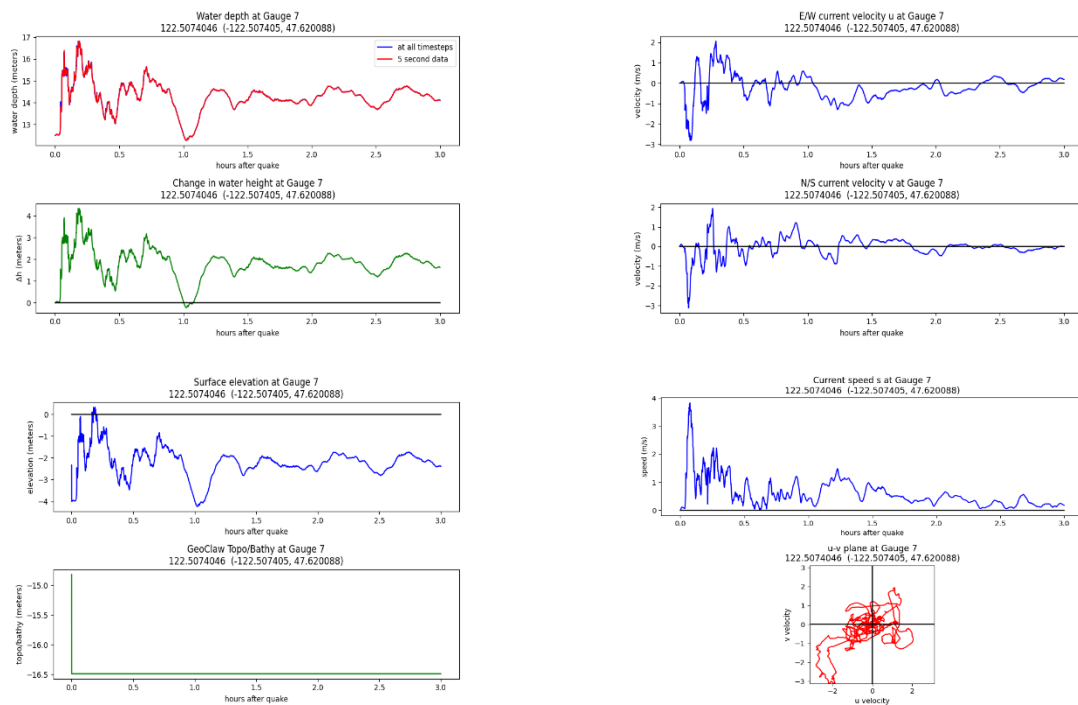
Cascadia subduction zone scenario, MLW:



## Seattle fault scenario, MHW:

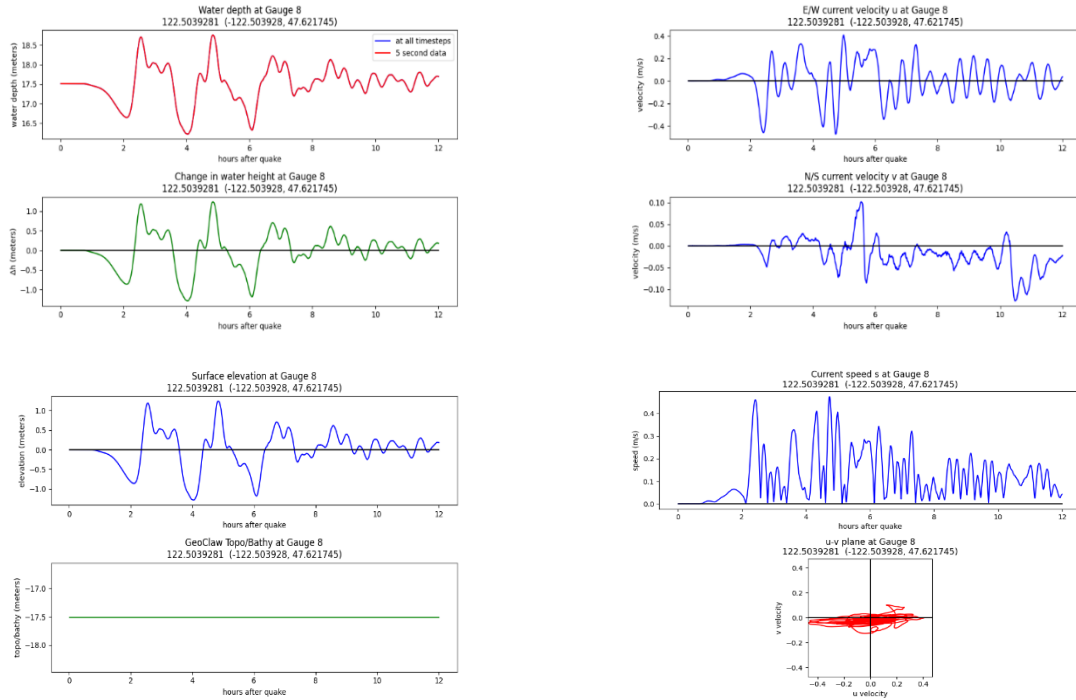


## Seattle fault scenario, MLW:

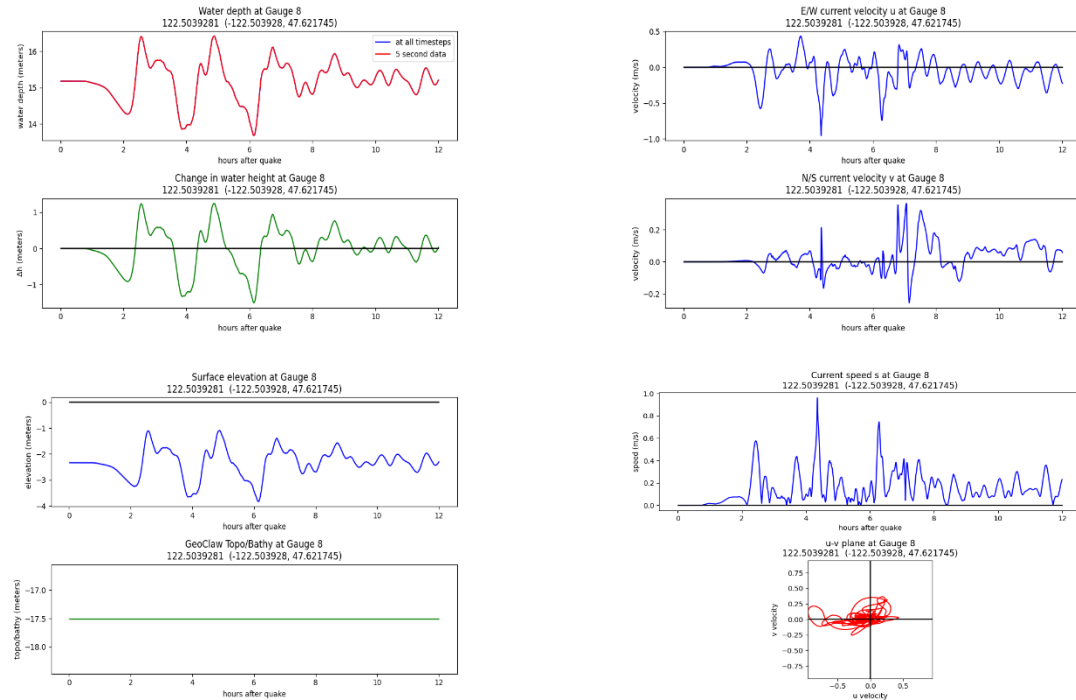


## Gauge 8: Center channel 7

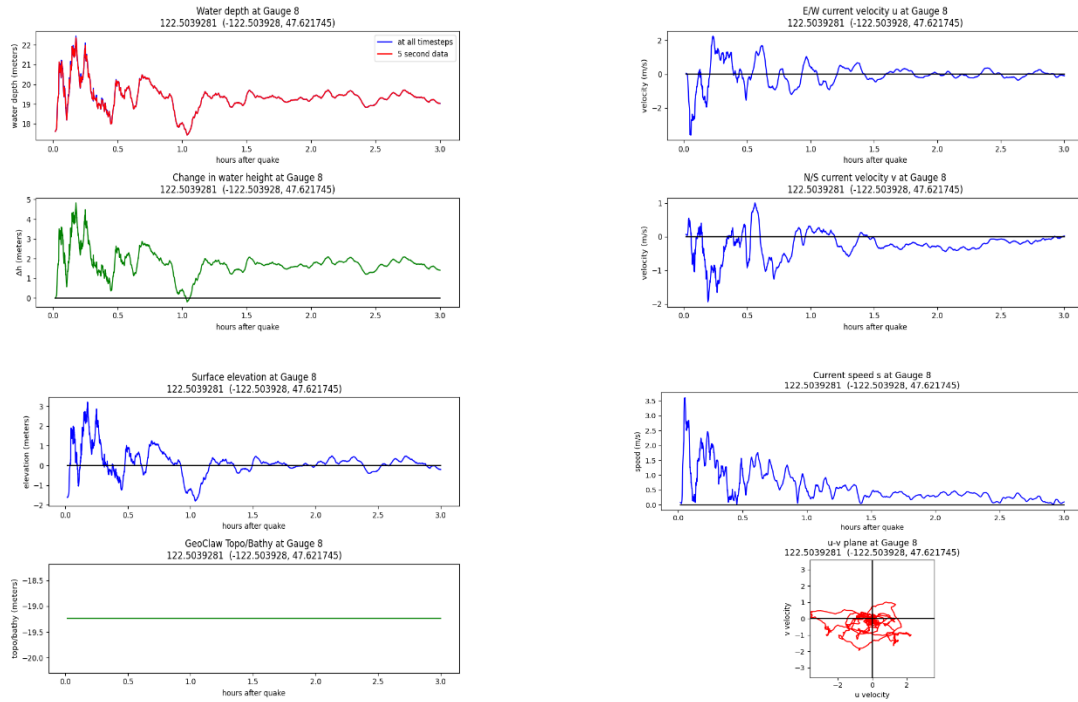
Cascadia subduction zone scenario, MHW:



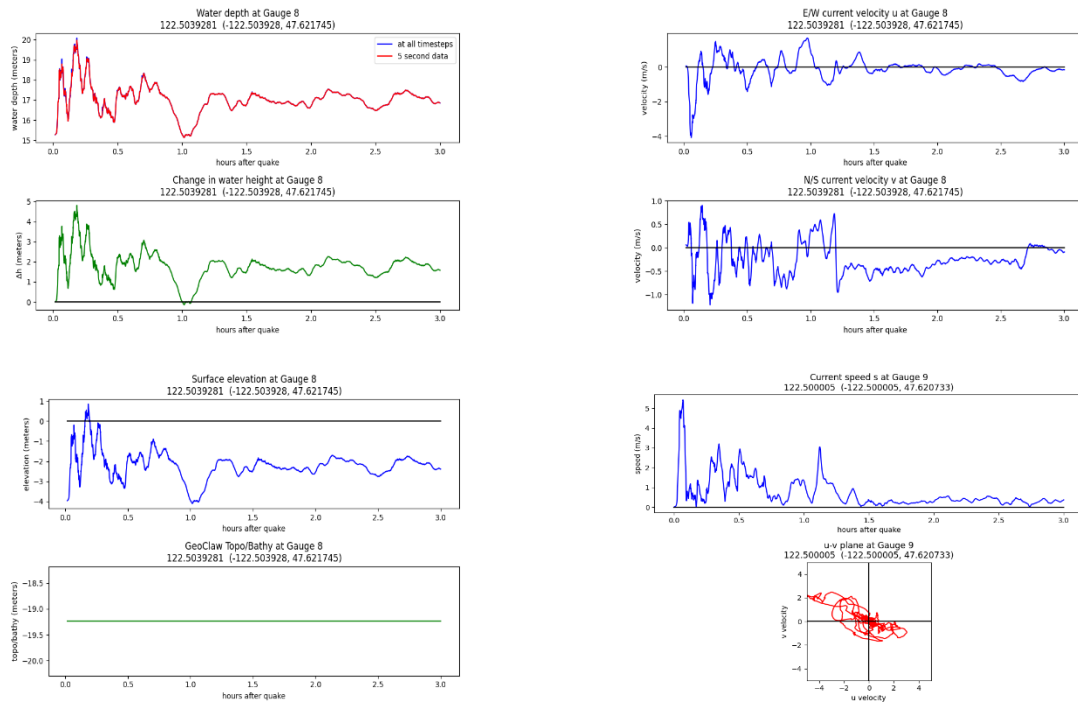
Cascadia subduction zone scenario, MLW:



## Seattle fault scenario, MHW:

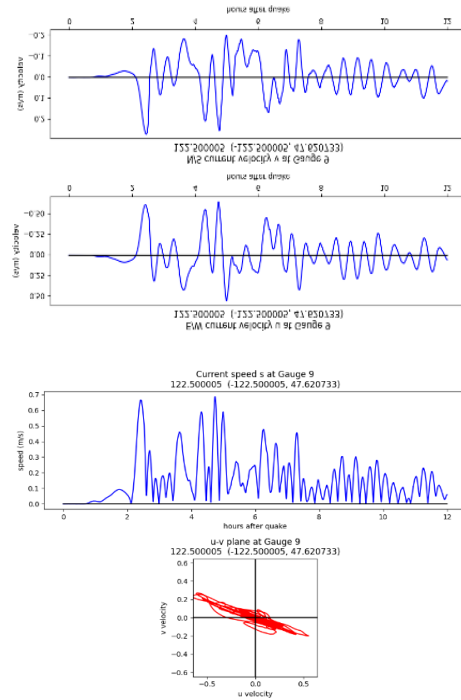
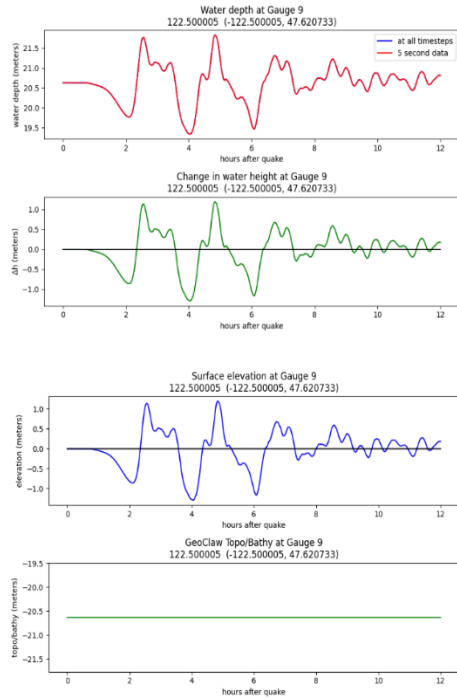


## Seattle fault scenario, MLW:

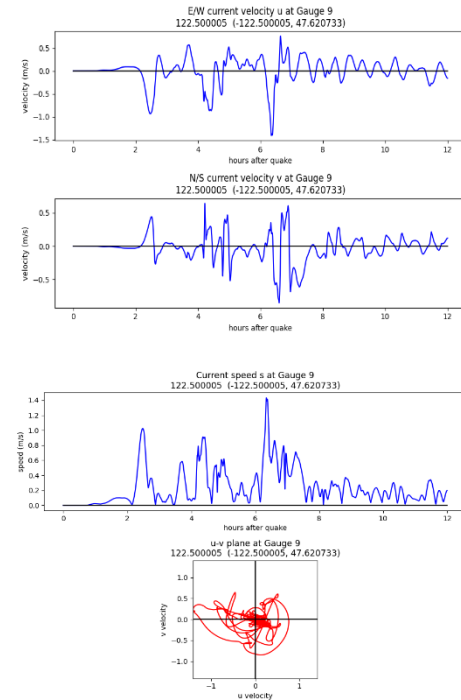
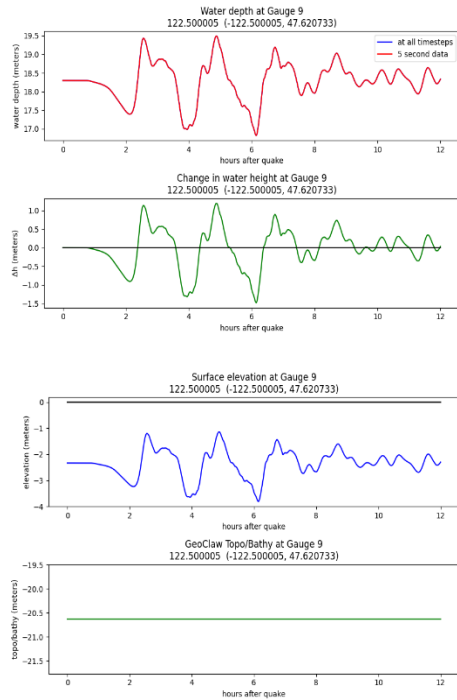




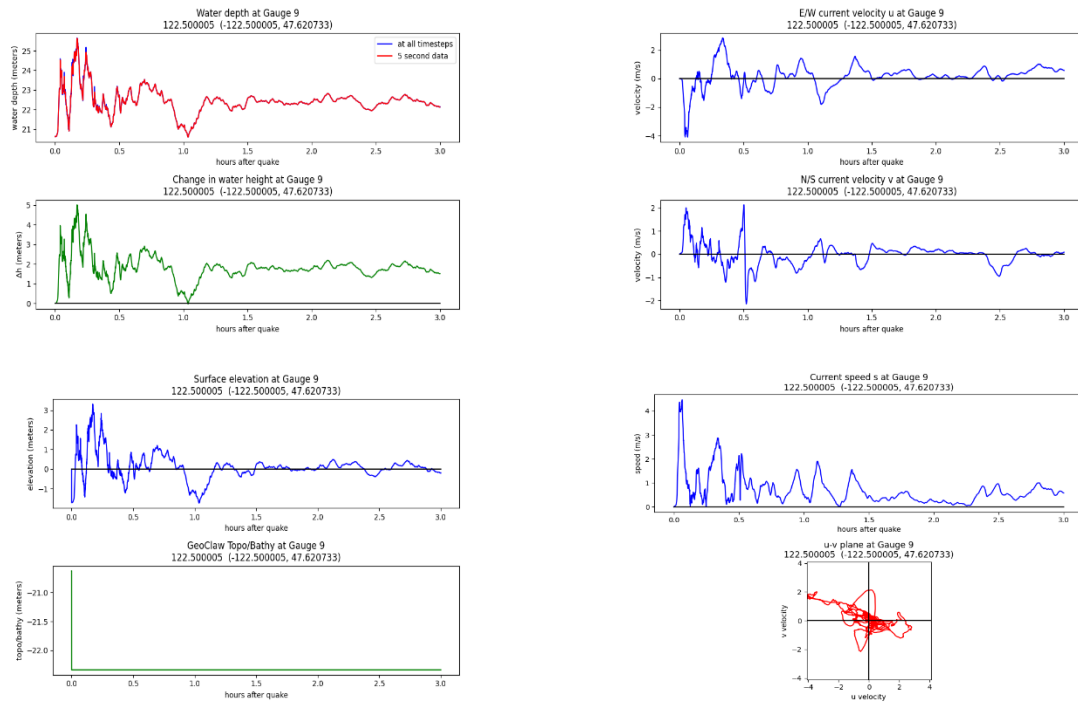
Gauge 9: Center channel 8 (DEM tile boundary)  
 Cascadia subduction zone scenario, MHW:



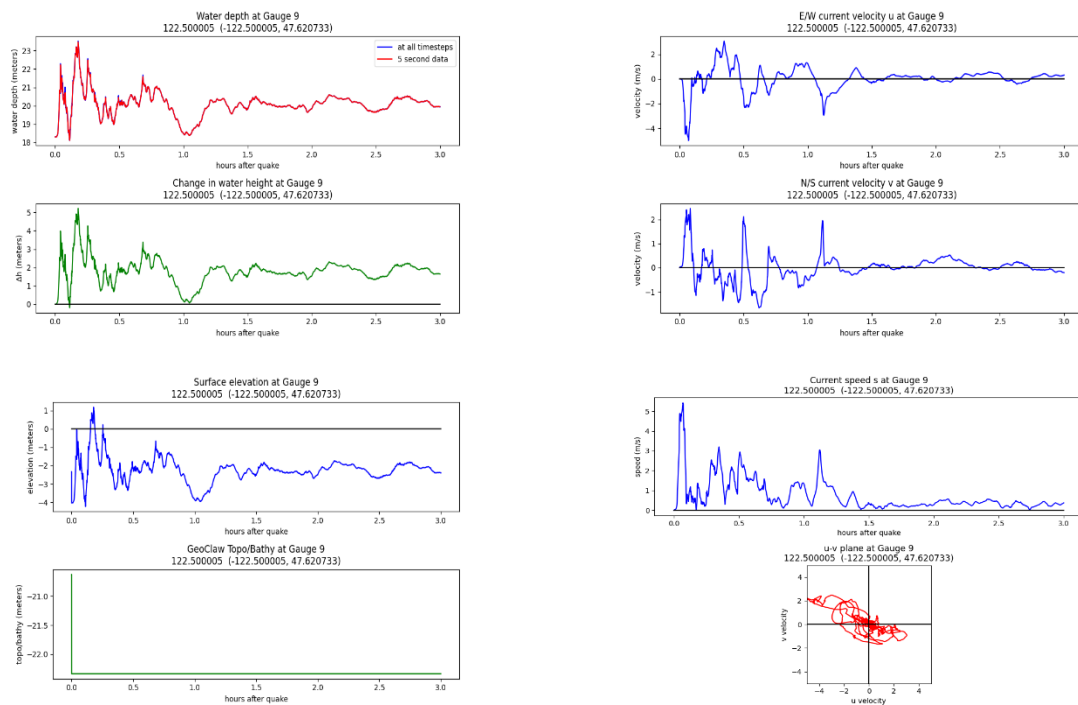
Cascadia subduction zone scenario, MLW:



## Seattle fault scenario, MHW:

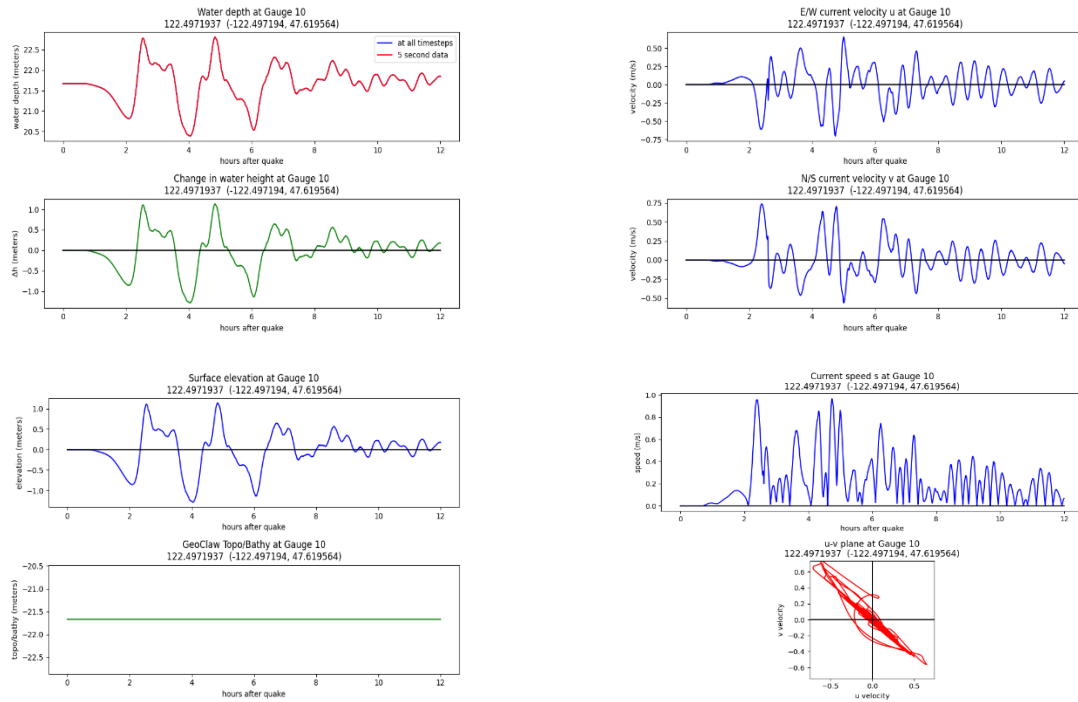


## Seattle fault scenario, MLW:

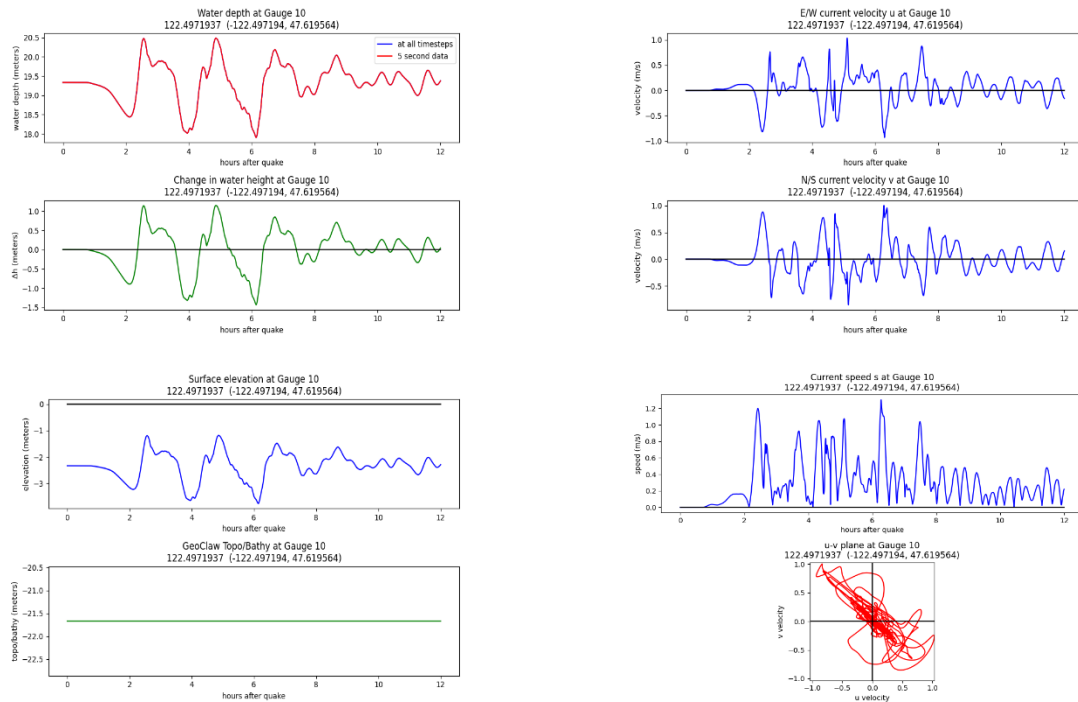


## Gauge 10: Channel entrance

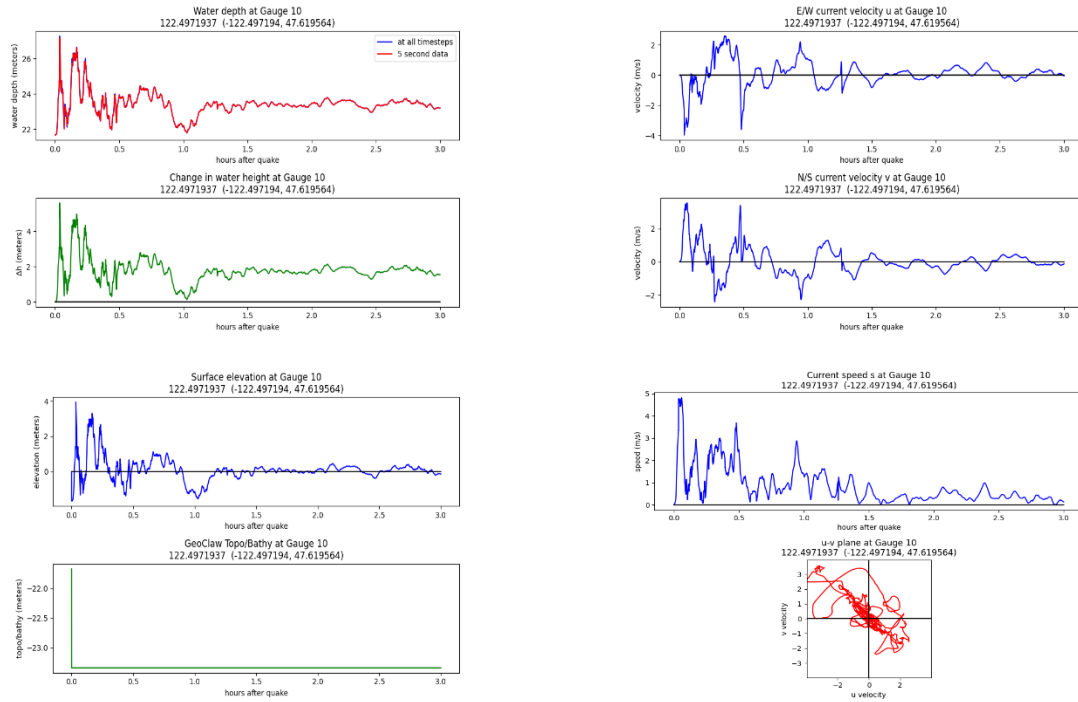
### Cascadia subduction zone scenario, MHW:



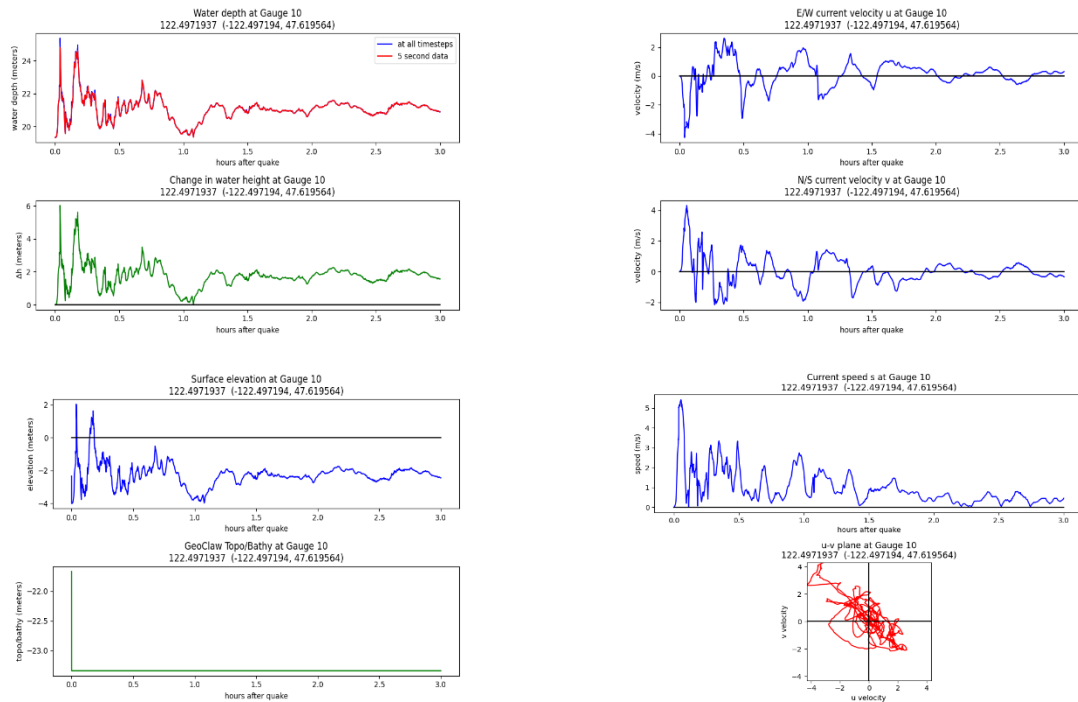
## Cascadia subduction zone scenario, MLW:



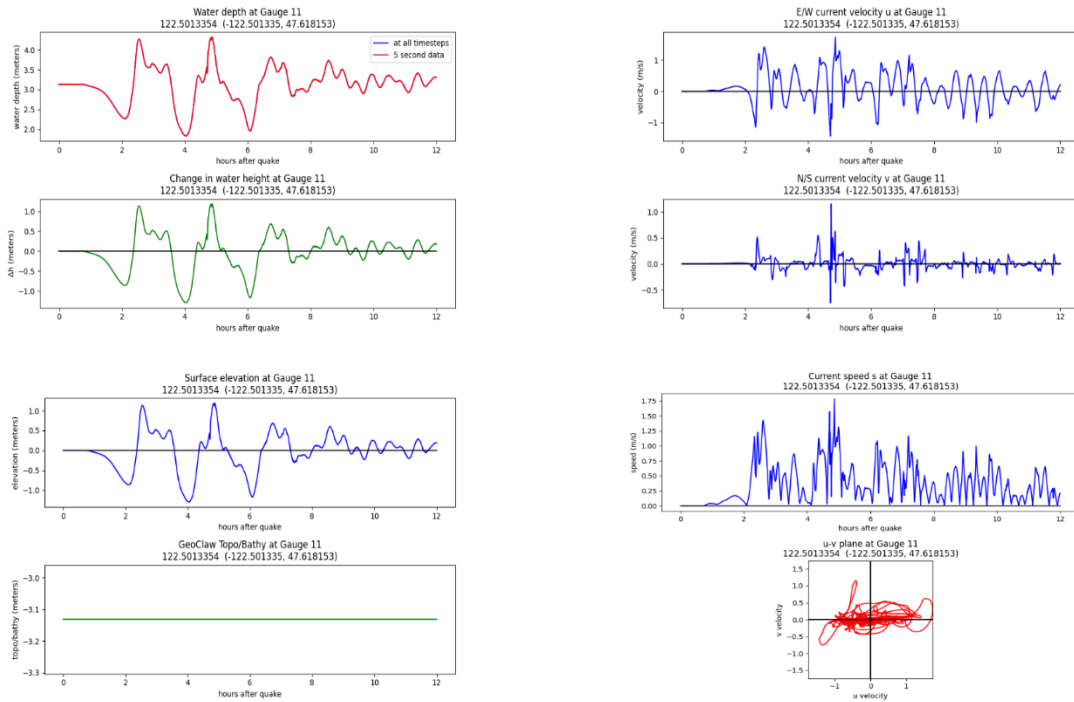
## Seattle fault scenario, MHW:



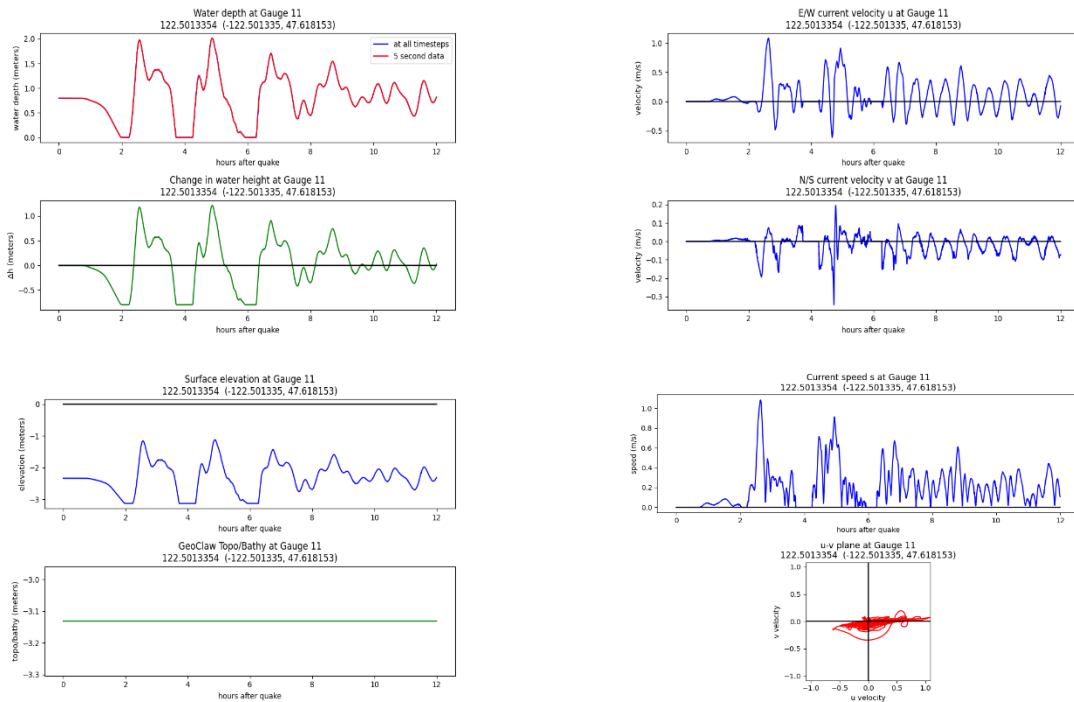
## Seattle fault scenario, MLW:



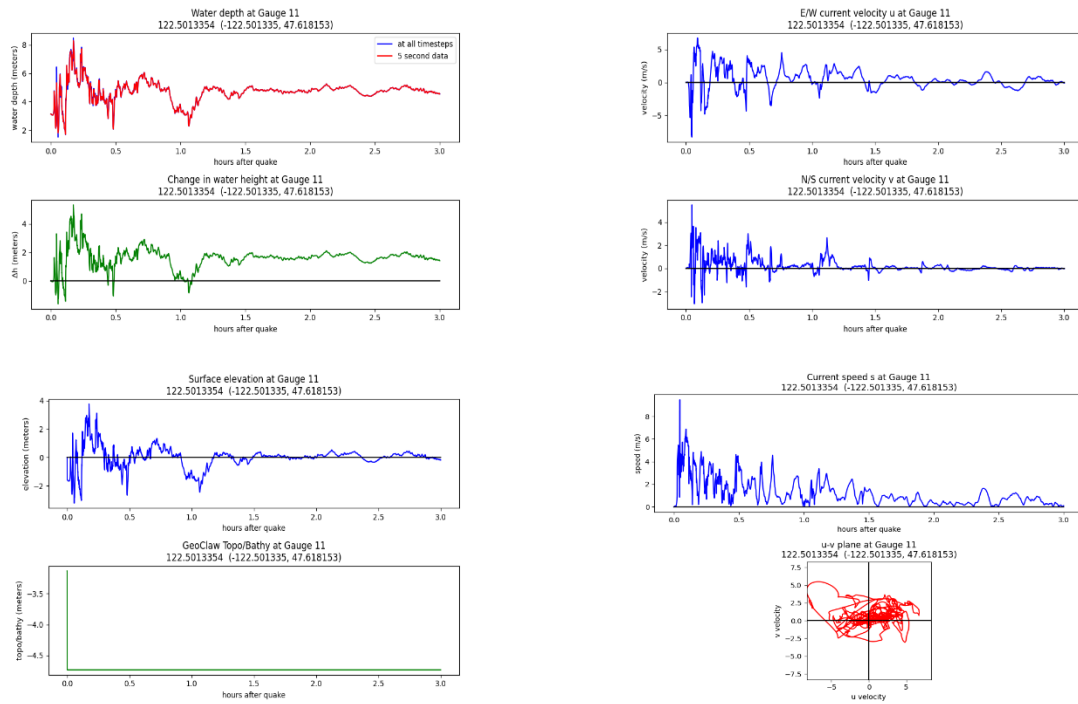
## Gauge 11: Offshore Pritchard Park Cascadia subduction zone scenario, MHW:



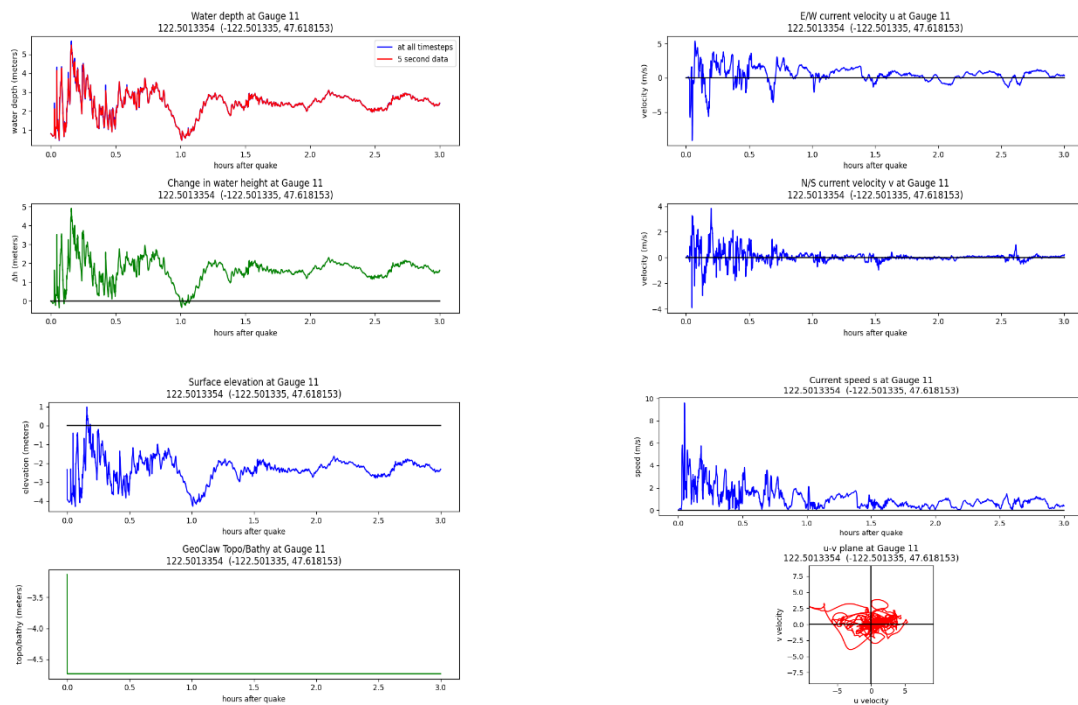
## Cascadia subduction zone scenario, MLW:



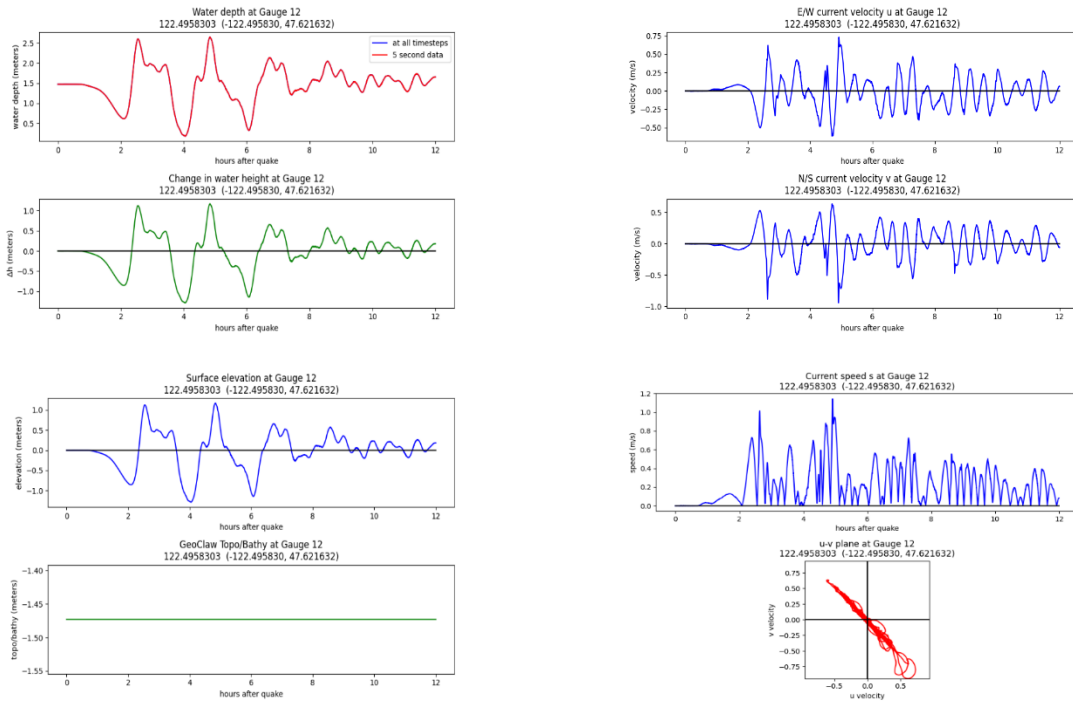
## Seattle fault scenario, MHW:



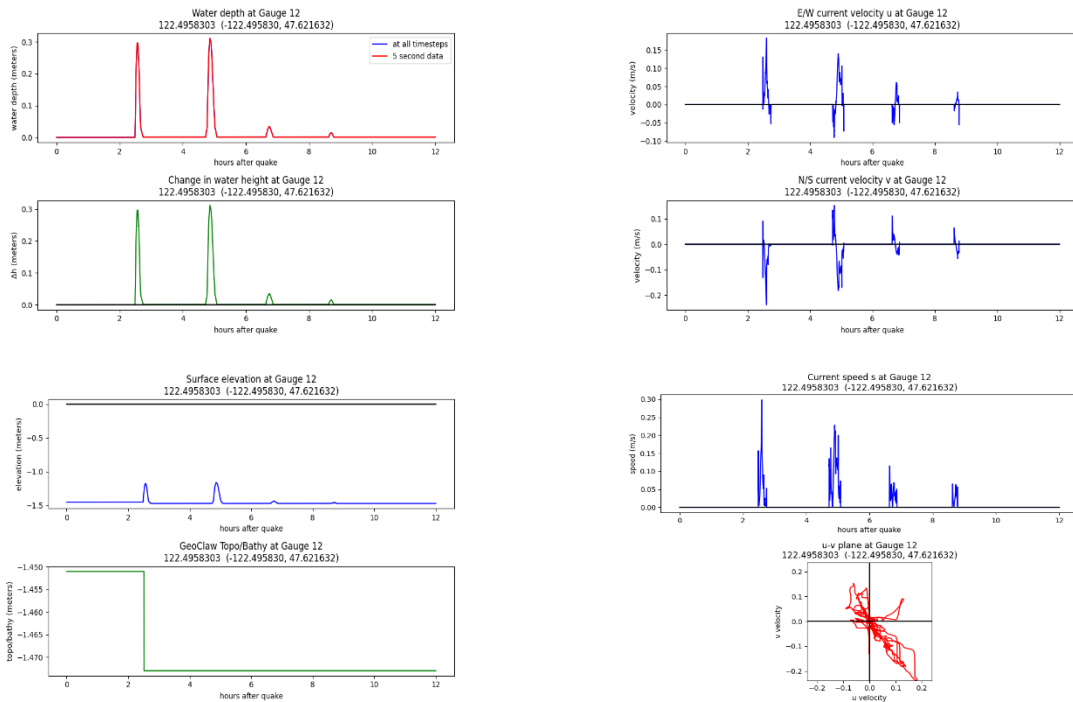
## Seattle fault scenario, MLW:



Gauge 12: West of Wing Point Rd NE  
 Cascadia subduction zone scenario, MHW:

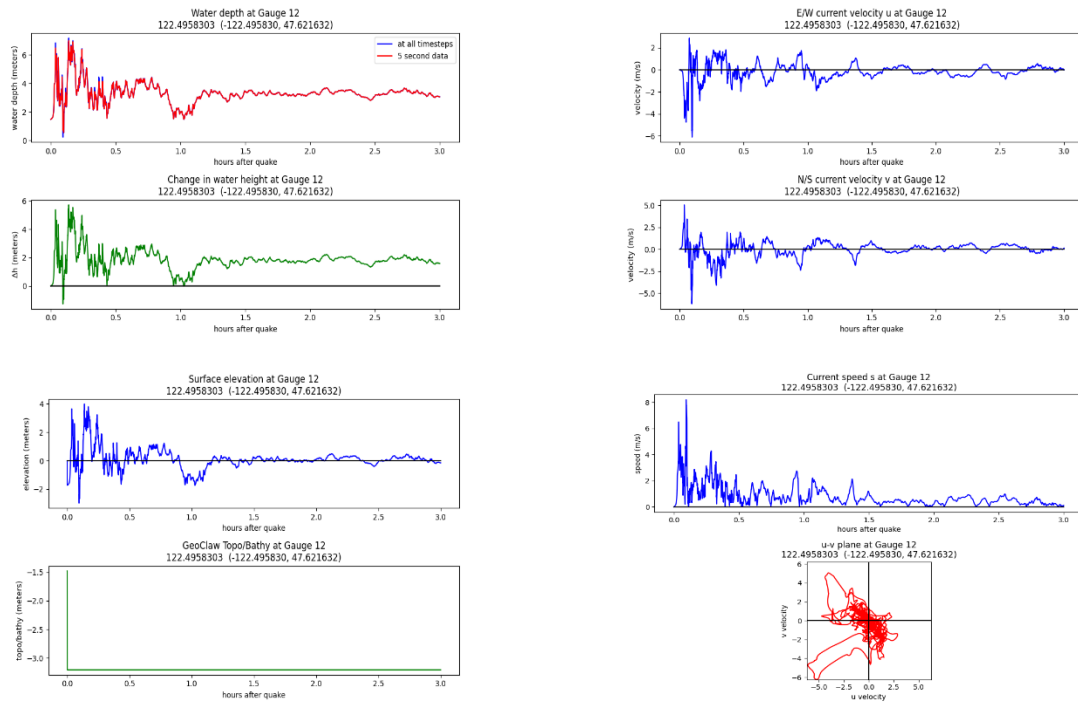


Cascadia subduction zone scenario, MLW:

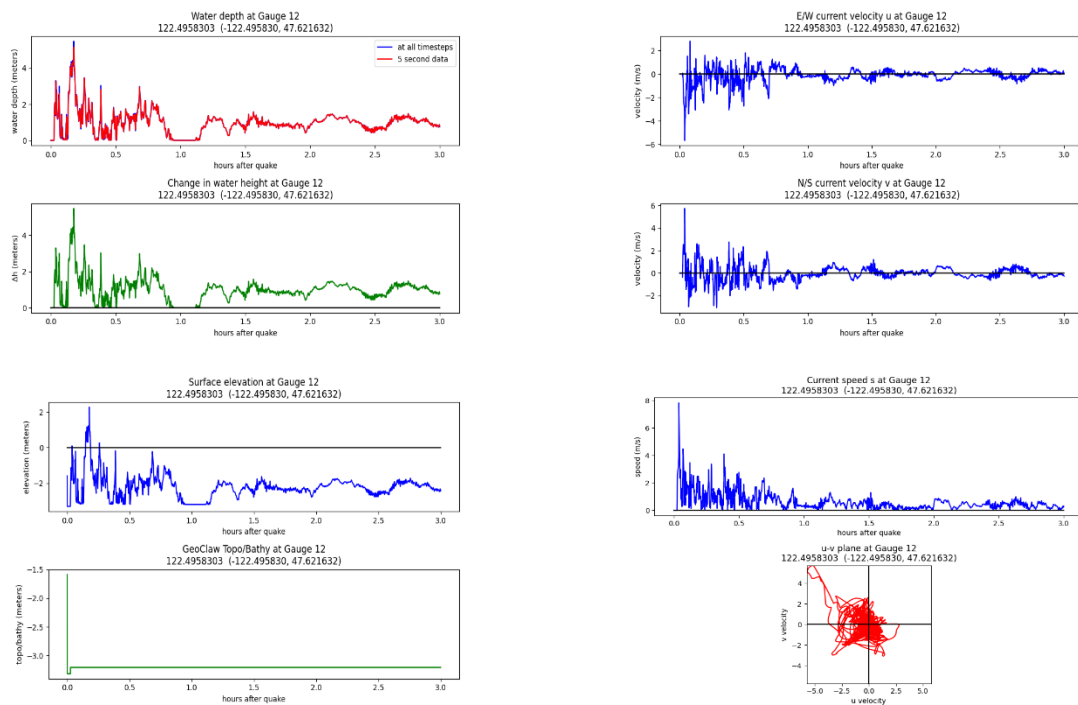




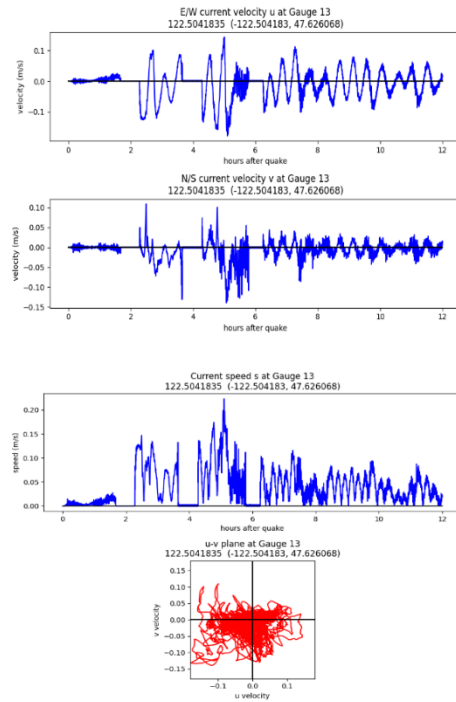
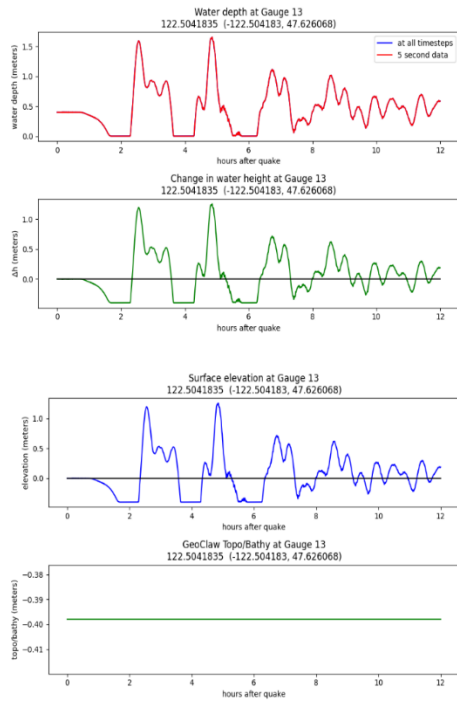
## Seattle fault scenario, MHW:



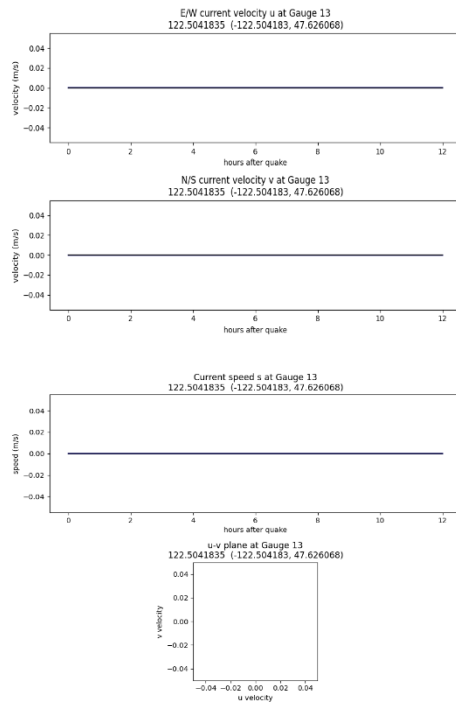
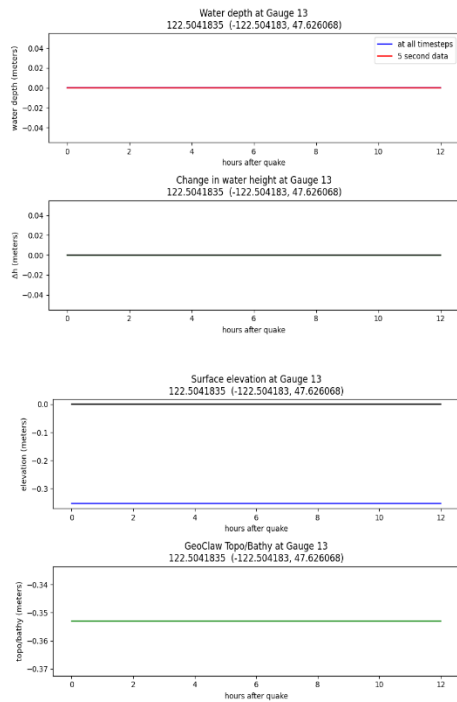
## Seattle fault scenario, MLW:



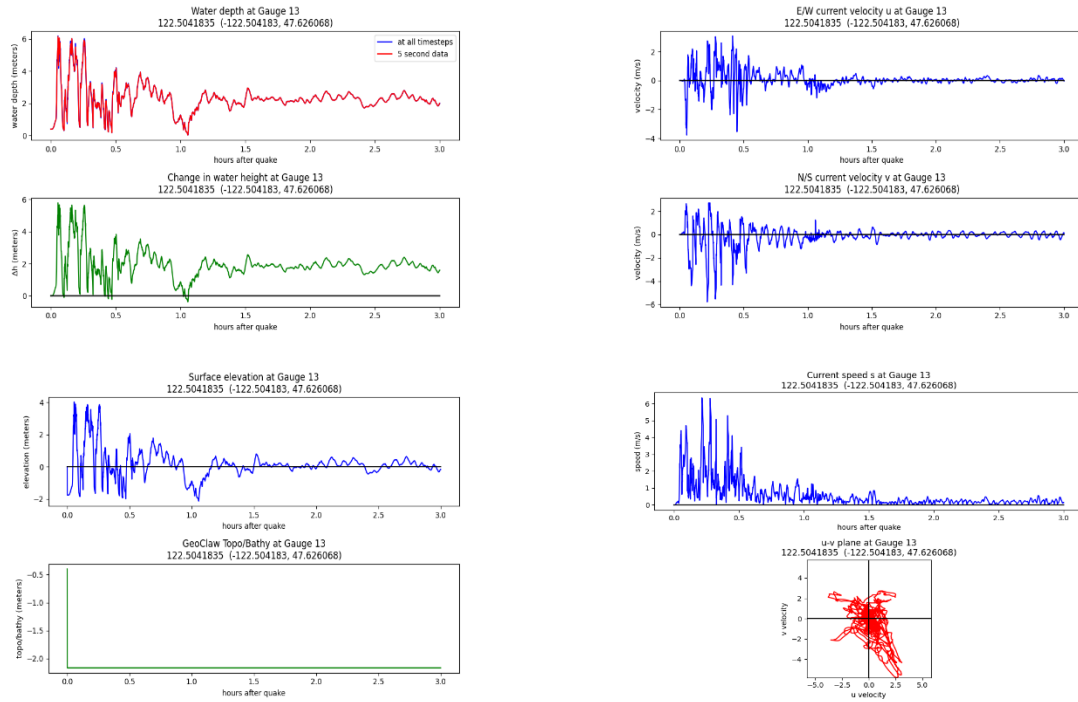
## Gauge 13: South of Hawley Cove Park Cascadia subduction zone scenario, MHW:



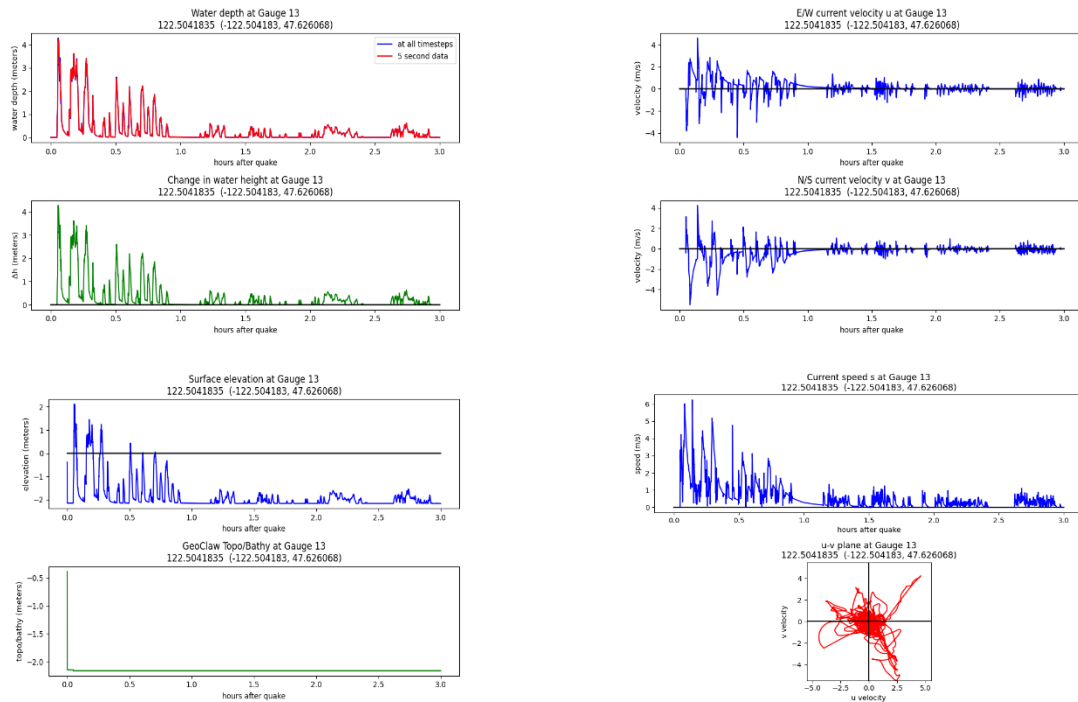
## Cascadia subduction zone scenario, MLW:



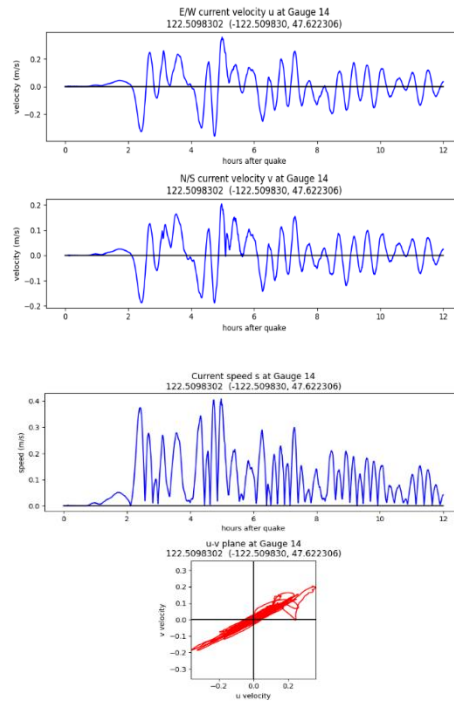
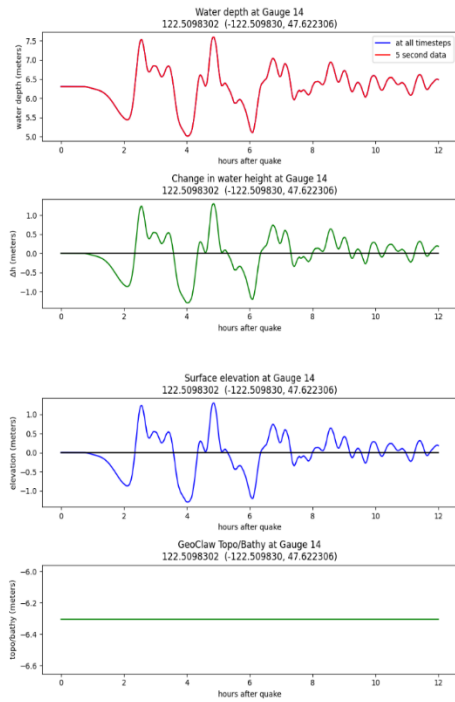
## Seattle fault scenario, MHW:



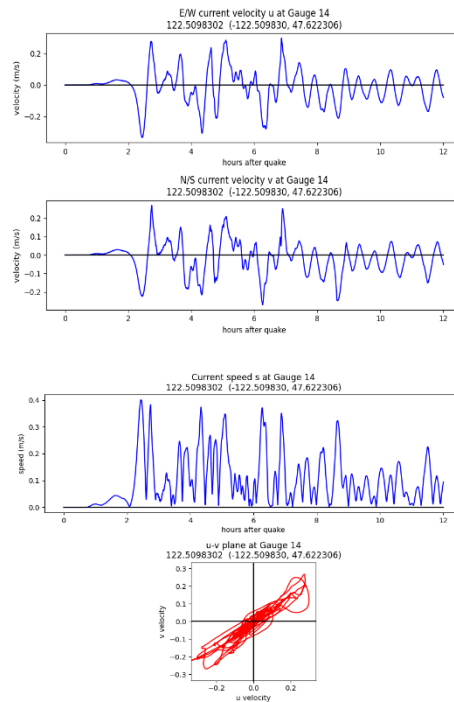
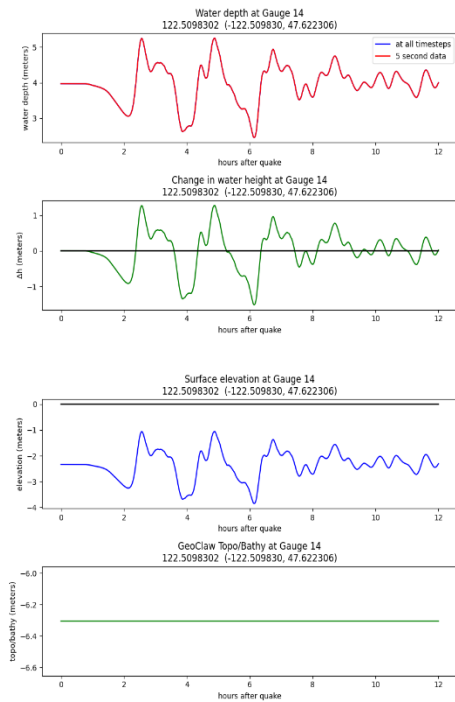
## Seattle fault scenario, MLW:



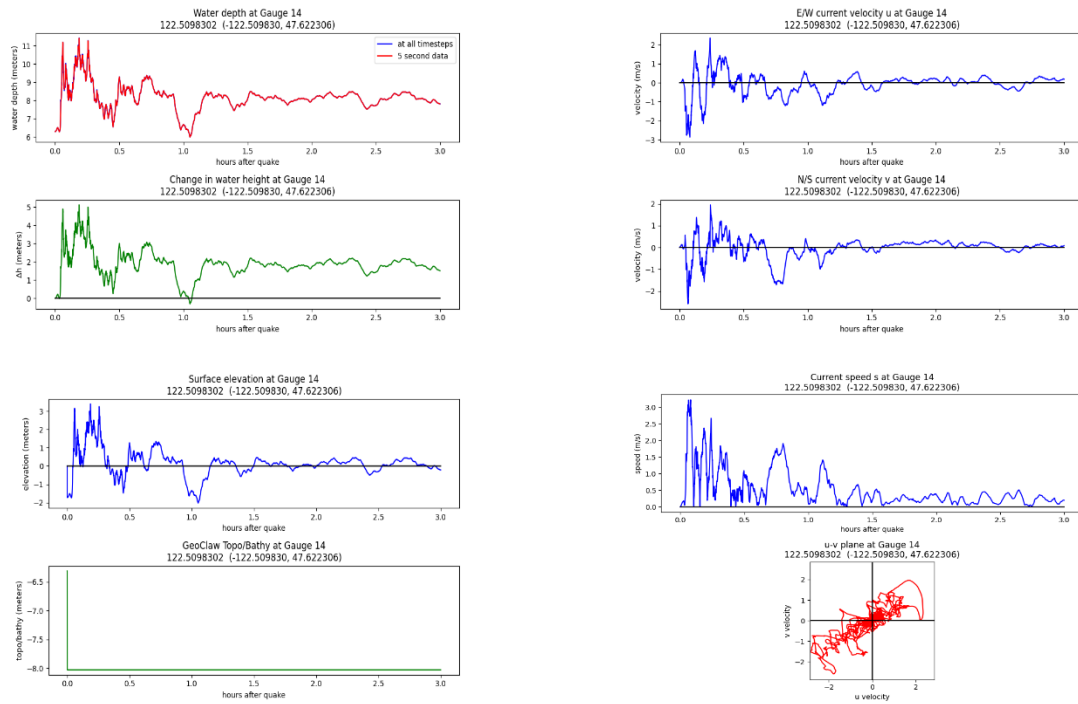
## Gauge 14: Bainbridge Island Ferry Terminal 1 Cascadia subduction zone scenario, MHW:



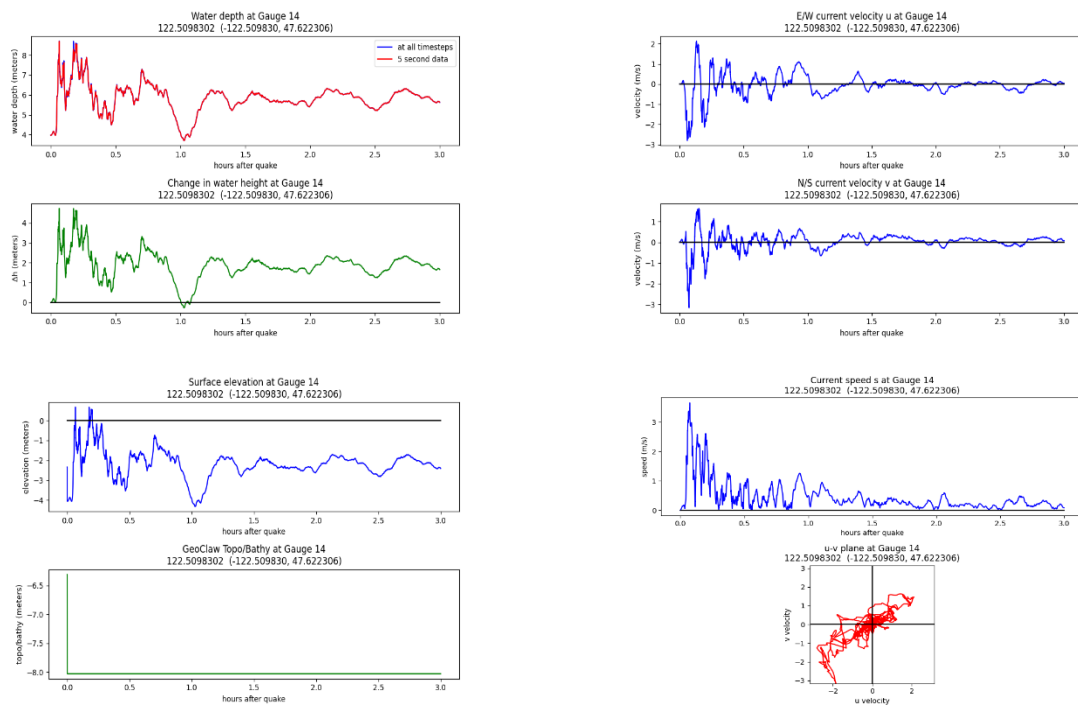
## Cascadia subduction zone scenario, MLW:



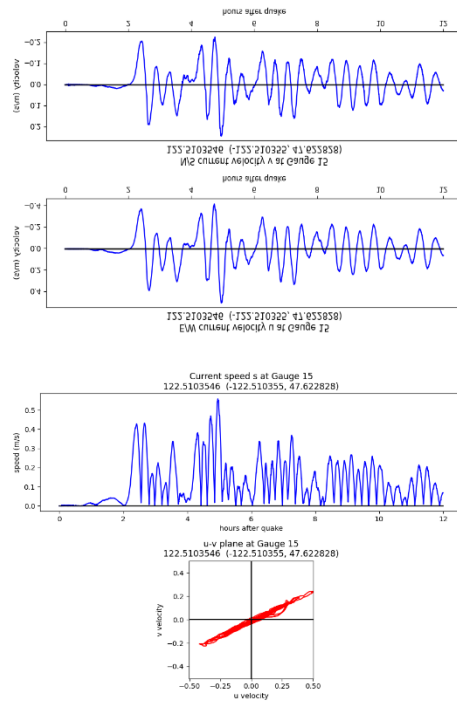
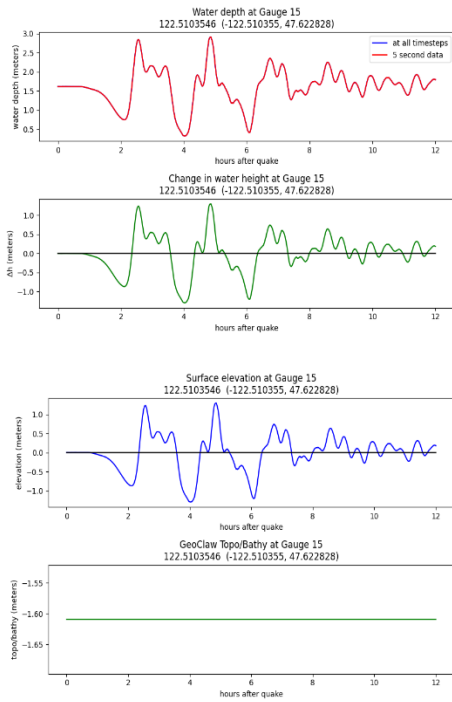
## Seattle fault scenario, MHW:



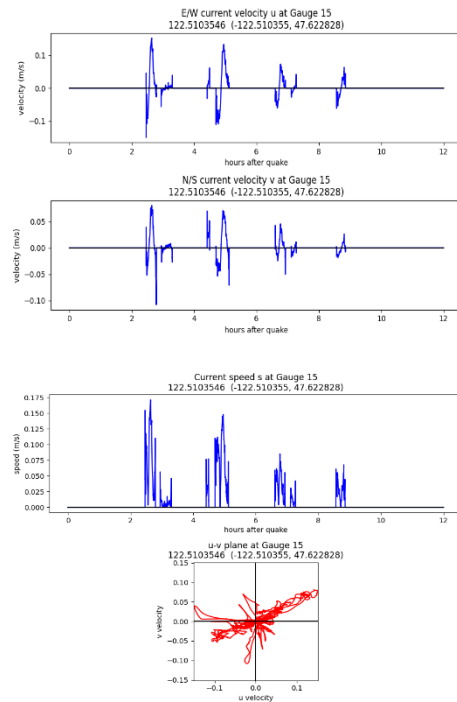
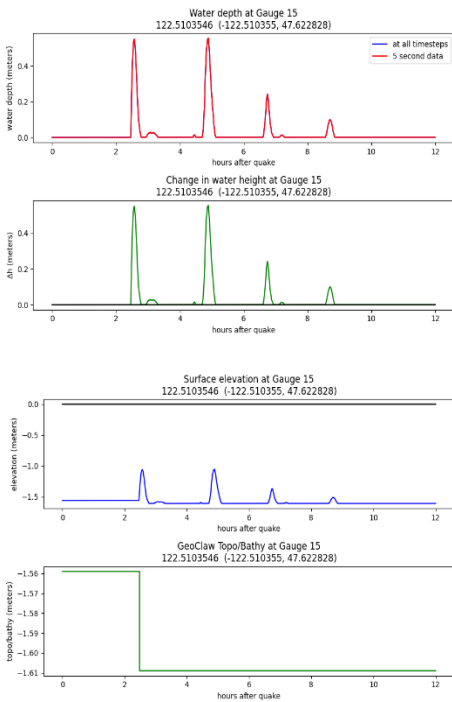
## Seattle fault scenario, MLW:



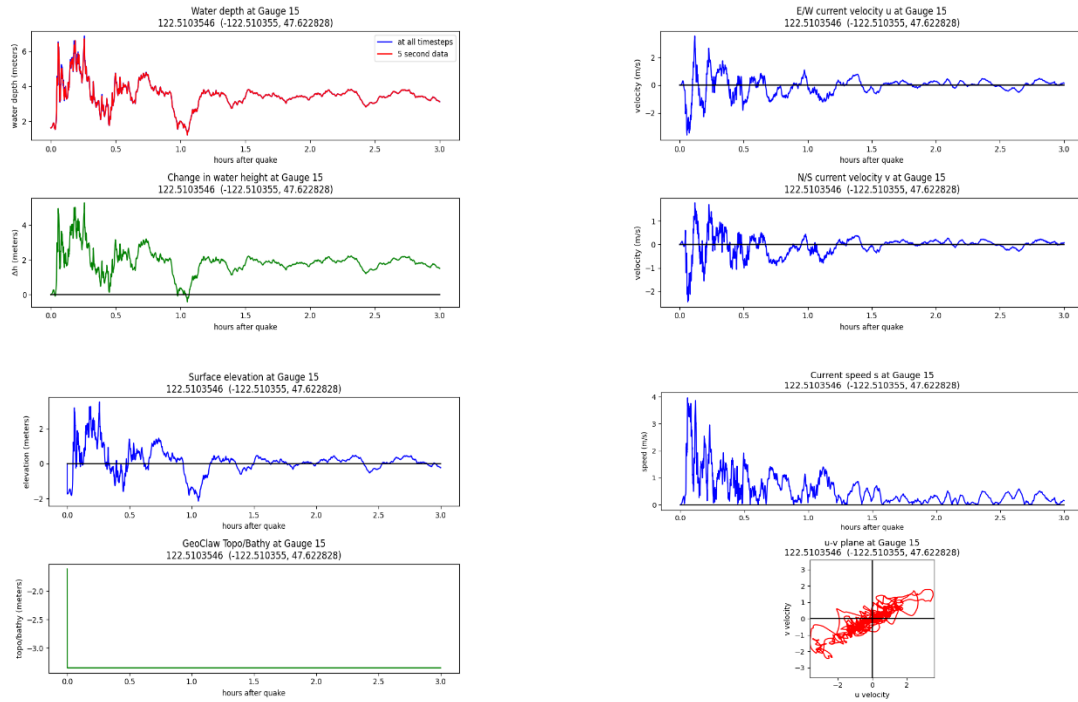
## Gauge 15: Bainbridge Island Ferry Terminal 2 Cascadia subduction zone scenario, MHW:



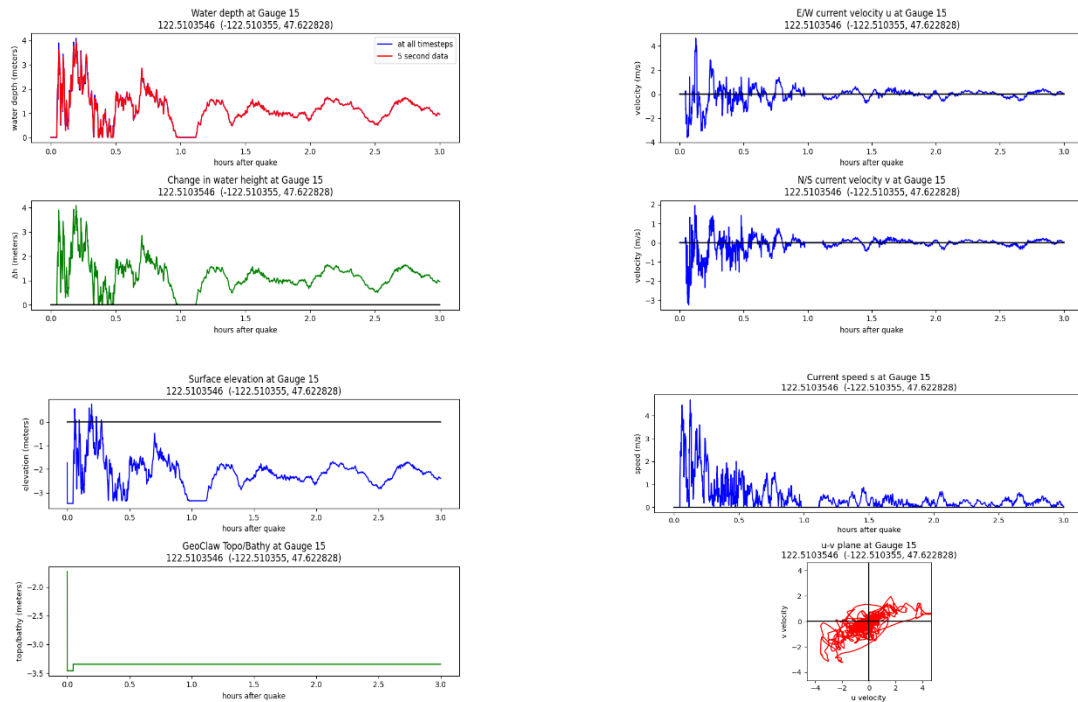
## Cascadia subduction zone scenario, MLW:



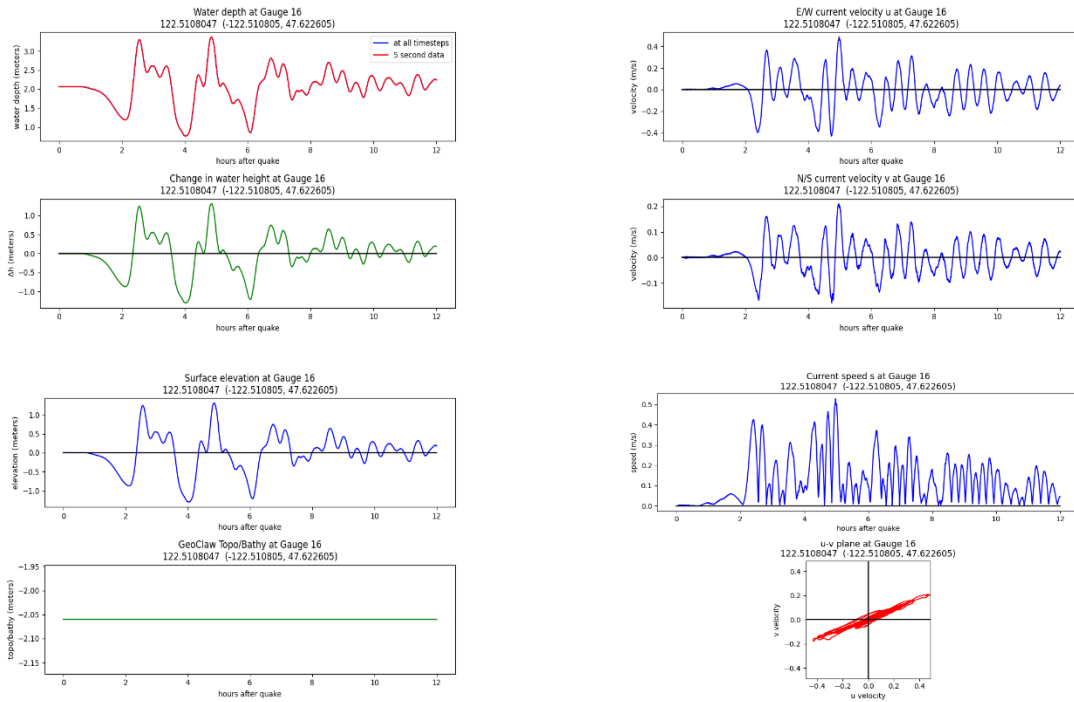
## Seattle fault scenario, MHW:



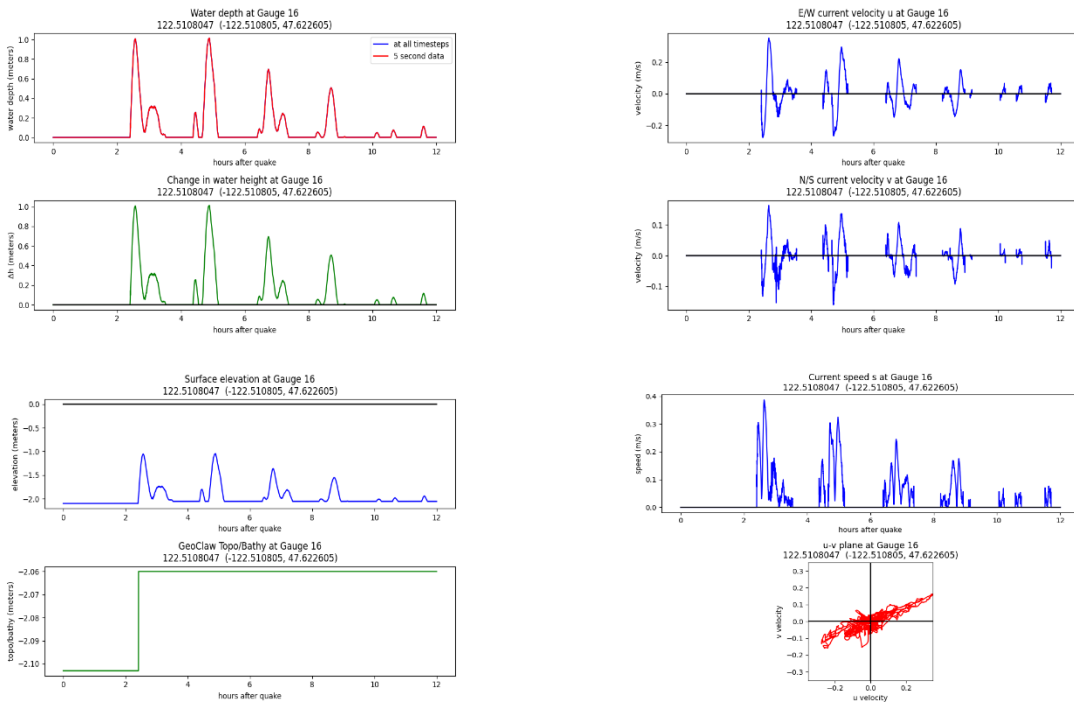
## Seattle fault scenario, MLW:



## Gauge 16: Bainbridge Island Ferry Terminal 3 Cascadia subduction zone scenario, MHW:

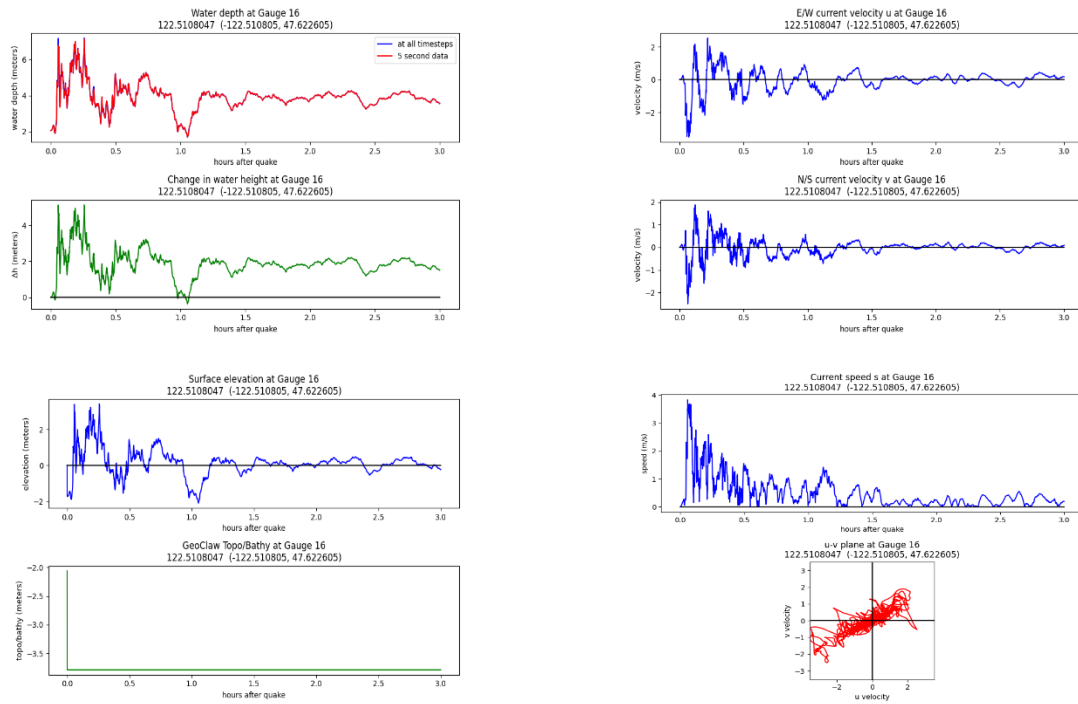


## Cascadia subduction zone scenario, MLW:

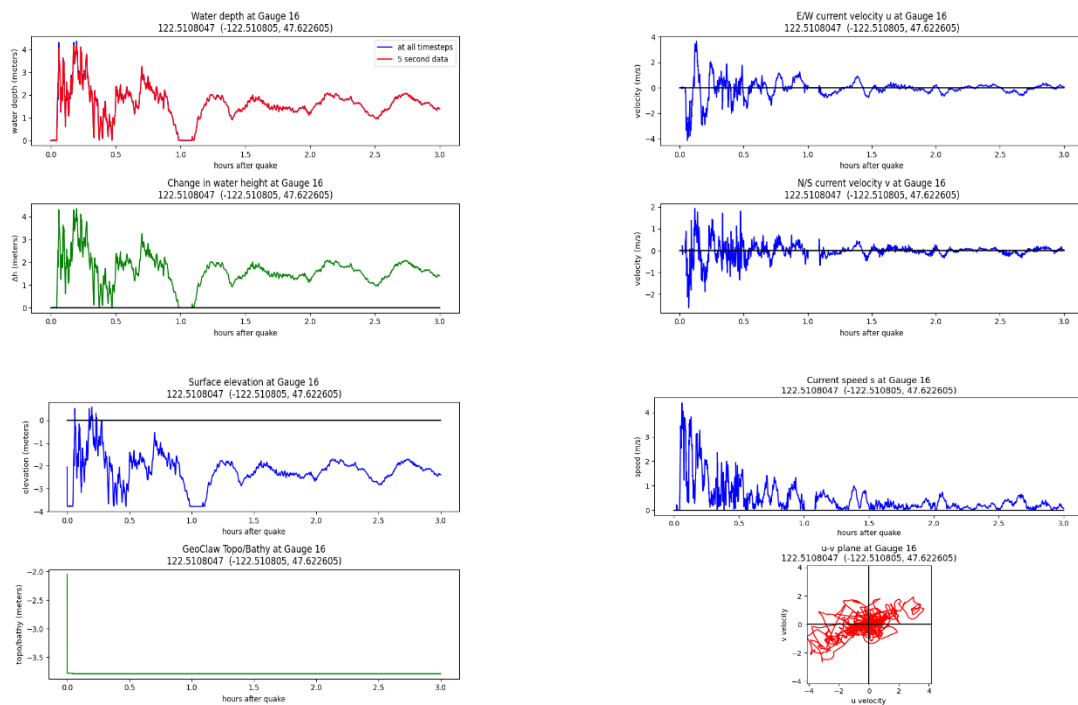




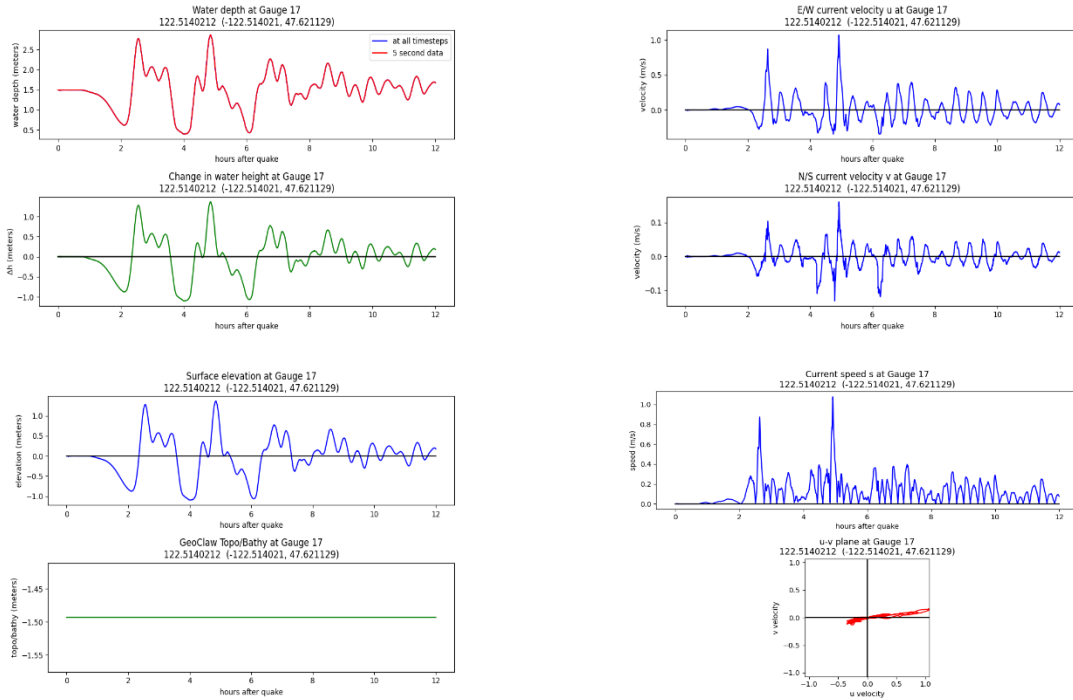
## Seattle fault scenario, MHW:



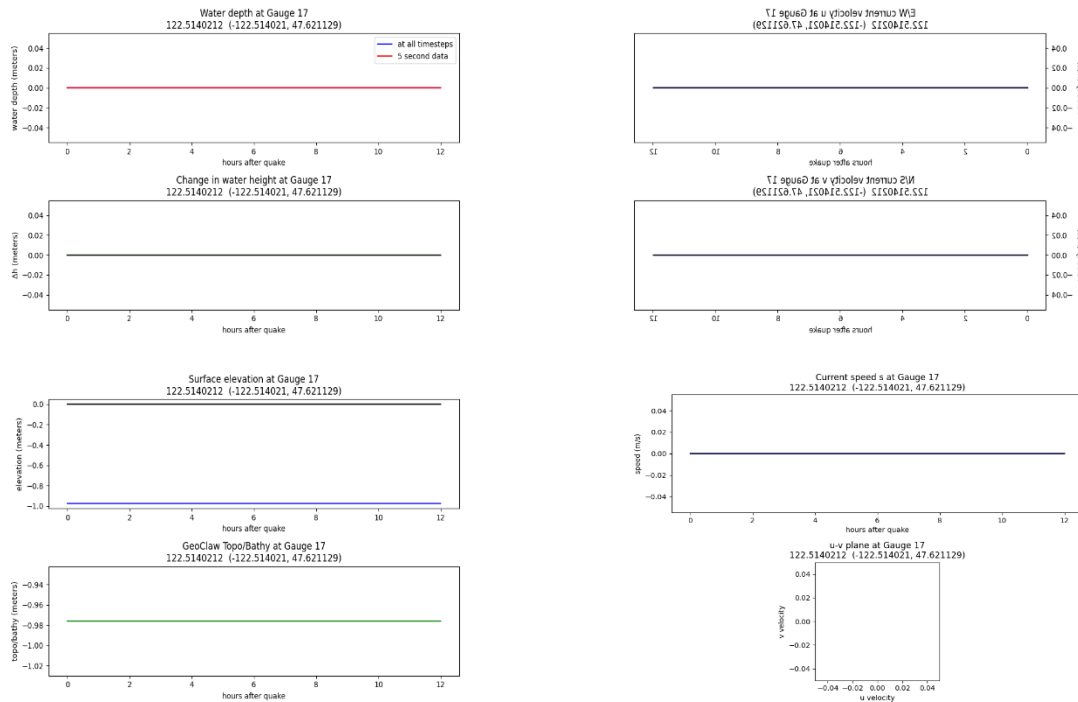
## Seattle fault scenario, MLW:



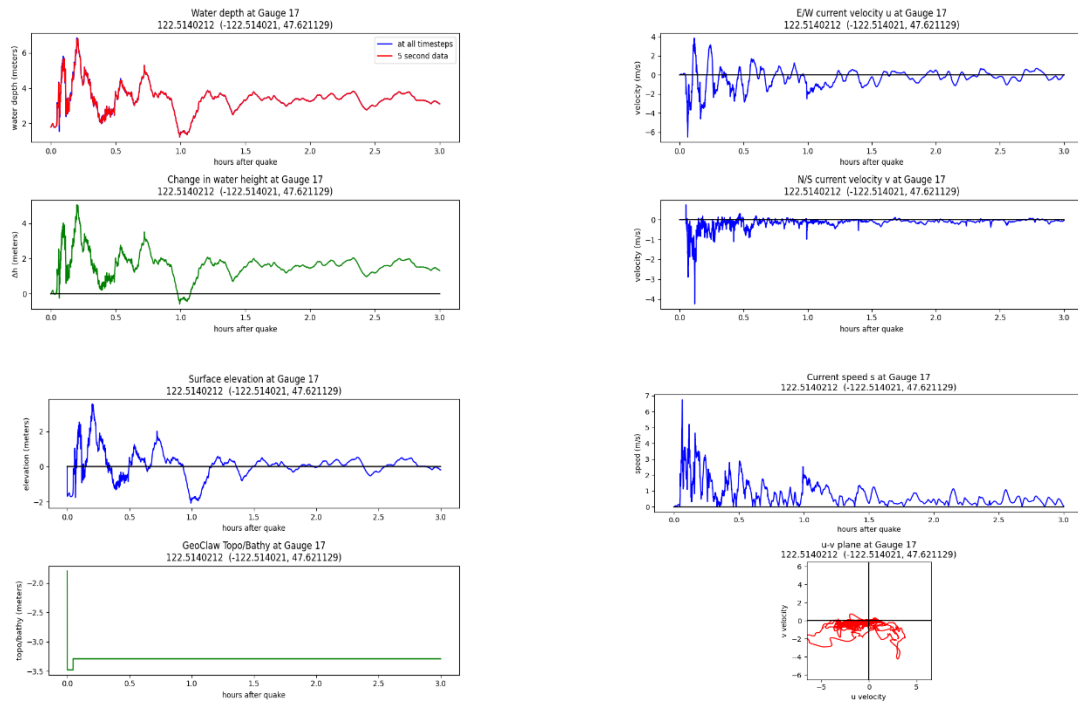
## Gauge 17: Offshore WSF Maintenance Facility Cascadia subduction zone scenario, MHW:



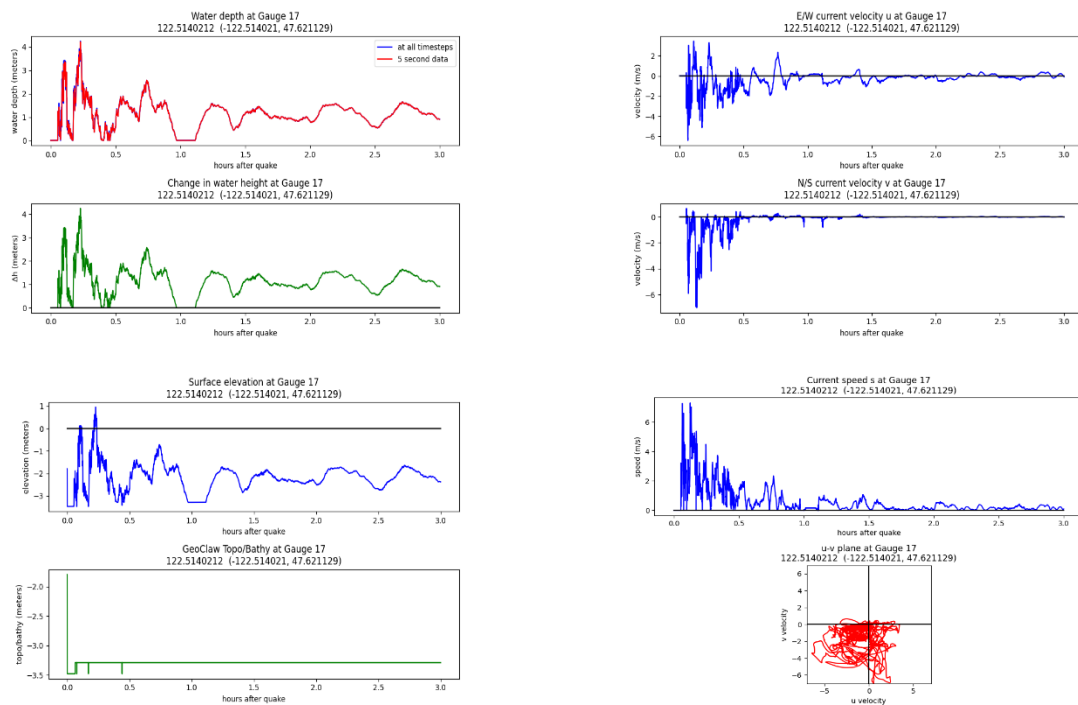
## Cascadia subduction zone scenario, MLW:



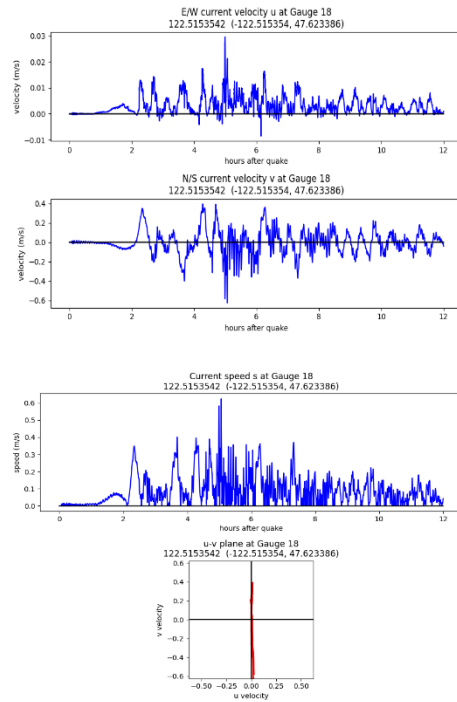
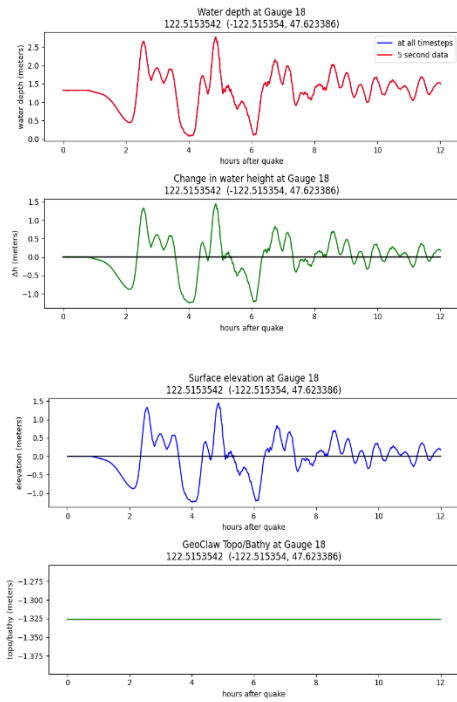
## Seattle fault scenario, MHW:



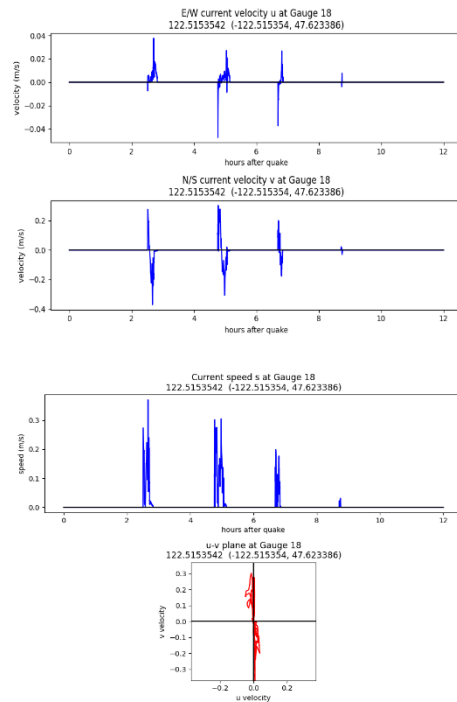
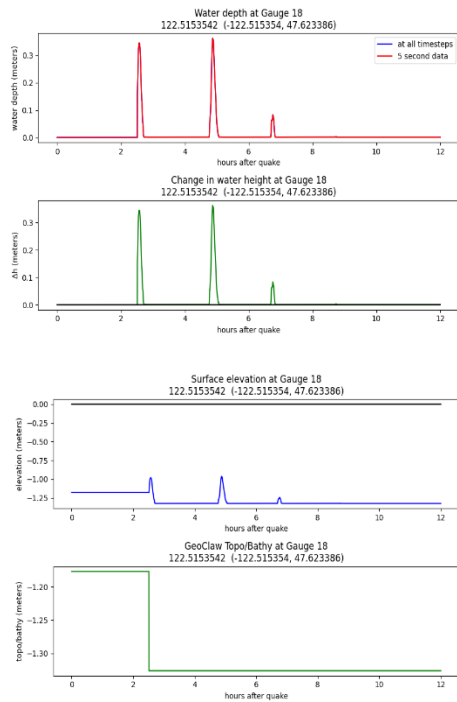
## Seattle fault scenario, MLW:



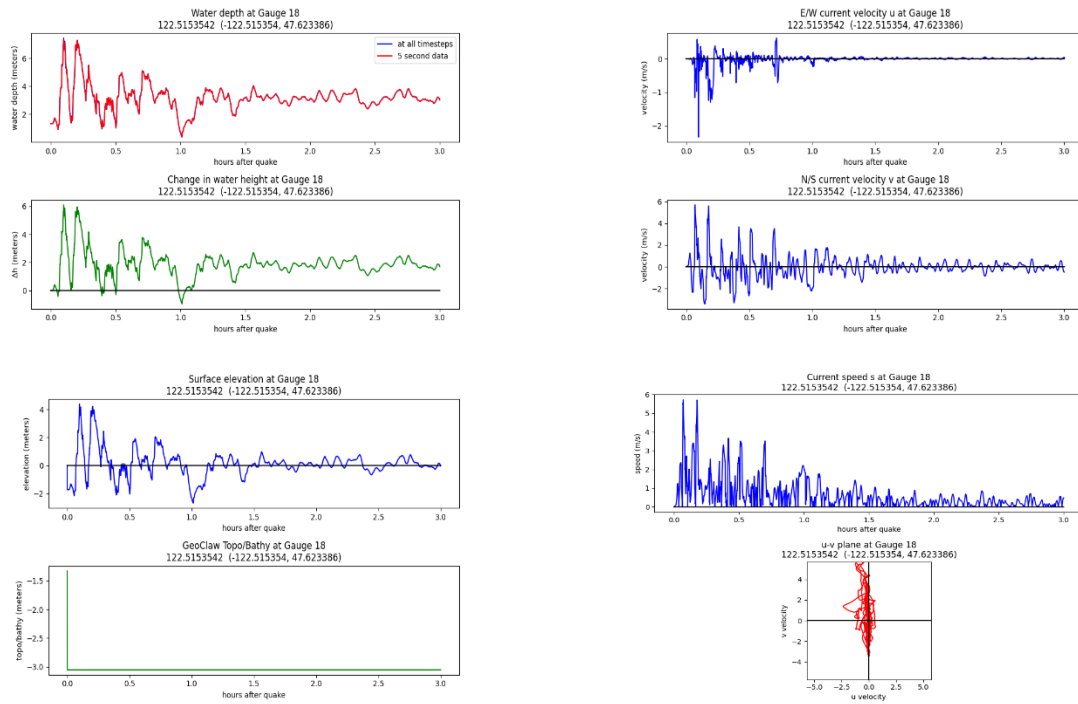
## Gauge 18: Offshore Waterfront Trail bridge Cascadia subduction zone scenario, MHW:



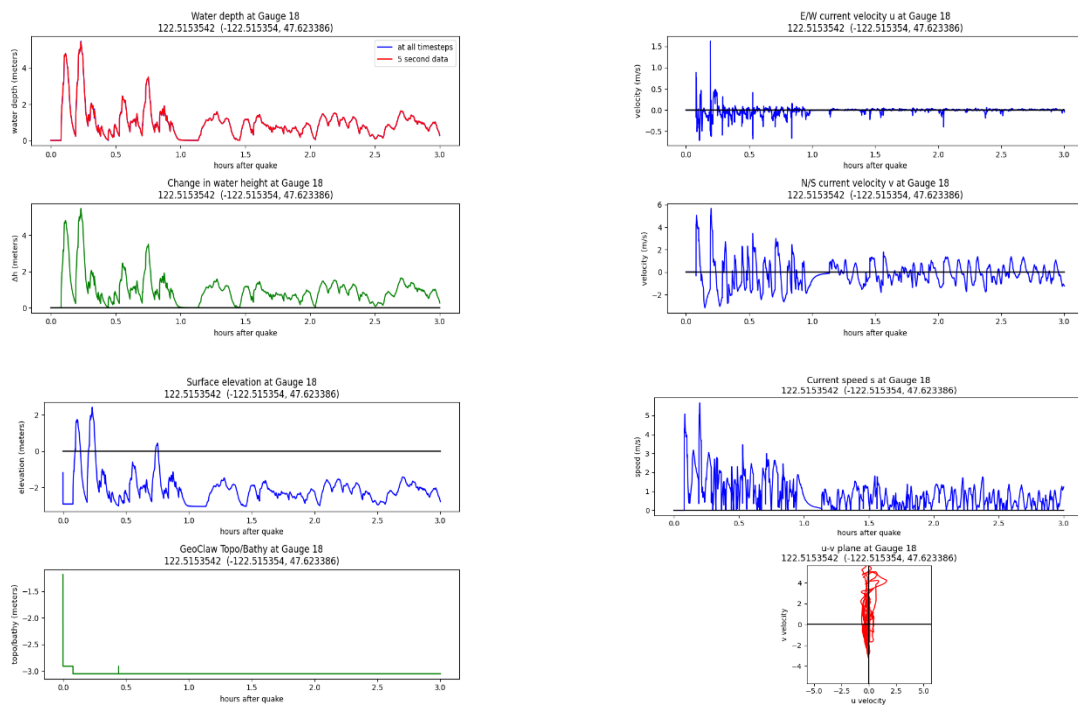
## Cascadia subduction zone scenario, MLW:



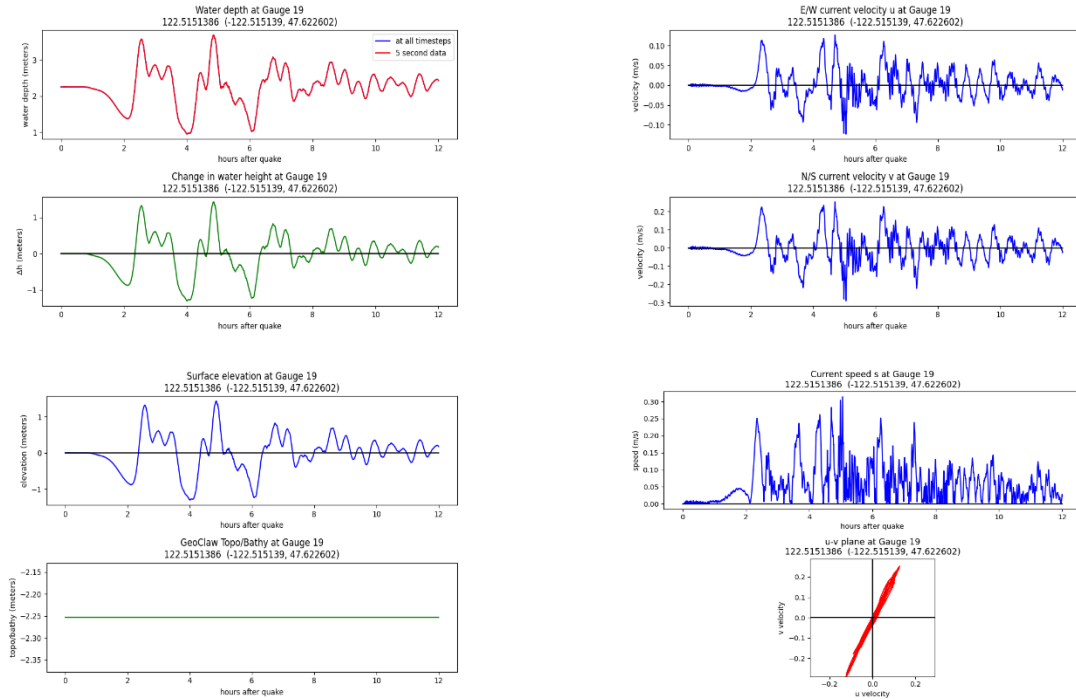
## Seattle fault scenario, MHW:



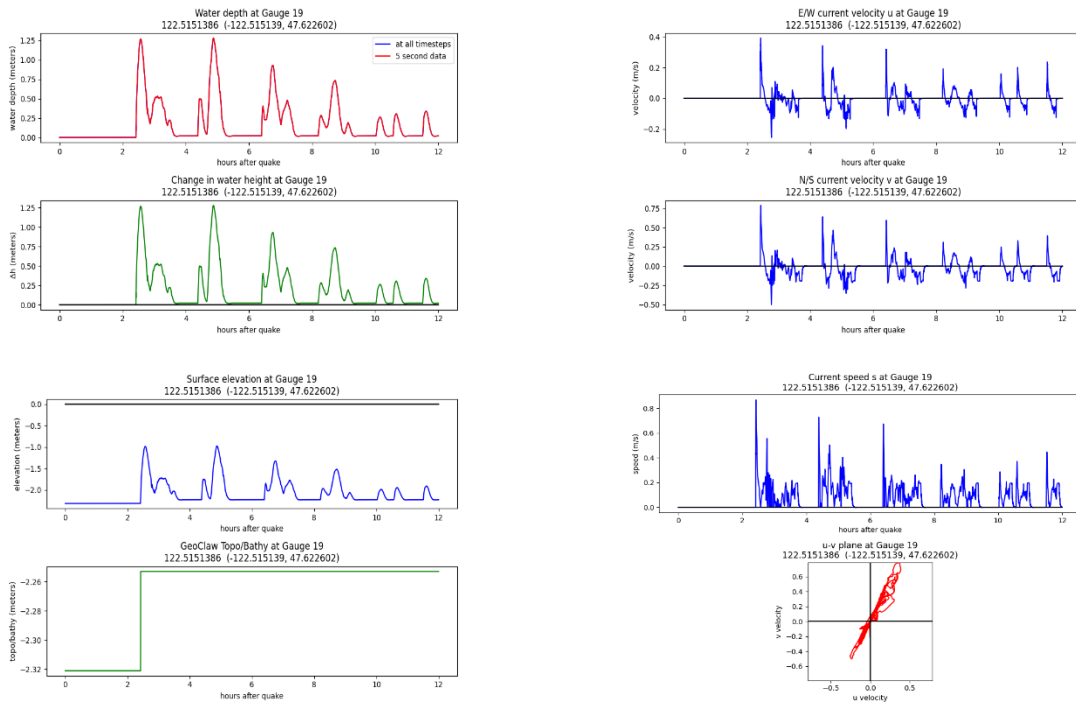
## Seattle fault scenario, MLW:



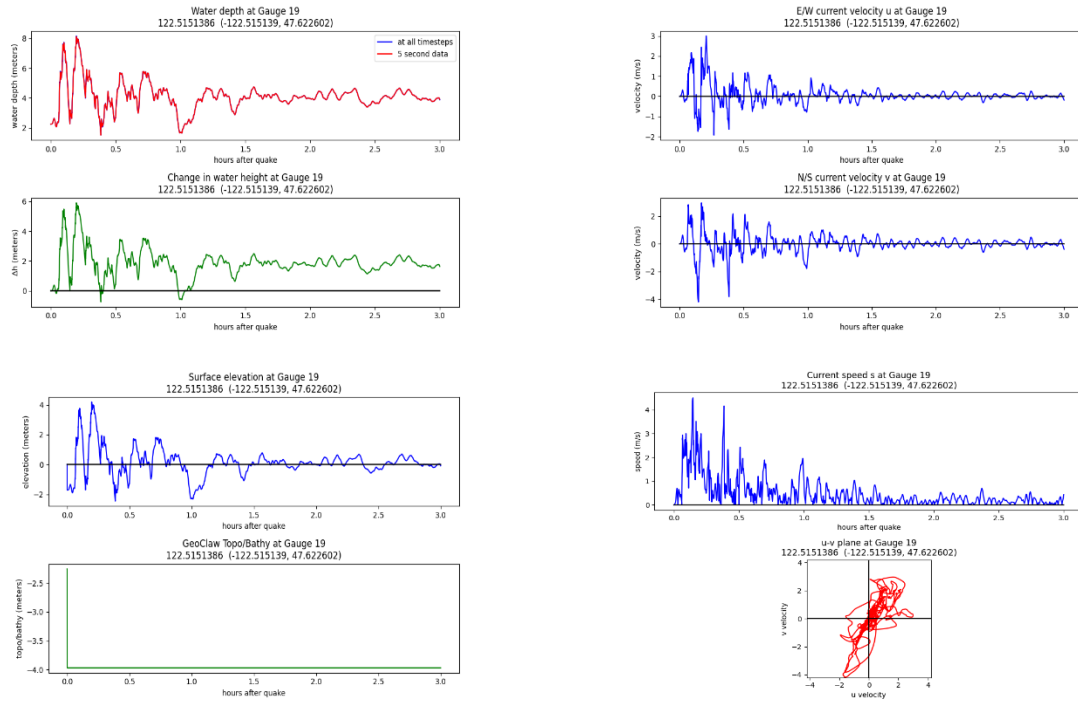
Gauge 19: West of WSF parking lot  
 Cascadia subduction zone scenario, MHW:



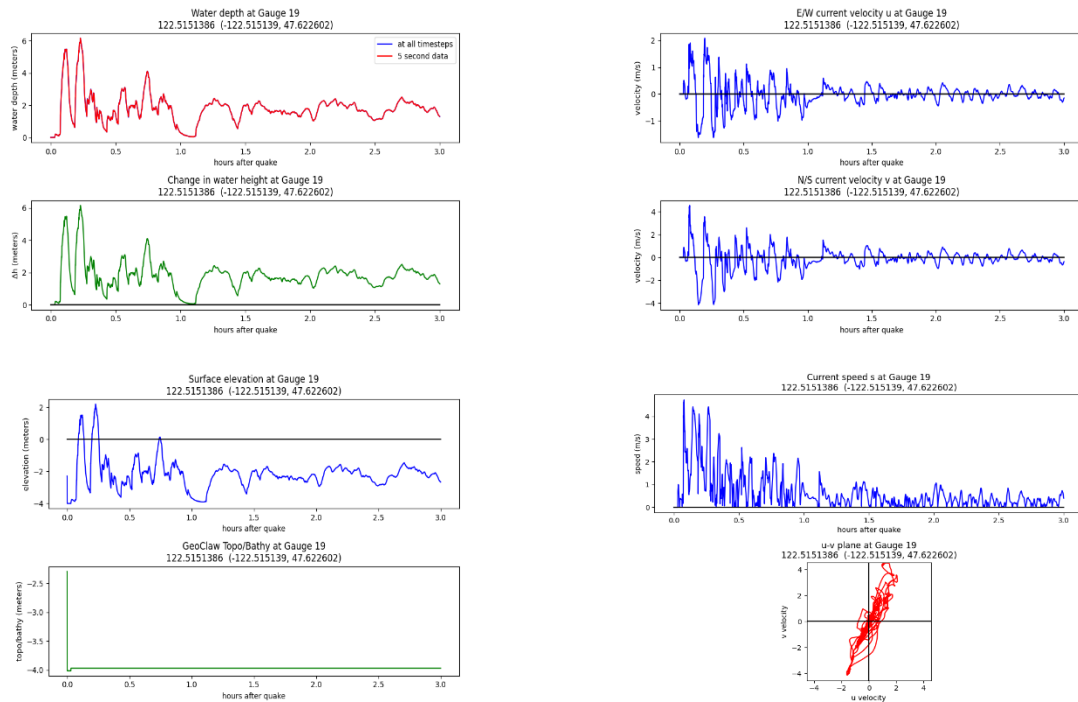
Cascadia subduction zone scenario, MLW:



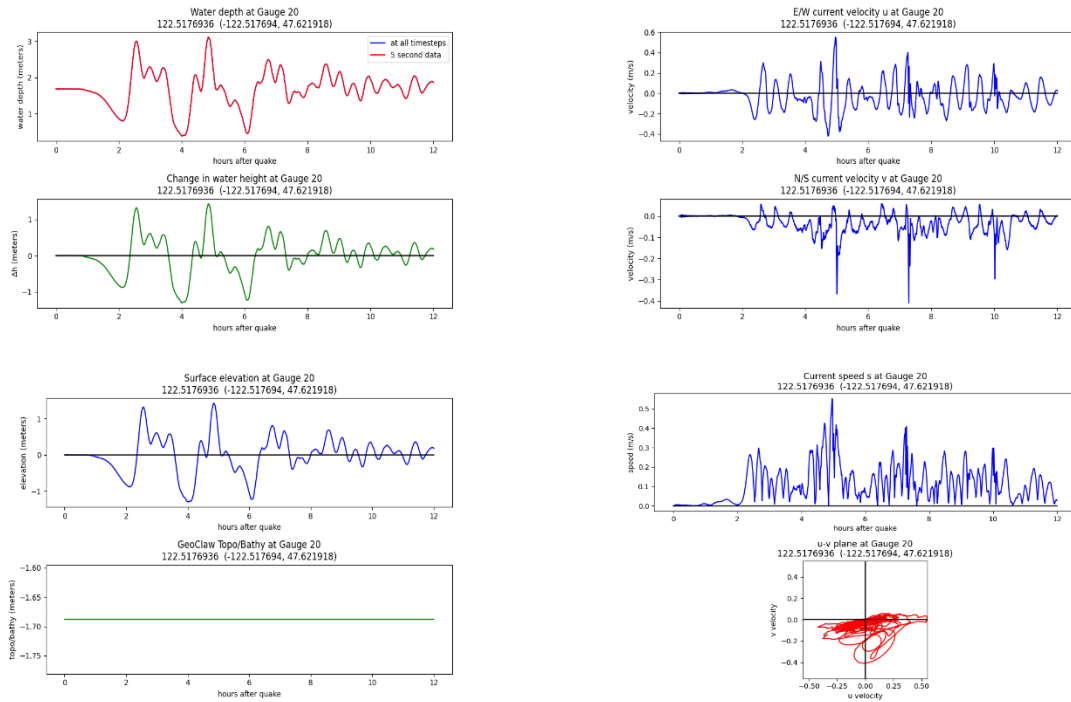
## Seattle fault scenario, MHW:



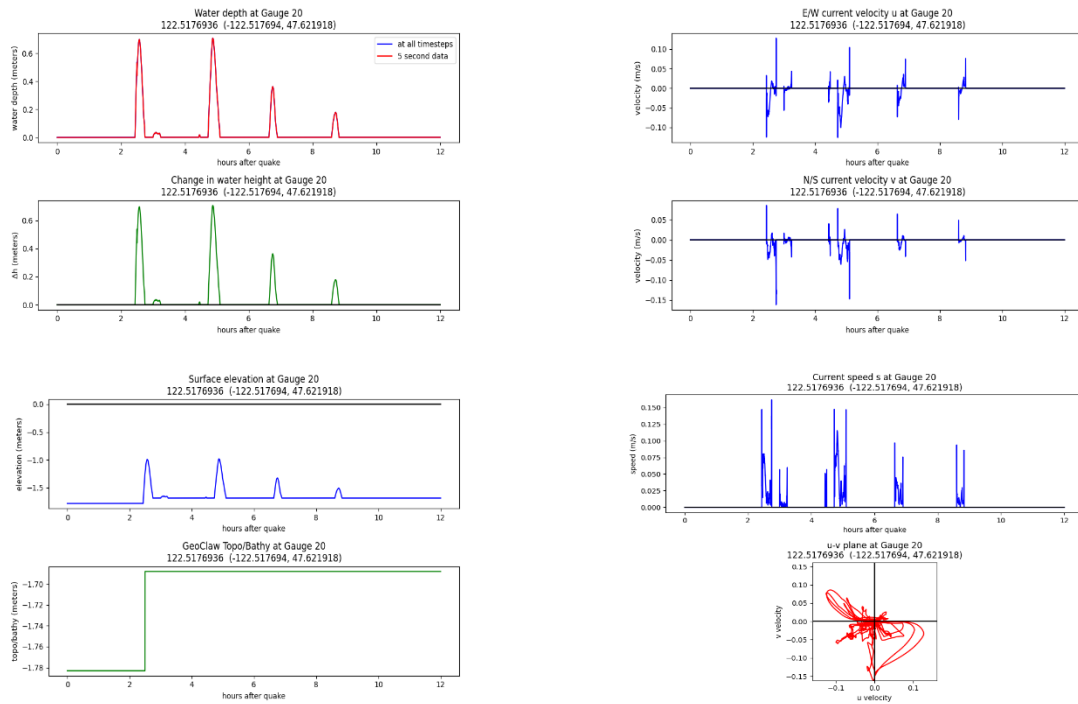
## Seattle fault scenario, MLW:



## Gauge 20: Exotic Aquatic Kayaks Dock Cascadia subduction zone scenario, MHW:

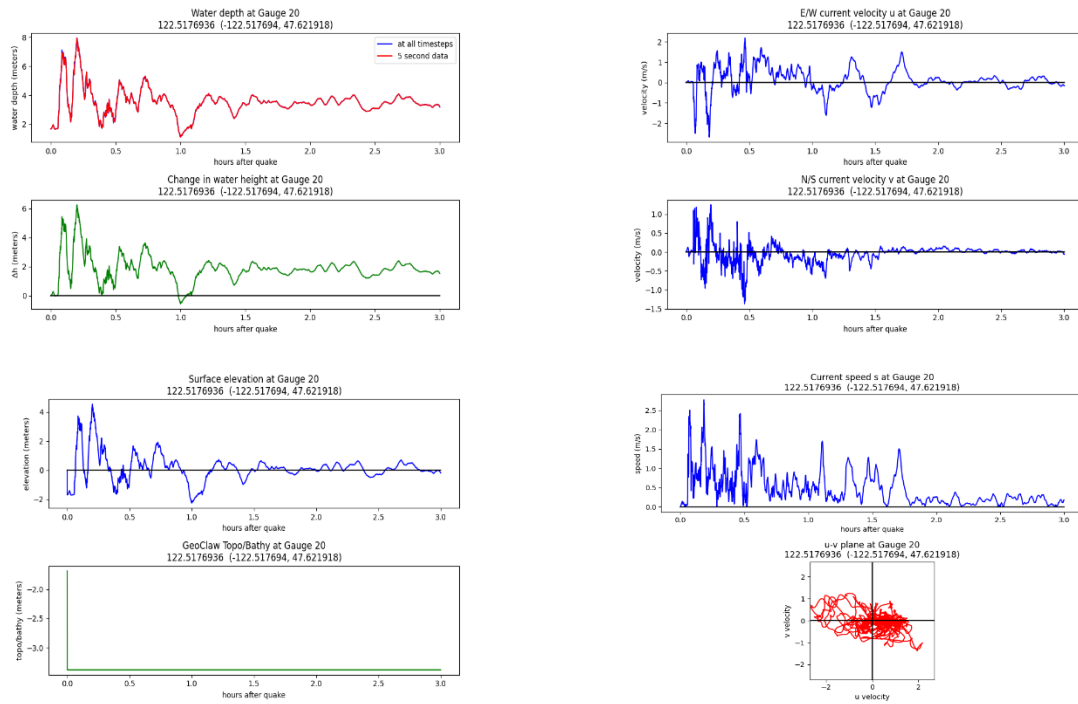


## Cascadia subduction zone scenario, MLW:

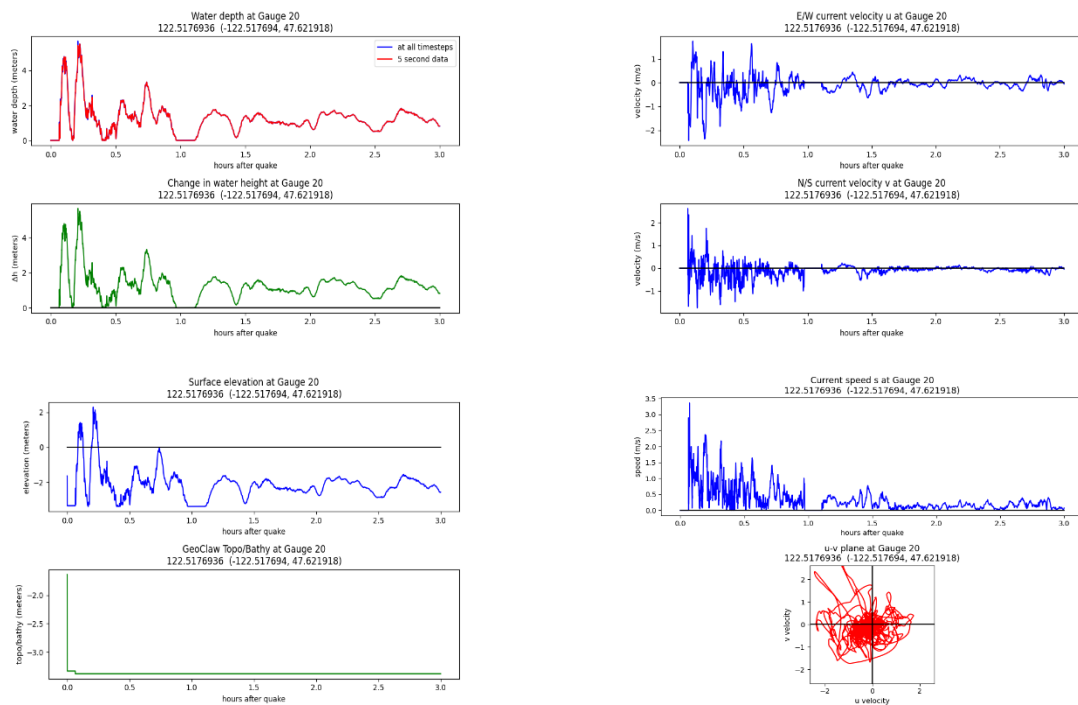




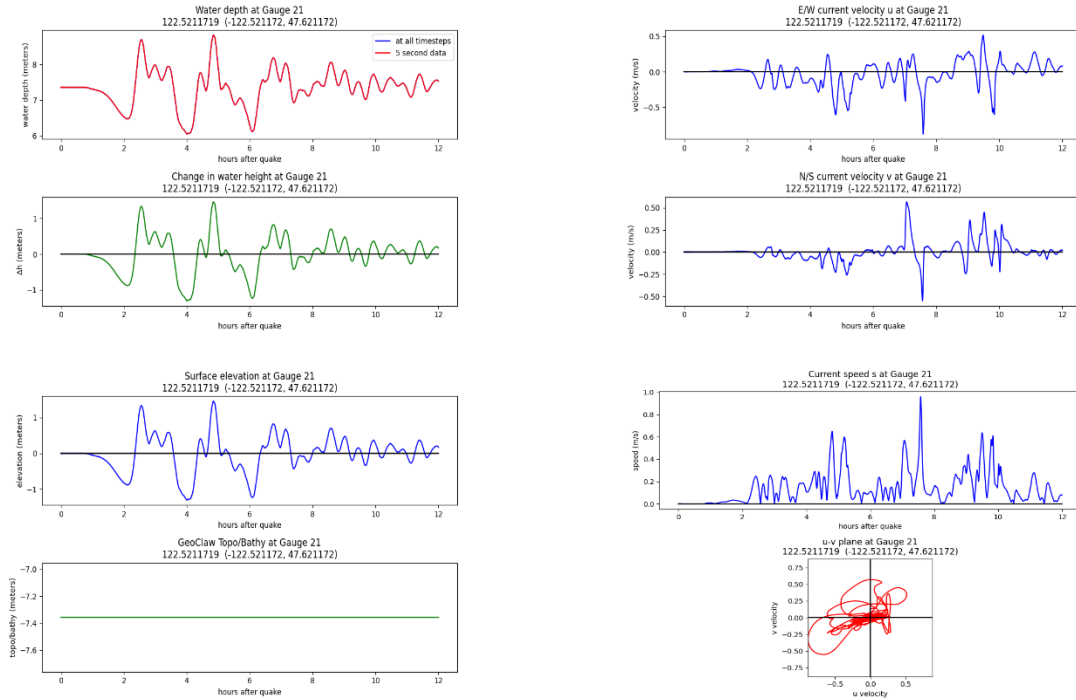
## Seattle fault scenario, MHW:



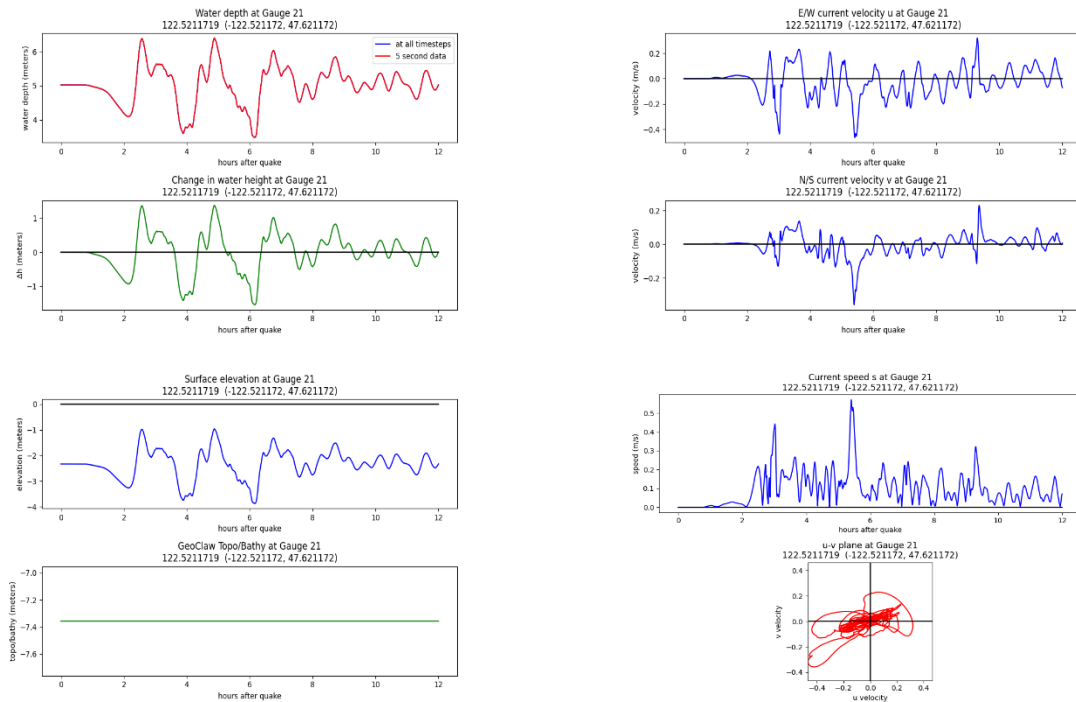
## Seattle fault scenario, MLW:



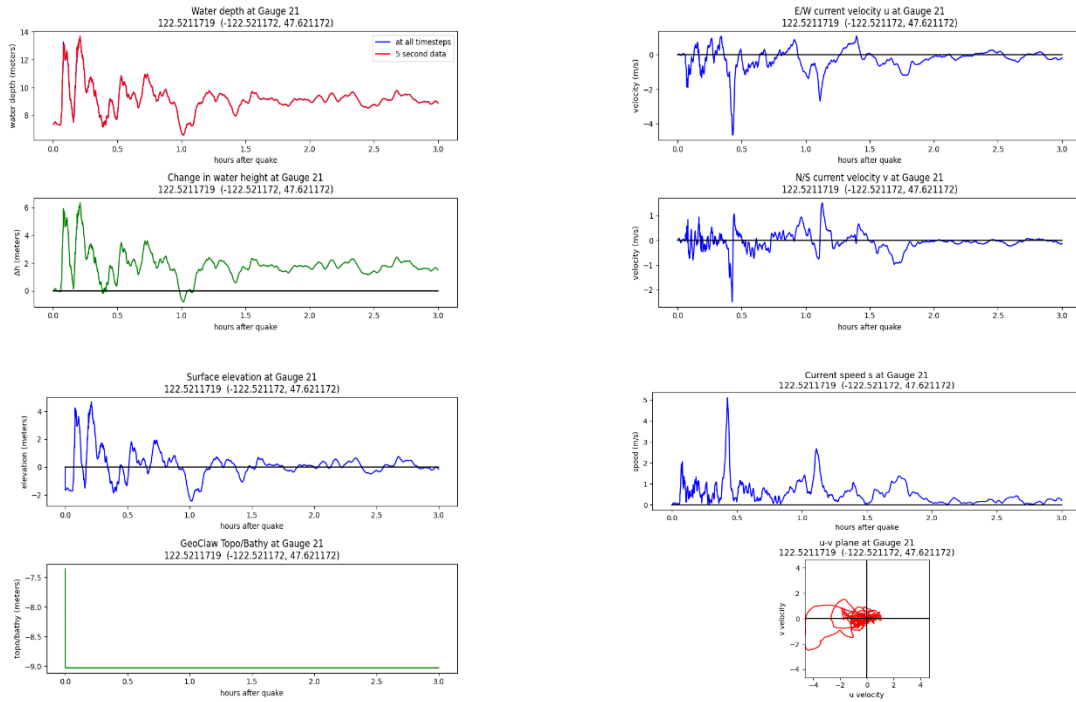
## Gauge 21: Winslow Wharf Marina center Cascadia subduction zone scenario, MHW:



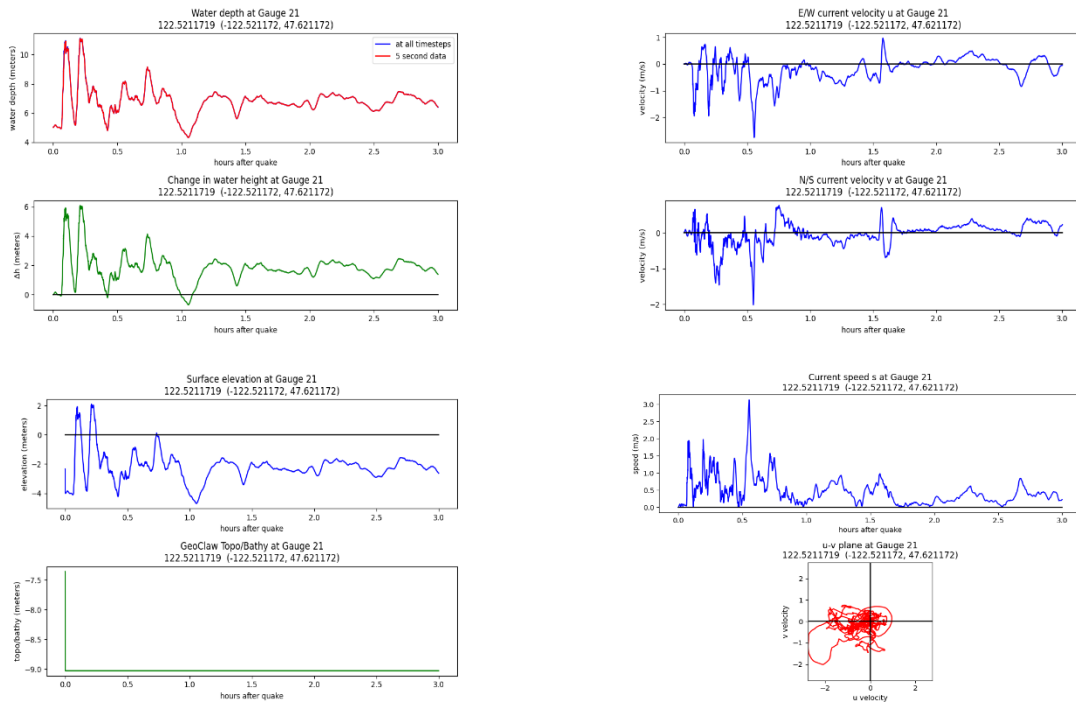
## Cascadia subduction zone scenario, MLW:



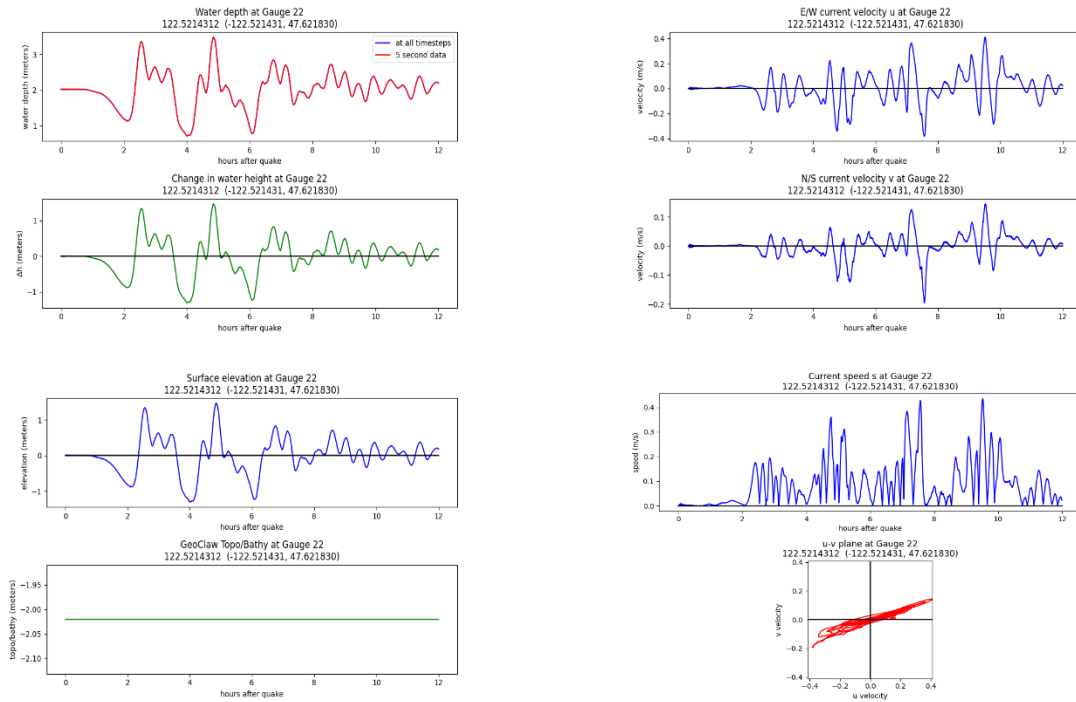
## Seattle fault scenario, MHW:



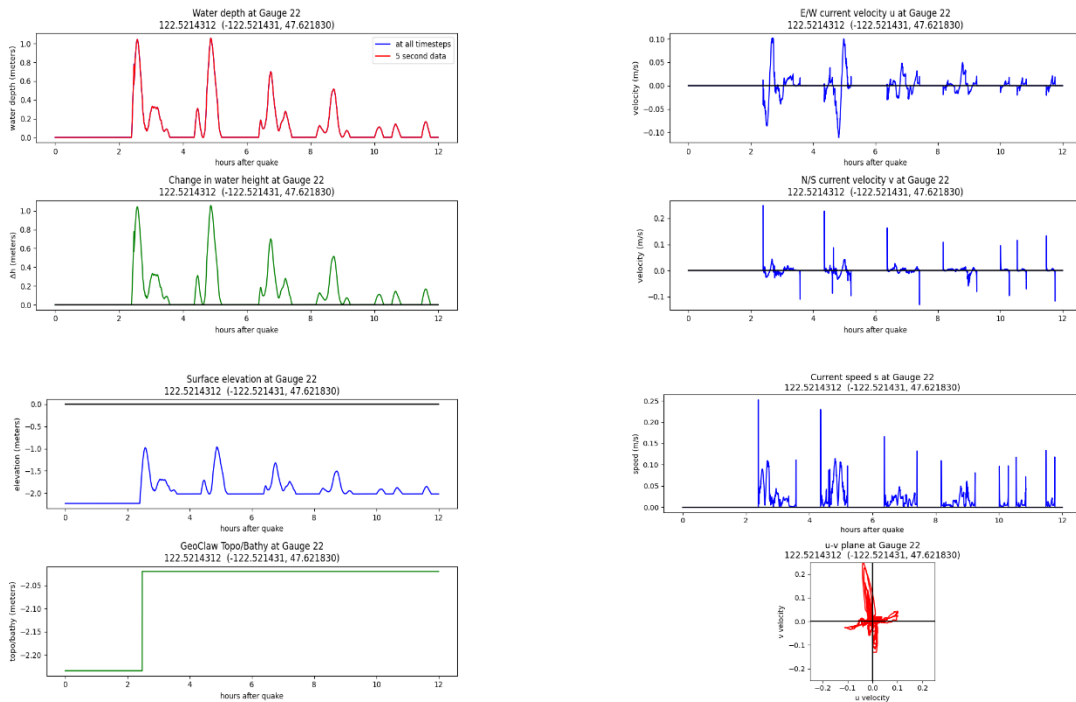
## Seattle fault scenario, MLW:



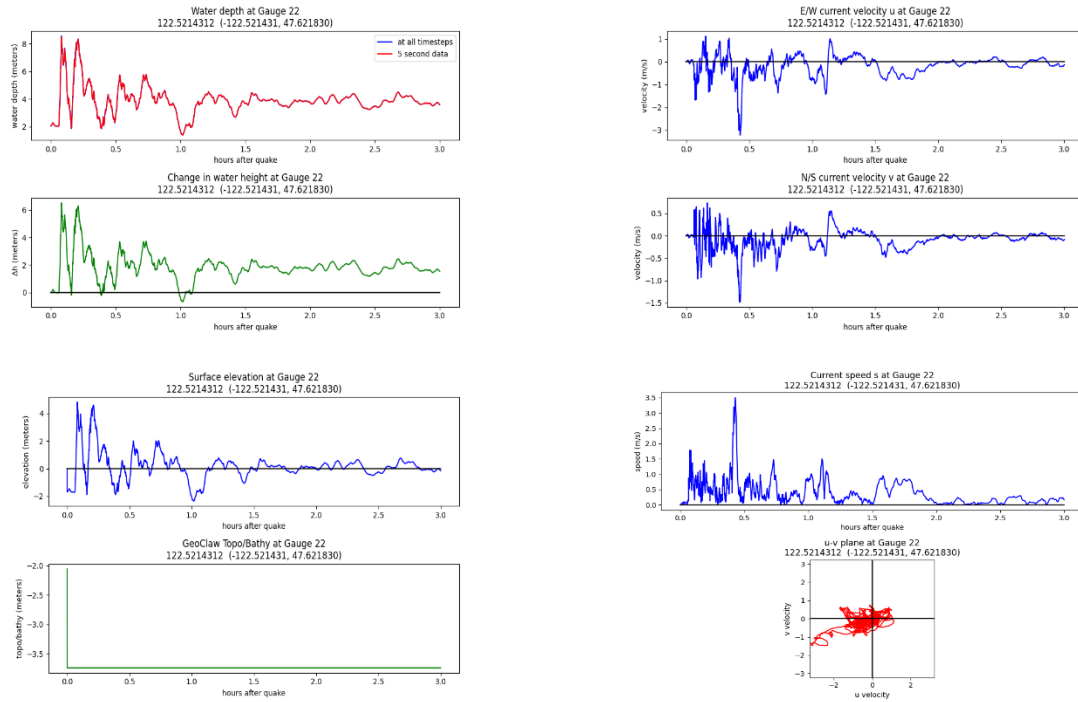
Gauge 22: Winslow Wharf Marina nearshore  
 Cascadia subduction zone scenario, MHW:



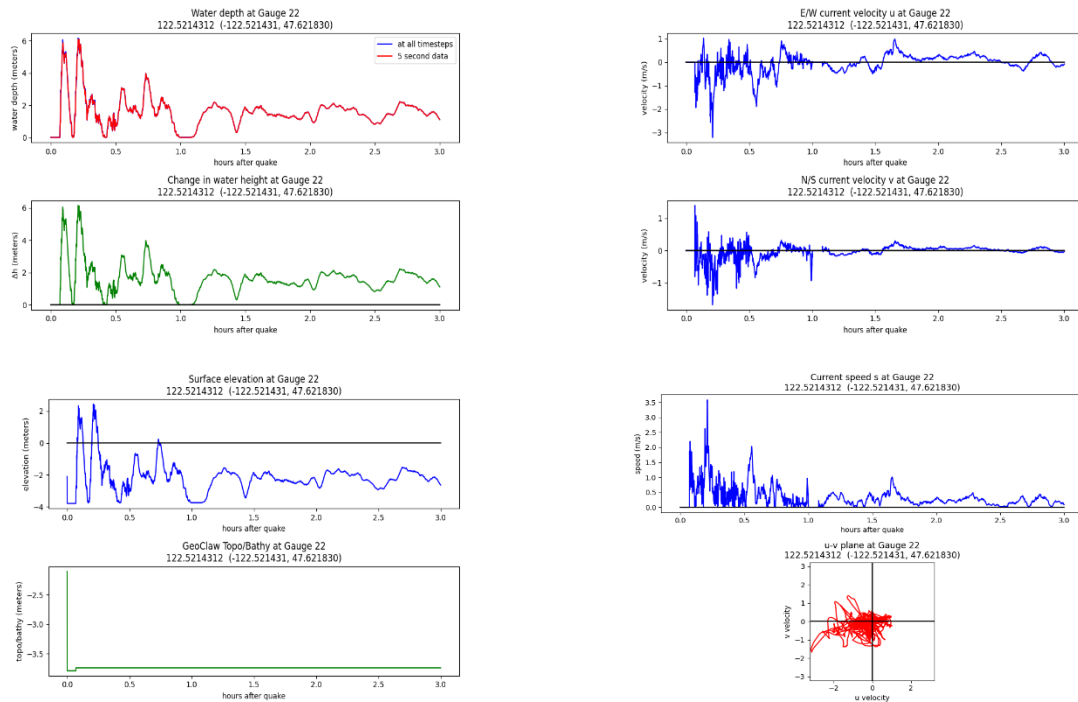
Cascadia subduction zone scenario, MLW:



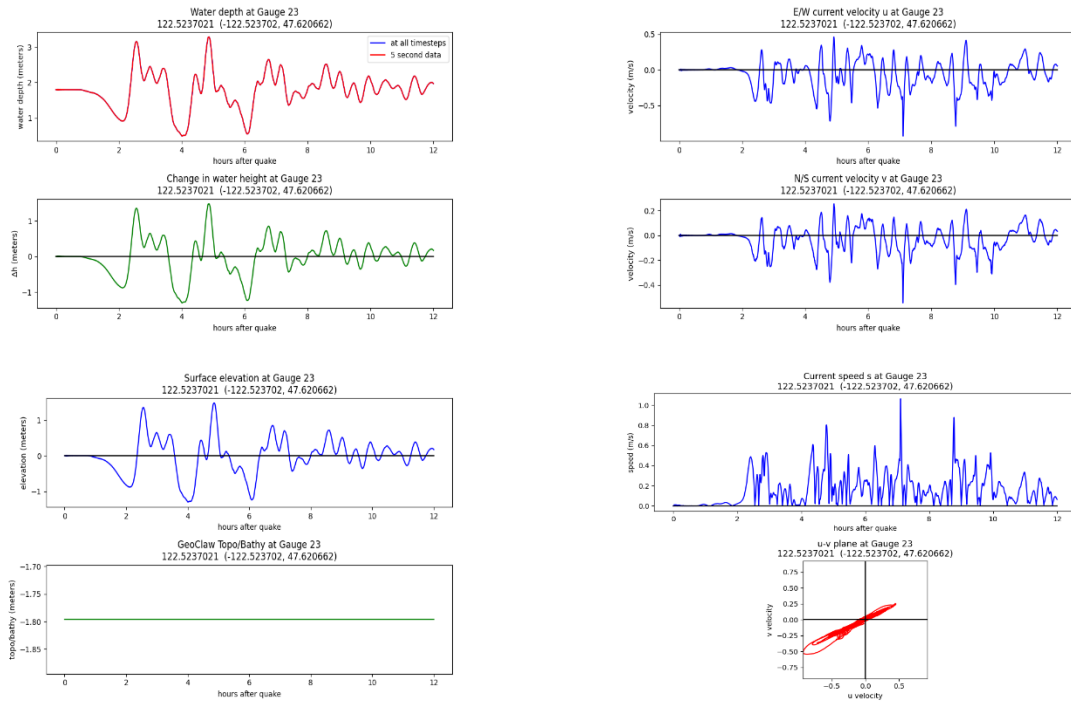
## Seattle fault scenario, MHW:



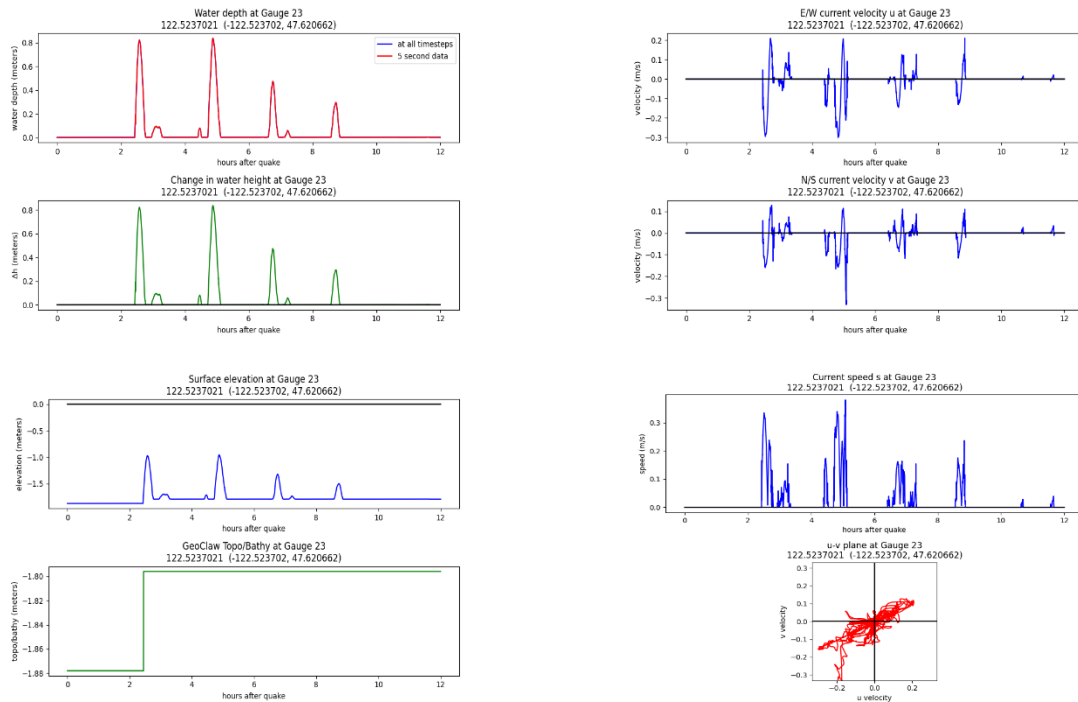
## Seattle fault scenario, MLW:



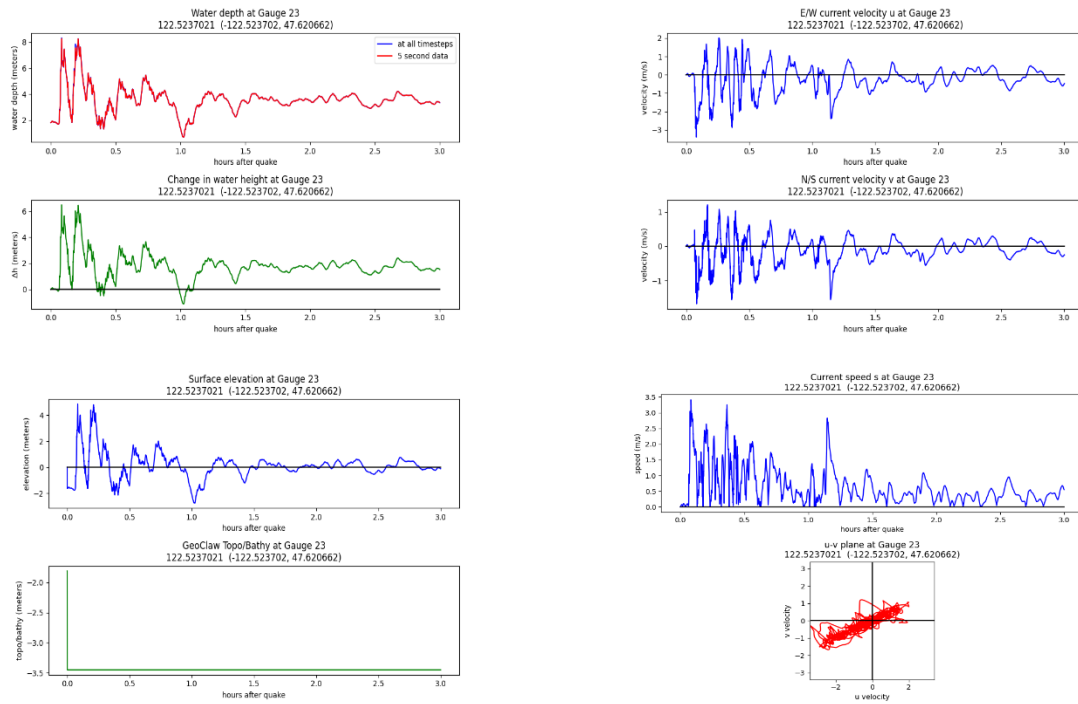
## Gauge 23: Offshore Williamson Landing Marina Cascadia subduction zone scenario, MHW:



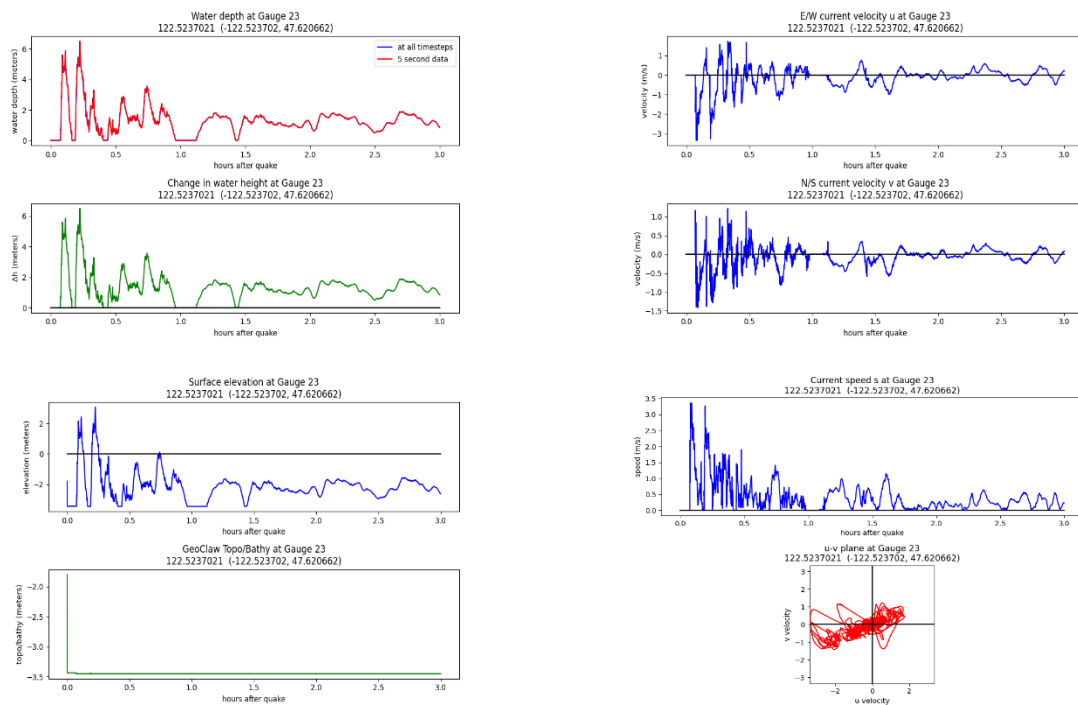
## Cascadia subduction zone scenario, MLW:



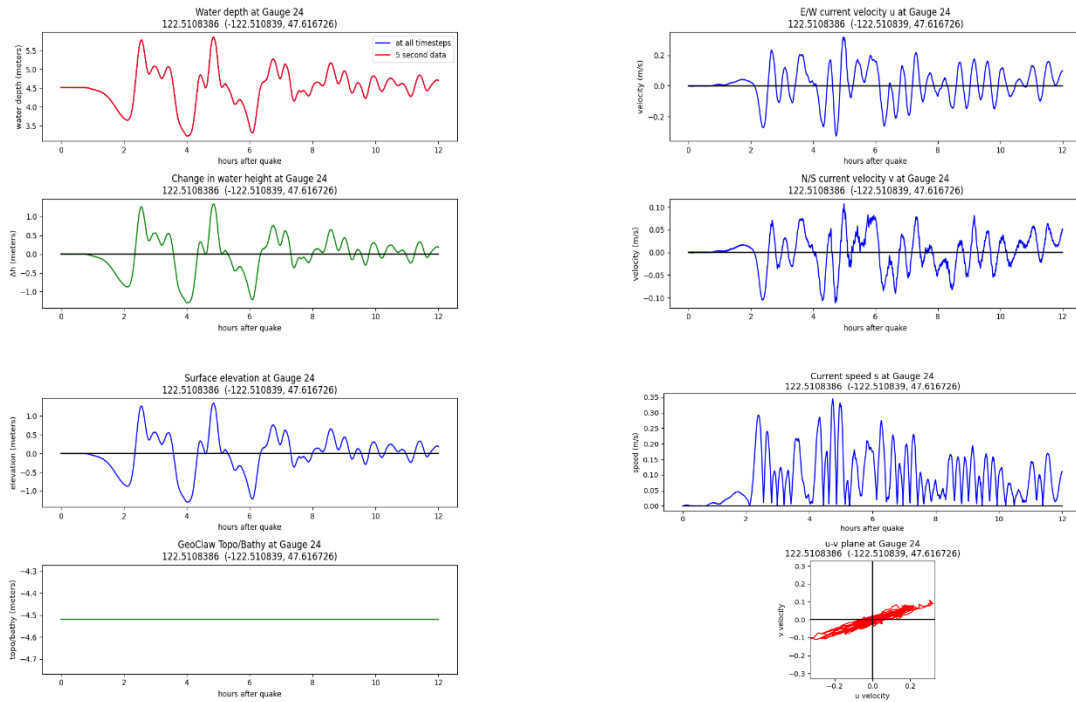
## Seattle fault scenario, MHW:



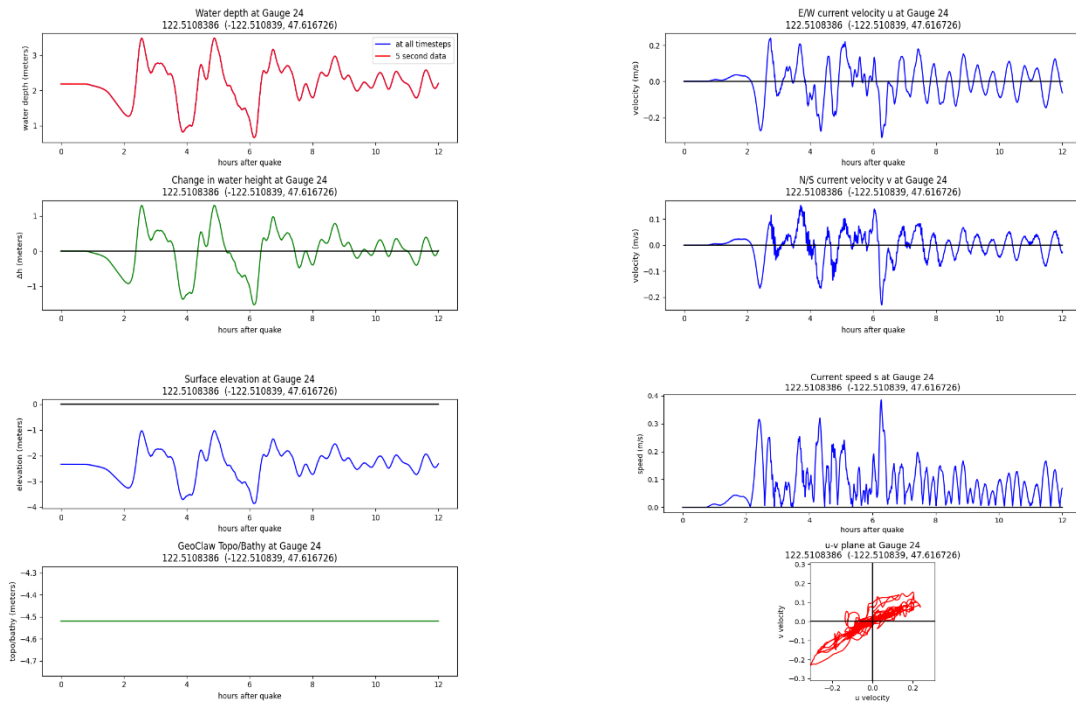
## Seattle fault scenario, MLW:



Gauge 24: Bainbridge Island Marina center  
Cascadia subduction zone scenario, MHW:

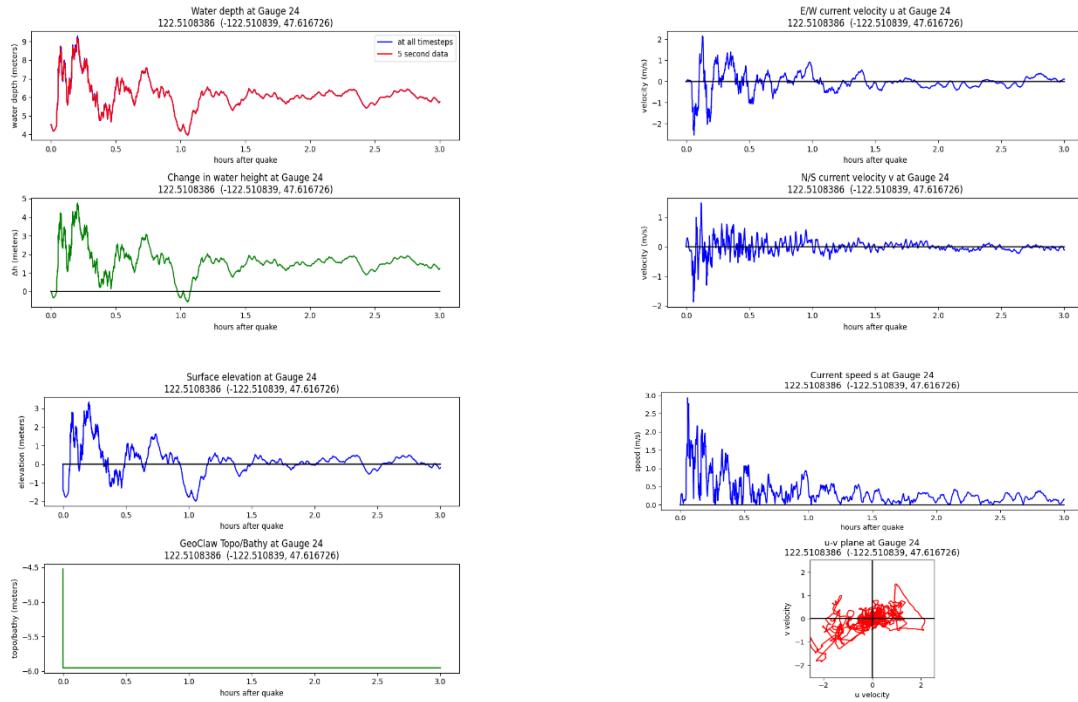


Cascadia subduction zone scenario, MLW:

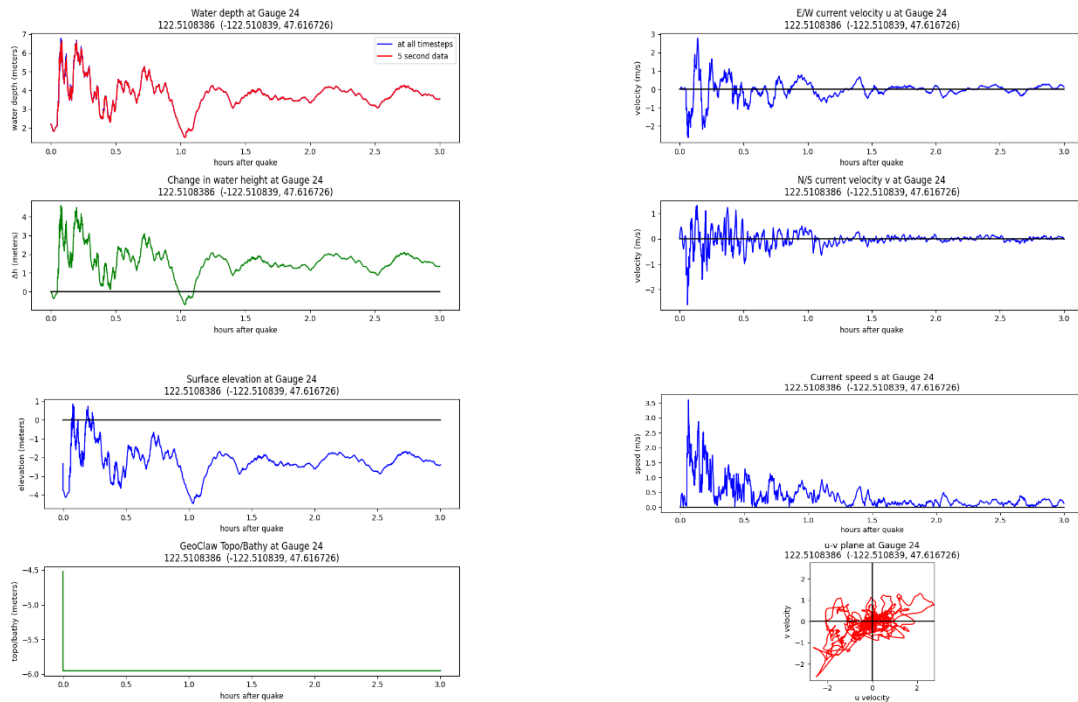




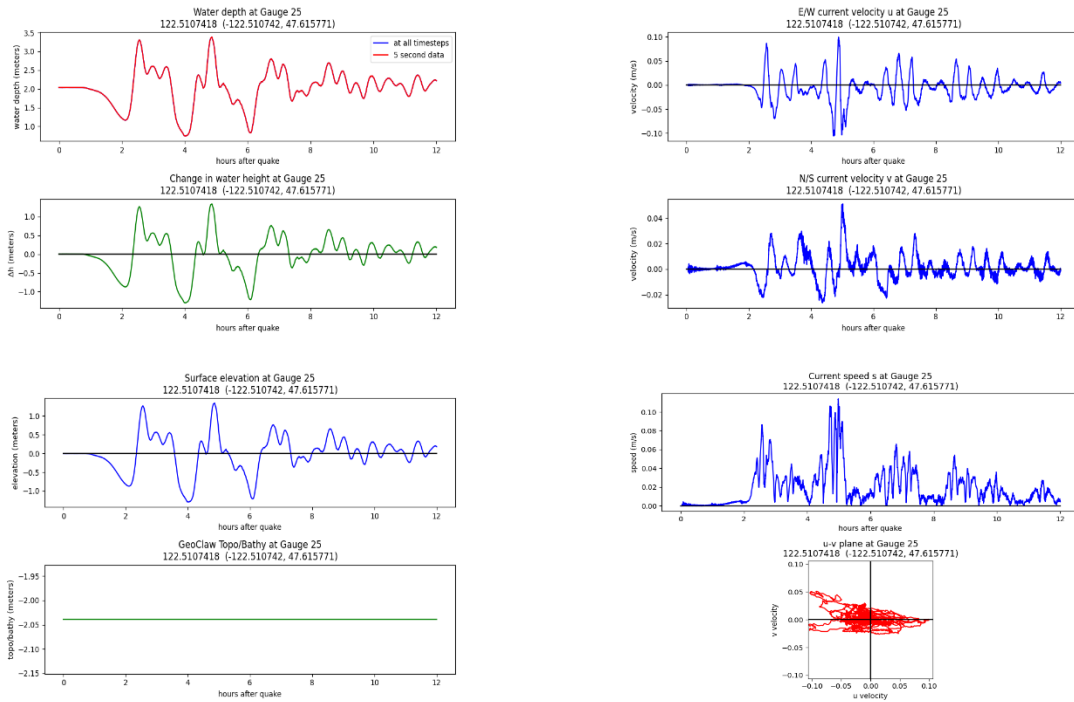
## Seattle fault scenario, MHW:



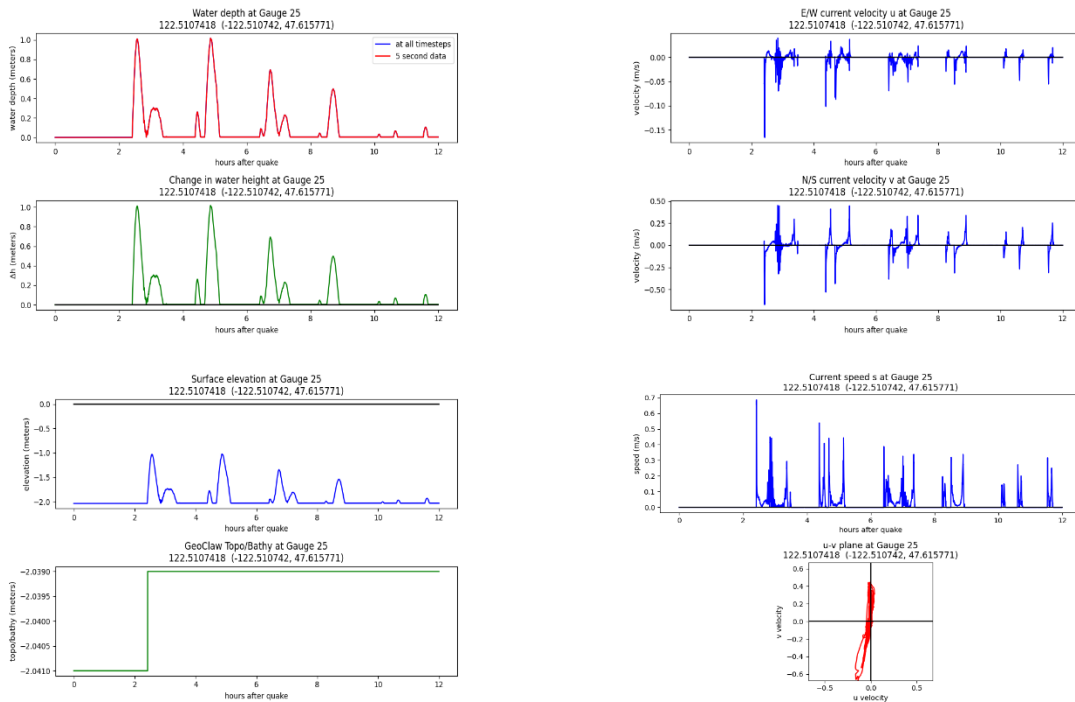
## Seattle fault scenario, MLW:



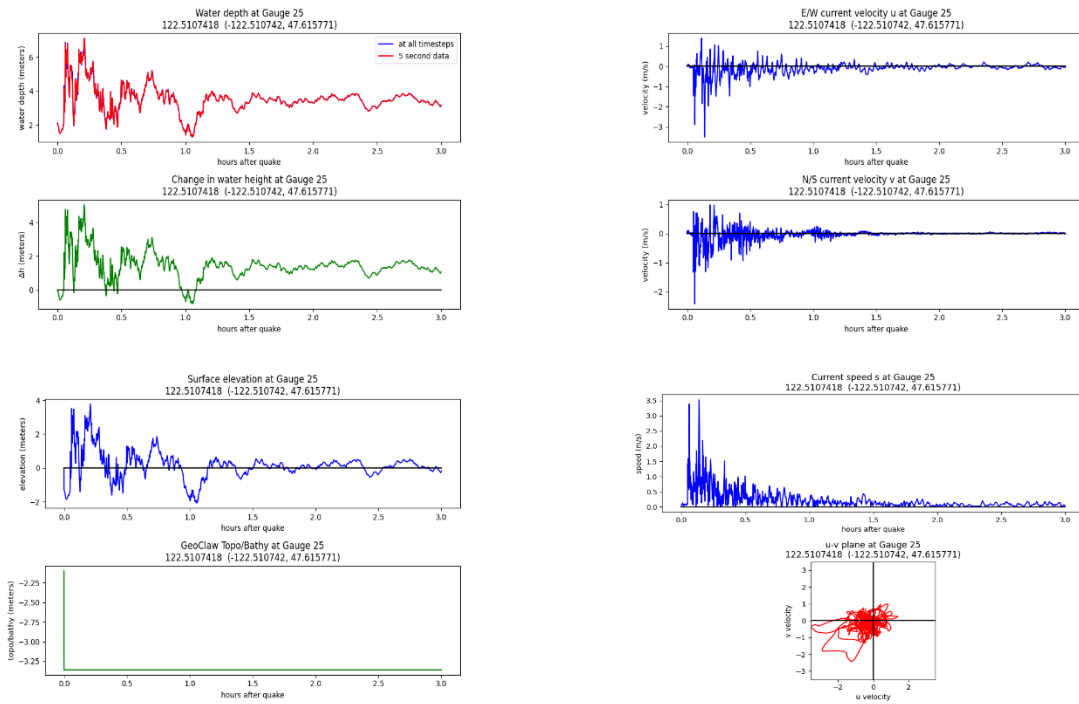
Gauge 25: Bainbridge Island Marina nearshore  
Cascadia subduction zone scenario, MHW:



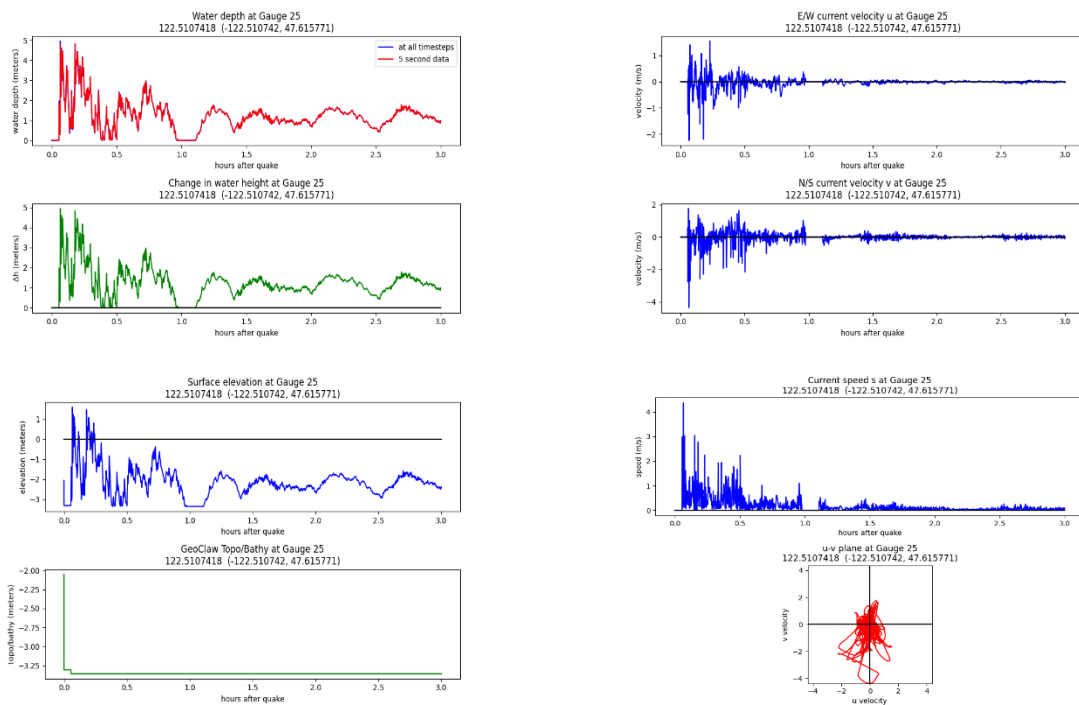
Cascadia subduction zone scenario, MLW:



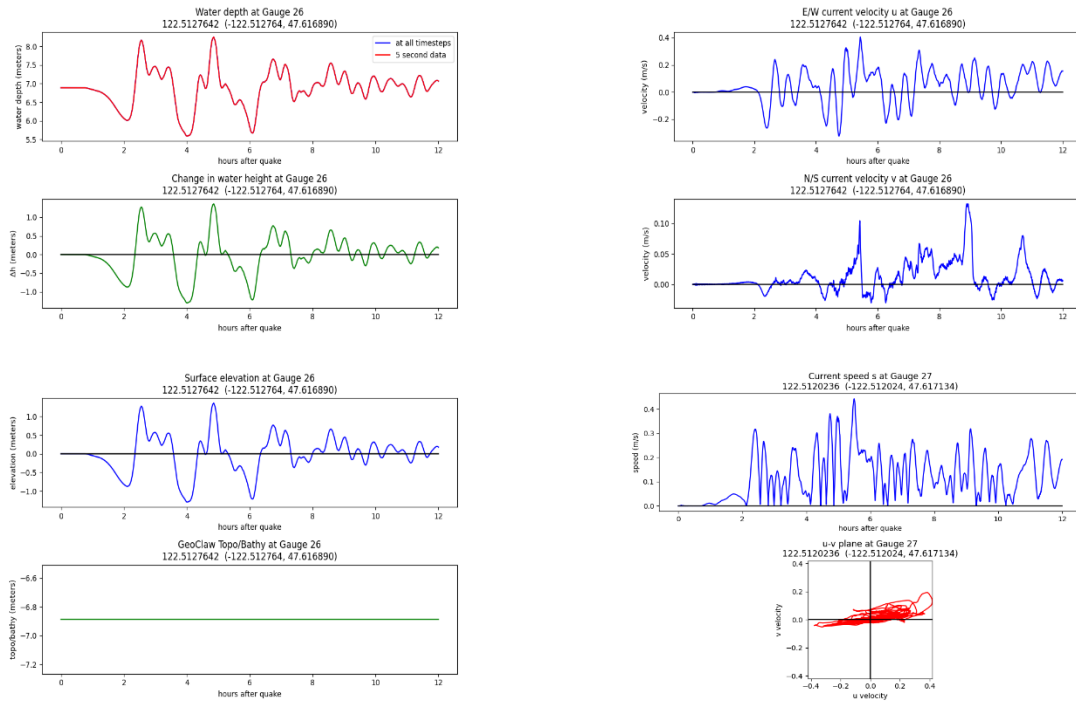
## Seattle fault scenario, MHW:



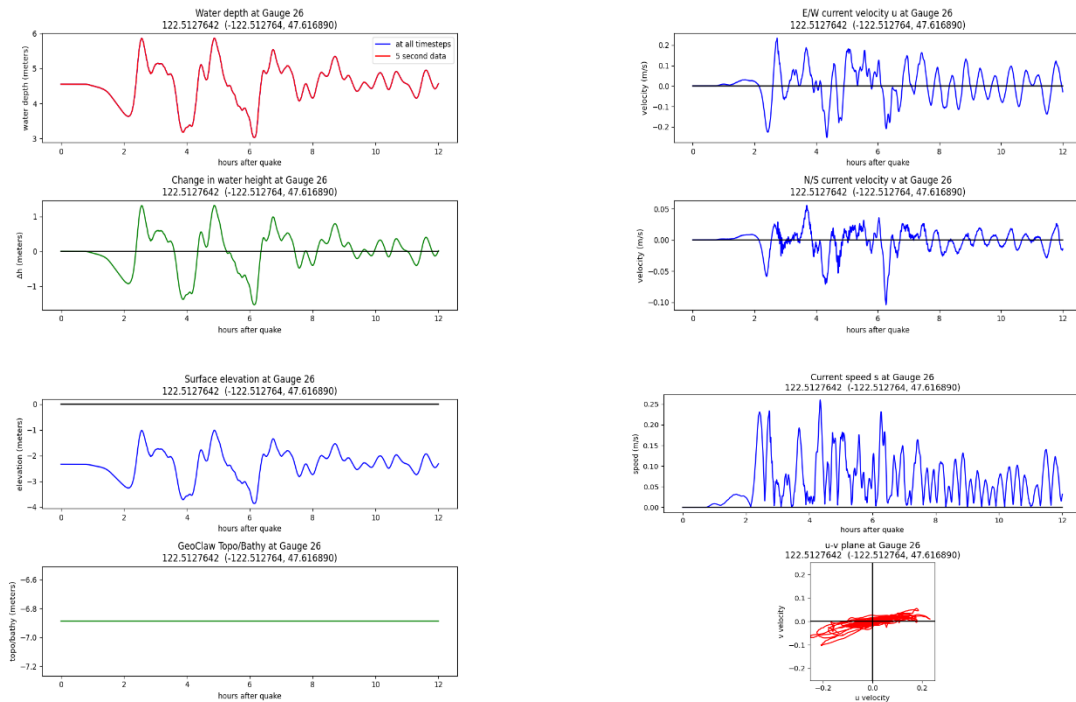
## Seattle fault scenario, MLW:



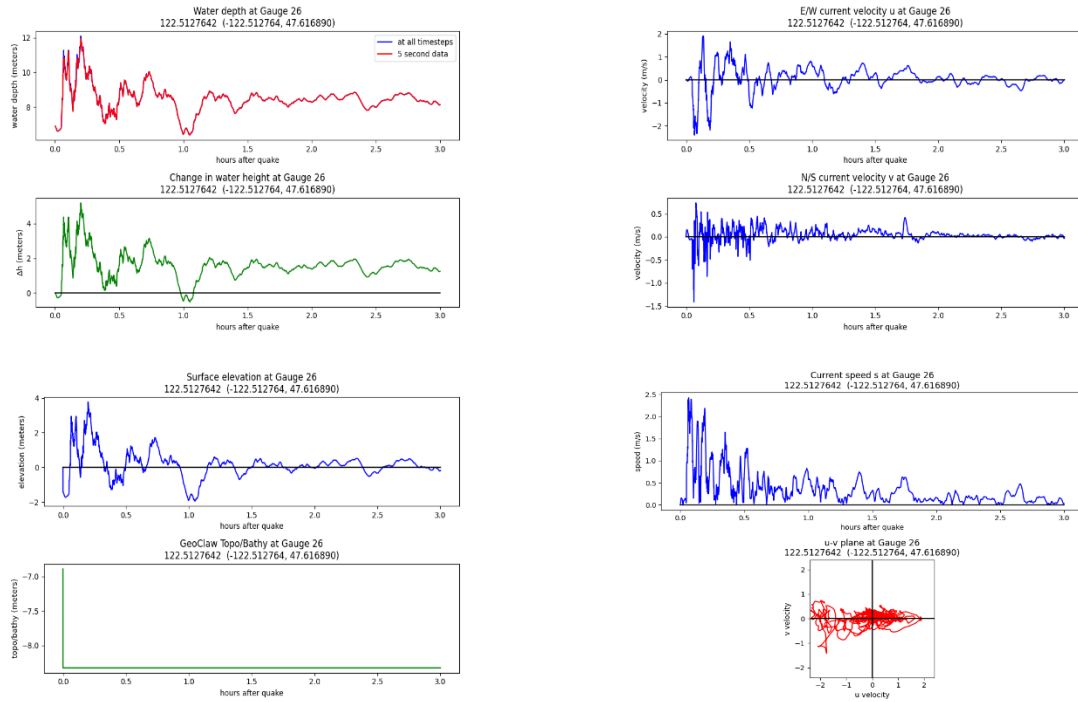
Gauge 26: Eagle Harbor Marina center  
Cascadia subduction zone scenario, MHW:



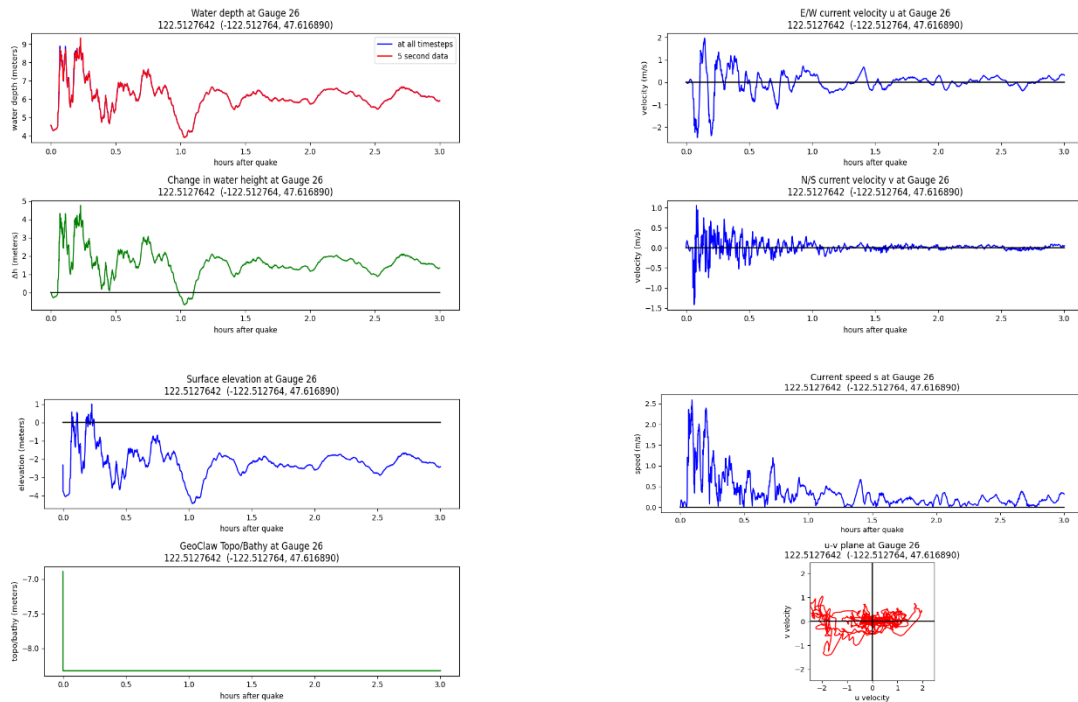
Cascadia subduction zone scenario, MLW:



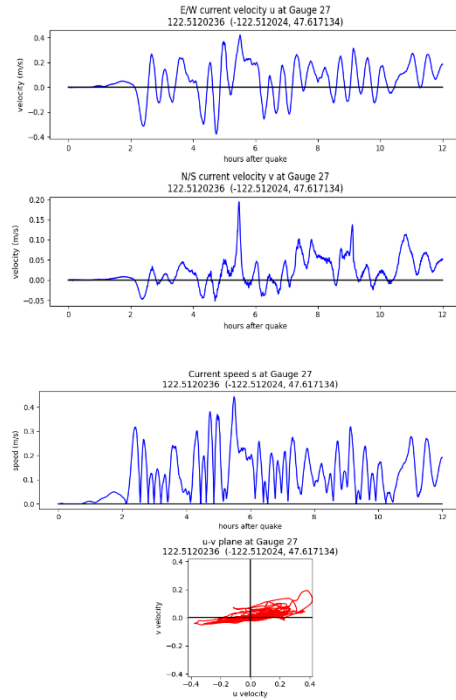
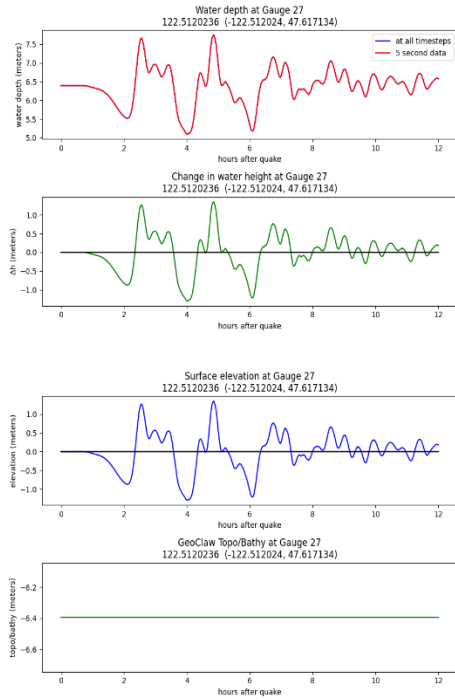
### Seattle fault scenario, MHW:



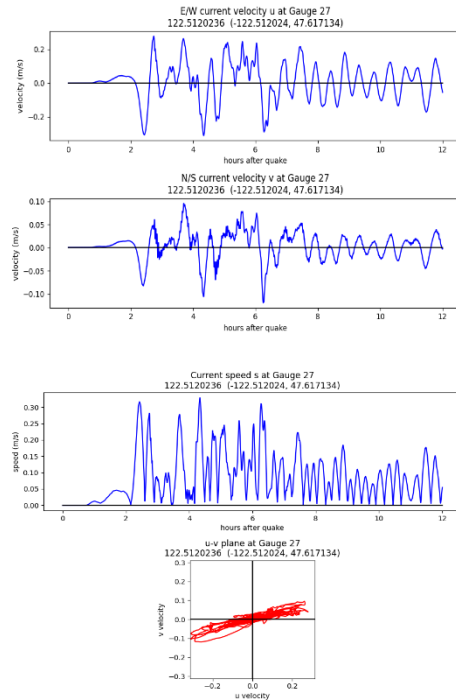
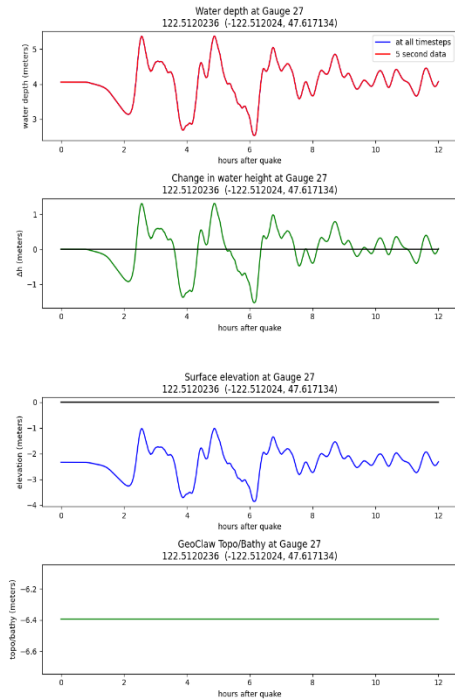
### Seattle fault scenario, MLW:



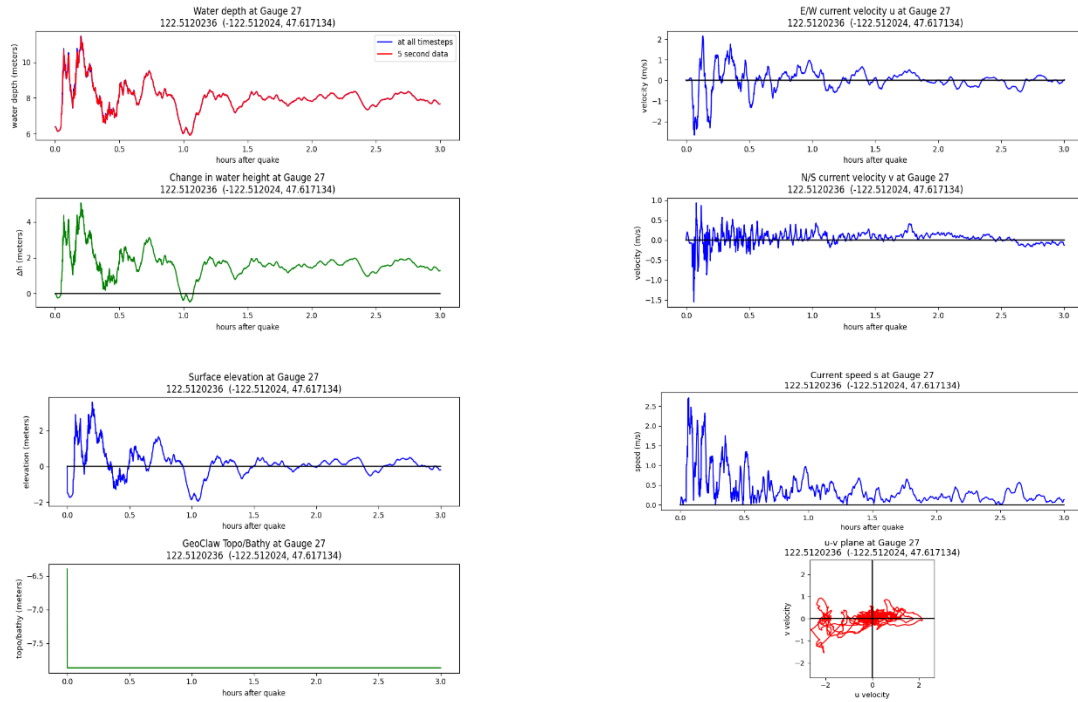
## Gauge 27: North of Eagle Harbor houseboats Cascadia subduction zone scenario, MHW:



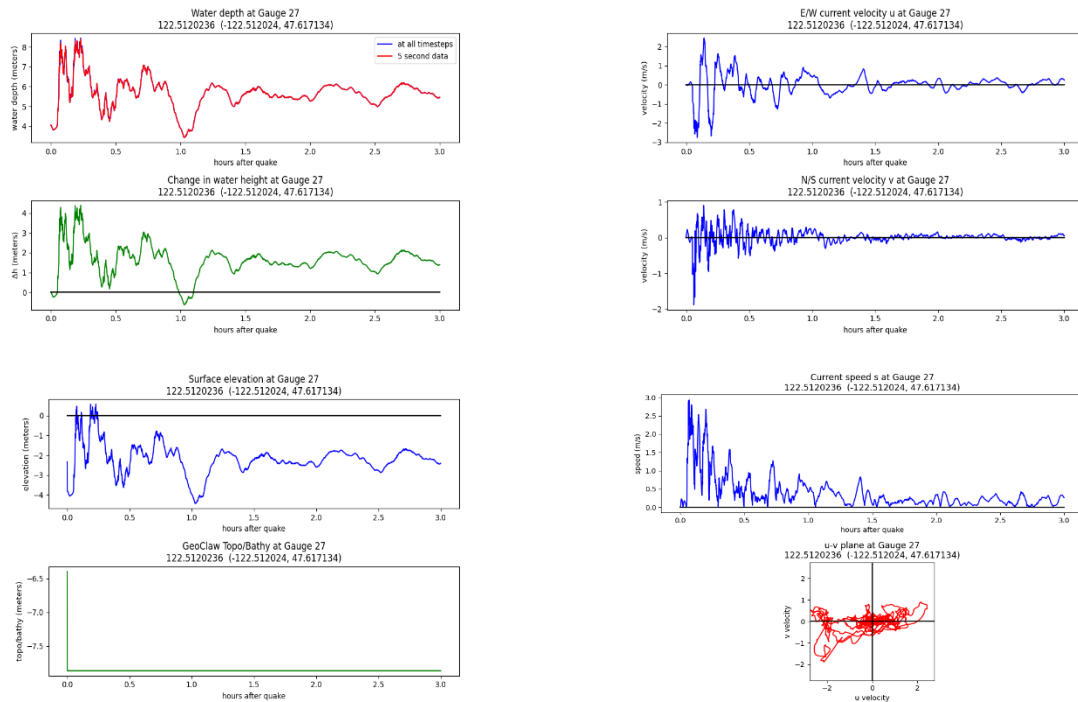
## Cascadia subduction zone scenario, MLW:



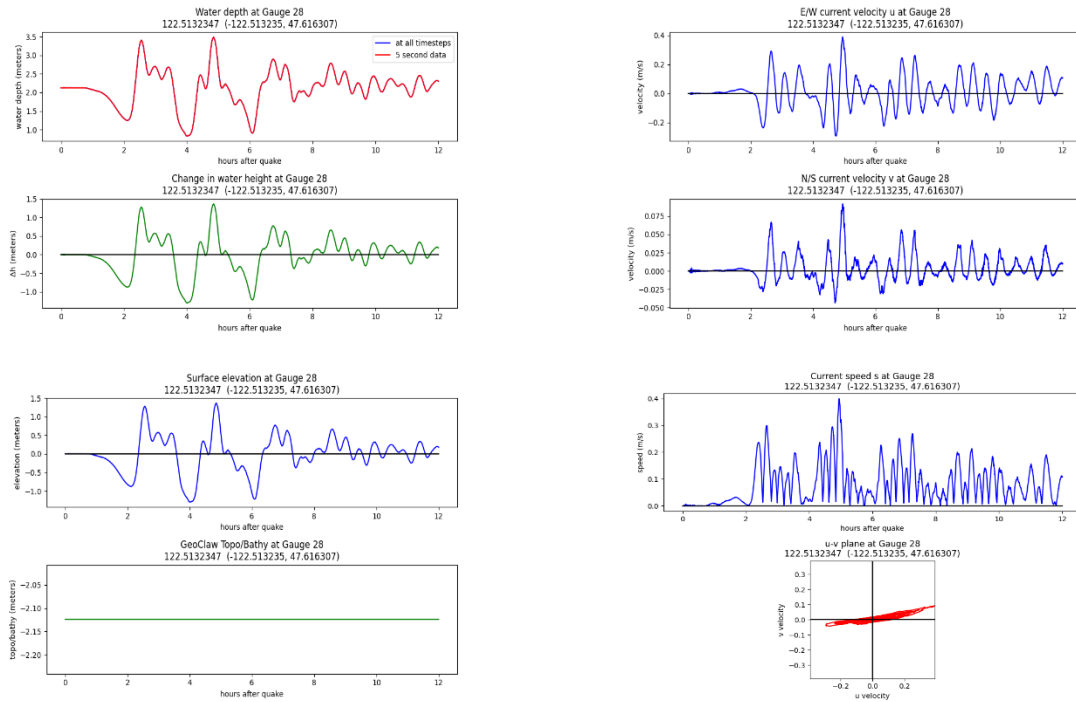
## Seattle fault scenario, MHW:



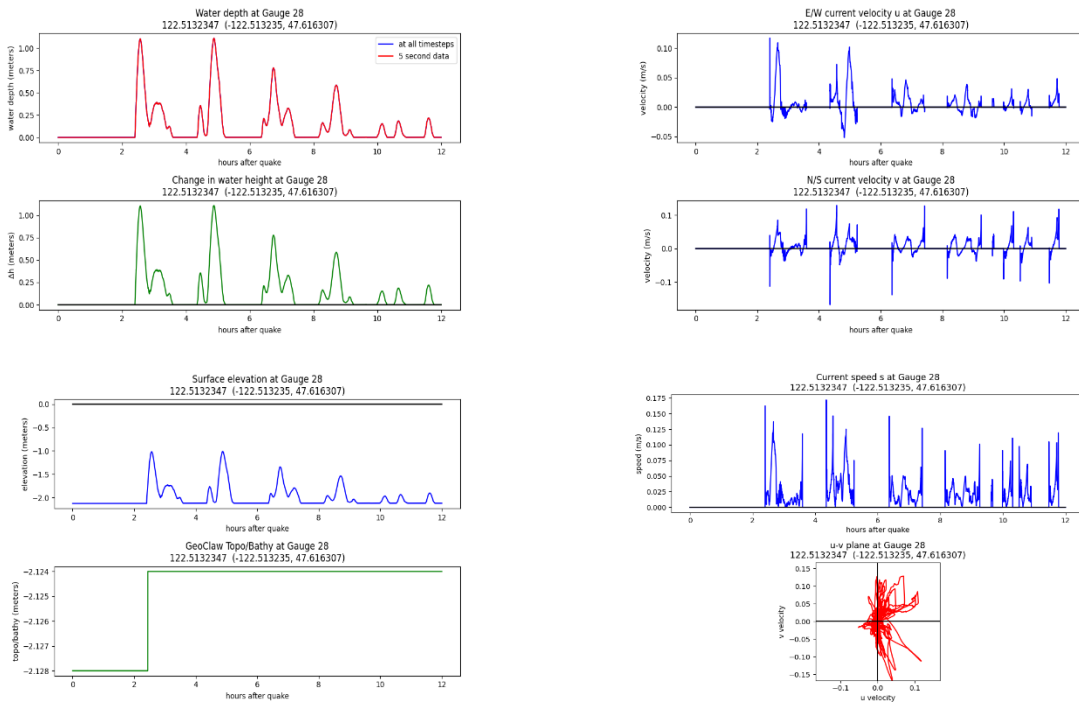
## Seattle fault scenario, MLW:



## Gauge 28: Eagle Harbor Marina nearshore Cascadia subduction zone scenario, MHW:

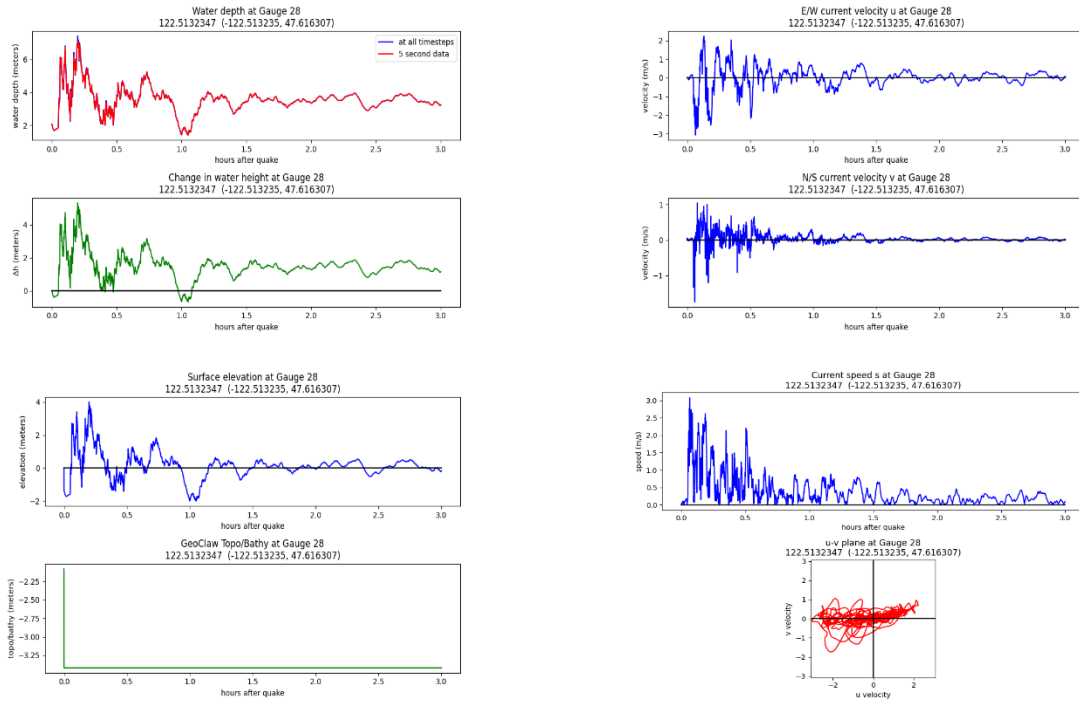


## Cascadia subduction zone scenario, MLW:

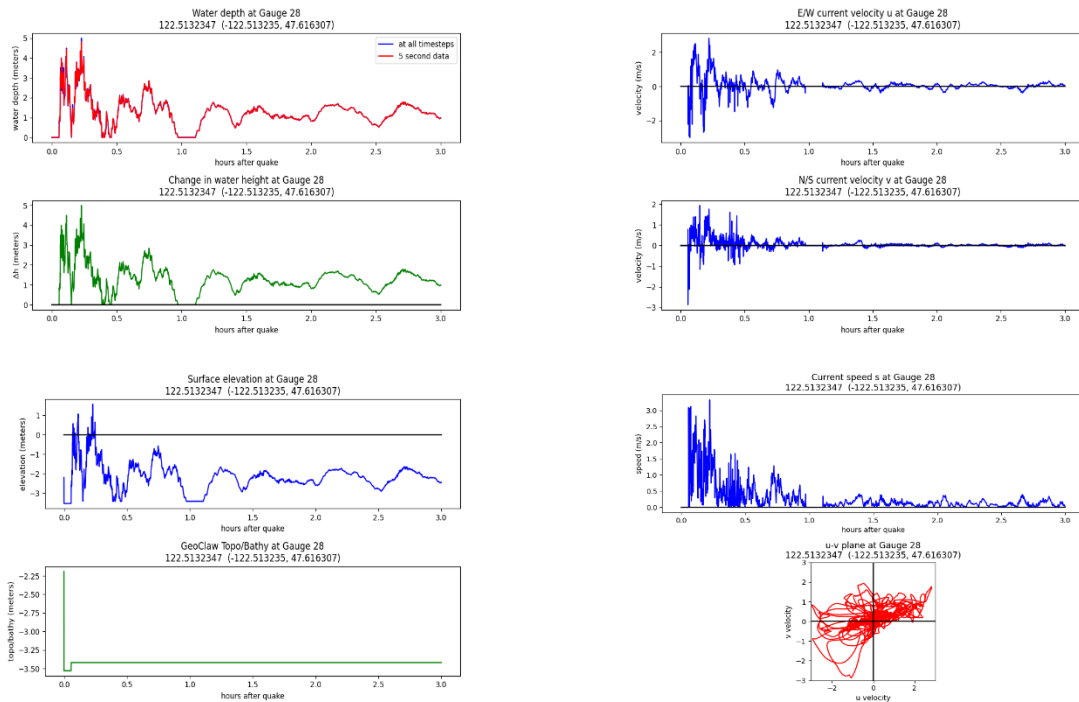




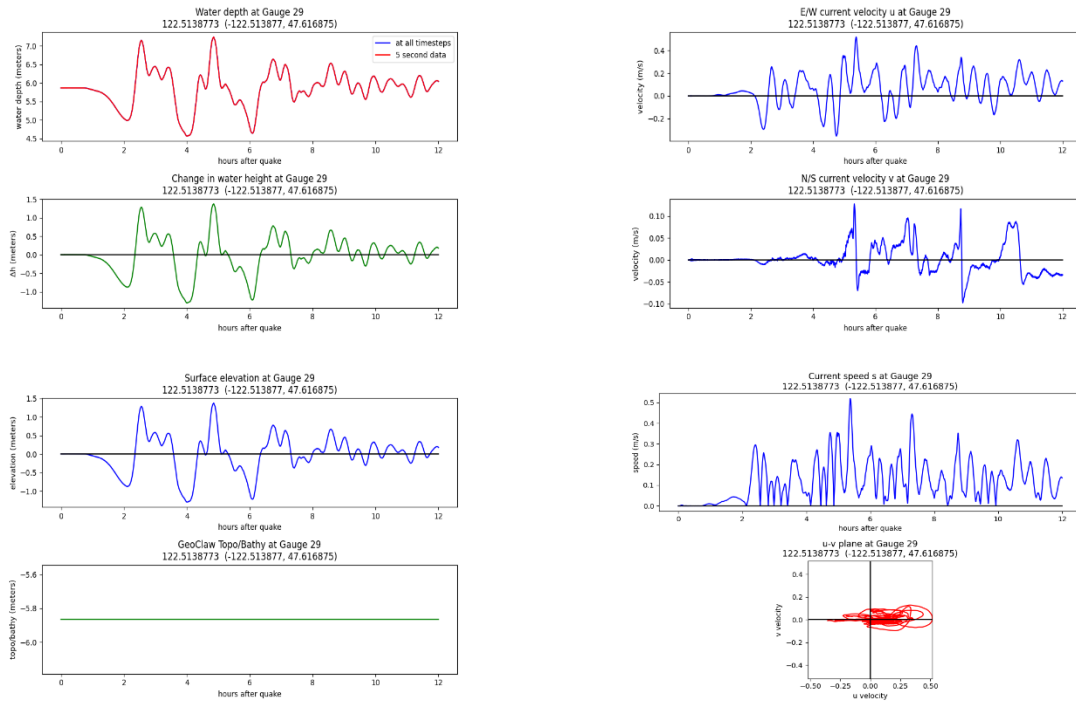
## Seattle fault scenario, MHW:



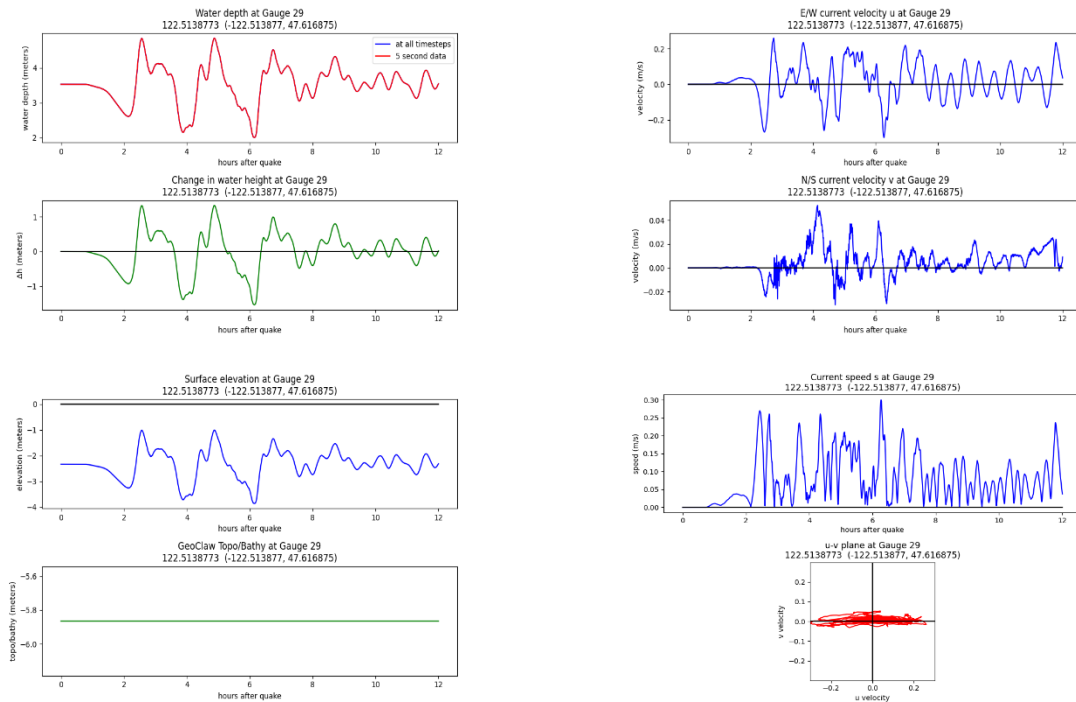
## Seattle fault scenario, MLW:



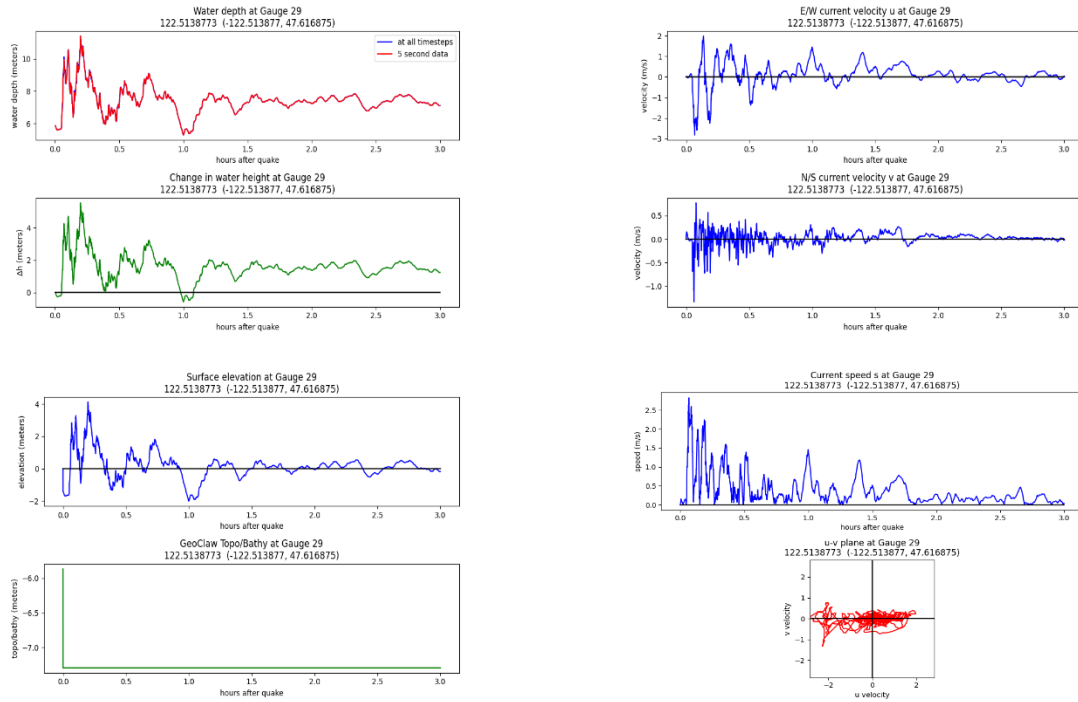
## Gauge 29: West of Eagle Harbor Cascadia subduction zone scenario, MHW:



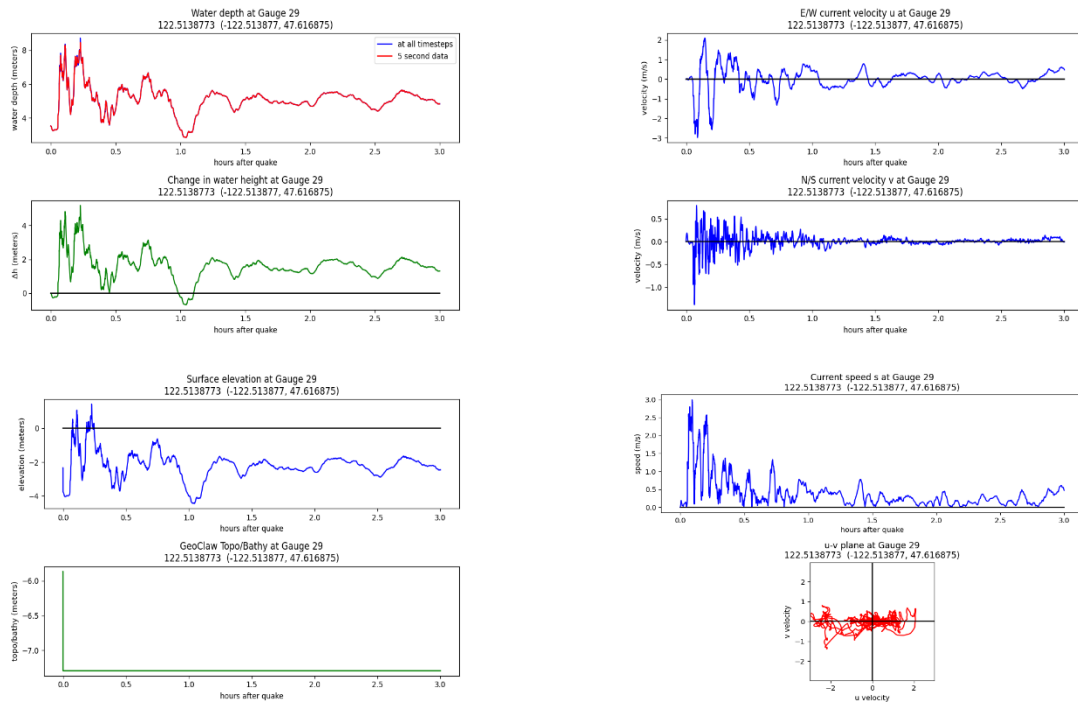
## Cascadia subduction zone scenario, MLW:



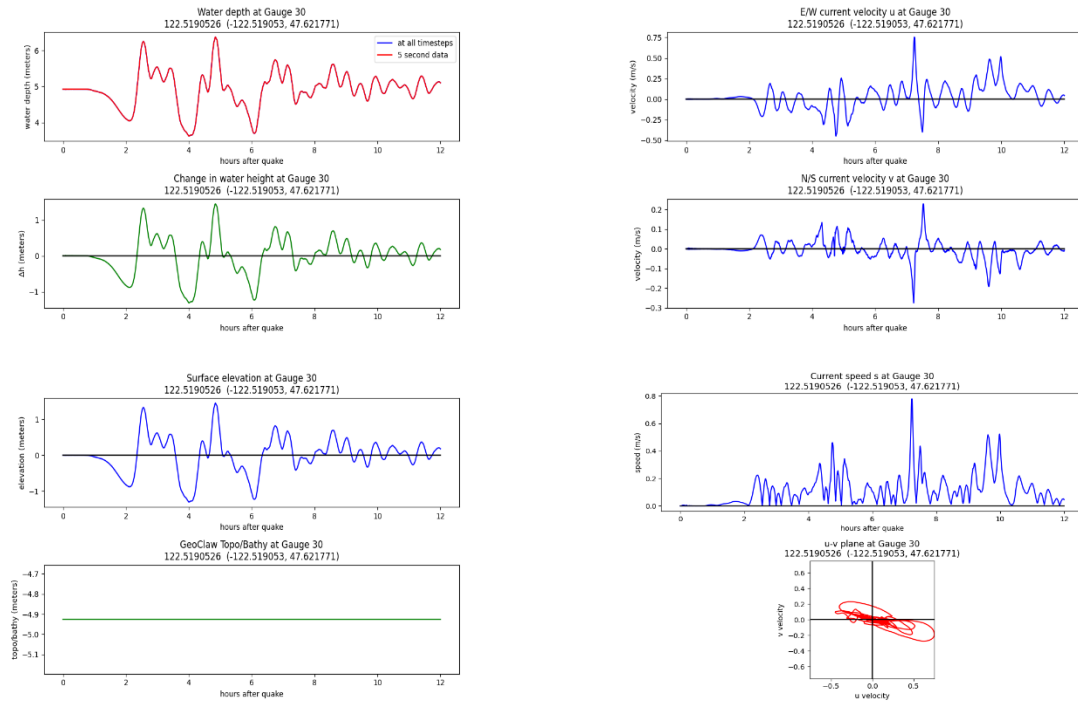
### Seattle fault scenario, MHW:



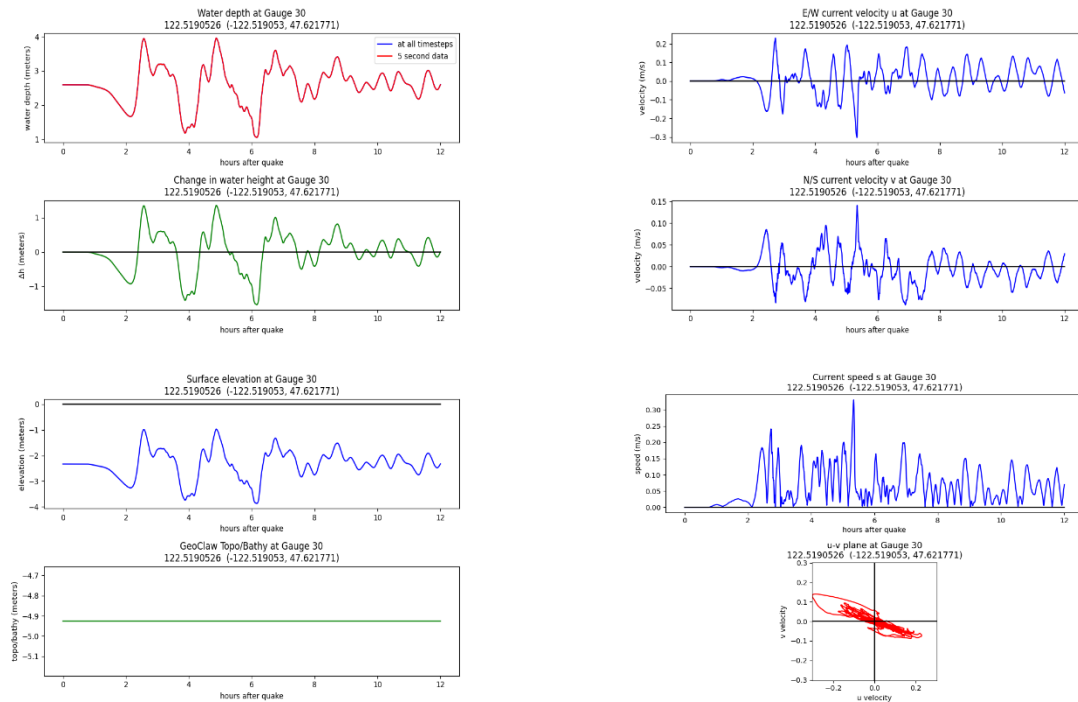
### Seattle fault scenario, MLW:



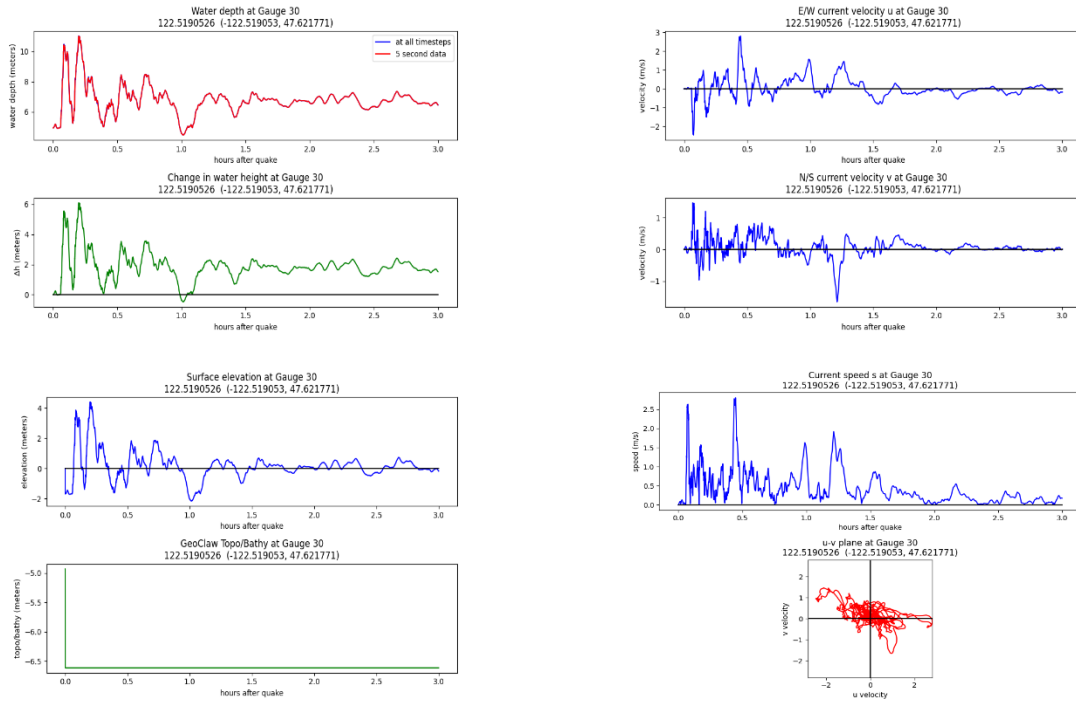
## Gauge 30: Police boat location Cascadia subduction zone scenario, MHW:



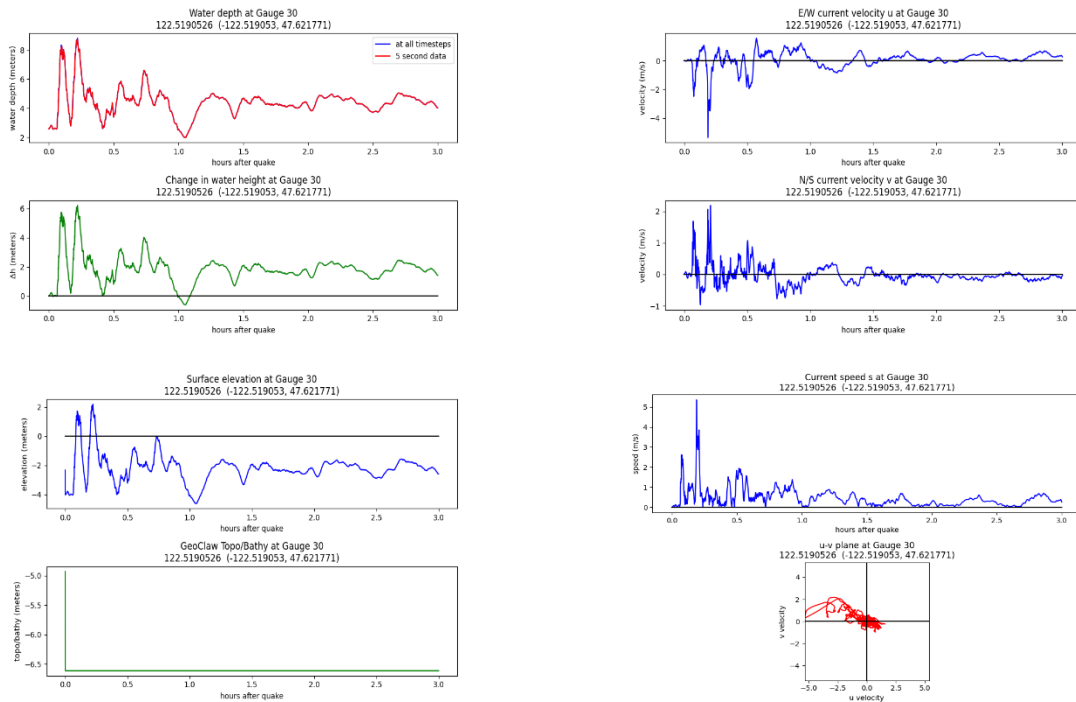
## Cascadia subduction zone scenario, MLW:



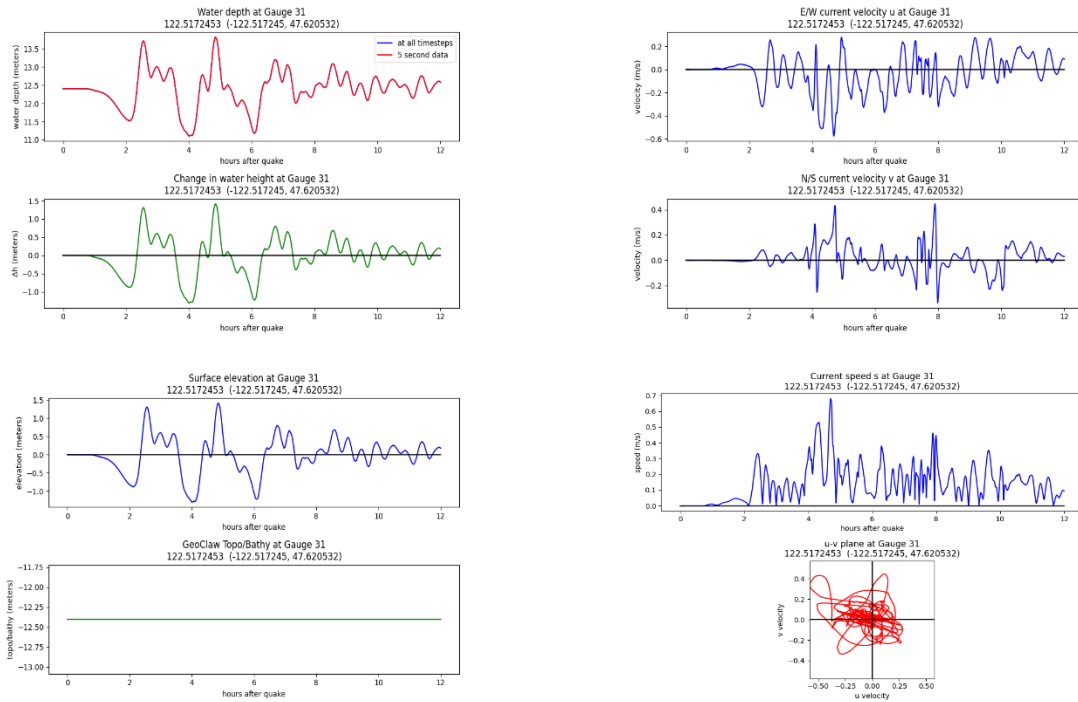
## Seattle fault scenario, MHW:



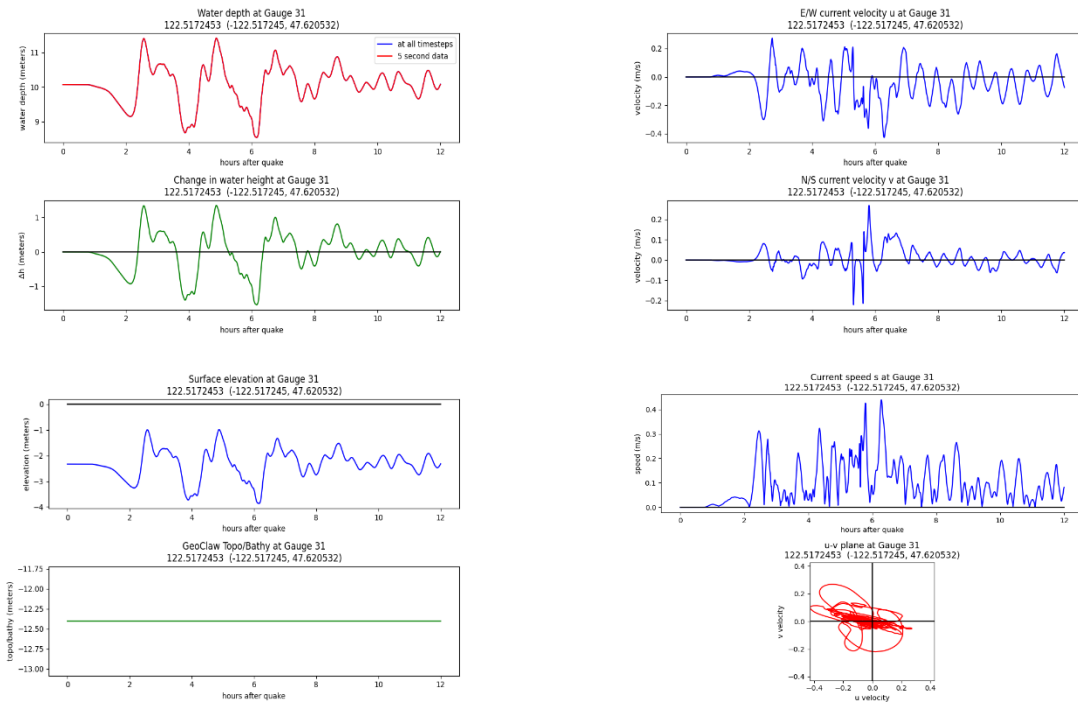
## Seattle fault scenario, MLW:



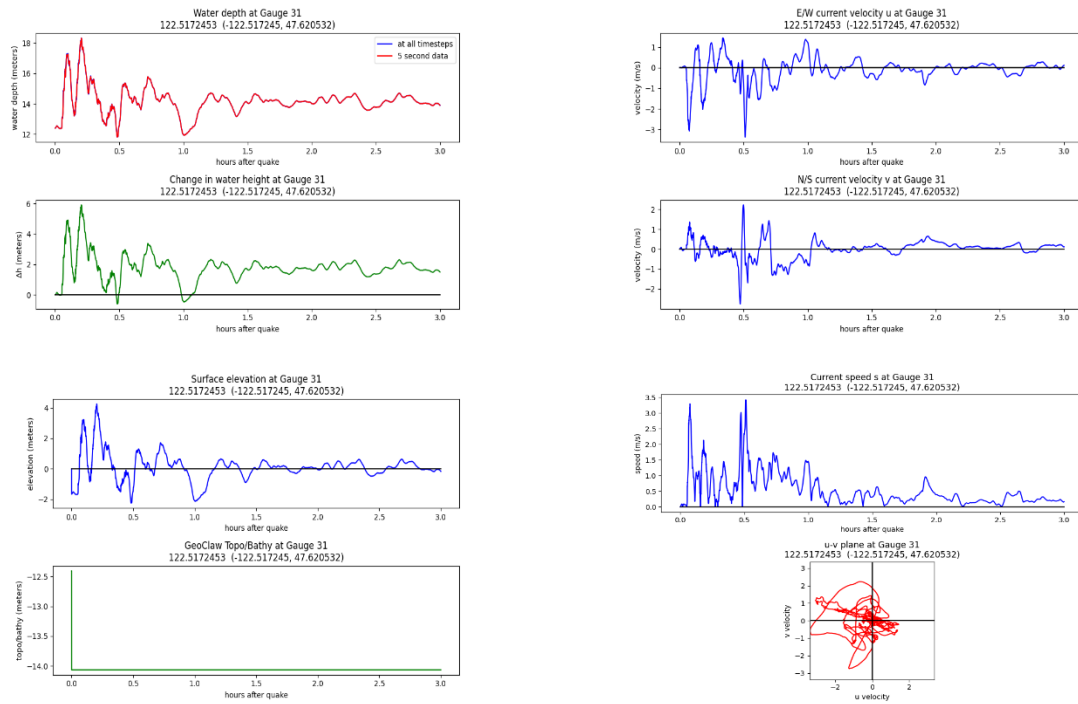
## Gauge 31: Bainbridge Island City Dock Cascadia subduction zone scenario, MHW:



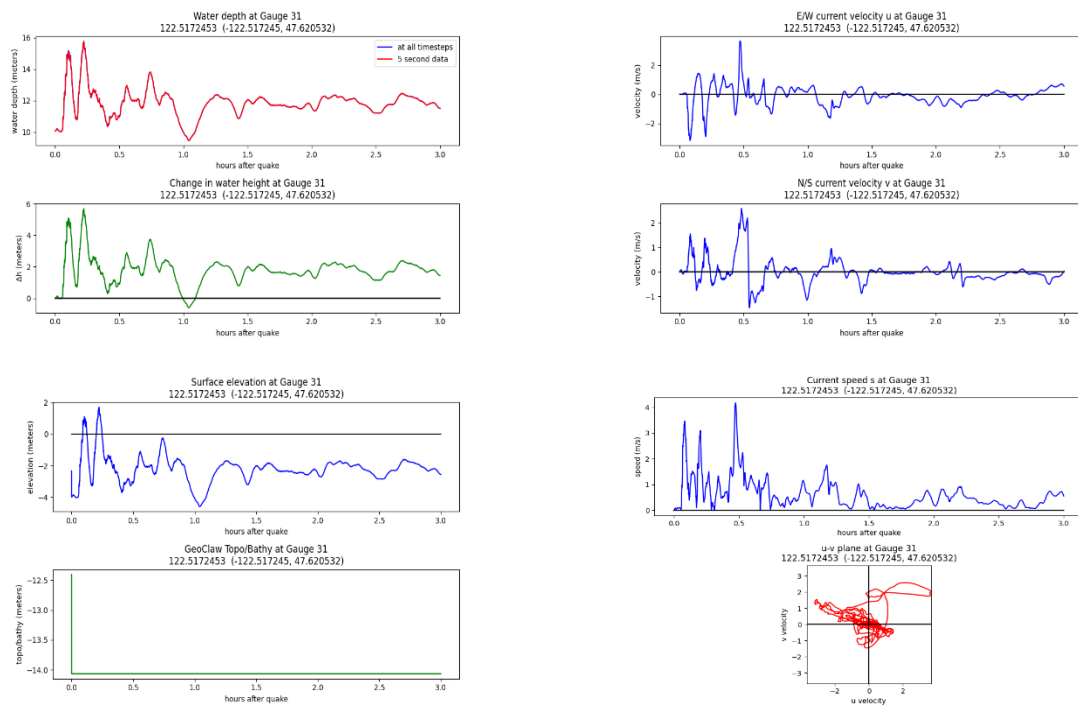
## Cascadia subduction zone scenario, MLW:



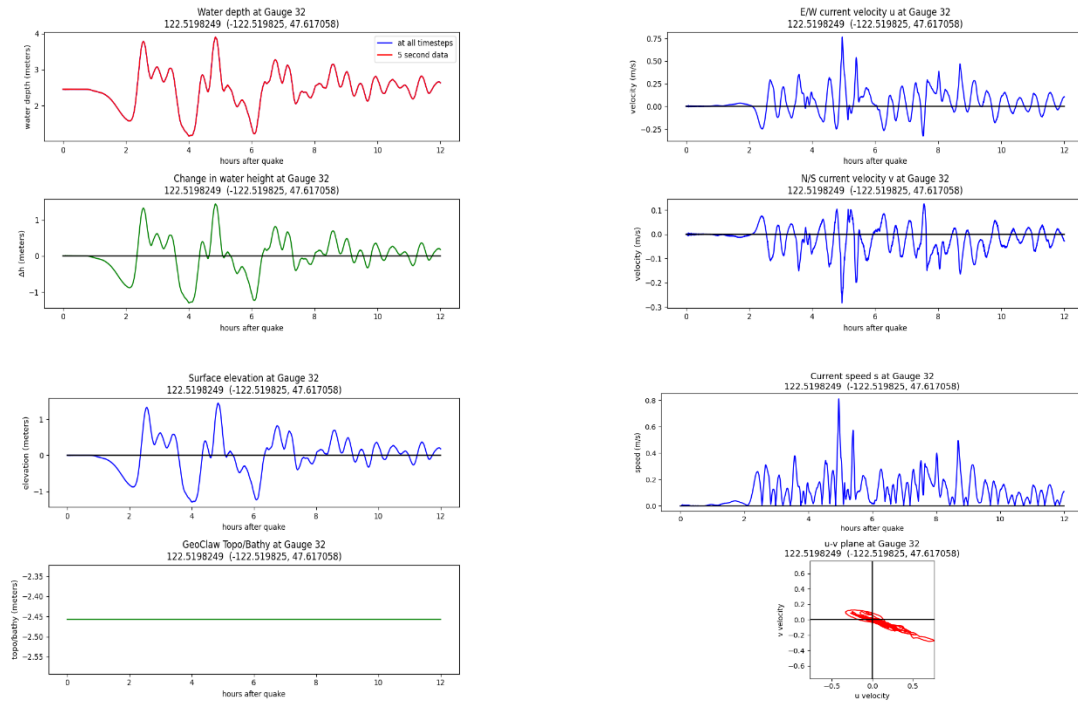
## Seattle fault scenario, MHW:



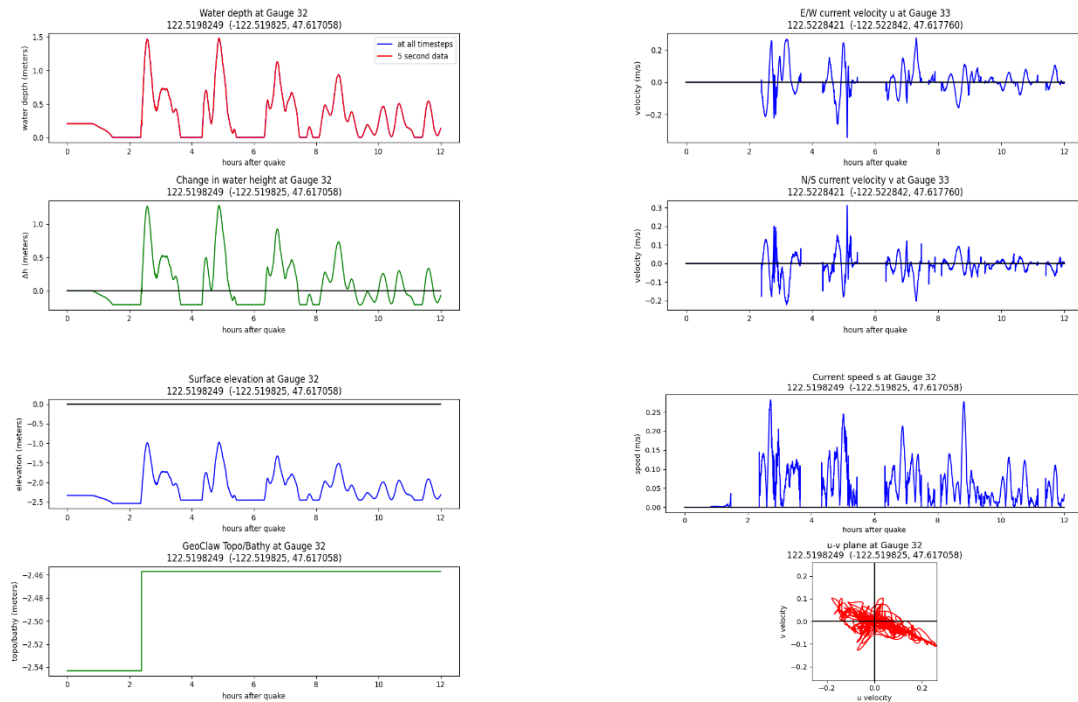
## Seattle fault scenario, MLW:



Gauge 32: Private dock center  
 Cascadia subduction zone scenario, MHW:

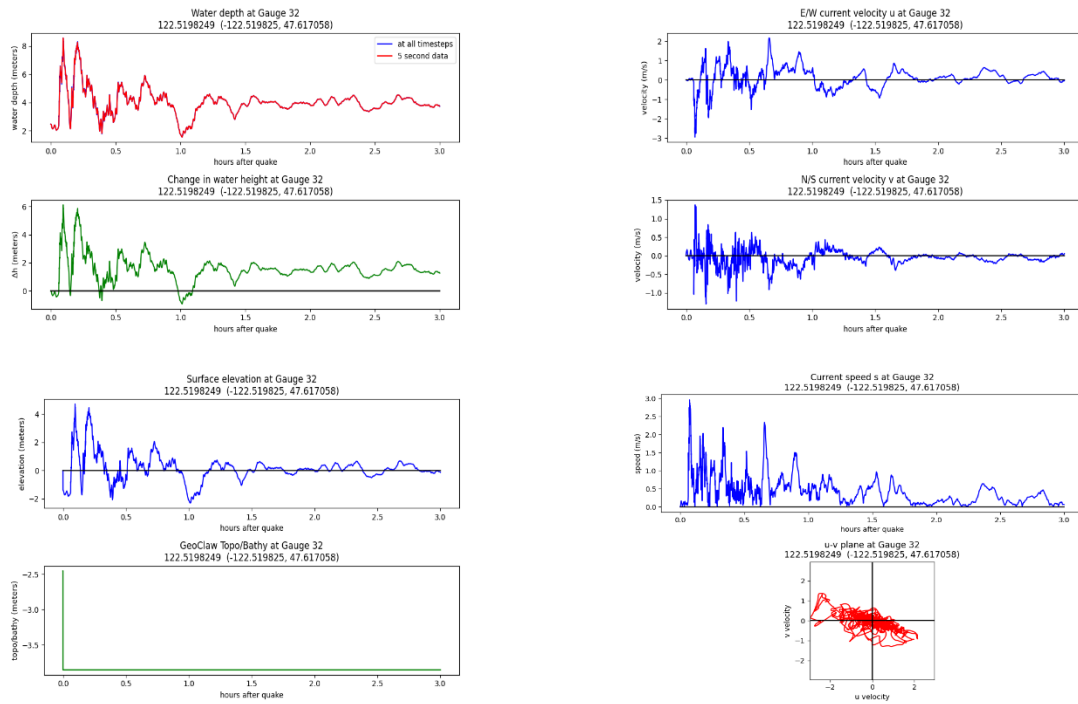


Cascadia subduction zone scenario, MLW:

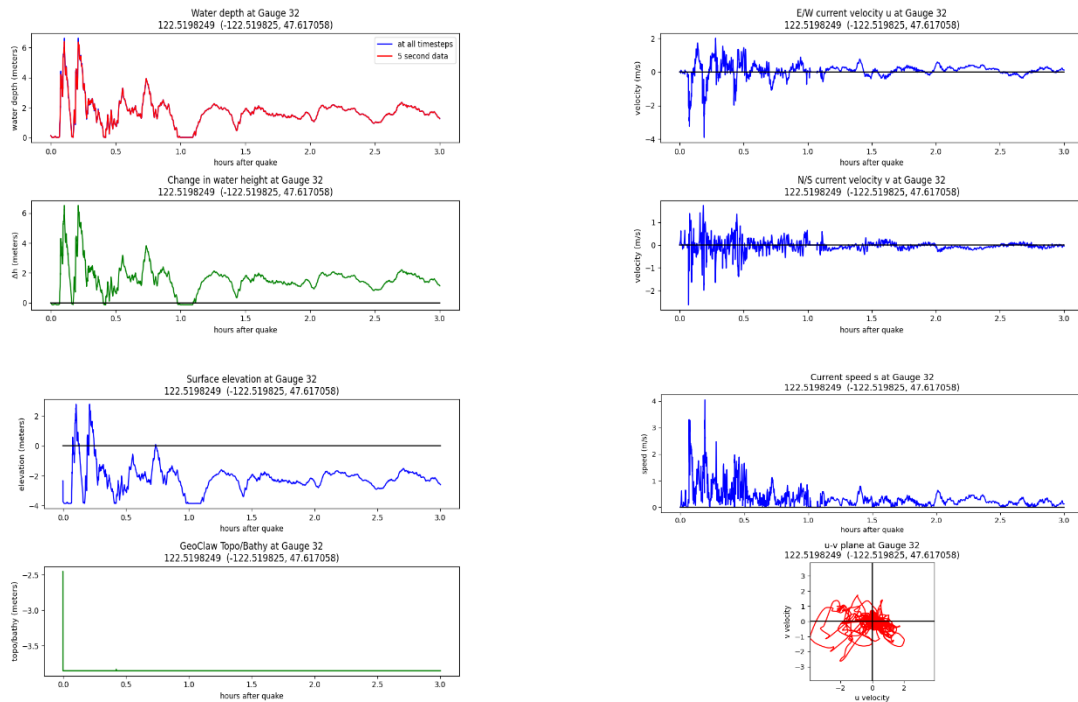




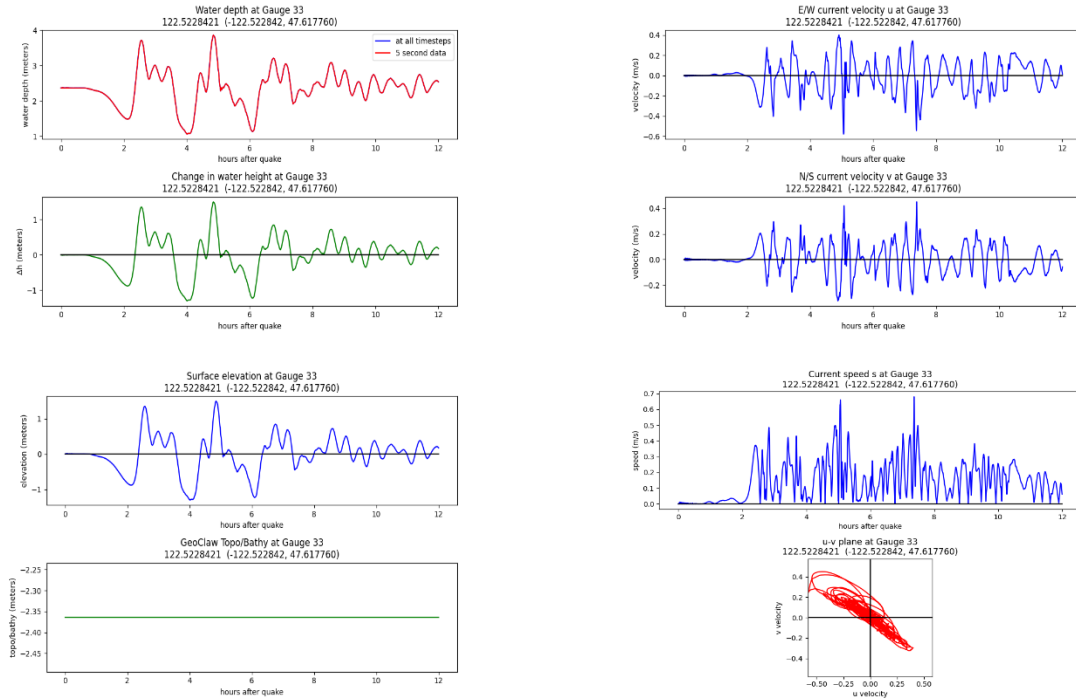
## Seattle fault scenario, MHW:



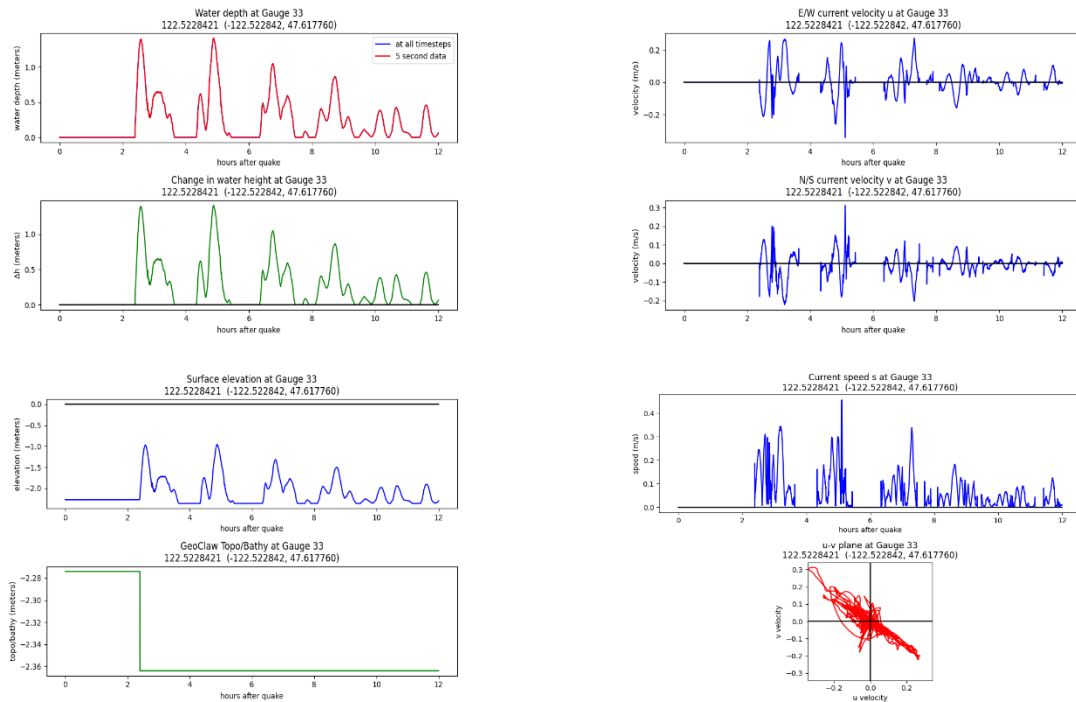
## Seattle fault scenario, MLW:



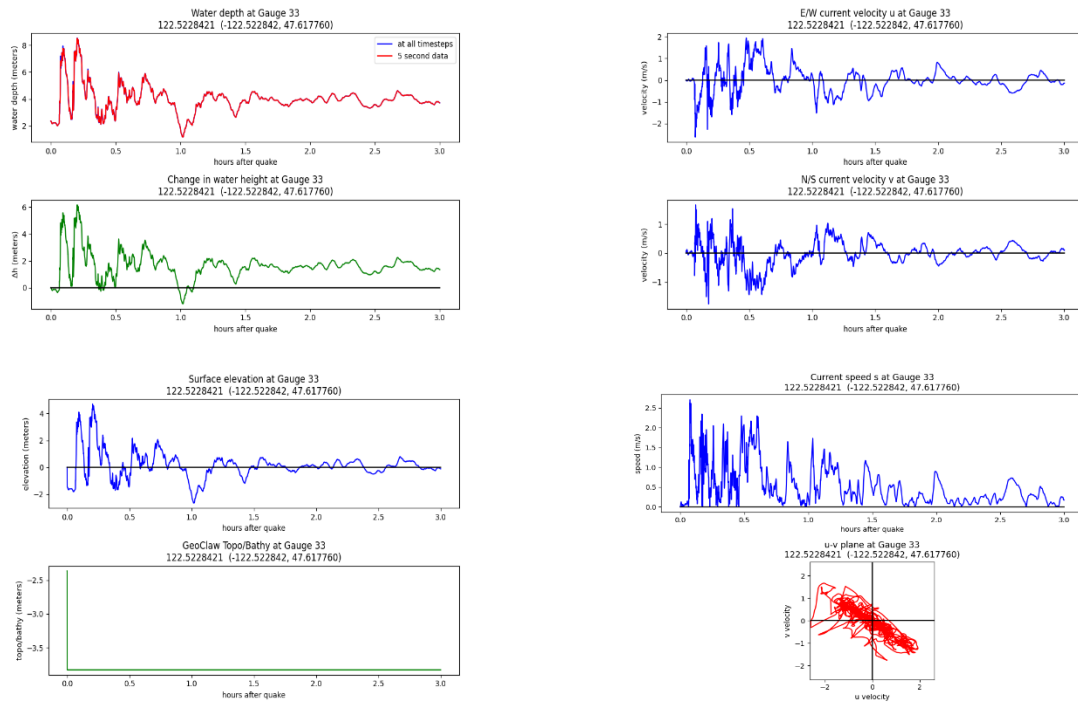
Gauge 33: Private dock west  
 Cascadia subduction zone scenario, MHW:



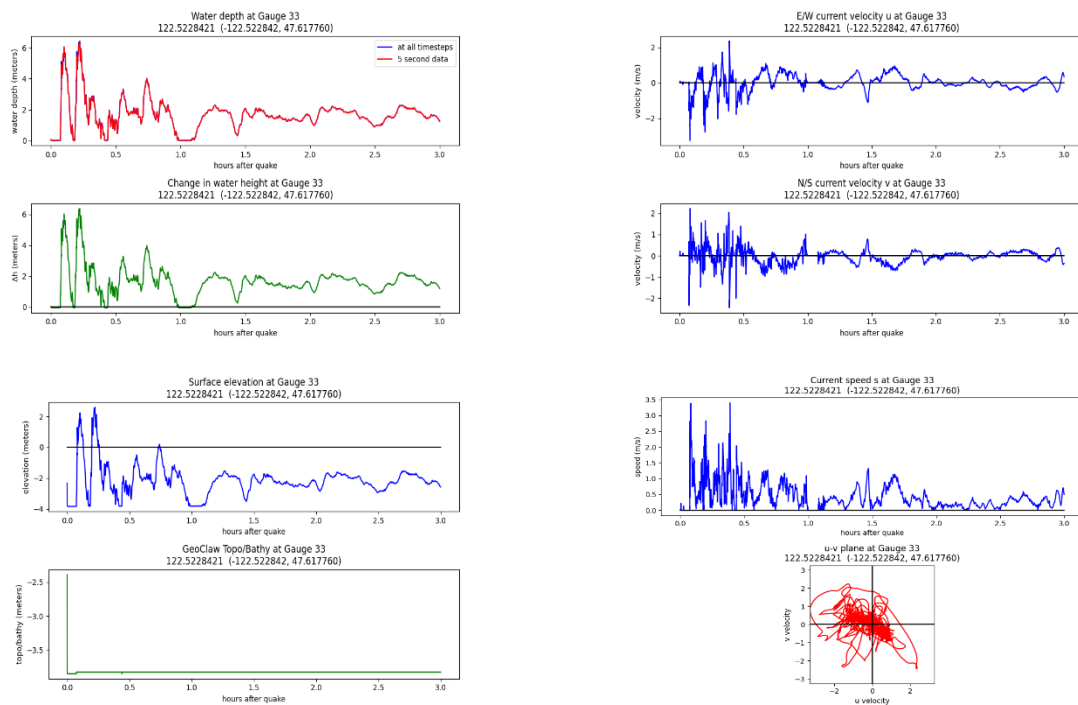
Cascadia subduction zone scenario, MLW:



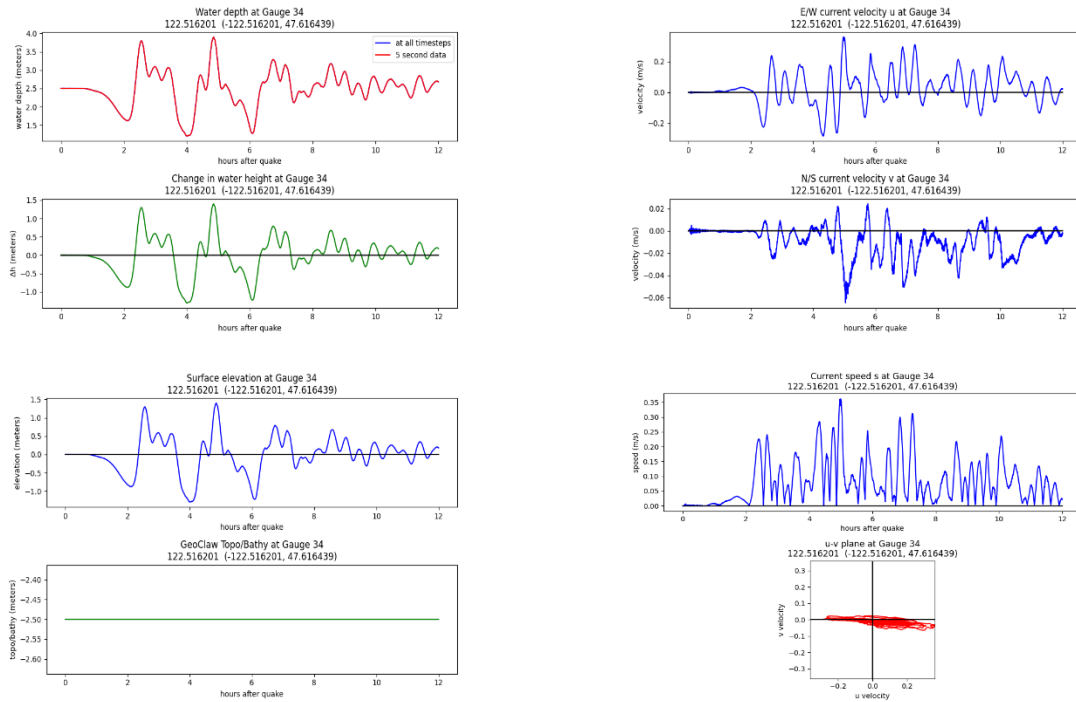
## Seattle fault scenario, MHW:



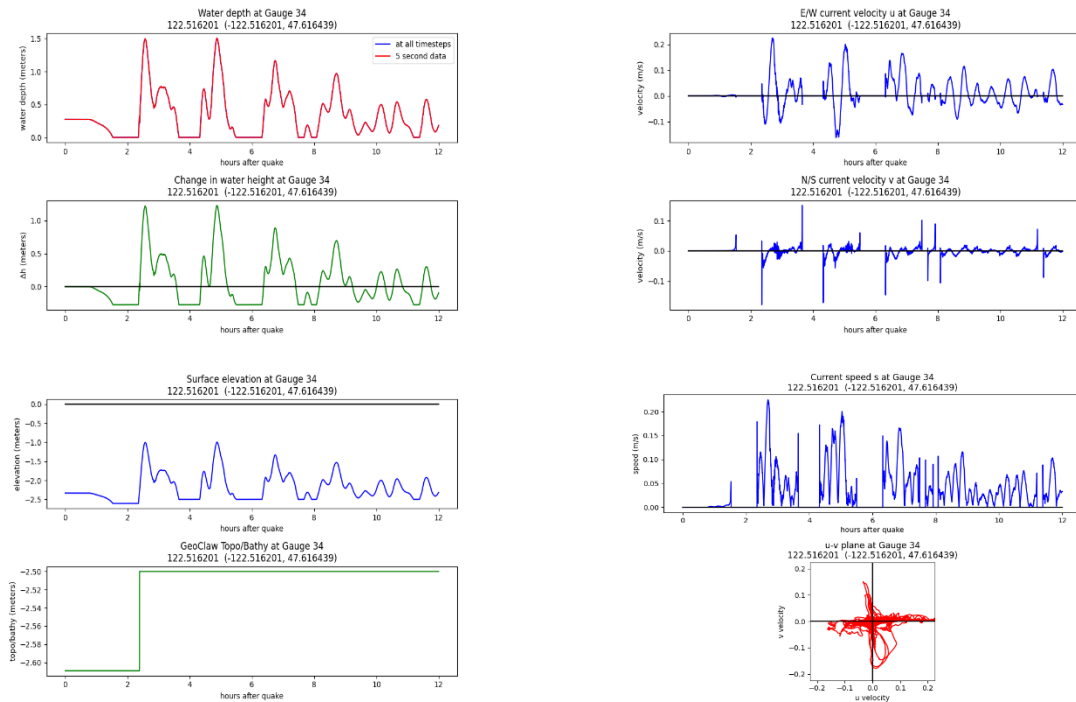
## Seattle fault scenario, MLW:



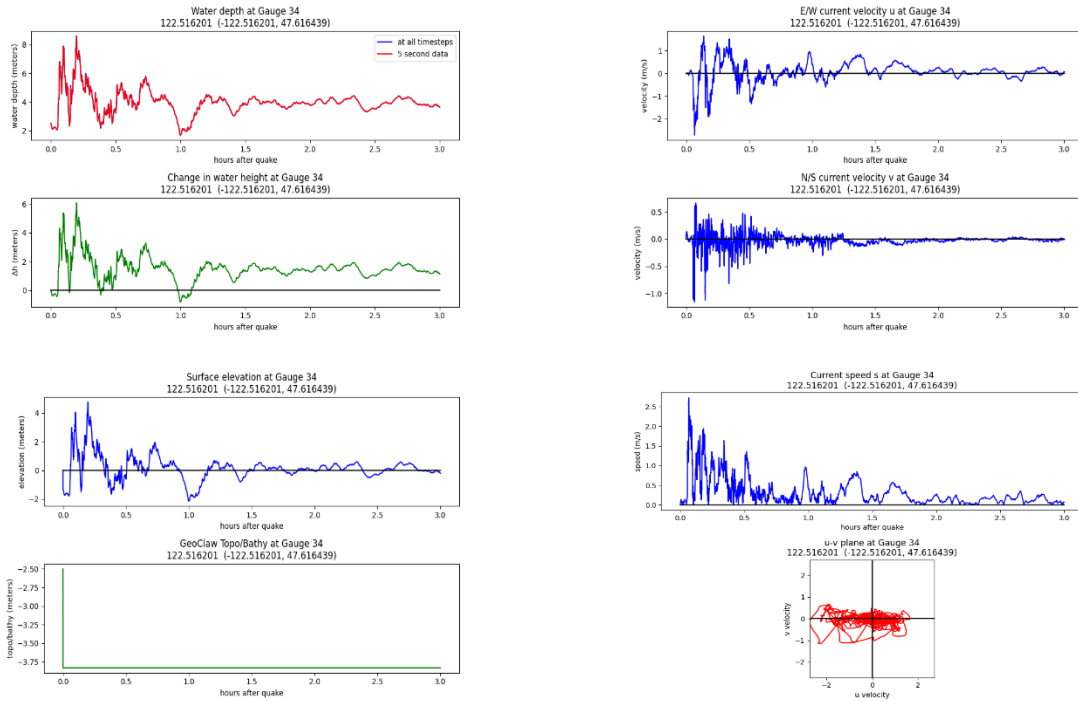
Gauge 34: Private dock east  
 Cascadia subduction zone scenario, MHW:



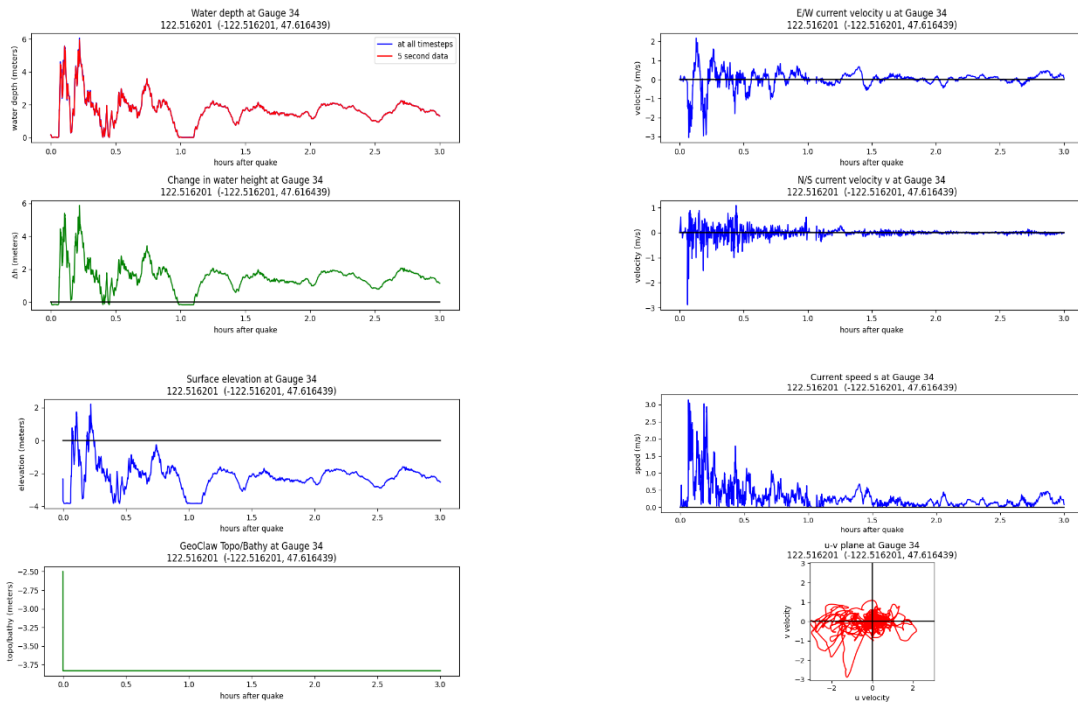
Cascadia subduction zone scenario, MLW:



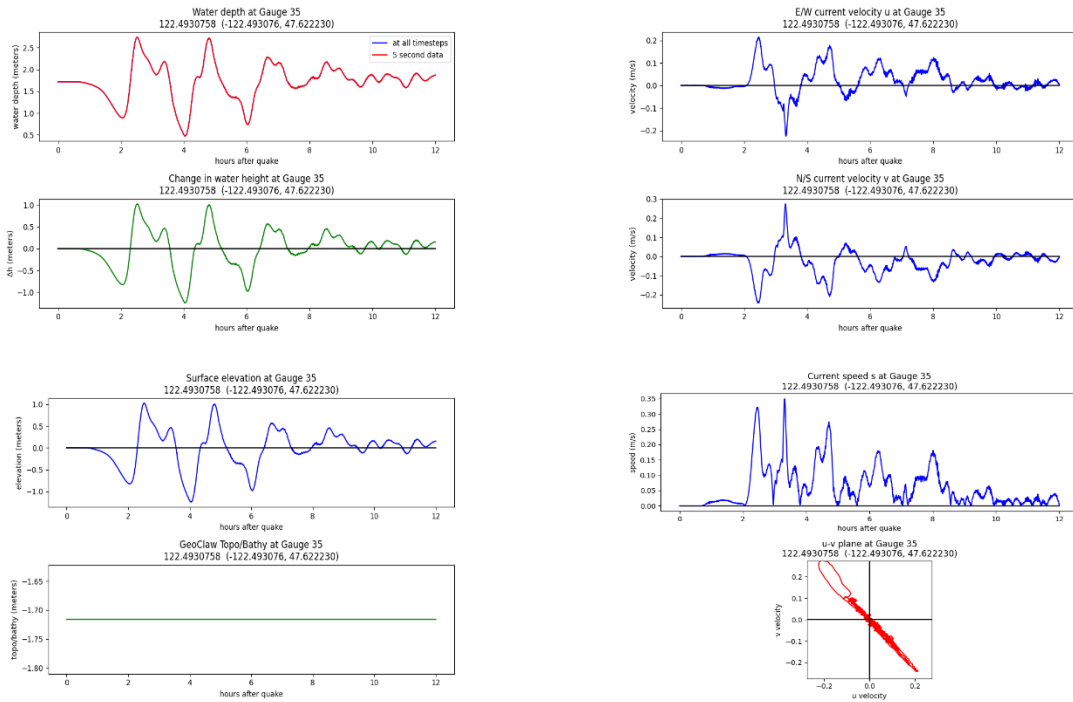
## Seattle fault scenario, MHW:



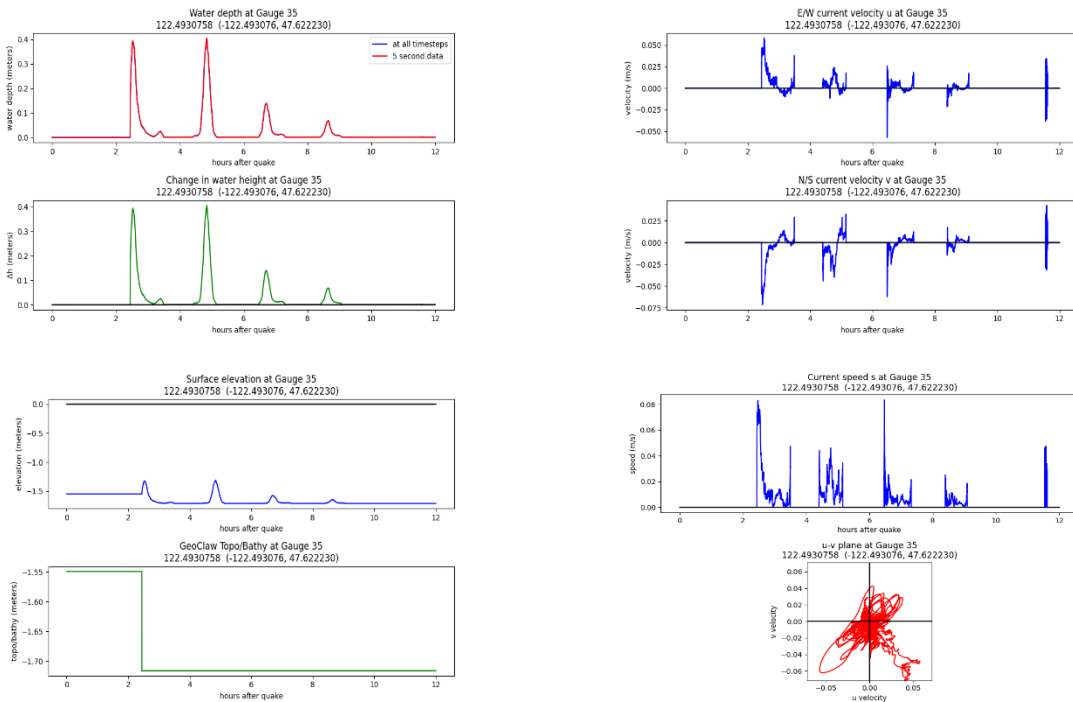
## Seattle fault scenario, MLW:



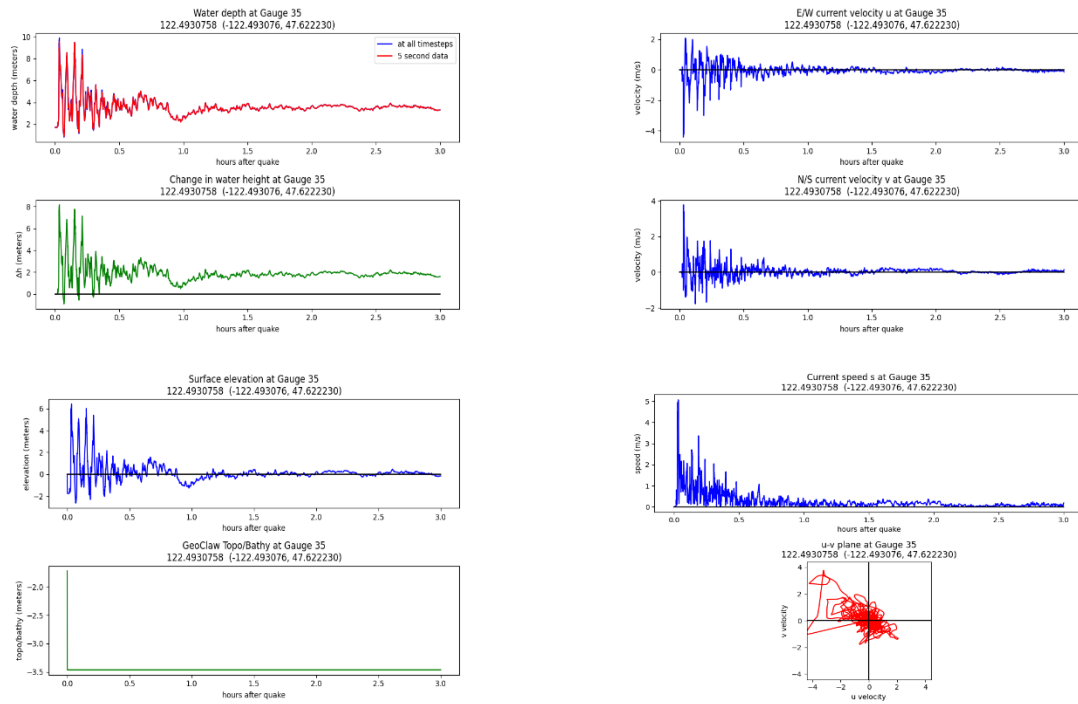
## Gauge 35: East of Wing Point Cascadia subduction zone scenario, MHW:



## Cascadia subduction zone scenario, MLW:



## Seattle fault scenario, MHW:



## Seattle fault scenario, MLW:

